51st International School & Conference on the Physics of Semiconductors

BOOK OF ABSTRACTS

JASZOWIEC 2023

Szczyrk, Poland 17 – 23 June 2023

ORGANIZED BY

IP PAN

FUW

Politechnika Wrocławska

unipress

Łukasiewicz Institute of Microelectronics and Photonics

PROGRAM COMMITTEE

Elżbieta Guziewicz – ***Chairman***
Tomasz Jakubczyk – ***Chair of the Tutorial Session***
Ewa Przeździecka – ***Secretary***

Witold Bardyszewski
Michał Borysiewicz
Aneta Drabińska
Joanna Jadczak
Maria Kamińska
Łukasz Kłopotowski
Piotr Kossacki
Paweł Machnikowski
Michał Matuszewski
Marcin Motyka
Czesław Skierbiszewski
Tomasz Story
Jacek Szczytko
Henryk Turski
Tomasz Wojtowicz
Jerzy Wróbel

ADVISORY COMMITTEE

Günther Bauer - Linz, Austria
Laurence Eaves, - Nottingham, UK
Jonathan Finley - Munchen, Germany
Jacek K. Furdyna - Notre Dame, USA
David Gershoni - Haifa, Israel
Paweł Hawrylak - Ottawa, Canada
Hideo Ohno - Sendai, Japan
Marek Potemski - Grenoble, France
Maurice S. Skolnick - Sheffield, UK
Luis Vina - Madrid, Spain
Dmitri Yakovlev - Dortmund, Germany

ORGANIZING COMMITTEE

Anna Reszka - ***Organizing Committee Chair***
Zbigniew Adamus
Jacek Szczepkowski

ORGANIZERS

Institute of Physics Polish Academy of Sciences

Faculty of Physics University of Warsaw

Wrocław University of Science and Technology

Politechnika Wrocławska

Institute of High Pressure Physics of the Polish Academy of Sciences

unipress

Łukasiewicz – the Institute of Microelectronics and Photonics

Łukasiewicz
Institute of
Microelectronics
and Photonics

SPONSORING ORGANIZATIONS

American Chemical Society International

US Army Combat Capabilities Development Command

EXHIBITORS

- Dr. Eberl MBE Komponenten
- EDVAC
- Labis
- Nextnano
- Quantum Design

WELCOMING ADDRESS

The 51st International School & Conference on the Physics of Semiconductors "Jaszowiec 2023" begins the second half-century of this conference, so it follows the long tradition of annual meetings of Polish physicists working in the field of semiconductors, in a beautiful mountain scenery.

We have 15 exciting invited lectures ahead, which will be delivered by 12 foreign and 3 Polish scientists. We will also listen to 36 oral presentations, carefully selected by the Scientific Committee from three times more submissions. Lectures and oral presentations cover many areas of novel physics, such as Fourier optics, 2D materials and Moiré heterostructures, semiconductor qubit architecture, topological photonics and ultra-wide bandgap materials. They are accompanied by 149 poster presentations, where apart from papers on photonic materials and 2D structures, you can also find reports on topological insulators, thermoelectrics, magnetic structures, solar cells and IV-VI materials. The conference is preceded by the School, a tutorial session addressed to students and young scientists.

I would like to thank the Program and Advisory Committees for their support in shaping the scientific program. I would also like to express my gratitude to the members of the Organizing Committee for their time and enthusiasm. Without your tremendous efforts the organization of "Jaszowiec 2023" conference would not be possible.

I wish you a successful conference, exciting discussions, striking up many acquaintances and sharing new ideas. If, in addition to participating in a rich scientific program, you find time for at least one mountain hike, I will consider that the conference has fulfilled its role.

Conference Chair

Elżbieta Guziewicz

CONFERENCE OFFICE

Conference office will be open:

10: 30 – 11:30, 16:30 – 18:00

Conference telephone number:

+48 502 962 261

CONFERENCE VENUE

HOTEL KLIMCZOK

ul. Poziomkowa 20

43-370 Szczyrk

Hotel reception:

mobile: +48 669 260 101

phone: +48 (33) 82 60 100

mail: recepcja@klimczok.pl

MBE
KOMPONENTEN | DR. EBERL

OCTOPLUS 600

MBE System

EDVAC

TECHNIKA PRÓŻNIOWA

Laboratoryjne pompy próżniowe

bezolejowe „scroll”

turbomolekularne

rotacyjne olejowe

EDWARDS

jonowe

kriogeniczne

multi-roots

oleje, filtry, czujniki, zawory, przyłącza próżniowe

SERWIS - DYSRTYBUCJA

www.edvac.pl

EDVAC Sp. z o.o.

ul. Lotnicza 27, 05-090 Raszyn

tel.: 22 490 41 81, e-mail: biuro@edvac.pl

Advanced Research Systems, Inc.

LABIS
Nanotechnology Tools and Systems

Aparatura badawcza do pomiarów w ultra-niskich temperaturach i polu magnetycznym

- Ultra stabilne **kriostaty helowe** pracujące w obiegu zamkniętym (3K – 800K)
- Kriogeniczne **stacje do pomiarów ostrzowych** mikro i nanostruktur
- Indywidualne **niestandardowe układy kriogeniczne**

WWW.LABIS.PL

nextnano
Software for semiconductor nanodevices

Software for the simulation of electronic and optoelectronic semiconductor nanodevices

- Quantum Cascade Lasers, RTDs
- LEDs, µ-LEDs
- Semiconductor Laser Diodes, VCSELs
- Nanotransistors, HEMTs
- Photodetectors, Solar Cells
- Nanowires, Quantum Dots
- Quantum Computing: Qubits
- Biosensors

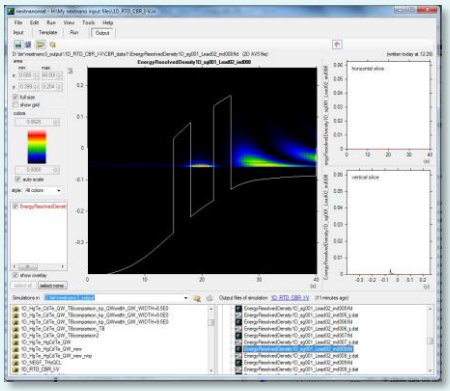

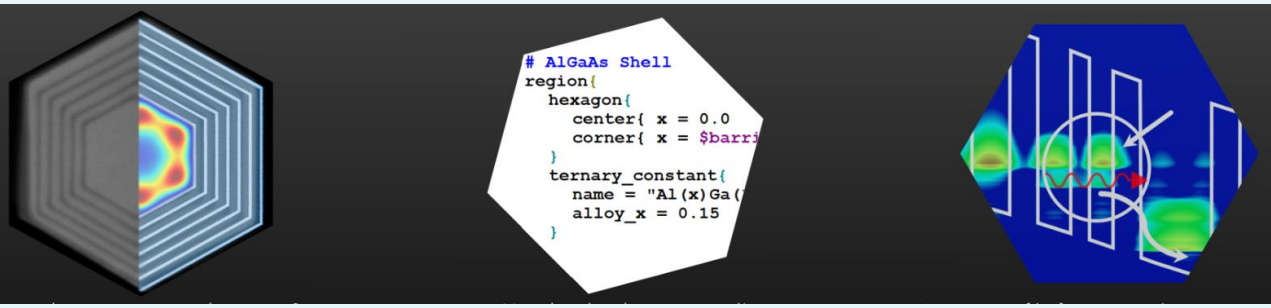

- Schrödinger-Poisson-Current solver in 1D, 2D & 3D
- Effective-mass, 8-band k·p, Quantum transport (NEGF)
- Strain, Piezo- & Pyroelectricity
- Materials: Group IV, III-V, II-VI (Zinc blende & Wurtzite)

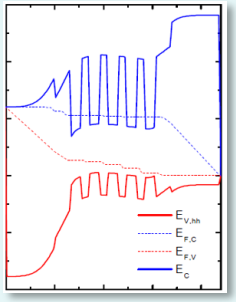

Try our new Python package: github.com/nextnanopy

Download trial version: www.nextnano.com/download

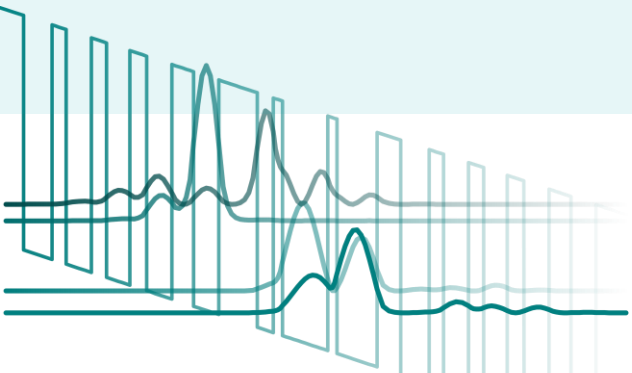

nextnano GmbH – Munich – Germany
Dr. Stefan Birner, stefan.birner@nextnano.com

nextnano Lab SAS – Grenoble – France
Dr. Thomas Grange, thomas.grange@nextnano.com

Quantum Design
EUROPE

qd-europe.com

High-tech instruments for research and industry
50 years of experience - 120 specialized experts in Europe

- Leading supplier of automated materials characterization systems incorporating superconducting technology
- Reliable distribution partner of:

OXFORD INSTRUMENTS ANDOR

Biolin Scientific

SPECIM
A Konica Minolta Company

OXFORD INSTRUMENTS WITec

Lake Shore CRYOTRONICS
ADVANCING SCIENCE

J.A. Woollam
Ellipsometry Solutions

Micro Materials
Excellence in Nanomechanics

and more...

Program of the 51st International School & Conference on the Physics of Semiconductors "Jaszowiec 2023" Szczyrk, Poland, 17 – 23 June 2023

School – Special Tutorial Session

SATURDAY, 17 JUNE 2023

15:30 – 15:45	**Tomasz Jakubczyk** – *School Opening*
15:45 – 17:30	**Michał Boćkowski** (Institute of High Pressure Physics PAS, Poland) *Bulk GaN growth* – **Sa1**
17:30 – 18:00	Coffee break
18:00 – 19:45	**Heike Riel** (IBM Research Europe, Switzerland) *Prospects and challenges of quantum computing* – **Sa2**
19:45	**Barbecue Dinner**

SUNDAY, 18 JUNE 2023

9:15 – 11:00	**Jagoda Sławińska** (University of Groningen, Netherlands) *Computational design of spintronics materials* – **Su1**
11:00 – 11:30	Coffee break
11:30 – 13:15	**Tim Schröder** (Humboldt-Universität zu Berlin, Germany) *Experimental Quantum Control of Spin Defects in Solids* – **Su2**
13:15 – 14:15	Lunch
17:30 –18:30	**Tutorial Session Quiz and Closing**
18:45 – 20:00	Dinner
20:00	**Concert and Welcoming glass of wine**

Conference

MONDAY, 19 JUNE 2023

8:45 – 9:00 **Elżbieta Guziewicz –** *Conference Opening*

Chair: Tomasz Dietl

9:00 – 9:45 **David Norris** (ETH Zurich, Switzerland)
Optical and Electronic Fourier Surfaces – **MoI1**

9:45 – 10:30 **Alexander Högele** (LMU München, Germany)
Excitons in moiré heterostructures – **MoI2**

10:30 – 10:45 **Dennis Kudlacik**, C. Harkort, N.E. Kopteva, D.R. Yakovlev, M. Karzel, E. Kirstein, O. Hordiichuk, M. Kovalenko, M. Bayer
Spin-Flip Raman Scattering on Electrons and Holes in Two-Dimensional $(PEA)_2PbI_4$ Perovskites – **MoO1**

10:45 –11:15 Coffee break

Chair: Witold Bardyszewski

11:15 – 12:00 **Sebastian Klembt** (Chair for Applied Physics, University of Würzburg, Germany)
Topological photonics and topological lasers – **MoI3**

12:00 – 12:15 **Helgi Sigurðsson,** J.D. Toepfer, L. Pickup, S. Harrison, T. Cookson, Y. Wang, A. Askitopoulos, S. Alyatkin, P.G. Lagoudakis
Networks of liquid light – **MoO2**

12:15 – 12:30 **Michał Kobecki**
Giant Photo-Elasticity of the Superlattice Polaritons for Detection of Coherent Phonons – **MoO3**

12:30 – 12:45 **Dąbrówka Biegańska,** M. Pieczarka, C. Schneider, S. Hofling, S. Klembt, M. Syperek
Anomalous dispersion and dissipative coupling in AlGaAs exciton-polariton structure – **MoO4**

12:45 – 13:00 **Amir Rahmani,** M. Kędziora, A. Opala, M. Matuszewski
Non-Hermitian synthetic lattice with light-matter coupling – **MoO5**

13:00 – 14:30 Lunch

14:30 – 16:00 **Monday Poster Session A**
TMDs, van der Waals crystals and solar cells

17:00 – 18:00 **Quantum Design**
Spectrographs – **MoE1**

18:00 – 19:30 Dinner

Chair: Maria Kamińska

19:30 – 20:15 **Panaiot Zotev** (University of Sheffield, UK)
Van der Waals materials for nanophotonic applications – **MoI4**

20:15 – 20:30 **Arka Karmakar,** T. Kazimierczuk, I. Antoniazzi, M. Raczyński, T. Taniguchi, K. Watanabe, A. Babiński, A. Al-Mahboob, M.R. Molas
Excitation Dependent Energy Transfer in 2D Heterostructure – **MoO6**

20:30 – 20:45 **Alessandro Surrente,** J. Jasinski, S. Palai, M. Smiertka, F. Gucci, A. Genco, S. Dal Conte, K. Watanabe, T. Taniguchi, M. Baranowski, P. Płochocka
Dexter induced inverted valley polarization in monolayer WSe_2 – **MoO7**

20:35 – 21:00 **Maciej Molas,** T. Woźniak, Ł. Kipczak, A. Babiński, S. Sun, C. Xu, W. Ren
Hot luminescence or Raman scattering in monolayers of $MoSi_2N_4$ – **MoO8**

21:00 – 22:30 **Monday Poster Session B**
Topological insulators, magnetic structures & termoelectrics

TUESDAY 20 JUNE 2023

Chair: David Norris

9:00 – 9:45 **Łukasz Cywiński** (Institute of Physics Polish Academy of Sciences, Poland)
Coherent shuttling of spins between silicon-based quantum dots – **TuI1**

9:45 – 10:30 **Maciej Bieniek** (University of Würzburg, Germany)
Spin valley qubits in gated quantum dots in 2D – **TuI2**

10:30 – 10:45 **Sarath Prem,** M.M. Wysokiński, M. Trif
Longitudinal coupling between electrically driven spin-qubits and a resonator – **TuO1**

10:45 – 11:15 Coffee break

Chair: Jacek Szczytko

11:15 – 12:00 **Doris E. Reiter** (TU Dortmund, Germany)
Optical control of solid-state quantum emitters – **TuI3**

12:00 – 12:15 **Anna Musiał,** M. Wasiluk, K. Roszak, M. Gawełczyk, P. Holewa, P. Wyborski, P. Podemski, M. Burakowski, H. Salamon, P. Mrowiński, M. Mikulicz, T. Smołka, K. Posmyk, A. Zielińska, J.P. Reithmaier, M. Benyoucef, G. Sęk, W. Rudno-Rudziński
Epitaxial InAs/InP quantum dots as emitters of single photons and entangled photon pairs for fiber-based quantum communication – **TuO2**

12:15 – 12:30 **Marcin Syperek,** P. Holewa, E. Zięba-Ostój, D.A. Vajner, T. Gao, M. Lach, M. Wasiluk, B. Gaal, A. Sakansas, M. Burakowski, P. Mrowiński, B. Krajnik, M. Xiong, A. Huck, K. Yvind, N. Gregersen, A. Musiał, T. Heindel, E. Semenova
State-of-the-art Quantum Dot-based Single-photon Sources for Quantum Key Distribution in Silica Fiber Networks at 1550 nm – **TuO3**

12:30 – 12:45 **Marek Burakowski,** P. Mrowiński, P. Holewa, A. Sakanas, E. Semenova, G. Sęk, M. Syperek
Heterogeneously Integrated InAs/InP Quantum Dot Single-photo n Emitter with the Si Platform for On-chip Quantum Photonics – **TuO4**

12:45 – 13:00 **Kacper Oreszczuk**, A. Rodek, L. Zinkiewicz, J. Howarth, T. Taniguchi, K. Watanabe, P. Kossacki
Electrically gated single photon emitters in monolayer transition metal dichalcogenides – **TuO5**

13:00 – 14:30 Lunch

14:30 – 16:00 **Tuesday Poster Session A**
Wide bandgap materials (h-BN, Ga2O3, ZnO, CdMgO, GaN)

17:00 – 18:00 **Quantum Design**
Detectors – **TuE1**

18:00 – 19:30 Dinner

Chair: Doris Reiter

19:30 – 19:45 **Nilesh Dalla,** P.K. Kulboka, P.S. Sojewski, K.O. Oreszczuk, T.K. Kazimierczuk, P.K. Kossacki, R.J.W. Warburton, T.J. Jakubczyk
Realization of a High Finesse Platform for Functionalization of Emitters – **TuO6**

19:45 – 20:00 **Mateusz Kędziora,** K. Łempicka-Mirek, M. Król, L.De. Marco, A. Coriolano, L. Polimeno, I. Viola, M. Muszyński, P. Morawiak, R. Mazur, P. Kula, W. Piecek, P. Fita, D. Sanvitto, J. Szczytko, B. Piętka
Electrical switching of a chiral lasing from polariton condensate in a Rashba-Dresselhaus regime – **TuO7**

20:00 – 20:15 **Magdalena Furman,** A. Opala, M. Król, R. Mirek, K. Tyszka, B. Seredyński, W. Pacuski, J. Szczytko, M. Matuszewski, B. Piętka
Natural Exceptional Points Appearing in Semiconductor Microcavity Systems – **TuO8**

20:15 – 20:30 **Maciej Pieczarka,** M. Gębski, A.N. Piasecka, M. Wasiak, J.A. Lott, T. Czyszanowski
Driven dissipative Bose Einstein condensation of photons in a VCSEL – **TuO9**

20:30 – 20:45 **Andrzej Opala,** P. Oliwa, M. Muszyński, B. Piętka, J. Szczytko, M. Matuszewski
Topologically protected interface states induced by spin-orbit coupling in liquid crystal microcavity – **TuO10**

20:45 – 21:00 **Przemysław Oliwa,** W. Bardyszewski, B. Piętka, J. Szczytko
Quantum Mechanical-like Approach with Effective Hamiltonians Based on Resonant States in Optical Cavities – **TuO11**

21:00 – 22:30 **Tuesday Poster Session B**
Photonic structures and photodetectors

WEDNESDAY 21 JUNE 2023

Chair: Czesław Skierbiszewski

9:00 – 9:45 **Bart Kuyken** (Ghent University, Belgium)
III-V-on-Silicon-Nitride Mode-Locked Lasers – **WeI1**

9:45 – 10:00 **Rafał Zdunek,** M. Chlipała, G. Muzioł, C. Skierbiszewski, J. Łusakowski, H. Turski
Recovering rectangular band profile in polar InGaN-based heterostructures utilizing junction field – **WeO1**

10:00 – 10:15 **Piotr Kruszewski,** J. Plesiewicz, V.P. Markevich, P. Prystawko, S. Bulka, M. Halsall, I. Crowe, L. Sun, A.R. Peaker
Deep-level traps in as-grown and electron-irradiated n-GaN layers grown by MOVPE on Ammono-GaN substrate – **WeO2**

10:15 – 10:30 **Tomasz Fąs,** D. Yavorskiy, E. Pruszyńska-Karbownik, M. Sawicka, J. Kacperski, J. Wróbel, P. Nowicki, A. Kazakov, J. Polaczyński, A. Feduniewicz-Żmuda, Cz. Skierbiszewski, D. Schiavon, P. Perlin, T. Czyszanowski, J. Suffczyński
Bound states in continuum confined in GaN based subwavelength gratings – **WeO3**

10:30 – 10:45 **Antonina Bieganowska,** C. Schneider, S. Höfling, S. Klembt, M. Syperek, M. Pieczarka
Dynamics and Effective Interactions of a Photonic Condensate in an Optical Trap – **WeO4**

10:45 – 11:15 Coffee break

Chair: Zbigniew Wasilewski

11:15 – 12:00 **Masataka Higashiwaki** (Osaka Metropolitan University, Japan)
Advances and Prospects of Gallium Oxide Material and Device Technologies – **WeI2**

12:00 – 12:45 **Katharina Lorenz** (Instituto Superior Técnico, University of Lisbon, Portugal)
Radiation Effects in Wide Bandgap Materials – **WeI3**

12:45 – 13:05 **Dinesh Soares**
"ACS Omega": A High Quality, Global, Open Access Journal from the American Chemical Society – **WeS1**

13:05 – 14:30 Lunch

14:30 – 17:00 **Nextnano**
Tutorial Session – **WeE1**

19:30 – 3:00 **Banquet**

THURSDAY 22 JUNE 2023

Chair: Piotr Kossacki

10:00 – 10:45 **Mark Greenaway** (Loughborough University, UK)
Magnetophonon resonances in graphene – **ThI1**

10:45 – 11:15 Coffee break

Chair: Paweł Machnikowski

11:15 – 12:00 **Sylvain Ravets** (CNRS, France)
Kardar-Parisi-Zhang universality in a one-dimensional polariton condensate – **ThI2**

12:00 – 12:45 **Daniel Wigger** (Trinity College Dublin, Ireland)
Time-resolved nonlinear optical spectroscopy of basic excitations in 2D materials – **ThI3**

12:45 – 13:00 **Leszek Bryja**, J. Andrzejewski, J. Debus, C.H. Ho, J. Jadczak
The study of resonant Raman scattering in semiconducting layered GeS – **ThO1**

13:00 – 14:30 Lunch

14:30 – 16:00 **Thursday Poster Session A**
Theoretical platform/ CdTe and PbTe-based structures/Si-based NWs

18:00 – 19:30 Dinner

Chair: Tomasz Story

19:30 – 19:45 **Kajetan Fijałkowski,** N. Liu, P. Mandal, S. Schreyeck, K. Brunner, C. Gould, L.W. Molenkamp
Macroscopic Quantum Tunneling of a Topological Ferromagnet – **ThO2**

19:45 – 20:00 **Md Shahin Alam,** F. Tafti, C. Autieri, M. Matusiak
Anomalous transverse response in topological magnet CeAlSi – **ThO3**

20:00 – 20:15 **Paweł Sidorczak,** W. Wołkanowicz, K. Gas, A. Kaleta, S. Gierałtowska, R. Minikayev, S. Kret, M. Sawicki, T. Wojtowicz, D. Wasik, M. Gryglas-Borysiewicz, K. Dybko
Superconductivity in PbTe/SnTe semiconductor heterostructure: a candidate for spin-triplet superconductor – **ThO4**

20:15 – 20:30 **Kacper P. Kluczyk,** K. Gas, M.J. Grzybowski, M.A. Borysiewicz, T. Fąs, J. Suffczyński, E. Łusakowska, W. Wołkanowicz, J.Z. Domagała, P. Skupiński, K. Grasza, A. Mycielski, K. Vyborny, M. Baj, M. Sawicki, M. Gryglas-Borysiewicz
Peculiar magnetic phase in antiferromagnet MnTe – **ThO5**

20:30 – 20:45 **Michał Szot,** P. Wojnar, J. Korczak, W. Zaleszczyk, L. Kowalczyk, S. Chusnutdinow, R. Minikayev, W. Wołkanowicz, T. Story, G. Karczewski
Photoluminescence studies of the futuristic SnSe semiconductor – **ThO6**

20:45 – 21:00 **Mujeeb Ahmad**, W. Wołkanowicz, S. Dad, P. Dziawa, T. Wojtowicz, K. Dybko
Investigating of the topological phase transition in $Pb_{1-x}Sn_xTe$ topological crystalline insulators by using nonlinear Hall effect measurements – **ThO7**

21:00 – 22:30 **On-line Poster Session**

FRIDAY 23 JUNE 2023

Chair: Wojciech Pacuski

9:00 – 9:45 **Johannes Binder** (University of Warsaw, Poland)
Epitaxial Hexagonal Boron Nitride – Growth, Properties and Applications – **FrI1**

9:45 – 10:00 **Piotr Tatarczak,** J. Iwański, J. Binder, A.K. Dąbrowska, M. Tokarczyk, R. Stępniewski, A. Wysmołek
h-BN bubbles – a step towards deterministic activation of single photon emission – **FrO1**

10:00 – 10:15 **Krzysztof Korona,** A.K. Dąbrowska, J. Iwański, T. Korona, A. Reszka, J. Binder, R. Stępniewski, A. Wysmołek
Nature of UV (3 – 5 eV) Emission from Hexagonal Boron Nitride – **FrO2**

10:15 – 10:30 **Aleksandra Łopion,** A. Bogucki, Z. Śnioch, K.E. Połczyńska, W. Pacuski, T. Kazimierczuk, A. Golnik, P. Kossacki
Optically Detected Magnetic Resonance of p- and n-type Doped (Cd,Mn)Te QWs – **FrO3**

10:30 – 10:45 **Magdalena Birowska**
Magnetic signatures in structural, electronic and optical properties of 2D MPX_3 crystals – **FrO4**

10:45 – 11:15 Coffee break

Chair: Andrzej Golnik

11:15 –12:00 **Mateusz Dyksik** (Wrocław University of Science and Technology,Poland)
Magneto-spectroscopy of excitons in two-dimensional layered perovskites – **FrI2**

12:00 – 12:15 **Andrzej Nowok,** M. Baranowski, M. Dyksik, A. Surrente, M. Mączka, P. Płochocka
Temperature Dependence of Effective Masses in Three-dimensional Methylammonium Lead Trihalides – **FrO5**

12:15 – 12:30 **Natalia Zawadzka,** M. Grzeszczyk, Z. Chen, M.I. Katsnelson, M.R. Molas, M. Koperski
Spin dimensionality in chromium trihalides – **FrO6**

12:30 – 12:45 **Elżbieta Guziewicz** - *Closing conference*

12:45 – 14:00 Lunch

MONDAY POSTER SESSION A

TMDs, van der Waals crystals and solar cells

14:30 - 16:00

MoPA1 *Automated Search For TMDs Monolayers On Exfoliated Samples*
W. Kolesiński, M. Goryca

MoPA2 *Electrical Tuning Of exciton lifetime in monolayer MoS_2*
P. H. Lankappa, P. Mondal, A. Bid,J K. Basu

MoPA3 *Fabrication and Strain Engineering of Transition Metal Dichalcogenides Monolayers on GaAs Nanomembranes*
E. Cybula, J. Jasiński, S. Palai, M. Śmiertka, A. Balgarkashi, V. Piazza, A. Fontcuberta i Morral, A. Surrente, M. Baranowski, A. Castellanos-Gomez, P. Płochocka

MoPA4 *Controlled coherent-coupling and dynamics of exciton complexes in a $MoSe_2$ monolayer*
A. Rodek, J. Howarth, T. Hahn, T. Taniguchi, K. Watanabe, M. Potemski, P. Kossacki, D. Wigger, J. Kasprzak

MoPA5 *Comparison of optical properties of $MoSe_2$ monolayers; samples grown by MBE technique vs mechanically exfoliated one*
M. Raczyński, W. Pacuski, T. Kazimierczuk, P. Kossacki

MoPA6 *Electron-phonon coupling in a WSe_2 monolayer unveiled by two-photon photoluminescence excitation spectroscopy*
M. Śmiertka, E. Cybula, K. Zalewska, K. Watanabe, T. Taniguchi, M. Dyksik, A. Surrente, M. Baranowski, P. Płochocka

MoPA7 *Electrical Control of Interlayer Physics in Type-II TMD Heterostructures*
K. Sadecka, M. Bieniek, J. Pawłowski, A. Wójs, P. Hawrylak

MoPA8 *Searching for moiré-induced quantum spin liquid - the DMRG and ED study of twisted TMD hetero-bilayers*
W.K. Pasek, J. Jastrzębski, M. Kupczyński, P. Potasz

MoPA9 *Exploring neutral and charged exciton optical properties in a $MoTe_2/SiO_2/Si$-based metal-oxide-semiconductor device*
E. Zięba-Ostój, E. Rogowicz, A. Paralikis, C. Piccinini, B. Munkhbat, M. Syperek

MoPA10 *Optimization of Contacts for van der Waals heterostructures by AFM ironing*
A. Zielińska, J. Eroms, D. Weiss, M. Ciorga

MoPA11 *Computational prediction of structure and electronic properties of monolayer and few-layer 2D polyimide covalent organic frameworks*
M. Wlazło, A. Nagai

MoPA12 *Tunable valley splitting in 2D MPX_3 crystals.*
M. Rybak, M. Birowska

MoPA13 *Optical markers of magnetic phase transition in layered CrSBr*
M. Rybak, M. Birowska

MoPA14 *Interplay between stacking and magnetic configurations in MPS_3 bilayers*
A.M. Leon, B. Guedes, T. Heine, T. Brumme

MoPA16 *Exploring structural, electronic, and magnetic properties of 2D Cr, Fe, and Zr monoborides*
I.M. Arias Camacho, N. Gonzalez-Szwacki

MoPA17 *Magnetic skyrmions of Ti2C MXenes doped with Cr, Mn, and Fe*
T. Kulka, J. Majewski

MoPA18 *The effect of temperature and excitation energy on Raman scattering in bulk HfS_2*
I. Antoniazzi, N. Zawadzka, M. Grzeszczyk, T. Woźniak, J. Ibáñez, Z. Muhammad, W. Zhao, M.R. Molas, A. Babiński

MoPA19 *Growth and characterization of metallic and oxidized forms of bismuthene*
K. Toczek, M. Rogala, P. Krukowski, M. Piskorski, M. Le Ster, I. Lutsyk, W. Kozłowski, P. Dąbrowski, R. Dunal, A. Nadolska, P. Przybysz, W. Ryś, K. Szałowski, D.A. Kowalczyk, P.J. Kowalczyk

MoPA20 *Transport signatures of Van Hove singularities in mesoscopic twisted bilayer graphene*
A. Sanjuan Ciepielewski, J. Tworzydło, T. Hyart, A. Lau

MoPA22 *MBE grown heterostructures of ZnSe, CdSe, $MoSe_2$, and hBN*
B. Tronowicz, J. Kucharek, R. Bożek, T. Taniguchi, K. Watanabe, W. Pacuski

MoPA23 *Structural, Optical and Electrical Properites of Quaternary Hafnium-Aluminium Zinc Oxide Films Grown by Atomic Layer Deposition for Transparent Conductive Oxide Applications*
M. Krajewski, M. Tokarczyk, P. Wróbel, A. Drabińska, M. Kamińska

MoPA24 *ALD Grown ZnMgO:Al on Si for Photovoltaic Applications: Effect of High Mg Alloying and Al Doping*
R. Schifano, J. Kurek, S. Gierałtowska, L. Wachnicki, U. Rehman, D. Budiakivska, S. Chusnutdinow, K. Kopalko, R. Minikayew, B. Witkowski, M. Godlewski, M. Pawłowski, C. Jastrzebski

MoPA25 *Construction and studies of a cathode for photoelectrocatalytic hydrogen generation by water splitting*
A. Bohdan, K. Korona, M. Krajewski, J. Kucharek, W. Pacuski, M. Tokarczyk, P. Podsadni, A. Czewriński, K. Zarębska, M. Skompska, M. Kamińska

MoPA26 *Degradation studies of $MAPbI_3$ perovskite using cathodoluminescence and microscopy techniques*
S. Piotrowska, A. Reszka, A. Wincukiewicz, M. Tokarczyk, B.J. Kowalski, M. Kamińska

MoPA27 *Polymer solar cells thermal annealing of active layers – impact of annealing temperature on efficiency and ageing rate*
W. Mech, M. Kamińska, K.P. Korona

MoPA28 *Towards Electrostatically Gated Perovskite Thin Films*
A. Szoła, W. Kolesiński, M. Kędziora, M. Goryca

MoPA29 The structure and properties of bilayer borophene
S. Rakshit, N. Gonzalez – Szwacki

MoPA30 *Towards Strain Engineering of High Quality 2D Perovskite Flakes*
K. Zalewska, K. Posmyk, M. Śmiertka, M. Mączka,K. Watanabe, T. Taniguchi, M. Dyksik, M. Baranowski,P. Płochocka, A. Surrente

MONDAY POSTER SESSION B

Topological insulators, magnetic structures & termoelectrics

21:00 - 22:30

MoPB1 *Surface and Structural Analysis of (110)-oriented $Pb_{1-x}Sn_xTe$ Topological Crystalline Insulator*
S. Dad, P. Dziawa, M. Wojcik, S. Kret, J.Z. Domagala, E. Łusakowska
P. Wojnar, J. Sadowski

MoPB2 *Ferromagnetic topological crystalline insulator $Sn_{1-x}Mn_xTe$ in an inhomogeneous magnetic field*
A. Kazakov, V.V. Volobuev, M. Chojnacki, T. Wojciechowski,
T. Wojtowicz

MoPB3 *Signatures of Weyl Fermions in Magnetotransport of Topological Semimetal α-Sn*
J. Polaczyński, A. Kazakov, W. Zaleszczyk, B. Turowski, C-W. Cho, B.A. Piot, R. Rudniewski, T. Wojciechowski, T. Wojtowicz, V.V. Volobuev

MoPB4 *Magnetic Circular Dichroism from Exchange Splitting in Intrinsic Magnetic Topological Insulator $MnBi_2Te_4$*
S.-K. Bac, F. Le Mardelé, J. Wang, L. Riney, K. Yoshimura, I. Mohelsky, M. Ozerov, M. Zhukovskyi, T. Orlova, M. Orlita, X. Liu, B.A. Assaf

MoPB5 *Non-trivial topological phases in transition metal rich half-Heusler Oxides*
B.R. Dhori, R.M. Sattigeri, P.K. Jha

MoPB6 *Topological phase transition in SnTe topological crystalline insulator thin films*
S. Samadi, R. Rechcinski, R. Buczko

MoPB7 *Scanning Gate Microscopy Probing of Electron-Hole Interference in a Normal-Superconductor Junction*
S. Maji, K. Sowa, M. Nowak

MoPB8 *Non-local Transport Signatures of Topological Superconductivity in Planar Josephson Junctions*
D. Kuiri, M. P. Nowak

MoPB9 *Quantum Anomalous Hall effect and axion insulator phase in HgTe material class*
C. Autieri

MoPB10 *Geometry of the (001) surface and electron dispersion relations of topological IV-VI semiconductors*
A. Łusakowski, P. Bogusławski, T. Story

MoPB11 *Magnetic and electrical properties of $CoRE_2W_2O_{10}$ ceramic materials*
B. Sawicki, E. Tomaszewicz, T. Groń, M. Oboz, I. Gruszka, A. Guzik, P. Urbanowicz

MoPB12 *Magnetic properties of semiconducting $ZnCr_2Se_4$:Re single crystals*
I. Jendrzejewska, T. Groń, B. Sawicki, J. Kusz, J. Goraus, Z. Stokłosa

MoPB13 *Magnetic and electrical properties of $CuCr_2Se_4$ nanoparticles*
E. Malicka, T. Groń, A. Gudwański, B. Sawicki, M. Oboz, M. Karolus

MoPB14 *Magnetic and electric properties of Nd^{3+} and Mn^{2+}-co-doped calcium molybdato-tungstate single crystals*
T. Groń, E. Tomaszewicz, B. Sawicki, M. Oboz, J. Kusz, M. Berkowski

MoPB15 *High-Quality MBE-grown Aluminum Layers for Experimental Realization of Majorana Bound States*
A. Elbaroudy, B. Khromets, E. Bergeron, T. Blaikie, Y. Shi, M.C. Tam, S. Sadeghi, F. Sfigakis, J. Baugh, Z.R. Wasilewski

MoPB16 *Majorana-Magnon Interactions in Topological Shiba Chains*
P. Shen, V. Perrin, P. Simon, M. Trif

MoPB17 *Temperature Dependence of Spin Pumping in $Y_3Fe_5O_{12}$/Pt, $Ni_{81}Fe_{19}$/Pt and SnTe/$Ni_{81}Fe_{19}$ Thin Films*
A. Moosarikandy, V.S. Bhat

MoPB18 *Size and curvature modulation of the magnetic properties of magnetite nanoshells*
B.C. Camargo, B. Semenenko, M. Gorke, M. Barasinski, G. Garnweitner, J. Szczytko

MoPB19 *Towards Spintronics of Antiferromagnetic Semiconductors - Characterization of MnSe on GaAs*
C.J. Krasucki, J.Z. Domagala, M. Gryglas-Borysiewicz, W. Pacuski, M.J. Grzybowski

MoPB20 *Raman spectroscopy as an indicator of antiferromagnetic to paramagnetic phase transition in transition metal thiophosphates*
M. Peter, J. Kopaczek, M. Rybak, Z. Sofer, R. Kudrawiec

MoPB21 *Resonant Raman scattering of few-layers $CrBr_3$*
Ł. Kipczak, A. Karmakar, M. Grzeszczyk, J. Pawłowski, A. Babiński, M. Koperski, M.R. Molas

MoPB22 *Nagaoka ferromagnetism in phosphorene quantum dots*
T. Thakur, B. Szafran

MoPB23 *Magneto-phonon interaction in layered $Cr_2Ge_2Te_6$ ferromagnet*
G. Krasucki, K. Olkowska-Pucko, M.I. Sturza, H. Kohlmann, A. Babiński, M.R. Molas

MoPB24 *Investigating the Proximity Effect in h-BN/ 2D Magnet Heterostructures*
K. Ludwiczak, J. Binder, A.K. Dąbrowska, P. Tatarczak, J. Siticka, J. Jasiński, R. Stępniewski, A. Wysmołek

MoPB25 *Thermoelectric properties of $Pb_{1-x}Sn_xTe$ crystals doped with vanadium deep donors*
T. Andrearczyk, A. Królicka, J. Korczak, M. Szot, R. Minikayev, P. Dziawa, E. Łusakowska, A. Szczerbakow, K. Dybko, T. Story

MoPB26 *Effect of Ni and Mn dopant on thermoelectric power generation performance of ZnO nanostructures synthesized via hydrothermal method*
U. ur Rehman, K. Mahmood, A. Ashfaq, M. F. Iqbal, K. ul Sahar, A. A. Khan, E. Hussain

MoPB27 *Outstanding Thermoelectric Properties (ZT ≈ 5 – 6) of Functionalized 2D Molybdenum Nitrides (MXenes)*
J. Kołodziejczyk, J.A. Majewski

MoPB28 *Photoemission study of the thermoelectric group IV-VI van der Waals crystals (GeS, SnS, and SnSe)*
A.K. Tołłoczko, S.J. Zelewski, M. Błaszczak, N. Olszowska, M. Rosmus, S. Tongay, R. Kudrawiec

MoPB29 *Extension of rapid estimation of the flake thickness by color for a magnetic van der Waals 2D material*
R. Komar, M. Raczyński, T. Kazimierczuk, P. Kossacki

TUESDAY POSTER SESSION A

Wide bandgap materials (h-BN, Ga_2O_3, ZnO, CdMgO, GaN)

14:30 - 16:00

TuPA1 *Epitaxial Boron Nitride Processing and Conductivity*
J. Rogoża, B. Furtak, J. Binder, A.K. Dąbrowska, R. Stępniewski, A. Wysmołek

TuPA2 *Direct MOVPE growth of high-quality h-BN on the wafer-scale: the role of substrate off-cut*
M. Tokarczyk, A.K. Dąbrowska, G. Kowalski, R. Bożek, J. Iwański J. Binder, R. Stępniewski, A. Wysmołek

TuPA3 *Manipulating hBN Bandgap Properties With Aluminum*
J. Iwański, M. Tokarczyk, K.P. Korona, P. Tatarczak, J. Pawłowski, A.K. Dąbrowska, J. Binder, R. Stępniewski, A. Wysmołek

TuPA4 *MBE growth of CdTe on hBN*
A. Szczerba, J. Kucharek, J. Pawłowski, T. Taniguchi, K. Watanabe, W. Pacuski

TuPA5 *Carbon-enriched Epitaxial Boron Nitride Layers as Contact Material for h-BN Devices*
B. Furtak, A. Wysmołek, J. Binder

TuPA6 *Determining Strain Components in a Diamond Waveguide from Asymmetric ODMR Spectra of NV- Center Ensembles*
M.S. Alam, D. Wigger, M. Gawełczyk, P. Machnikowski

TuPA7 *Post-implantation Defect Accumulation in Crystal Lattice of β-Ga_2O_3 Implanted with Yb ion*
M. Sarwar, R. Ratajczak, E. Guziewicz

TuPA8 *The structural properties anisotropy of beta-Ga_2O_3 implanted with Yb*
R. Ratajczak, M. Sarwar, C. Mieszczynski, P. Jozwik, W. Wozniak, U. Kentsch, R. Heller, E. Guziewicz

TuPA9 *Electron Paramagnetic Resonance of Beta-Gallium Oxide Modified by High-Energy Electron Irradiation*
A. Wołoś, J. Sitnicka, R. Grasset, M. Konczykowski

TuPA10 *Effects of Si/N Ion Implantation on Defect formation and Doping of Gallium Oxide*
I.N. Demchenko, Y. Syryanyy, A. Shokri, Y. Melikhov, M. Chernyshova

TuPA11 *PA-MBE Grown CdMgO:Eu Ternary Alloy on m- and c-Oriented Al_2O_3 Substrates*
J.K. Jadoon, A. Adhikari, A. Lysak, A. Wierzbicka, W. Lisowski M. Stachowicz, A. Kozanecki, E. Przeździecka

TuPA12 *MBE growth of wide band gap wurtzite MgZnO superlattices doped with Eu for effective visible emission*
M. Stachowicz, J.A. Mathew, J.M. Sajkowski, R. Jakiela, Y. Zhydachevskyy, S. Magalhaes, E. Alves, A. Kozanecki

TuPA13 *Initial optimization of the growth conditions of GaAs homo-epitaxial layers after cleaning and restarting the MBE reactor.*
D. Jarosz, M. Stachowicz, P. Krzemiński, M. Ruszala, A. Juś, P. Śliż D. Płoch, M. Marchewka

TuPA14 *Geometrical selection during MBE growth of nanowires on polycrystalline substrates*
K. Olszewski, M. Sobańska, A. Wierzbicka, Z.R. Żytkiewicz

TuPA15 *Insights into Raman spectra and doping concentration profiles of Eu-doped {ZnCdO/ZnO} superlattices*
I. Perlikowski, E. Zielony, A. Lysak, E. Przeździecka

TuPA16 *Electrical and thermal transport properties of CdO and CdMgO alloys grown using plasma-assisted MBE technique*
A. Adhikari, Z. Adamus, M. Pawlak, A. Lysak, E. Przeździecka

TuPA17 *Characterization of MBE grown {Zn(Mg)O/ZnCdO}m superlattices doped in-situ with Eu*
A. Lysak, E. Przeździecka, A. Wierzbicka, A. Reszka, M. Stachowicz, R. Jakiela, P. Dłużewski, A. Adhikari, A. Kozanecki

TuPA18 *n-ZnO/ZnCdO/p-Si and n-ZnCdO/ZnO/p-Si diodes: studies on the influence of the junction interlayer on electrical properties and structural defects*
R. Szymon, E. Zielony, M.A. Pietrzyk, A. Lysak

TuPA19 *An insight into the optical properties of GaN nanowires with Al_2O_3 and HfO_2 shells*
R. Szymon, E. Zielony, M. Sobańska, A. Wierzbicka,A. Reszka, S. Gieraltowska, Z.R. Żytkiewicz

TuPA20 *Effect of strain and surface proximity on the acceptor grouping in ZnO:N*
O. Volnianska, S. Mishra, E. Guziewicz

TuPA21 *Tailoring of the optical and electrical characteristics of ZnO:Ga heterostructures by a metallic buffer layer*
A. Hassan, A.A. Khan, M. Azam, U. Farooq, M. Zubair, Y. Cao

TuPA22 *Ferromagnetic Resonance Studies of (Ga,Mn)N*
Y.K. Edathumkandy, K. Gas, D. Sztenkiel, K. Das, D. Hommel, H. Przybylińska, M. Sawicki

TuPA23 *Impact of current flow direction on the distribution of carriers in multiple, color-coded InGaN quantum wells*
M. Chlipała, H. Turski, K. Nowakowski-Szudlarek, A. Feduniewicz-Żmuda, C. Skierbiszewski

TuPA24 *Extreme InGaN growth conditions by plasma assisted molecular beam epitaxy*
M. Siekacz, M. Żak, K. Gołyga, M. Kryśko, A. Feduniewicz-Żmuda, H. Turski, C. Skierbiszewski, G. Muziol

TuPA25 *Doping inhomogeneity at the nanoscale in GaN:Si studied by electrochemical etching*
A. Feduniewicz-Żmuda, M. Siekacz, N. Fiuczek, O. Gołyga M. Sawicka, K. Sobczak, C. Skierbiszewski

TuPA26 *Visible luminescence of BGaN based structures: towards defects related LEDs*
M. Guziewicz, E.B. Możdżyńska, P. Ciepielewski, E. Dumiszewska, B. Stańczyk, M. Wzorek, K. Kościewicz

TuPA27 *Modification of luminescence of the nitride nanowires by chemical treatment of their surface*
B.J. Kowalski, A. Reszka, M. Klepka, A. Wolska, M. Sobańska, Z.R. Żytkiewicz

TuPA28 *Strain relation in GaN nanowires with HfO_2 and Al_2O_3 shells examined by X-ray diffraction and Raman spectroscopy techniques*
A. Wierzbicka, R. Szymon, E. Zielony, A. Reszka, M. Sobańska, S. Gieraltowska, P. Sybilski, Z.R. Żytkiewicz

TuPA29 *Investigation of strain relation and lattice dynamics in {CdO/MgO} superlattices grown by plasma-assisted molecular beam epitaxy*
A. Wierzbicka, E. Przeździecka, I. Perlikowski, E. Zielony

TuPA30 *Band parameters of group IV semiconductors in wurtzite structure*
J. Ziembicki, P. Scharoch, M.P. Polak, M. Wiśniewski, R. Kudrawiec

TUESDAY POSTER SESSION B

Photonic structures and photodetectors

21:00 - 22:30

TuPB1 *Merons in Reciprocal Space as a Result of Photonic Spin-Orbit Interaction in Birefringent Microcavity*
M. Popławska, P. Oliwa, M. Król, W. Bardyszewski, B. Piętka, J. Szczytko

TuPB2 *Numerical Approach to Determine the Fourier Plane of Light Propagation Through Cartesian-Oval Shaped Microlenses*
Z. Werner, J. Lewandowski, M. Popławska, M. Furman, P. Oliwa, A. Bogucki, Ł. Zinkiewicz, B. Seredyński, W. Pacuski, J. Szczytko, B. Piętka

TuPB3 *Localization of light on defects in microcavities with built-in uniform lying helix*
J. Czapiński, M. Muszyński, E. Otón, P. Oliwa, R. Mazur, P. Morawiak, W. Piecek, P. Kula, B. Piętka, J. Szczytko

TuPB4 *Self-Organizing Photonic Potential with Tunable Band Structures Coupled by Spin-Orbit Interaction in Birefringent Optical Cavity*
M. Muszyński, P. Oliwa, E. Oton, R. Mazur, P. Morawiak, W. Piecek, P. Kula, B. Piętka, J. Szczytko

TuPB5 *Flow of an exciton-polariton condensate in optical microcavities with the natural structural disorder*
S. Świerczewski, R. Mirek, M. Król, M. Furman, M. Matuszewski, A. Opala, J. Szczytko, B. Piętka

TuPB6 *Experimental Evaluation of the Indistinguishability of Single Photons at 1.55 μm Generated by InAs(P)/InP Quantum Dots*
D.A. Vajner, M. Wasiluk, P. Holewa, E. Zięba-Ostój, B. Gaál, A. Sakanas, B. Krajnik, M. Xiong, K. Yvind, N. Gregersen, M. Syperek, E. Semenova, A. Musiał, T. Heindel

TuPB7 *Magneto-Optical Properties of Single Symmetric InAs/InP Quantum Dots Emitting in the Telecom C-band*
M. Wasiluk, A. Musiał, M. Burakowski, J.P. Reithmaier, M. Benyoucef, W. Rudno-Rudziński

TuPB8 *Optimization of on-chip photonic structures for a hybrid InP/Si platform via deep learning approach*
P. Mrowiński, G. Sęk, M. Syperek

TuPB9 *Optical Characteristics of Monolithic High-Contrast Gratings for Quantum-Dot Vertical-Cavity Surface-Emitting Lasers at 940 nm.*
B. Kamiński, J. Boniecki, M. Janczak, N. Heermeir, F. Laudani, S. Rodt, S. Reitzenstein, M. Gębski, T. Czyszanowski, G. Sęk, A. Musiał

TuPB10 *Methods for Determining High Finesse in Open Cavity Systems*
P. Kulboka, N. Dalla, T. Kazimierczuk, P. Kossacki, T. Jakubczyk

TuPB11 *Reflectivity spectra of GaAs/AlAs Distributed Bragg Reflector in the MIR Calculated by the Transfer Matrix Method*
H. Janowska, A. Zielińska, A. Musiał, G. Sęk

TuPB12 *Optimization of the polarization state of an ensemble of quantum dots for chiral emission*
J. Rosiński, M. Gawełczyk, K. Tarnowski, D. Wigger, P. Karwat, P. Machnikowski

TuPB13 *Controlled coherent coupling in a quantum dot molecule measured with nonlinear spectroscopy*
D.W. Wigger, J.S. Schall, M.D. Deconinck, N. Bart, P.M. Mrowinski, M.K. Krzykowski, K.G. Gawarecki, M.H. von Helversen, R.S. Schmidt, L. Bremer, F. Bopp, D.R. Reuter, A.W. Wieck, S.R. Rodt, J.R. Renard, G.N. Nogues, A.L. Ludwig, P.M. Machnikowski, J.F. Finley, S.R. Reitzenstein, J.K. Kasprzak

TuPB14 *Diffusion of quantum well excitons measured with nonlinear spectroscopy*
K.P. Połczyńska, M.R. Raczynski, Z.S. Snioch, G.N. Nogues, W.L. Langbein, W.P. Pacuski, P.K. Kossacki, J.K. Kasprzak

TuPB15 *Coherent imaging and dynamics of exciton complexes in $MoSe_2$ monolayers epitaxially grown on a hexagonal boron nitride*
K.E. Połczyńska, S.L. Denmat, T. Taniguchi, K. Watanabe, M. Potemski, P. Kossacki, W. Pacuski, J. Kasprzak

TuPB16 *Probing the Local Temperature Distribution in Electrically Pumped Broad-Area VCSELs*
A.N. Piasecka, M. Gębski, M. Wasiak, J.A. Lott, T. Czyszanowski, M. Pieczarka

TuPB17 *Modeling InAs/GaSb Type-II Superlattices for Mid-Wavelength Infrared Photodetectors with the nextnano++ Software*
H.S. Mączko

TuPB18 *Applications of InAs/$InAs_{0.625}Sb_{0.375}$ Superlattice in Far-infrared Detection*
G. Hussain, G. Cuono, C. Autieri, T. Dietl

TuPB19 *Magnetic properties of TRS broken ferrovalley semiconductors*
G. Hussain, G. Cuono, C. Autieri

TuPB20 *Bulk And Contact Low Frequency Noise Investigated With Transmission-Line-Model: InAs case*
Ł. Ciura, J. Wróbel, P. Martyniuk

TuPB21 *Optical characterization and pump-probe measurements of InAs/GaSb and InAs/InAsSb type-II superlattices*
M. Rygała, A. Bader, T. Smołka, F. Hartmann, G. Sęk, S. Höfling, M. Motyka

TuPB22 *Modelling of Band Structure and Optical Properties of InAsP/InP Quantum Dots in Nanowires*
J. Boniecki, G. Bucci, V. Zannier, L. Sorba, A. Musiał, G. Sęk

TuPB23 *Temperature Dependence of Refractive Indices of $In_{0.53}Ga_{0.47}As$ and InP in the Mid-Infrared Spectra Range Determined by Fourier Transform Spectroscopy*
M. Mikulicz, M. Rygała, T. Smołka, M. Badura, W. Kijaszek, A. Łozińska, D. Radziewicz, B. Ściana, M. Motyka

TuPB24 *Carrier dynamics of type-II quantum wells emitting in mid-infrared*
T. Smołka, M. Rygała, K. Ryczko, A. Bader, F. Hartmann, B. Petrovic, S. Höffling, M. Motyka

TuPB25 *Influence of Mg^{2+} codoping on excitation relaxation and emission properties of $(Lu,Gd)_3(Ga,Al)_5O_{12}$:Ce,Mg scintillators*
A. Solovjovas, S. Nargelas, M. Kučera, G. Tamulaitis

TuPB26 *Characterization of the Microwave Strip Antenna in the Experiment of Optically Detected Magnetic Resonance*
Z. Śnioch, A. Łopion, A. Bogucki, K.E. Połczyńska, W. Pacuski, T. Kazimierczuk, A. Golnik, P. Kossacki

TuPB27 *Hybrid Acousto-Optic Driving of Rabi Oscillations of Electron Spin in a Quantum Dot*
M. Kuniej, M. Gawełczyk, P. Machnikowski

TuPB28 *Noise effects on the resonance fluorescence from acoustically modulated quantum dots*
R.A. Bogaczewicz, P. Machnikowski

TuPB29 *Energy gap determination from photoacoustic spectroscopy measurements*
K. Misztal, J. Kopaczek, R. Kudrawiec

TuPB30 *Magnetic field and temperature dependence of the Mn^{2+} spin relaxation rate in a (Cd, Mn)Te/(Cd, Mg)Te quantum well*
A. Bogucki, Z. Śnioch, A. Łopion, K.E. Połczyńska, W. Pacuski, T. Kazimierczuk, A. Golnik, P. Kossacki

THURSDAY POSTER SESSION A

Theoretical platform/ CdTe and PbTe-based structures/Si-based NWs

14:30 - 16:00

ThPA1 *Quantum anomalous Hall insulator in ionic Rashba lattice of correlated electrons*
M.M. Wysokiński, W. Brzezicki

ThPA2 *Exciton Diffusion in an Ensemble of Self-Assembled Semiconductor Quantum Dots*
K. Kawa, P. Machnikowski

ThPA3 *Introducing the step Monte Carlo method for simulating dynamic properties*
D. Sztenkiel

ThPA4 *Novel Te-bearing half-Heusler phases and their potential thermoelectric performance*
K. Bilińska, M.J. Winiarski

ThPA5 *Optimizing the cap thickness in fabrication of quantum dot photonic structures by focused ion beam*
M.J. Jaworski, A.C. Chudzyńska, P.M. Mrowiński, G.S. Sęk

ThPA6 *Facile Synthesis of Semiconductor Nanostructures with Variable Plasmonic Properties Using Pulsed Laser Ablation Technique*
Yu.V. Ryabchikov

ThPA7 *Optical Properties of Silicon Nanowires-Based Composites*
Yu.V. Ryabchikov

ThPA8 *Non-equilibrium transport theory for dopant arrays in silicon*
M. Gawełczyk, G.W. Bryant, M. Zieliński

ThPA10 *Elimination of Early Breakdowns in Fully-Depleted Detectors of Ionizing Radiation*
K. Kucharski, P. Janus, A. Panas, G. Głuszko, D. Tomaszewski, K. Krzyżak

ThPA11 *Intervalley hybridization and optical properties of GeSn quantum dots*
K. Gawarecki, P. Scharoch, J. Ziembicki, N. Janik, R. Kudrawiec

ThPA12 *Evaluation of Reaction Parameters in Polymeric Carbon Nitride Hybridized ZnO Nanocomposite for Improving Photocatalytic Activity using Thermal Synthesis*
N.N. Som, A. Opalinska, W. Lojkowski

ThPA13 *Pressure-driven tuning of bandgap in methylammonium lead iodide*
A. Pieniążek, F. Dybała, M. Polak, Ł. Przypis, A.P. Herman, J. Kopaczek, R. Kudrawiec

ThPA14 *Nanoprobe-based approach for electrical characterization of semiconductors nanostructures*
S. Tiagulskyi, R. Yatskiv, O. Černohorský, N. Bašinová, Š. Kučerová, J. Vaniš, A. Reszka, J. Grym

ThPA15 *Young's Modulus and Microhardness of (Pb,Cd)Te Solid Solution Grown by SSVG and MBE Method*
S. Adamiak, W. Wołkanowicz, A. Juś, E. Łusakowska, R. Minikayev, D. Płoch, J. Korczak, A. Szczerbakow, W. Szuszkiewicz

ThPA16 *Characterization of (Cd,Mn)Te and (Cd,Mn)(Te,Se) material and contact properties*
D.M. Kochanowska, A. Wardak, K. Gościński, P. Sybilski, A. Reszka, A. Sulich, A. Mycielski

ThPA17 *Comparison of (Cd,Mn)Te and (Cd,Mn)(Te,Se) Compounds for Room Temperature X and Gamma Ray Detection: Optical Properties and Detector Response*
A. Wardak, D.M. Kochanowska, M. Szot, M. Kochański,M. Dopierała, A. Mycielski

ThPA18 *Mn^{2+}-V_{Zn}- charge transfer complexes in $Zn_{1-x}Mn_xTe$*
V.K. Le, A. Avdonin, A. Mycielski

ThPA19 *Dynamics of direct and indirect excitons in (Cd,Mn)Te/(CdTe) double QW structure controlled by magnetic field*
V.Yu. Ivanov, S.M. Ryabchenko, V.I. Sugakov, G.V. Vertsimakha, G. Karczewski

ThPA20 *Properties of Infrared Detectors Made of $Pb_{1-x}Mn_xTe$/CdTe Multilayer Composite*
S. Chusnutdinow, A. Kazakov, M. Szot, S. Schreyeck, R. Jakieła, K. Brunner, G. Karczewski

ThPA21 *Terahertz Spectroscopy of Hyperbolic Metamaterial Based on CdTe/$Cd_{1-x}Mg_xTe$ Multiple Quantum Wells*
J. Łusakowski, A. Frączak, E. Imos, A. Siemaszko, M. Zaremba, K. Karpierz, Z. Adamus, T. Słupiński, T. Wojtowicz

ThPA22 *Near-band-gap Optical Properties of Modulation-doped CdTe/$Cd_{1-x}Mg_xTe$ Multiple Quantum Well Structures*
J. Łusakowski, M. Grymuza, W. Solarska, K. Karpierz, Z. Adamus, T. Słupiński, T. Wojtowicz

ThPA23 *Terahertz Emission from CdTe-based Multiple Quantum Wells*
D. Yavorskiy, R. Zdunek, K. Karpierz, Z. Adamus, T. Słupiński, T. Wojtowicz, J. Łusakowski

ThPA24 *Simulation of Optical Properties of Terahertz Hyperbolic Metamaterials Based on Multiple Quantum Wells*
J. Łusakowski, T. Kazimierczuk

ThPA25 *Diffusional dependent structures on the crystal surface*
M. Chabowska, M. Załuska-Kotur

ThPA26 *Fitting parameters of atomic orbitals to reproduce optical properties of III-V systems*
K. Kwas, K. Gawarecki

ThPA27 *Excited electronic states of Sr_2: ab initio predictions and experimental observation of the $2^1\Sigma_u^+$ state*
J. Szczepkowski, M. Gronowski, A. Grochola, W. Jastrzebski, M. Tomza, P. Kowalczyk

ThPA28 *Excellent excitonic properties of novel hexagonal MA_2Z_4 monolayers*
T. Woźniak, P.E. Faria Junior, U. Umm-e-hani, M.S. Ramzan, A.B. Kuc

THURSDAY POSTER SESSION B
ON-LINE ONLY
21:00 - 22:30

ThPB1 *Electrical Properties of Anisotype ZnO:Al/ZnSe/p-CdTe Heterostructures*
E.V. Maistruk, I.G. Orletskyi, M.I. Ilashchuk, I.P. Koziarskyi, D.P. Koziarskyi

ThPB2 *Current Transfer Mechanisms in $CuMoO_4$/n-Si Heterostructure*
I.P. Koziarskyi, E.V. Maistruk, D.P. Koziarskyi

ThPB3 *Kinetics of Fe Island Films degradation in Air*
K.A. Korotkov, A.M. Kasumov, A.I. Dmitriev, V.M. Karavaeva, A.I. Ievtushenko

ThPB4 *Isolation of responsive elements of coordinate p-i-n photodiodes by p^+-layer*
M.S. Kukurudziak

ThPB5 *Damping of open circuit photovoltage in a Si homojunction*
B.A. Orłowski, K. Gwozdz, K. Goscinski, M. Chabowska, E. Guziewicz, B.J. Kowalski

Bulk GaN growth

M. Bockowski*

Institute of High Pressure Physics, Polish Academy of Sciences, Warsaw, Poland
*email: bocian@unipress.waw.pl

Application of gallium nitride (GaN) substrates in electronic and optoelectronic industries is constantly increasing. In order to fabricate wafers, GaN crystals of the highest structural quality and desired electrical (and sometimes optical) properties must be grown. Today, there are three main GaN crystallization methods: i/ halide vapor phase epitaxy (HVPE) with its derivatives: halide-free VPE and oxide VPE [1-3]; ii/ sodium-flux [4]; and iii/ ammonothermal. The last approach can be basic or acidic depending on what mineralizer is used to increase the solubility of GaN in the feedstock zone [5,6].
In this paper we will focus on HVPE and basic ammonothermal growth of GaN. Wherein, the HVPE as the best method for crystallization of drift layers necessary for construction of high-power vertical electronic devices (FET transistors, Schottky diodes) will also be discussed.
Recent results obtained in the basic ammonothermal growth will be shown. Structural, electrical, and optical properties of ammonothermal highly conductive (n-type) and semi-insulating (SI) GaN (Am-GaN) will be analyzed. Based on the presented results, main limiting factors of bulk Am-GaN crystallization and new ways for improving this process will be discussed. It will be shown: i/ how to eliminate lateral growth during crystallization in vertical directions; ii/ how to prepare the surface of a native seed in order to minimize residual stress in the growing crystal; iii/ how to obtain a uniform and constant supersaturation in the growth zone where more than fifty 2.2-inch crystals are placed; iv/ what kind of growth mode is required to obtain a uniform concentration of wanted and unwanted dopants in bulk Am-GaN.
In the case of HVPE-GaN growth, the advantages of using native seeds will be demonstrated. All barriers for growing truly bulk HVPE-GaN will be analyzed. They will be compared to the limiting factors existing in Am-GaN growth. Morphology and its influence on uniform doping of bulk HVPE-GaN crystals will be discussed in detail. The main dopants used for growing n-type and SI crystals will be shown.
In conclusion, it will be explained what else we need to know about the crystallization of truly bulk GaN by the two methods described above. Some aspects of wafering of GaN crystals into substrates as well as seeds will also be summarized.

References

[1] M. Bockowski, M. Iwinska, M. Amilusik, M. Fijalkowski, B. Lucznik, T. Sochacki, Semicond. Sci. Technol. **31** 093002 (2016)
[2] D. Nakamura and T. Kimura, Appl. Phys. Express **11**, 065502 (2018)
[3] J. Takino, T. Sumi, Y. Okayama, M. Nobuoka, A. Kitamoto, M. Imanishi, M. Yoshimura, and Y. Mori, Jpn. J. Appl. Phys. **58**, SC1043 (2019)
[4] M. Imanishi, K. Murakami, T. Yamada, K. Kakinouchi, K. Nakamura, T. Kitamura, K. Okumura, M. Yoshimura, and Y. Mori, Appl. Phys. Express **12**, 045508 (2019)
[5] R. Kucharski, T. Sochacki, B. Lucznik, M. Bockowski, Growth of bulk GaN crystals. J. Appl. Phys. **128**, 050902 (2020)
[6] Y. Mikawa, T. Ishinabe, Y. Kagamitani, T. Mochizuki, H. Ikeda, K. Iso, T. Takahashi, K. Kubota, Y. Enatsu, Y. Tsukada, S, Izumisawa, in Proceedings of the SPIE OPTO 2020, Volume **11280** (2020)

Computational Design of Materials for Spintronics

Jagoda Sławińska

Zernike Institute for Advanced Materials, University of Groningen,
Nijenborgh 4, 9747AG Groningen, The Netherlands

Exploring materials that exhibit spin-orbit-related phenomena holds great promise for advancing alternative computing devices beyond the traditional von Neumann paradigm. By leveraging the manipulation of spins through control of material symmetries, we can pave the way for next-generation electronic devices that minimize power consumption.

In this talk, I will provide a comprehensive overview of the computational design methods employed in the study of electronic materials. Delving deeper, I will discuss the remarkable properties of several recently (re-)discovered crystals that unveil intriguing spin-orbit-related phenomena, along with various techniques for controlling spins. My focus will be on the utilization of low-symmetry crystals, which facilitate unconventional charge-to-spin conversion configurations, enabling the generation of highly efficient spin-orbit torques.

Furthermore, I will discuss the fascinating realm of chiral crystals, which exhibit collinear charge-to-spin conversion akin to the chirality-induced spin selectivity observed in molecules. Noteworthy examples include trigonal Te, Se, and TaSi2, which demonstrate high efficiency in charge-to-spin conversion and possess a remarkable attribute called the persistent spin texture, potentially leading to significantly prolonged spin lifetimes. Although the precise role of the persistent spin texture in protecting spin transport necessitates further elucidation, chiral materials with substantial spin-orbit coupling show immense potential in resolving one of the pivotal trade-offs in spintronics.

To conclude, I will explore the exciting prospects of high-throughput computational design in materials science, highlighting its potential in accelerating the discovery and development of novel materials with desirable properties.

[1] S. Varotto, L. Nessi, S. Cecchi, J. Sławińska, et al., *Nature Electronics* **4**, 740–747 (2021)
[2] H. Wang, P. Gopal, S. Picozzi, S. Curtarolo, M. Buongiorno Nardelli, J. Sławińska, *npj Computational Materials* **6** (7), 1-7 (2020)
[3] A. Roy, M. Guimarães, J. Sławińska, *Physical Review Materials* **6**, 045004 (2022)
[4] A. Roy, F. Cerasoli, A. Jayaraj, K. Tenzin, M. Buongiorno Nardelli, J. Sławińska, *npj Computational Materials* **8** (1), 243 (2022)
[5] H. Jafari, A. Roy, J. Sławińska, *Physical Review Materials* **6**, L091404 (2022)
[6] K. Tenzin, A. Roy, H. Jafari, B. Banas, F. T. Cerasoli, A. Jayaraj, M. Buongiorno Nardelli, J. Sławińska, *Physical Review B* **107**, 165140 (2023)
[7] K. Tenzin, A. Roy, F. Cerasoli, A. Jayaraj, M. Buongiorno Nardelli, J. Sławińska, *arXiv:2304.05287* (2023)

Experimental Quantum Control of Spin Defects in Solids

Tim Schröder

Humboldt-Universität zu Berlin / Ferdinand-Braun-Institut Berlin

Optically active spin defects in diamond have proven to be a promising resource for the implementation of quantum communication and have recently enabled the first demonstration of a 3-node network. In this presentation I bridge ongoing and anticipated work in the control, analysis and engineering of single spin defects for applications in quantum communication. I introduce a recent proposal in which we demonstrate theoretically that the realization of quantum communication over 1000 km becomes achievable with relatively few solid-state spin qubits that are efficiently coupled to an optical nanostructure. These coupled spin defects and their coherent control, however, have complex requirements that go beyond current state-of-the-art.

In our work, we focus on understanding the spin qubits‘ nano- and microscopic noise environment, on coupling to nanostructures, and on system control schemes. To illustrate these efforts, I outline how to coherently control diamond spin qubits, how to enhance qubit-to-photon coupling with nanostructures, and how to mitigate noise in such nanostructures. In particular, I discuss how to achieve single ‘central’ spin qubits with long coherence times through decoupling from spin bath noise, and how several of such quantum memories can be controlled simultaneously in a sub- diffraction volume. For enhanced qubit-to-photon coupling I introduce photonic nanostructures and methods for their fabrication, and demonstrate how such qubit-nanostructure devices facilitate flux control of electromagnetic radiation. One important (yet undesired) ‘side-effect’ of nanostructures is spectral diffusion of the spin system’s optical transition frequency induced by time-varying electrostatic field noise. I introduce ways to investigate and mitigate the impact of this noise, and show that certain spin defects are immune to electric field noise to first order. Finally, I look into the near future and lay out how we plan to generate multi-qubit entangled states—an important step towards applying solid-state spin defects for the implementation of long-distance quantum communication and quantum networks.

Optical and Electronic Fourier Surfaces

Nolan Lassaline [1], Raphael Brechbühler [1], Deepankur Thureja [1,2], Sander J. W. Vonk [1,3], Korneel Ridderbeek [1], Martin Spieser [4], Samuel Bisig [4], Boris le Feber [1], Thibault Chervy [2], Puneet A. Murthy [2], Armin Knoll [5], Freddy T. Rabouw [1,3], Daniel Petter [1] and David J. Norris [1]

[1] Optical Materials Engineering Laboratory, ETH Zurich, Zurich, Switzerland
[2] Quantum Photonics Group, ETH Zurich, Zurich, Switzerland
[3] Debye Institute for Nanomaterials Science, Utrecht University, Utrecht, The Netherlands
[4] Heidelberg Instruments Nano/SwissLitho, Zurich, Switzerland
[5] IBM Research – Zurich, Rueschlikon, Switzerland

Gratings and holograms are patterned surfaces that tailor optical signals by diffraction. Despite the long history of such structures, variants with remarkable functionalities continue to be discovered. Further advances could exploit Fourier optics, which specifies the surface pattern that generates a desired diffracted output through its Fourier transform. The required surface profile should contain a precise sum of sinusoidal waves, each with a well-defined amplitude, spatial frequency, and phase, to shape the optical wavefront. However, because fabrication techniques typically yield profiles with at most a few depth levels, complex "wavy" surfaces cannot be obtained, limiting the straightforward mathematical design and implementation of sophisticated diffractive optics. In this presentation, we will discuss a simple yet powerful approach to eliminate this design–fabrication mismatch by demonstrating optical surfaces that contain an arbitrary number of specified sinusoids [1]. Multicomponent linear gratings allow precise manipulation of the dispersion, stopbands, and coupling of electromagnetic signals. More broadly, we analytically design and accurately replicate intricate two-dimensional Moiré patterns, quasicrystals, and holograms, demonstrating a variety of previously impossible diffractive surfaces. Finally, we show that such patterns can be reduced to nanometer length scales, creating wavy Fourier surfaces for 2D electronics [2]. Therefore, this approach provides benefit for optical devices and emerging topics in photonics and 2D optoelectronics.

[1] N. Lassaline, R. Brechbühler, S. J. W. Vonk, K. Ridderbeek, M. Spieser, S. Bisig, B. le Feber, F. T. Rabouw, D. J. Norris, *Nature* **582**, 506 (2020).
[2] N. Lassaline, D. Thureja, T. Chervy, D. Petter, P. A. Murthy, A. W. Knoll, D. J. Norris, *Nano Lett.* **21**, 8175 (2021).

Excitons in moiré heterostructures

Alexander Högele[1]

[1] *Fakultät für Physik, Center for NanoScience (CeNS), Munich Quantum Center and Munich Center for Quantum Science and Technology (MCQST), Ludwig-Maximilians-Universität München, Geschwister-Scholl-Platz 1, 80539 München, Germany*

Van der Waals crystals of two-dimensional semiconducting transition metal dichalcogenides have evolved as an increasingly significant material platform in condensed matter research. With access to a variety of single-crystal monolayers, a wide range of van der Waals heterostructures can be assembled into rationally designed vertical stacks with emergent flat bands of correlated electrons and tailored optical properties of strongly bound excitons. In my talk, I will discuss our recent insight into the roles of layer constituents, atomic registry and twist angle for the formation of excitons with distinct spin-valley degrees of freedom and layer character. In particular, I will highlight the effect of charge carrier doping on moiré excitons in MoSe2-WS2 heterobilayers with canonical moiré superlattices [1] and present contrasting phenomena in MoSe2-WSe2 heterostacks subject to mesoscopic reconstruction [2,3].

[1] B. Polovnikov, J. Scherzer, S. Misra, X. Huang, C. Mohl, Z. Li, J. Göser, J. Förste, I. Bilgin, K. Watanabe, T. Taniguchi, A. S. Baimuratov, and A. Högele, Coulomb-correlated states of moiré excitons and elementary charges on a semiconductor moiré lattice at integer and fractional fillings, *arXiv:2208.04056* (2022).
[2] S. Zhao, Z. Li, A. Rupp, J. Göser, I. A. Vovk, S. Yu. Kruchinin, K. Watanabe, T. Taniguchi, I. Bilgin, A. S. Baimuratov, and A. Högele, Excitons in mesoscopically reconstructed moiré heterostructures, https://doi.org/10.1038/s41565-023-01356-9 *Nature Nanotechnology* (2023).
[3] Z. Li, F. Tabataba-Vakili, S. Zhao, A. Rupp, I. Bilgin, Z. Herdegen, B. März, K. Watanabe, T. Taniguchi, G. Schleder, A. S. Baimuratov, E. Kaxiras, K. Müller-Caspary, and A. Högele, Lattice reconstruction in MoSe2-WSe2 heterobilayers synthesized by chemical vapor deposition, *arXiv:2212.07686* (2022).

Spin-Flip Raman Scattering on Electrons and Holes in Two-Dimensional $(PEA)_2PbI_4$ Perovskites

D. Kudlacik[1], C. Harkort[1], N. E. Kopteva[1], D. R. Yakovlev[1], M. Karzel[1], E. Kirstein[1], O. Hordiichuk[2,3], M. Kovalenko[2,3], and M. Bayer[1]

[1] *Experimentelle Physik 2, Technische Universität Dortmund, Dortmund, Germany*
[2] *Department of Chemistry and Applied Biosciences, ETH Zürich, Zürich, Switzerland*
[3] *Laboratory for Thin Films and Photovoltaics, Empa-Swiss Federal Laboratories for Materials Science and Technology, Dübendorf, Switzerland*

The class of Ruddlesden-Popper type $(PEA)_2PbI_4$ perovskites comprises two-dimensional (2D) structures which are promising materials for photovoltaic and optoelectronic applications as their optical properties are determined by excitons with a large binding energy of about 260 meV. In 2D perovskites, a similar degree of optical spin control can be achieved as in conventional III-V and II-VI semiconductors, whose band structure is inverted compared to lead halide perovskites. We present our recent studies using spin-flip Raman scattering to measure the Zeeman splitting of electrons and holes in a magnetic field up to 10 T (see Fig. 1a)[1]. From the recorded data, the electron and hole Landé factors (g-factors) are evaluated (see Fig. 1b), their anisotropies are measured, and the hole sign is determined. The electron g-factor value changes from +2.11 out-of-plane to +2.50 in-plane, while the hole g-factor ranges between −0.13 and −0.51. Spin-flips of resident electrons and holes have been observed through their interaction with photo-generated excitons, as well as double spin-flip processes in which a resident electron and hole interact with the same exciton. Furthermore, we demonstrate the hyperfine hole-nuclei interaction in 2D perovskites by means of the dynamic nuclear polarization detected in corresponding changes of the hole Zeeman splitting (see Fig. 1c). Due to the small g-factor of the hole, we are able to achieve an Overhauser field value of $B_{N,h} = 0.6$ T.

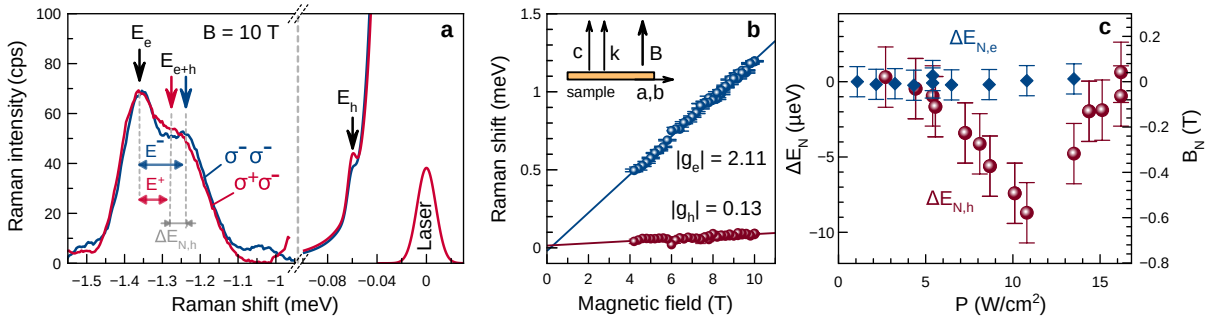

Figure 1: (a) Spin-flip Raman spectrum in the anti-Stokes spectral range in cross polarizations for $B = 10$ T. The hole E_h, electron E_e, and their double spin-flip E_{e+h} lines are highlighted by arrows. (b) Electron and hole Raman shift as function of the magnetic field in out-of-plane geometry ($\mathbf{B} \parallel \mathbf{k}$). (c) Power density dependences of the energy splitting $\Delta E_N = E^+ - E^-$ (the superscript indicates the excitation polarization) for the electron and hole shifts. Right axis gives the corresponding Overhauser field B_N.

[1] C. Harkort, D. Kudlacik, N. E. Kopteva, D. R. Yakovlev, M. Karzel, E. Kirstein, O. Hordiichuk, M. Kovalenko, M. Bayer, *arXiv*:2302.02349 (2023).

Topological photonics and topological lasers

Sebastian Klembt[1]

[1] *Chair for Applied Physics, Julius-Maximilians-University Würzburg & Würzburg-Dresden Cluster of Excellence ct.qmat*

Topological Photonics is an emerging and novel field of research, adapting concepts from condensed matter physics to photonic systems adding new degrees of freedom. After the first demonstrations of topological photonic insulators [1,2], the field has moved on to study and exploit the inherent non-hermiticity of photonic systems and the interplay with their topological nature. In my talk, I will attempt to give an overview about the quickly emerging field of topological photonics. In this context, I will discuss topological lasers as a prime example of using topological concepts potentially for new technologies in the broad context of synthetic (photonic) matter. Examples will be given from novel photonic lattice devices resulting from the coupling of individual vertical III-V semiconductor microresonators.

Here, the so-called exciton-polaritons – hybrid states of light and matter – can emerge in the strong coupling regime. By choosing precise lattice geometries we are able to tailor optical band structures realizing novel photonic lattice. Here, the specific geometry as well as the hybrid light-matter nature allow for ways to break time-reversal symmetry and implement topologically non-trivial systems. Here, we were able to experimentally demonstrate the first exciton-polariton topological insulator, manifesting in chiral, topologically protected edge modes [3]. In order to study topological effects in combination with optical non-linearities, so-called topological lasers have been envisaged and realized. They exploit topological effects to efficiently couple and phase-lock extended arrays of lasers to behave like one single coherent laser. The major drawback so far is that the emission appears in the plane of the topologically protected light propagation, thus hindering light extraction. Here, we have presented the first experimental demonstration of a topological insulator vertical cavity laser array [4], using the so-called crystalline topological insulator model. Starting for the above mentioned examples, I will give an overview of the field of topological optical lattices and lasers and give an outlook on emerging novel materials beyond III-V semiconductors, such as organic materials, transition metal dichalcogenides and perovskites [5,6].

[1] Rechtsman et al. Nature **496**, 196–200 (2013).

[2] Hafezi et al., Nat. Photon. **7**, 1001–1005 (2013).

[3] Klembt et al., Nature **562**, 552–556 (2018).

[4] Dikopoltsev et al., Science **373**, 1514–1517 (2021).

[5] Dusel et al. Nano Lett. **21**, 6398–6405 (2021).

[6] Shan et al., Nat. Commun. **12**, 6406 (2021).

Networks of liquid light

H. Sigurðsson[1,2], J. D. Töpfer[1], L. Pickup[1], S. Harrison[1], T. Cookson[1], Y. Wang[1], A. Askitopoulos, S. Alyatkin, and P. G. Lagoudakis[1]

[1] *School of Physics and Astronomy, University of Southampton, Southampton SO17 1BJ, United Kingdom*
[2] *Science Institute, University of Iceland, Dunhagi 3, IS-107, Reykjavík, Iceland*

Recent years have seen a surge of advancements in optical manipulation over bosonic light-matter quasiparticles known as exciton-polaritons in semiconductor microcavities. These particles appear under strong-coupling conditions between cavity photons and embedded quantum-well excitons. Characterised by very high interaction strengths, nonlinearities, and picosecond timescales, these coherent light sources provide an exciting testbed to explore room-temperature nonequilibrium Bose-Einstein condensation in the optical regime.

In this talk, I will present results on all-optically engineered macroscopic networks of connected exciton-polariton condensates, which permit studies on fundamental emergent behaviours in complex nonequilibrium dynamical systems while subject to a drive and bosonic final-state stimulation. I will explain how a uniquely polaritonic feature gives rise to so-called “ballistic condensates” which, when spatially coupled, form a bosonic condensed matter analog of time-delay coupled oscillators that are ubiquitous in nature. I will present experimental and theoretical results on large-scale condensate networks displaying aforementioned emergent behaviors, including: spontaneous synchronization with unprecedented long-range spatial and temporal correlations [1,2], geometric frustration and formation of persistent superfluid currents [3], non-invasive optical control of the network coupling weights [4], synthesis of artificial lattices for studies of non-Hermitian topological physics [5], flatbands [6], and vortex frustration [7].

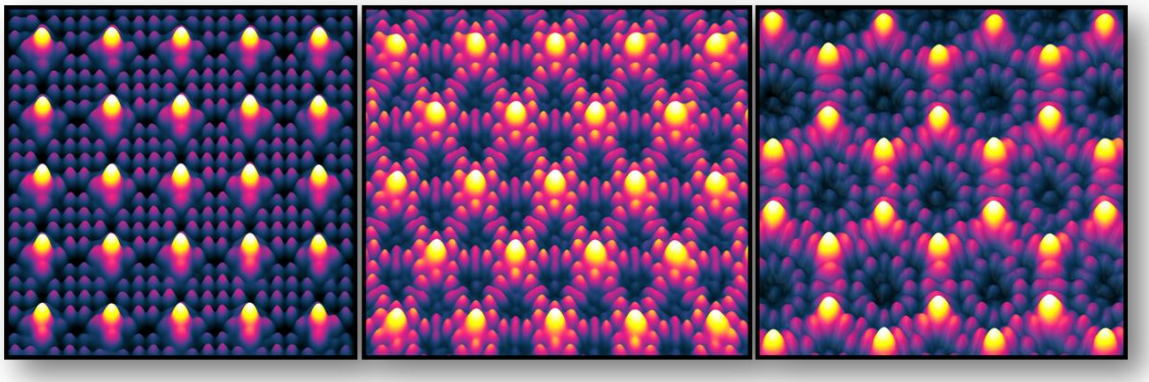

[1] Töpfer et al., Communication Physics **3**, 2 (2020).
[2] Töpfer et al., Optica **8**, 106 (2021).
[3] Cookson et al., Nature Communications **12**, 2120 (2021).
[4] Alyatkin et al., Physical Review Letters **124**, 207402 (2020).
[5] Pickup et al., Nature Communications **11**, 4431 (2020).
[6] Alyatkin et al., Nature Communications **12**, 5571 (2021).
[7] Alyatkin et al., arXiv:2207.01850 (2022).

Giant Photo-Elasticity of the Superlattice Polaritons for Detection of Coherent Phonons

M. Kobecki [(1)], A.V. Scherbakov [(1)], S.M. Kukhtaruk[(1,2)], D.D. Yaremkevich [(1)], T.Henksmeier [(3)], A.Trapp [(3)], D.Reuter [(3)], V.E. Gusev [(4)], A.V. Akimov [(5)], M. Bayer[(1)]

(1) Experimentelle Physik 2, Technische Universitat Dortmund, Dortmund, Germany

(2) Department of Theoretical Physics, V.E. Lashkaryov Institute, Kyiv, Ukraine

(3) Department Physik, Universitat Paderborn, Paderborn, Germany

(4) Universite du Mans (LAUM), CNRS, Le Mans Universite, Le Mans, France

(5) School of Physics and Astronomy, University of Nottingham, Nottingham NG7 2RD, UK

*

High-frequency coherent phonons in the GHz range have a potential for application in quantum technologies due to their nanometer wavelengths being comparable with the size of quantum nanodevices. Therefore, increasing strength of photon-photon coupling became of interest to the community [1,2]. In this work, we show that it is possible to reach quantum sensitivity of the phonon detection with a standard pump-probe set-up by exploiting giant photoelasticity of exciton-polariton resonance in a short period GaAs/AlAs superlattice (SL) [3].

For excitation and detection of the coherent phonon wave packet, we used a standard pump-probe experimental set-up with a mechanical delay line and a lock-in amplifier. A coherent acoustic phonon wave packet is generated by absorption of the pump laser pulse by a metal transducer at the back of the sample. Strain pulse propagates into GaAs substrate and reaches the GaAs/AlAs SL at the front, where it gets detected. By sweeping the central wavelength of the probe in the vicinity of the polariton resonance we obtained signals for several detuning values of probe photon energy. The amplitude of the measured signal depends strongly on the photon energy of the probe.

Our experiments reveal giant photo-elasticity of polaritons and extremely high sensitivity to propagating coherent phonons. The strong dispersion of the dielectric permittivity in the vicinity of the polariton resonance results in a strong ultrafast response of the optical properties to dynamical strain which accompanies the coherent phonons. This discovery opens new possibilities of ultrasensitive measurements of extremely low-density phonon fluxes.

[1] B. Jusserand, A.N. Poddubny, A.V. Poshakinskiy, A. Fainstein, A. Lemaitre, Phys. Rev. Lett. 115
[2] A.N. Poddubny A.V. Poshakinkiy, B. Jusserand, A. Lemaitre, Phys. Rev. B. 89
[3] M. Kobecki, A.V. Scherbakov, S. M. Kukhtaruk, D.D. Yaremkevich, T. Henksmeier, A. Trapp, D. Reuter, V.E. Gusev, A.V. Akimov, M. Bayer, Phys. Rev. Lett. 128, 157401

Anomalous dispersion and dissipative coupling in AlGaAs exciton-polariton structure

D. Biegańska [1], M. Pieczarka [1], C. Schneider [2], S. Hofling [3], S. Klembt [3], and M. Syperek [2]

[1] *Department of Experimental Physics, Wrocław University of Science and Technology, Wyb. Wyspiańskiego 27, 50-370 Wrocław, Poland*
[2] *Institute of Physics, University of Oldenburg, D-26129 Oldenburg, Germany*
[3] *Technische Physik, Wilhelm-Conrad-Röntgen-Research Center for Complex Material Systems, and Würzburg-Dresden Cluster of Excellence ct.qmat, University of Würzburg, D-97074 Würzburg, Germany*

Strong light-matter coupling in semiconductor microcavities leads to the formation of quasiparticles called exciton polaritons, in which the energy is coherently exchanged between quantum-well (QW) excitons and bound photons. However, continuous photon loss due to the mirror imperfections, together with the exciton decay via radiative and nonradiative channels, makes it a highly lossy, dissipative system. It has been shown that dissipative light-matter coupling can be a result of various forms of decay channels [1], for instance when both resonances decay to the shared photonic environment [2]. Dissipative terms in Hamiltonian can greatly affect polariton dispersions, particularly when dissipative coupling is strong enough in comparison to the inherent coherent coupling. Then it may lead to an anomalous shape of the dispersion, with inverted lower state branch. Such energy-wavevector dependence has only recently been observed, and solely in microcavities containing transition metal dichalcogenides (TMDCs) [1,3]. With a negative particle mass, linked to its group velocity, such states have a great potential in dispersion engineering and in studies of non-Hermitian phases of quantum matter in a solid state.

In this work, we observe anomalous inverted dispersion of exciton polaritons in AlGaAs-based microcavity at low temperature. This material system is superior to microcavities with TMDCs in quality factors, linewidths, reproducibility, stability and ease of design, hence it has a large potential in reliable structure production and engineering. Our sample hosts both standard Γ-excitons in the QWs, coherently coupled to photons, but also lower-energy spatially and momentum indirect X-excitons, prone to dissipation. We show how the X-exciton resonance couples to the photonic mode in a wide range of exciton-photon detunings, leading to the inverted-mass eigenstates, observed in photoluminescence (PL) measurements. We present the evolution of polaritonic level attraction strength with the detuning, clearly showing a transition between monotonic (with a single maximum at k=0) and nonmonotonic (with maxima at finite wavevectors) |k|-dependence in lower branch dispersion. By implementing the non-Hermitian dissipative-coupling model, we characterize decay channels and interactions between resonances. Moreover, we present the temporal evolution of such states, as well as the dispersion of eigenstate lifetimes, showing a difference in branches' PL decay. Our work is the first realization of anomalous polariton states in a non-organic III-V semiconductor-based microcavity with wide detuning availability and with such a detailed characterization, which is crucial in understanding the unique nature of dissipative coupling in semiconductor microcavities and in future design of new non-Hermitian quantum phases.

[1] M. Wurdack, T. Yun, M. Katzer, A. G. Truscott, A. Knorr, M. Selig, E. A. Ostrovskaya, E. Estrecho, *Nat. Commun.* **14**, 1026 (2023).
[2] O. Bleu, K. Choo, J. Levinsen, M. M. Parish, *arXiv:2301.02221*, (2023).
[3] S. Dhara, C. Chakraborty, K. Goodfellow, L. Qiu, T. A. O'Loughlin, G. W. Wicks, S. Bhattacharjee, A. N. Vamivakas, *Nat. Phys.* **14**, 130-133 (2018).

Non-Hermitian synthetic lattice with light-matter coupling

Amir Rahmani[1], Mateusz Kedziora[2], Andrzej Opala[1,2], and Michał Matuszewski[1]

[1] *Institute of Physics Polish Academy of Sciences, Al. Lotników 32/46, 02-668 Warsaw, Poland*

[2] *Institute of Experimental Physics, Faculty of Physics, University of Warsaw, ul. Pasteura 5, PL-02-093 Warsaw, Poland*

We propose that light-matter coupling can be used to realize a synthetic lattice. In particular, we consider a one-dimensional chain of exciton-photon sites to create a synthetic comb lattice (see Figure 1) that exhibits a transition from a Lieb lattice flat band to a finite mass dispersion by tuning site-dependent light-matter coupling. Moreover, in a non-Hermitian system with gain and loss, the flat band phase is much more robust and the transition is accompanied by the appearance of exceptional points in the complex energy spectrum. We demonstrate that by engineering the light-matter coupling in the synthetic comb lattice, one can explore various phases in the polariton lasing regime. Our proposal paves the way for studying non-Hermitian systems in higher dimensions.

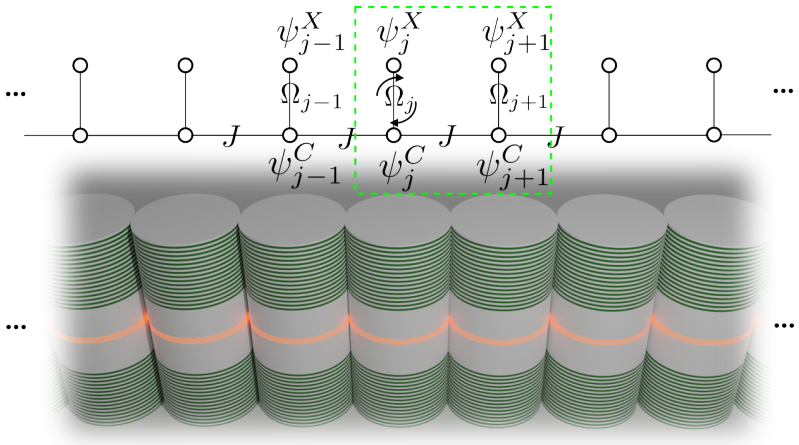

Figure 1: Scheme of our model. (Top) At lattice site j photonic (ψ^C_j) and excitonic (ψ^X_j) states are coupled. The neighboring photonic sites are coupled to each other with coupling rate J. A possible choice of a unit cell is marked by the green square. (Bottom) In practice the model can be implemented in a lattice of coupled micropillars.

[1] O. Boada, A. Celi, J. I. Latorre, and M. Lewenstein, *Phys. Rev. Lett.* **108**, 133001 (2012).

[2] M. A. Miri, and A. Alù, *Science* **363**, 6422 (2019).

Automated Search For TMDs Monolayers On Exfoliated Samples

W. Kolesiński[1], **M. Goryca**[1]

[1] *Institute of Experimental Physics, Faculty of Physics, University of Warsaw, Pasteura 5, 02-093 Warsaw, Poland*

Despite the constant development of the transition metal dichalcogenide (TMD) monolayer fabrication methods, the exfoliated TMD flakes still exhibit the best optical properties. However, by its nature, exfoliation is pretty much a random process, which results in a chaotic distribution of different multilayers on the substrate's surface. The search for monolayers suitable for further processing and measurements is often mostly done manually, which is tedious and time-consuming due to monolayers' size. It turns out that using simple optical properties and computer calculations can significantly speed up this process.

Thin TMD multilayers of different thicknesses deposited on a reflective substrate, such as a silicon wafer, reflect the white light differently due to internal interferences and absorption within the TMD material (Fig. 1). Because of this effect, it is possible to assess the number of layers in a given flake by eye test using an optical microscope with a white light source. By analysing images of silicon wafers covered in exfoliated TMDs, one can select monolayer flakes and, by further analysis of their size and shape, find samples usable for purposes such as fabricating heterostructures.

In this presentation computer program capable of such identification will be shown. The software can find monolayers from saved images of exfoliated TMDs. Statistical analysis of previously found monolayers allows the algorithm to locate monolayers on photos taken under different conditions, such as differing exposure time or light intensity. The scope of this program's usability is also easily expandable to other layered materials.

The main advantages of that approach over manual search are the significantly shorter time required to search through the entire surface of the wafer and the nearly complete elimination of the chance of missing a good flake. It also potentially outperforms other deterministic methods of finding monolayers, such as PLE measurement, because of accessibility, as it does not require any additional experimental setup other than a microscope with a camera.

The presentation will cover statistical analysis used to determine the colour of monolayers in a given image alongside the main coding ideas used in the software.

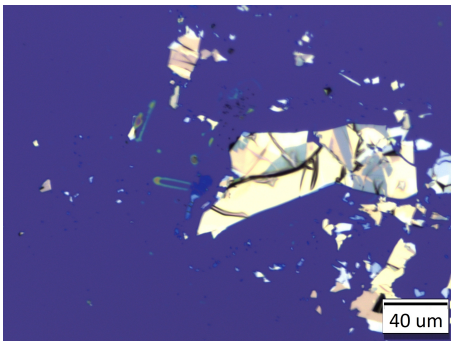

Figure 1: A microscope image of the exfoliated WSe_2 on the silicon substrate. Layers of different thicknesses have distinctively different colours. The orange and yellow are the thickest, while the dark blue spot near the centre of the image is a monolayer.

Electrical Tuning Of Exciton Lifetime In Monolayer MoS_2

H L Pradeepa[1,2], Pralay Mondal[1], Aveek Bid[1] and J K Basu[1].

[1] *Department of Physics, Indian Institute of Science, Bangalore 560012, India.*

[2] *Department of Physics, Wroclaw University of Science and Technology, Wroclaw- 50-370, Poland.*

The recent studies of low-dimensional semiconductors and their hybrid structure have led to discovering of many fascinating properties that are absent in their bulk counterparts. [1] Here, we studied the dynamics of excitons, which have high binding energy at room temperature using steady-state photoluminescence (PL) and time-resolved photoluminescence (TRPL) by systematically controlling the carrier density. We observed neutral and charged exciton(trions) dominant regimes in some specific carrier density.[2] In pristine MoS_2 devices, we observed an exciton dominant regime with an exciton lifetime of 3 ns, when we doped electrostatically with holes. Interestingly, we observe a sharp decrease in exciton lifetime with an increase of the electron density by electrostatic doping, with a corresponding increase in negative trion population, as shown in Fig. 1(a). This indicates the formation of negative trion. With increased hole doping by a chemical method, the exciton lifetime decreases, but it remains almost constant with electrostatic doping, which is visible in Fig. 1(b). This might be due to the exciton-exciton annihilation mechanism. Further hole doping by a chemical method leads to a transition to a positive trion dominated regime, as shown in Fig(c). Our observations suggest that when calculating the lifetime of excitons, the exciton-to-trions formation and exciton-exciton annihilation mechanisms should be considered.

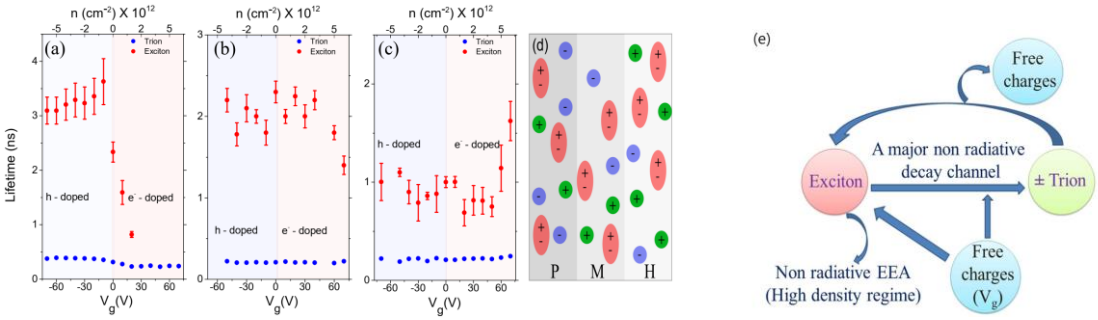

Fig.1. Lifetime of A-exciton (red circles) and trions (blue circles) at different doping levels achieved via chemical treatment and electrostatic doping: (a) pristine sample(P); (b) medium-hole-doped sample(M); (c) high-hole-doped sample(H). The lifetime of the A-exciton depends strongly on doping level. (d) Schematic of the exciton interaction at different regimes. (e) Schematic showing the various channels available for excitons and trions.

[1] Wang, Gang et al. Colloquium: Excitons in atomically thin transition metal dichalcogenides. *Reviews of Modern Physics*, 90, 2, 021001, 2018.
[2] H L Pradeepa et al. Electrical and Chemical Tuning of Exciton Lifetime in Monolayer MoS_2 for Field-Effect Transistors. *ACS Applied Nano Materials*, 3, 1, 641-647, 2020.

Fabrication and Strain Engineering of Transition Metal Dichalcogenides Monolayers on GaAs Nanomembranes

E. Cybula [1], J. Jasiński[1,2], S. Palai [2], M. Śmiertka [1], A. Balgarkashi[3], V. Piazza[3], A. Fontcuberta i Morral [3], A. Surrente [1], M. Baranowski [1], A. Castellanos-Gomez [4], and P. Płochocka[1,2]

[1] *Wroclaw University of Science and Technology, Wroclaw, Poland*
[2] *Laboratoire National des Champs Magnétiques Intenses, Toulouse, France*
[3] *École Polytechnique Fédérale de Lausanne, Lausanne, Switzerland*
[4] *Instituto de Ciencia de Materiales de Madrid, Campus de Cantoblanco, Madrid, Spain*

Transition metal dichalcogenides (TMDs) possess an excellent mechanical robustness and flexibility withstanding strains as high as 10% before breaking. Therefore, strain engineering has become a particularly attractive tool to tailor their electronic and vibrational properties or to preferentially funnel photoexcited carriers towards defects, which act as single photon emitters [1]. One of the approaches to site-control these quantum light emitters is the deposition of TMD monolayers on patterned substrates [1], thereby imposing strain on the two-dimensional layers.

So far, patterned substrates consist mainly of SiO_2 nanostructures, which, however, suffer from surface charge instability. This provokes spectral wandering and blinking of single photon emitters. Here, we explore an alternative approach to deterministically imposing strain on TMD layers by making use of high-quality, epitaxially grown III-V semiconductor nanostructures.

We show a successful deposition of WSe_2 monolayers on 100 nm wide GaAs nanomembranes with 10 μm pitch in Fig. 1a. By performing photoluminescence spectroscopy, we show that the TMD monolayers deposited on GaAs nanomembranes effectively funnel carriers to the potential minima corresponding to strain, which is demonstrated by photoluminescence and Raman spectroscopy. At low temperature, we observe a blue shift of the A exciton of WSe_2 monolayer measured on a nanomembrane, as compared to the same resonance measured on the flat part. (See Fig. 1b) Intensity on the nanomembrane is lower than on the flat part and some resonances are polarization dependent. In addition, we found that the most intense Raman mode splits and shifts to the higher frequency on the nanomembrane, compared to the flat part. (See Fig. 1c) This observation suggests the presence of compressive strain, differently than expected.

This confirms that the applied stress allows to efficiently funnel photocreated carriers to the potential minima. In perspective, we will investigated the single photon emission properties of localized states by photon correlation spectroscopy.

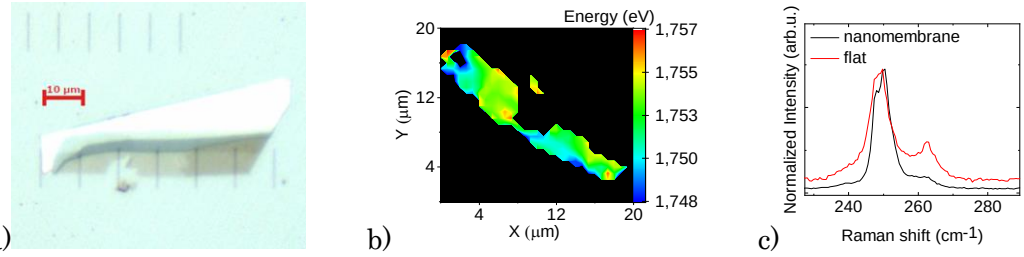

Figure 1. (a) Micrograph of the WSe_2 flake deposited on GaAs nanomembranes. (b) PL map energy of the A exciton. (c) Raman measurements on the nanomembrane (red) and on the flat part (black).

[1] Branny, A., Kumar, S., Proux, R. et al., *Nat Commun* **8**, 15053 (2017).

Controlled coherent-coupling and dynamics of exciton complexes in a $MoSe_2$ monolayer

A. Rodek[1] J. Howarth[2] , T. Hahn[3], T. Taniguchi[4], K. Watanabe[5], M. Potemski[1,6,7], P. Kossacki[1], D. Wigger[8] and J. Kasprzak[1,9,10]

[1] *Faculty of Physics, University of Warsaw, ul. Pasteura 5, 02-093 Warszawa, Poland*
[2] *National Graphene Institute, University of Manchester, Booth St E, M13 9PL UK*
[3] *Institute of Solid State Theory, University of Münster, 48149 Münster, Germany*
[4] *International Center for Materials Nanoarchitectonics, National Institute for Materials Science, 1-1 Namiki, Tsukuba 305-0044, Japan*
[5] *Research Center for Functional Materials, National Institute for Materials Science, 1-1 Namiki, Tsukuba 305-0044, Japan*
[6] *Laboratoire National des Champs Magnétiques Intenses, CNRS-UGA-UPS-INSA-EMFL, 25 Av. des Martyrs, 38042 Grenoble, France*
[7] *CENTERA Labs, Institute of High Pressure Physics, PAS, 01- 142 Warsaw, Poland*
[8] *School of Physics, Trinity College Dublin, Dublin 2, Ireland*
[9] *Univ. Grenoble Alpes, CNRS, Grenoble INP, Institut Néel, 38000 Grenoble, France*
[10] *Walter Schottky Institut and TUM School of Natural Sciences, Technische Universität München, 85748 Garching, Germany*

Quantifying and controlling the coherent dynamics and coupling of optical transitions in solids is of paramount importance in fundamental considerations in condensed matter optics and for their prospective optoelectronics applications in quantum technologies. Here we perform Four-Wave-Mixing microspectroscopy of a charge-tunable $MoSe_2$ monolayer. The experiments show that the homogeneous linewidth and the population decay of exciton complexes hosted by this material can be directly tuned by an applied gate voltage, which governs the free carrier density.

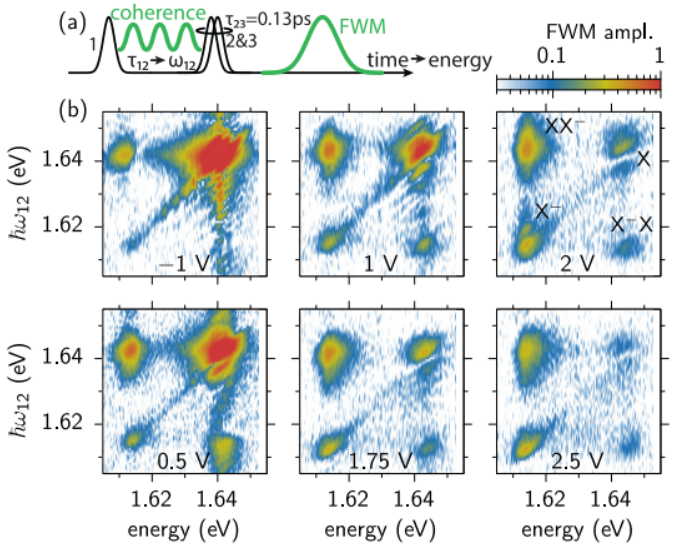

By performing two-dimensional spectroscopy, we also show that the same bias tuning approach permits us to control the coherent coupling strength between different exciton species.

Our findings yield exciting prospects for forthcoming investigations of coherence phenomena in the context of recent discoveries of strongly correlated exciton phases in solids, optically probed quantum Hall states, Moiré superlatices, and magnetic two-dimensional materials.

Figure 1: Phase-referenced two-dimensional FWM spectroscopy of X and X^- (a) The pulse sequence used in the 2D FWM experiment. (b) Examples of 2D FWM spectra for different gate biases as given in the plots.

[1] A. Rodek et al.,*arXiv* **2302.13109** (2023) *accepted for 2D Materials.*

Comparison of optical properties of $MoSe_2$ monolayers; samples grown by MBE technique vs mechanically exfoliated one.

Mateusz Raczyński[1], Tomasz Kazimierczuk[1], Wojciech Pacuski[1] and Piotr Kossacki[1]

[1] *Division of Solid State Physics, Institute of Experimental Physics, Faculty of Physics, University of Warsaw, ul. Pasteura 5, 02-093 Warsaw, Poland*

Semiconducting transition metal dichalcogenides (s–TMD) exhibit strong optical response within the limit of a single atomic layer. It was first observed for molybdenum disulfide, which exhibits strong photoluminescence due to direct bandgap.[1] The state of the art s–TMD monolayer samples are produced by the process of mechanical exfoliation, which became famous with the first graphene sample produced by this method.[2] The bulk crystals that are used for mechanical exfoliation can be grown with low defects concentration within their volume, especially when compared to defects concentrated on their surfaces. Therefore, the subsequent thinning of the bulk–grown sample with an adhesive tape allows for the exfoliation of atomically thin layered crystals (top–down approach). The amount of defects in such layers is similarly small as in the case of the original bulk crystal. For that reason – the surface of the sample is the sample – epitaxial techniques (bottom–up approach) were expected to be always inferior when compared to the manually exfoliated ones from the bulk crystal. The breakthrough happened with $MoSe_2$ monolayer sample grown by molecular beam epitaxy on high–quality substrate of hexagonal boron nitride.[3] It showed the possibility of producing TMD monolayer sample with an optical response comparable to the best – state–of–the–art – exfoliated ones. The development of TMD monolayer MBE–growth technique is crucial for industrial application due to its unprecedented spatial homogeneity and repeatability unachievable by the technique based on manual mechanical exfoliation. Moreover, MBE–grown $MoSe_2$ monolayers are folds– and ripples–free, and those are the intrinsic features of mechanically exfoliated samples that are very hard to get rid of.

In our work, we investigate the differences in optical properties of MBE-grown and mechanically exfoliated samples. We show that the photoluminescence intensity variation in MBE–grown samples can be explained by three major factors – the interference effects within the h–BN substrate, incomplete surface coverage by epitaxial monolayer (measured with atomic force microscope) and the radiatively non-active edge of $MoSe_2$ flakes. Additionally, we performed polarisation–resolved magnetospectroscopy and time–resolved measurements of exciton photoluminescence. We extract the exciton intervalley scattering time of $\sim$16 ps that is universal for both types of samples – exfoliated and MBE–grown. We also show variations of the charged exciton formation time among different samples caused by the changes in intrinsic carrier density.

[1] K. F. Mak, C. Lee, J. Hone, J. Shan, T. F. Heinz, *Phys. Rev. Lett.* **105**, 13 (2010).
[2] K. S. Novoselov, D. Jiang, F. Schedin, T. J. Booth, V. V. Khotkevich, S. V. Morozov, and A. K. Geim, *PNAS* **102**, 30 (2005)
[3] W. Pacuski, M. Grzeszczyk, K. Nogajewski, A. Bogucki, K. Oreszczuk, J. Kucharek, K. E. Połczyńska, B. Seredyński, A. Rodek, R. Bożek, T. Taniguchi, K. Watanabe, S. Kret, J. Sadowski, T. Kazimierczuk, M. Potemski, and P. Kossacki, *Nano Lett.* **20**, 5 (2020).

Electron-phonon coupling in a WSe_2 monolayer unveiled by two-photon photoluminescence excitation spectroscopy

M. Śmiertka[1], E. Cybula[1], K. Zalewska[1], K. Watanabe[3], T. Taniguchi[4], M. Dyksik[1], A. Surrente[1], M. Baranowski[1], P. Płochocka[1,2]

[1] *Wrocław University of Science and Technology, Wrocław, Poland*
[2] *Laboratoire National des Champs Magnétiques Intenses, CNRS Toulouse, France*
[3] *Research Center for Functional Materials, NIMS, Tsukuba, Japan*
[4] *International Center for Materials Nanoarchitectonics, NIMS, Tsukuba, Japan*

The "all-surface" character of two-dimensional semiconductors leads to strong interacrions of the electronic and vibrational degrees of freedom of a monolayer semiconductor to its surroundings [1]. Here, we investigate this aspect by performing a detailed investigation of the two-photon photoluminescence excitation (PLE) spectrum of a high quality WSe_2 monolayer, which we show in Fig. 1(a).

The low-temperature photoluminescence (PL) and reflection contrast spectra, shown in Fig. 1(b), show resonances of neutral and charged exciton species, as well as higher order excitonic transitions, like the 2s state of the A exciton. Figure 1(c), is a false-color map of the two-photon PLE experiment, with the horizontal axis corresponding to the emission energy and the vertical axis corresponding to two times the excitation energy. From the PLE spectrum, we extract the intensity of the two-photon PL of the exciton and plot it in Fig. 1(b), where we see pronounced resonances related to the absorption of the 2p and 3p states. We show in Fig. 1(d,e) selected PL spectra and close-up views, excited at the energies indicated in Fig. 1(c), respectively. In Fig. 1(e), we note a peak, separated by 108 meV from the doubled energy of the laser. Its shifts by the exact same amount as the doubled energy of the laser is a distinctive sign of its phonon-related nature. Ongoing work is devoted to a more precise understanding of this phonon line.

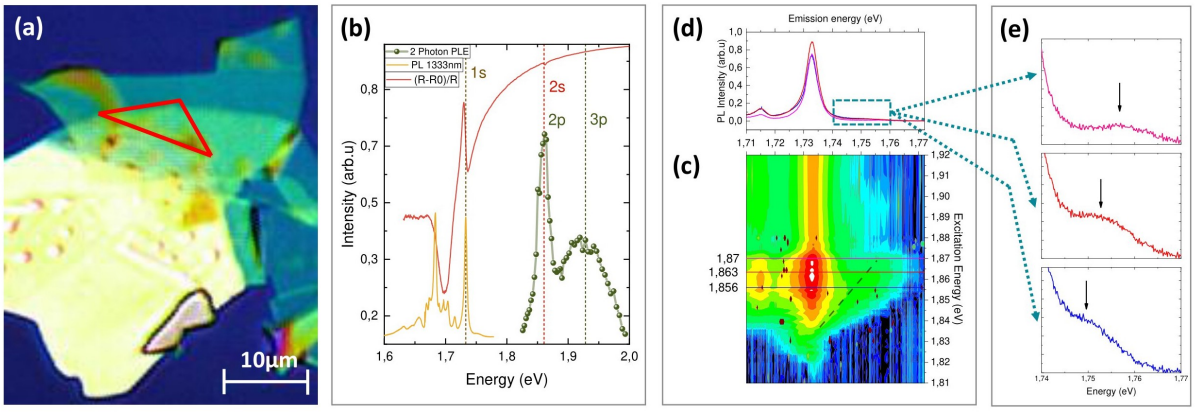

Figure 1: (a) Micrograph of the hBN-encapsulated $WSe2_2$ flake. The monolayer region is framed by the red triangle. (b) PL and reflectivity contrast and two-photon PLE spectra of the WSe_2 monolayer. The relevant excitonic resonances are indicated by dashed vertical lines. (c) False color map depicting two-photon PLE spectra. (d) Two-photon PL spectra extracted at selected excitation energies. (e) Close-up of the PL spectra. The phonon line shifting with the excitation laser is indicated by arrows.

[1] C. Jin, *et al.*, Nature Physics **13**, 127 (2017).

Electrical Control of Interlayer Physics in Type-II TMD Heterostructures

K. Sadecka[1,2], M. Bieniek[1,2,3], J. Pawłowski[1], A. Wójs[1], P. Hawrylak[2]

[1] *Institute of Theoretical Physics, Wrocław University of Science and Technology, Wybrzeże Wyspiańskiego 27, 50-370 Wrocław, Poland*
[2] *Department of Physics, University of Ottawa, Ottawa, Ontario, Canada K1N 6N5*
[3] *Institut für Theoretische Physik und Astrophysik, Universität Würzburg, 97074 Würzburg, Germany*

We describe the electronic and topological properties of $MoSe_2/WSe_2$ heterostructure using a combination of density functional theory (DFT) and tight-binding (TB) approximation. We start with determining the electronic structure of $MoSe_2/WSe_2$ from first principles, using the PBE parametrization of the GGA for the exchange-correlation potentials and including atomistic spin-orbit interaction. We obtain type-II band alignment and conduction band minima at Q points in agreement with previous works [1,2]. We include the analysis of Kohn-Sham wavefunctions allowing to describe the leading layer, spin and orbital contribution for a given band and given point in the reciprocal space, as well as to capture the interplay between two types of valleys present in the conduction band, i.e. K and Q. Following our previous work on monolayers we construct the *ab initio*-based TB model [3] for $MoSe_2/WSe_2$ heterostructure, which allows us to understand orbital contributions to Bloch states and will enable further studies of both twisted transition metal dichalcogenide (TMD) heterostructures and TMD-based multi-million atom nanostructures. To validate the model, we perform the analysis of topological properties of the system manifested in the Berry curvature. Finally, we perform a study of the effect of electric field on the interlayer properties of the $MoSe_2/WSe_2$ heterostructure towards the construction of gate-tunable spin-valley qubits [4] in TMD heterostructures.

[1] K. Sadecka, *Acta Physica Polonica A* **141**, 2 (2022).
[2] M Bieniek, K Sadecka, L Szulakowska, P Hawrylak, *Nanomaterials* **12**, 1582 (2022).
[3] M. Bieniek, L. Szulakowska, P. Hawrylak, *Phys. Rev. B* **101**, 125423 (2020).
[4] A. Altıntaş, M. Bieniek, A. Dusko, M. Korkusiński, J. Pawłowski, P. Hawrylak, *Phys. Rev. B* **104**, 195412 (2021).

K.S. and J.P. acknowledges financial support from National Science Centre (NCN), Poland, grant 2021/43/D/ST3/01989. K.S., M.B. and P.H. acknowledges support by NSERC Discovery and Strategic Grant and uOttawa Research Chair. Computing resources from Digital Alliance Canada and Wroclaw Center for Networking and Supercomputing are gratefully acknowledged.

Searching for moiré-induced quantum spin liquid - the DMRG and ED study of twisted TMD hetero-bilayers

Weronika K. Pasek[1], Jakub Jastrzębski[2], Michał Kupczyński[2], and Paweł Potasz[1]

[1] *Nicolaus Copernicus University, Faculty of Physics, Astronomy and Informatics, Grudziądzka 5, 87-100 Torun, Poland*
[2] *Wroclaw University of Science and Technology, 27 Wybrzeże Wyspiańskiego st. 50-370 Wroclaw, Poland*

Quantum spin liquid (QSL) is an exotic, highly correlated phase of matter characterized by the absence of long-range order and extremely large entanglement. The most intriguing property of QSL is its ability to support non-local excitations [1]. Such a phase occurs in frustrated triangular lattices and can be described by the Hamiltonian with four-spin terms [2].

Twisted hetero-bilayers of transition metal dichalcogenides are advantageous platforms for the study of correlated phases. Due to the mismatch between the lattice constants and a nonzero twist, a new periodicity called the moiré pattern arises in such materials, which can be effectively described by the Hubbard model on the triangular lattice [3,4]. For a range of twist angles, analyzed by us in previous work [5], moiré TMD materials at the half-filling can also be adequately described by the spin Hamiltonian.

In our work, we study finite structures craved from twisted TMD hetero-bilayers described by a spin Hamiltonian with four-spin terms. Using the DMRG method, we search for the range of parameters for which the QSL phase occurs and compare it with the results from the exact diagonalization analysis. In addition, we investigate the entanglement entropy of ground states.

[1] L. Savary, and L. Balents, *Rep. Prog. Phys.* **80**, 016502 (2017).
[2] T. Cookmeyer, J. Motruk, and J. E. Moore, *Phys. Rev. Lett.* **127**, 087201 (2021).
[3] F. Wu, T. Lovorn, E. Tutuc, and A. H. Maconald *Phys. Rev. Lett.* **121**, 026402 (2018).
[3] N. Morales-Duran, N. C. Hu, P. Potasz, and A. H. Maconald *Phys. Rev. Lett.* **128**, 217202 (2022).
[5] W. Pasek, M. Kupczynski, and P. Potasz, arXiv:2208.04636 (2022).

Exploring neutral and charged exciton optical properties in a $MoTe_2/SiO_2/Si$-based metal-oxide-semiconductor device

Emilia Zięba-Ostój[1], Ernest Rogowicz[1], Athanasios Paralikis[2], Claudia Piccinini[2], Battulga Munkhbat[2] and Marcin Syperek[1]

[1] *Department of Experimental Physics, Faculty of Fundamental Problems of Technology, Wrocław University of Science and Technology, 50-370 Wrocław, Poland*
[2] *DTU Electro, Technical University of Denmark, Kongens Lyngby 2800, Denmark*

Molybdenum ditelluride ($MoTe_2$) belongs to a broad family of transition-metal dichalcogenides (TMDs). In its 2H semiconducting phase, as a single-layer crystal, it has a direct optical bandgap at ~1.17 eV at 5 K, translated to ~1.0 eV at 300 K.[1] It makes this material the only TMD with optoelectronic device applicability in the near-infrared spectral range (>1 μm photon wavelength). However, many properties of single-layer $MoTe_2$ crystals are still unknown, including those related to the control of optical bandgap, interactions and excitation dynamics. It is predicted that the excess carrier density, charge polarity and electric field in $MoTe_2$ should effectively control these properties.[2] In this contribution, we examine the role of excess carrier density in monolayer (ML) $MoTe_2$ and examine to what extent one can control the optical gap, interactions in excitonic complexes and excitation dynamics.

We fabricated a metal-oxide-semiconductor (MOS) device allowing control over the excess carrier density and carrier type, switching from electrons to holes, in ML $MoTe_2$. The device consists of large-area exfoliated ML $MoTe_2$ placed partially on a gold electrode pre-patterned on a SiO_2/doped Si substrate. The Si plays a role of a second electrode. The MOS device can be biased with externally applied voltage (V_g), ranging from –30 V to +30 V and operates at cryogenic temperatures. Sweeping the voltage, we achieved a high range of charge tunability tracked by the optical response from the crystal at T = 5 K using the high-spatially-resolved photoluminescence (μPL) and contrast reflectivity experiments (μCR). By increasing V_g, one can observe the conversion of neutral excitons (X) to trions\polarons (T) through the monotonous increase in the T transition-related μPL intensity at the cost of a decrease in the X transition intensity. At roughly +/–20 V, the X population is almost entirely drained, and the T intensity is saturated. This observation is confirmed in the μCR, where at higher V_g, a new T-related resonance appears on a low-energy side of the always present X resonance. Interestingly, the voltage sweeping allows tuning energies of the X-related optical transition observed in μPL, showing a nearly linear increase from ~1.181 eV at ~0 V to 1.185 eV at –20 V and ~1.184 eV at +20 V. Under the same conditions, the T transition (when visible) remains almost unchanged at ~1.158 eV for negative bias and ~1.159 eV for positive. The trion/polaron binding energy ($E_{b,T}$) depends on the V_g polarity. For the negative Vg, $E_{b,T}$ reaches ~27 meV, whereas, for the positive Vg, it amounts to roughly 25 meV.

Finally, we tested the dynamics of X and T excitations using a non-degenerated pump-probe transient reflectivity experiment. We observe at least two fast and slow recombination channels for each species. At Vg~0 V, near the charge-neutrality condition, the X decays within ~9 ps and ~70 ps, whereas T decay with ~12 ps and ~90 ps. Interestingly, the decay channels can be controlled mainly by negative Vg, shortening the short component by a few ps and the long component by a few tens of ps.

[1] J. Kutrowska-Girzycka, E. Zięba-Ostój, D. Biegańska, M. Florian, A. Steinhoff, E. Rogowicz, P. Mrowiński, K. Watanabe, T. Taniguchi, C. Gies, S. Tongay, C. Schneider, and M. Syperek, *Appl. Phys. Reviews* **9**, 041410 (2022).
[2] G. Wang, A. Chernikov, M. M. Glazov, T. F. Heinz, X. Marie, T. Amand, and B. Urbaszek, *Rev. Mod. Phys.* **90**, 021001 (2018)

Optimization of Contacts for van der Waals heterostructures by AFM ironing

Agata Zielińska[1], Jonathan Eroms[2], Dieter Weiss[2], and Mariusz Ciorga[1,2]

[1] *Department of Experimental Physics, Wrocław University of Science and Technology, Wybrzeże Wyspiańskiego 27, 50-370 Wrocław, Poland*
[2] *Institute for Experimental and Applied Physics, University of Regensburg, Universitätstraße 31, 93053 Regensburg, Germany*

Semiconducting transition metal dichalcogenides (TMDCs) like MoS_2, $MoSe_2$, WS_2 and WSe_2 offer many new possibilities of structure engineering from the spintronics' point of view and are, therefore, attractive for future novel electronic devices. Integration of any device with an external circuitry requires, however, an efficient contacting scheme, which is challenging for TMDCs. Between a metal and a semiconductor (SC) the Schottky barrier (SB) is typically formed, which is theoretically dependent on the difference between the work function of the metal and the electron affinity of the SC [1]. In practice, the Fermi level at the metal/SC interface is typically pinned as a result of metal-induced gap states. This problem can be ommited by introducing a tunnel barrier in the form of an additional interlayer, e.g., hBN layer, between the metal and the TMDC, which limits the wavefunction spreading from the metal into the TMDC [2]. Transfer techniques commonly used to stack individual 2D layers into vdW structures can lead to inhomogeneities due to contaminants trapped between a 2D layer and a substrate or a metal layer [3]. One of the recently suggested methods to circumvent this problem is the so-called AFM ironing, when a contact-mode AFM scan is used to remove any possible imperfections like organic residues, bubbles or wrinkles, and improve adjacency of layers and, therefore, contact's resistance. This method has been used with success in many experiments [4-6].

Here, we investigate the effect of AFM ironing on the quality of Ti/Au contacts to MoS_2. MoS_2 flakes were produced by means of mechanical exfoliation and deposited on Si/SiO_2 substrates. Apart from investigating the direct metal/MoS_2 contacts, we studied also the influence of a thin hBN layer, acting as a tunnel barrier between the metal and the MoS_2 flake, on contact parameters. To study the influence of AFM ironing on the quality of such prepared contacts, the electrical and optical properties of the ironed and the non-ironed samples were compared using transport measurements and photoluminescence spectroscopy, respectively.

[1] A. Allain, J. Kang, K. Banerjee, and A. Kis, *Nature Materials* **14**, 1195-1205 (2015).
[2] M. Farmanbar, and G. Brocks, *Physical Review B* **91**, 161304(R) (2015).
[3] S.J. Haigh et al., *Nature Materials* **11**, 764-767 (2012).
[4] S. Chen et al., *ACS Omega* **6**, 4013-4021 (2021).
[5] Y. Kim et al., *ACS Nano* **13**, 14182-14190 (2019).
[6] M.R. Rosenberger et al., *ACS Applied Materials & Interfaces* **10**, 12 (2018).

Computational prediction of structure and electronic properties of monolayer and few-layer 2D polyimide covalent organic frameworks

Mateusz Wlazło, Atsushi Nagai

Ensemble³ Centre of Excellence, Łukasiewicz Research Network - Institute of Microelectronics and Photonics, Wólczyńska 133, 01-919 Warsaw, Poland

In contrast to similar and more established groups of materials, such as zeolites and metal organic frameworks, covalent organic frameworks (COFs) are distinctively built only from organic elements – carbon, oxygen, hydrogen, and often nitrogen or boron. They create light, mechanically rigid and chemically inert networks which have many advantages but also create issues with developing large-scale films or membranes because of low solubility and processability [1]. Together with a lack of strong coordination bonds, which direct the design and synthesis in case of frameworks that contain transition metal ions, it has slowed the progress in COF synthesis and characterization. Recently though, more robust design strategies have led, e.g., to first reports of bulk produced and single-crystal 2D COFs [2]. With the possibility in sight of controllable synthesis of monolayer and few-layer frameworks, they are on the path to becoming interesting candidates for integration in optoelectronic devices, similar to other layered 2D materials. Meanwhile, the rigidity and low solubility of COF that have hampered their development are becoming their valuable traits in device integration.

Imide COFs [3] in particular exemplify these characteristics by containing sp^2 carbon and a fair amount of enamine (-C-N-) instead of imine (-C=N-) bonds, both of which stabilize the crystal structure [1]. Here, we report the results of DFT calculations of such materials in the form of monolayers and AA and AB-stacked multilayers. We find the multilayers to be stable and with varying electronic properties. In particular, the finite band gap exhibited by every structure (monolayer and stacked) is sensitive to atomic arrangement of the atoms.

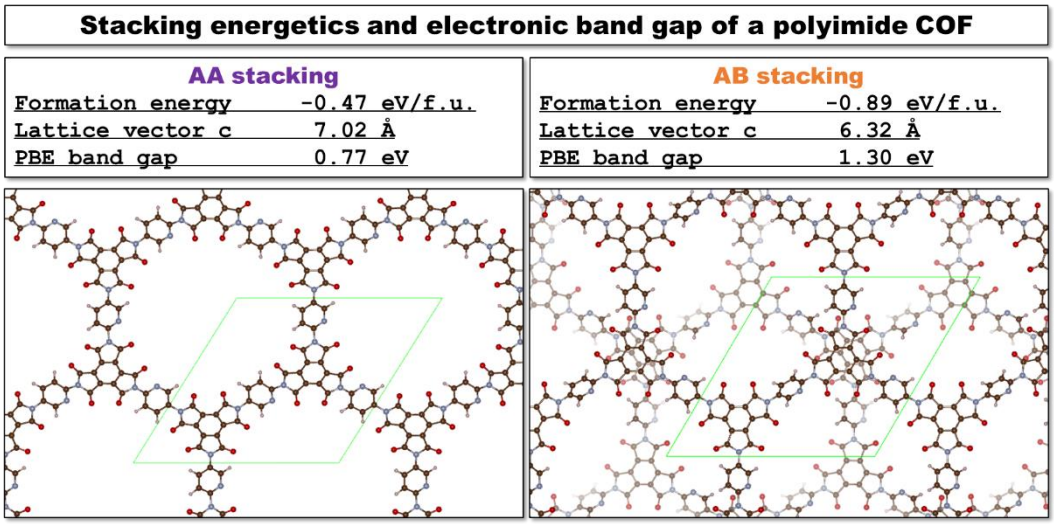

Figure 1: Formation energies (with respect to the flat monolayer), c lattice vector (out-of-plane) lengths, and PBE band gaps of AA and AB stacked polyimide COFs. The unit cell comprised of a monolayer relaxed towards a minimum with significant torsion (between 37 - 45 deg) between outer rings. The relaxed monolayer exhibits an energy lowering of -0.25 eV per formula unit (f.u., $\mathbf{C_{13}N_3O_4H_3}$). The PBE band gap of the monolayer varies between 1.02 (flat) and 1.68 eV (relaxed).

[1] S. Kandambeth, K. Dey, R. Banerjee, *J. Am. Chem. Soc.* ***141****, 1807−1822 (2019)*
[2] A. M. Evans et al., *Science* ***361****, 52−57 (2018)*
[3] H. Veldhuizen , A. Vasileiadis, M. Wagemaker, T. Mahon, D.P. Mainali, L. Zong, S. Zwaag, A. Nagai, *J. Polym. Sci. Part A: Polym. Chem.* ***57*** *2373-2377 (2019)*

Tunable valley splitting in 2D MPX_3 crystals.

Miłosz Rybak [1] **and Magdalena Birowska**[2]

[1] *Department of Semiconductor Materials Engineering, Faculty of Fundamental Problems of Technology, Wrocław University of Science and Technology, Wybrzeże Wyspiańskiego 27, 50-370 Wrocław, Poland*
[2] *Institute of Theoretical Physics, Faculty of Physics, University of Warsaw, Pasteura 5, 02-093 Warsaw, Poland*

Valleytronics has attracted a great interest in 2D materials, due to number of intriguing properties such as spin-valley locking and valley Hall effect [1]. Tailoring valley degrees of freedom offers unique playground to realize pecular phenomena and novel applications, Here, we have demonstrated that the monolayer of transition metal trichalcogenides $MnPX_3$ (X=S, Se), which are layered antiferomagnts [2,3], could be viewed as promising valley electronics materials. In particular, we have shown that the valley splitting at the K+/K- can be effectively control by the direction of the magnetic moments. In particular, the sizable valley splitting occurs for the out-of plane direction of the magnetic moments in monolayer of MnPSe3, resulting in valley dependent gaps, as it is presented in Fig. 1. On the other hand, the valley dependent gaps rely on the type of the chalcogen atoms. Moreover, the K+/K- valleys are spin degenerated, which might hinder their spintronic applications. Hence, we have also propose a novel way how the valley polarization can be achieved. We have suggested that particular deformation of the hexagonal lattice of $MnPX_3$ could lead to the spin resolved valley splitting. Our results give insight into the valley splitting realization in 2D antiferromagnets.

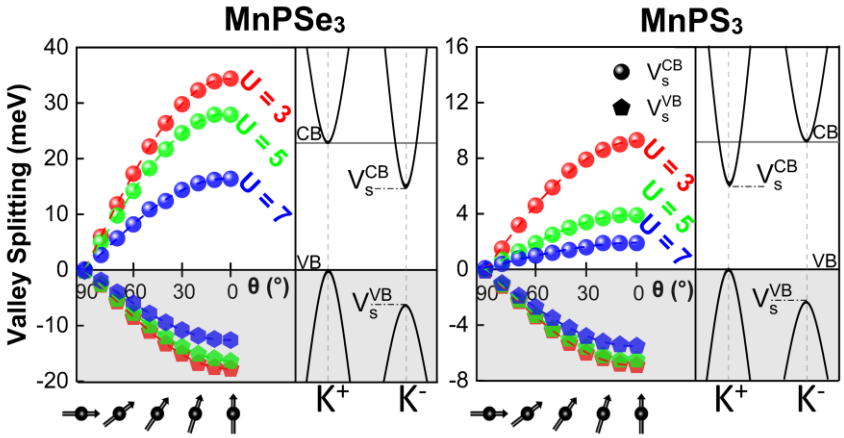

Fig. 1. Tunable Valley splitting upon the change of the direction of Mn spins from the in-plane to out-of plane direction.

We acknowledge support from the University of Warsaw within the project "Excellence Initiative-Research University" program. Access to computing facilities of PL-Grid Polish Infrastructure for Supporting Computational Science in the European Research Space, the Wroclaw Centre for Networking and of the Interdisciplinary Center of Modeling (ICM), University of Warsaw are gratefully acknowledged.

[1] J. R. Schaibley, 2016. "Valleytronics in 2D materials". United States.
[2] B. L. Chittari et al. Phys. Rev. B 94, 184428 (2016).
[3] M. Birowska, et al. Phys. Rev. B 103, L121108 (2021)

Optical markers of magnetic phase transition in layered CrSBr.

Miłosz Rybak [1], Wojciech M. Linhart [1], Magdalena Birowska[2], Paweł Scharoch[1] and Robert Kudrawiec [1]

[1] *Department of Semiconductor Materials Engineering, Faculty of Fundamental Problems of Technology, Wrocław University of Science and Technology, Wybrzeże Wyspiańskiego 27, 50-370 Wrocław, Poland*
[2] *Institute of Theoretical Physics, Faculty of Physics, University of Warsaw, Pasteura 5, 02-093 Warsaw, Poland*

Two-dimensional (2D) magnetic semiconductors give the opportunity to take advantage of the electron charge and the electron spin at the same time, which gives the possibility of broadening modern semiconductor technology and spintronic devices. It can greatly expand the applications of ferromagnets (FM) in other devices such as transformers, electromagnets, high-density storage, and magnetic random access memory [1].

Here, we investigate the role of the interlayer magnetic ordering of CrSBr: antiferromagnetic van der Waals crystal whose single monolayer is intrinsic ferromagnetic (AFM:A), in the framework of ab initio calculations, and by using optical spectroscopy [2]. We have demonstrated that optically induced band-to-band transitions visible in optical measurement are remarkably well assigned to the band structure by the momentum matrix elements and energy differences for magnetic ground state (A-AFM). In addition, our study reveals significant differences in electronic properties for two different interlayer magnetic phases. When the magnetic ordering of A-AFM to FM is changed, the crucial modification of the band structure reflected in the direct-to-indirect band gap transition and the significant splitting of the conduction bands are obtained.

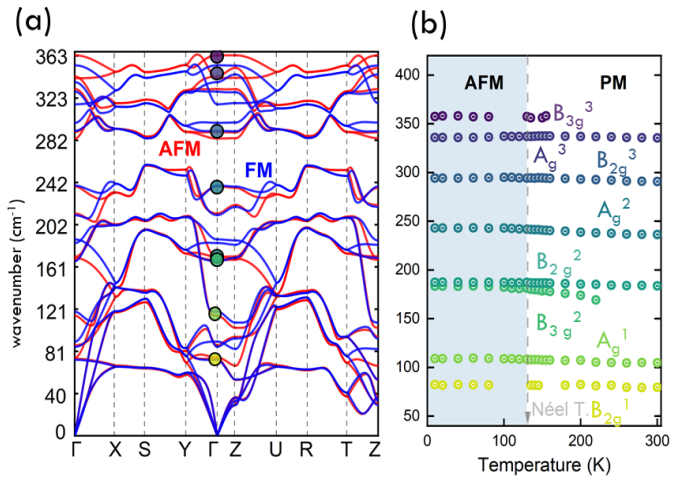

Fig. 1 (a) Phonon dispersion for AFM, FM magnetic states (b) Experimentally measured raman peaks positions in function of temperature.

In addition, Raman measurements (Fig.(b)) demonstrate a splitting between the in-plane modes B_{2g}^2/B_{3g}^2, which is temperature dependent and can be assigned to different interlayer magnetic states, corroborated by the DFT+U study (Fig.(a)). Finally, our results point out the origin of interlayer magnetism, which has its origin in electronic rather than structural properties. Our results reveal a new approach for tuning the optical and electronic properties of van der Waals magnets by controlling the interlayer magnetic ordering in adjacent layers.

[1] S. Chen,C. Huang, H. Sun, J. Ding, P. E. Jena, J. Kan, J. Phys. Chem. C 2019, 123, 17987–17993
[2]W. Linhart, M. Rybak, M. Birowska, K. Mosina, V. Mazanek,P. Scharoch, D. Kaczorowski, Z. Sofer, and R. Kudrawiec, Optical markers of magnetic phase transition in CrSBr, under review in ACS Nano

Interplay between stacking and magnetic configurations in MPS_3 bilayers

Andrea M. León,[1,2] *Beatriz Costa Guedes,*[1,3]
Thomas Heine,[1,3] *Thomas Brumme*[1]
[1] *Chair of Theoretical Chemistry, TU Dresden, Germany*
[2] *Physics Faculty, Pontifical Catholic University of Chile*
[3] *Helmholtz-Zentrum Dresden-Rossendorf, Leipzig, Germany*
andrea.leon@uc.cl

The two-dimensional transition metal thiophosphates MPS_3 (M = Mn, Fe, and Ni) have attracted a lot of attention recently because they exhibit a long-range antiferromagnetic (AFM) order and display interesting electronic-optical properties associated with their magnetic state [1]. In these materials, the AFM ground state is governed by the competition between direct M–M exchange and indirect M–S–M superexchange interactions within atomic layers, as well as the d-electron occupancy of the metal ion [2]. However, how the stacking between layers influences the electronic properties of MPS_3 is largely unknown. Here, we perform first-principles calculations to study the interplay between AFM and ferromagnetic (FM) configurations under different layer stacking (see Figure 1). Our results provide insight into understanding the interlayer AFM-FM coupling in those systems, revealing that different magnetic states can be stabilized through layer stacking. We suggest that these systems provide a unique playground for studying different aspects of magnetism in 2D systems.

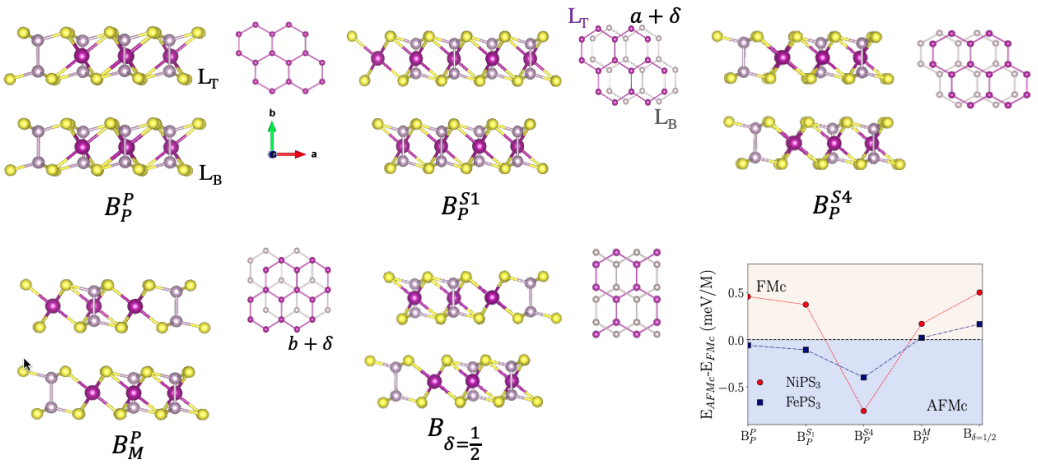

Figure 1. Different high-symmetry stacking configurations in bilayer MPS_3. The top view to the right of each structure indicates the stacking of the two hexagonal lattices of the transition metals. The low-right panel shows the interlayer exchange energy for each stacking.

References

[1] X. Jiang et al., Applied Physics Reviews, **8** 031305 (2021).
[2] B. L. Chittari et al., Physical Review B, **94** 184428 (2016).

Exploring structural, electronic, and magnetic properties of 2D Cr, Fe, and Zr monoborides

Isabel Arias Camacho and Nevill Gonzalez Szwacki

Institute of Experimental Physics, Faculty of Physics, University of Warsaw, Pasteura 5, PL-02093 Warsaw, Poland

MBenes, a family of two-dimensional transition metal borides, has recently attracted significant attention [1]. Their elemental compositions, surface terminations, geometrical forms, and chemical and physical properties are unique and fascinating. These two-dimensional compounds hold promising applications in various fields such as molecular sensing, Li- and Na-ion batteries, electrocatalysis, and magnetic devices. Also important are their exceptional electrical conductivity, high hydrophilicity, rich surface chemistry, and outstanding stability.

In this work [2], we present the results of density functional theory-based calculations for 2D Fe_2B_2, Cr_2B_2, and Zr_2B_2 hexagonal and orthorhombic MBenes. According to our calculations, the orthorhombic form of the 2D structures is the most energetically favorable for Fe_2B_2 and Cr_2B_2, whereas, Zr_2B_2 MBene prefers to adopt the hexagonal form. From phonon calculations, we can also deduce that the orthorhombic structure of Zr_2B_2 and the hexagonal Fe_2B_2 are also structurally stable. The magnetic properties of the two-dimensional systems were also studied and Fe_2B_2 and Cr_2B_2 are found to be ferromagnetic, whereas Zr_2B_2 is nonmagnetic. The Fe_2B_2 structure exhibits a magnetic moment of 3.73 Bohr magnetons per unit cell (see the DOS picture shown in Fig. 1) followed by Cr_2B_2, with 2.58 Bohr magnetons per unit cell. Transport computations reveal that the highest conductivity may be expected for Zr_2B_2 and the smallest for Fe_2B_2. A detailed comparison with available data in the literature will be provided.

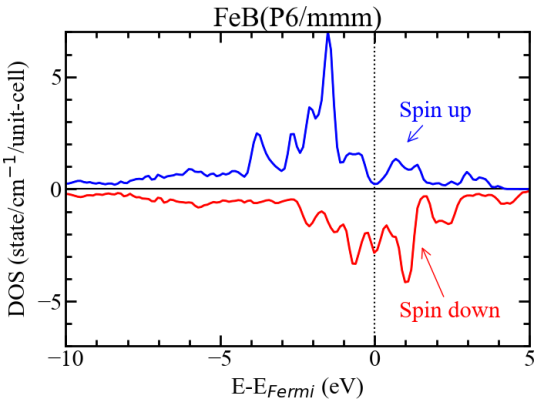

Figure 1: Spin resolved density of states (DOS) of ferromagnetic Fe_2B_2. The upward and downward plots show the majority and minority states, respectively, and the dashed line shows the Fermi energy.

[1] B. Zhang, J. Zhou, and Z. Sun , *J. Mater. Chem. A* **10**, 15865 (2022).
[2] I. Arias Camacho and N. Gonzalez Szwacki, *Materials - Special Issue* (2023).

Magnetic skyrmions of Ti2C MXenes doped with Cr, Mn, and Fe

Teresa Kulka[1], **and Jacek Majewski**[1]

[1] *Faculty of Physics, University of Warsaw, Ludwika Pasteura 5, 02-093 Warsaw, Poland*

Two-dimensional titanium carbides Ti2C, MXenes, have been attracted scientific effort, mostly owing to their intriguing properties and promising applications [1]. The magnetic moments of the external metallic Ti layers are ferromagnetically or antiferromagnetically oriented to each other depending on the remnants from the technological processes that cover the surface. The possibility to tune magnetic moments of the external MXenes layers through suitable functionalization could be utillized in numerous spintronic applications [2].

We have investigated the change of the magnetic properties of MXenes caused by the substitutional doping of Ti layers with transition metal (TM) atoms such as Mn, Cr, and Fe. The introduction of TM atoms with different number of d-electrons (and therefore different magnetic moment) leads to breaking of the homogeneity of the spontaneous magnetization and formation of the skyrmionic-like patterns (see Figure below). Magnetic skyrmions are small swirling topological defects in the magnetization texture, which are regarded as novel information carriers in future spintronic devices [3].

Our studies are based on the first principles calculations within the Kohn-Sham realization of the density functional theory (DFT) employing the Quantum Espresso computer package. We take spin-orbit interaction into account and therefore our calculations have to be performed in the non-collinear magnetism regime. To facilitate eventual future comparison with experiments, we have undertaken an attempt to compute the spin tunnelling current between the non-uniformly spin-polarized electrons of the MXenes surface and magnetic tip of the scanning tunnelling microscope (STM), in close analogy to codes providing the STM images from the electronic density obtained in DFT calculations.

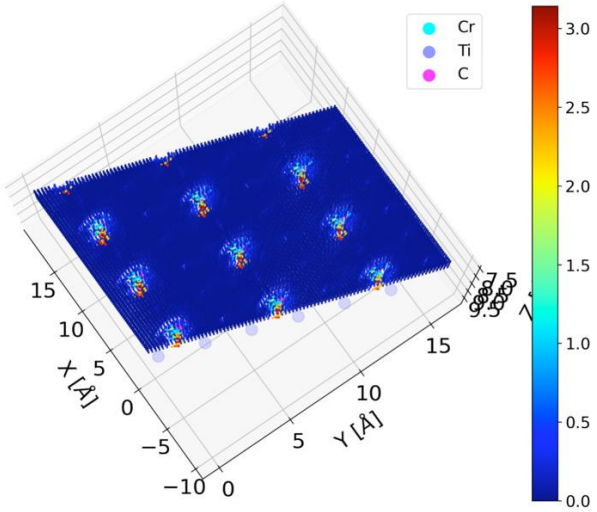

Acknowledgement: Authors acknowledge the support of National Science Centre in Poland under the project OPUS-16 (UMO-2018/31/B/ST3/03758).

[1] Y. Wang, Y. Xu, M. Hu, H. Ling, and X. Zhu, MXenes: focus on optical and electronic properties and corresponding applications, *Nanophotonics* **9**, 1601 (2020).

[2] S. Sugahara and J. Nitta, Spin-Transistor Electronics: An Overview and Outlook, *Proceedings of the Institute of Electrical and Electronics Engineers* **98**, 12 (2010).

[3] A. Fert, N. Reyren, V. Cros, Magnetic skyrmions: advances in physics and potential applications, *Nature Reviews Materials* **2**, 17031 (2017).

The effect of temperature and excitation energy on Raman scattering in bulk HfS_2

Igor Antoniazzi[1], Natalia Zawadzka[1], Magdalena Grzeszczyk[1], Tomasz Woźniak[2], Jordi Ibáñez[3], Zahir Muhammad[4], Weisheng Zhao[4], Maciej R. Molas[1] and Adam Babiński[1]

[1] *Faculty of Physics, University of Warsaw, Warsaw, Poland*
[2] *Faculty of Fundamental Problems of Technology, Wrocław University of Science and Technology, Wrocław, Poland*
[3] *Geosciences Barcelona, CSIC, Lluís Solé i Sabarís s.n., 08028, Barcelona, Spain*
[4] *Hefei Innovation Research Institute, Beihang University, Hefei 230013, P. R. China*

Raman scattering (RS) in bulk hafnium disulfide (HfS_2) is investigated as a function of temperature and excitation of several laser energies (fig. 1). The low-temperature quenching of ω_1 (134 cm^{-1}) and the emergence of a new mode at approx. 184 cm^{-1}, labeled Z, is reported (fig. 1.a). An unexpected blue-shift of the main Raman-active modes (A_{1g} and E_g) as temperature increases, was observed (fig. 1.b). The excitation-dependent RS is reported. The apparent quenching of the A_{1g} mode at T=5 K and of the E_g mode at T=300 K in the RS spectrum excited with 3.06 eV excitation is also observed. We discuss the results in the context of possible resonant character of light-phonon interactions. Analyzed is also a possible effect of the iodine molecules intercalated in the van der Waals gaps between neighboring HfS_2 layers, which inevitably result from the growth procedure.

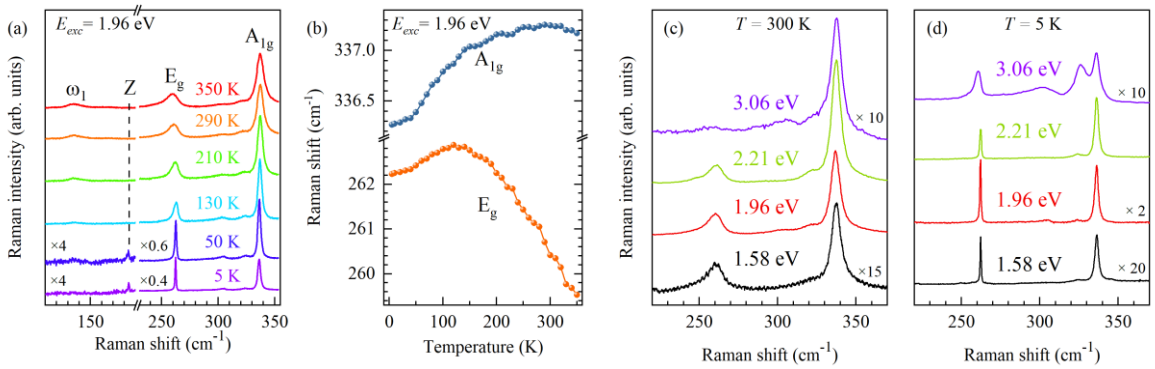

Fig. 1 (a) The temperature evolution of RS spectra measured on HfS2 bulk under excitation of E_{exc}=1.96 eV. For temperatures lower than 100 K a new mode, called here Z, has been observed and the quenching of ω_1. (b) Temperature evolution of the Raman shift of the A_{1g} and E_g modes under excitation of E_{exc}=1.96 eV. The Raman scattering spectra measured on Hf_2 bulk at (c) T =300 K and (d) T =5 K under a series of different excitation energies, indicated in the Figure.

Growth and characterization of metallic and oxidized forms of bismuthene

K. Toczek[1], M. Rogala[1], P. Krukowski[1], M. Piskorski[1], M. Le Ster[1], I. Lutsyk[1], W. Kozłowski[1], P. Dąbrowski[1], R. Dunal[1], A. Nadolska[1], P. Przybysz[1], W. Ryś[1], K. Szałowski[1], D. A. Kowalczyk[1], P. J. Kowalczyk[1]

[1] *Department of Solid State Physics, Faculty of Physics and Applied Informatics, University of Lodz, Pomorska 149/153, 90-236 Lodz, Poland*

Bismuth is in the XVth group of the periodic table, with the electronic configuration $6s^2 6p^3$, and as a semi-metal it is the last non-radioactive element in the periodic table with unusual electronic properties.

These properties are of interest due to spin-orbital effects and surface and edge states.[1] It was in bismuth that many quantum phenomena such as, for example, magnetoresistance, quantum size effects and recently also topologically protected edge states were first detected. It was recently shown that bismuth can grow in two dimensional form material known as bismuthene.[1,2] It is extremely important to understand the growth and degradation paths of these new material.

We will present the properties and morphology of bismuth nanostructures growing epitaxially on a pyrolytic graphite (HOPG), as well as insulating materials such as mica and hBN, on which the growth of bismuthene islands (2D bismuth with black phosphorus structure) can be observed.

We will focus on the conducted experimental research using scanning tunneling microscopy and atomic force microscopy, thanks to which we were able to study the electronic and atomic structure of bismuth single layers. X-ray photoelectron spectroscopy was used to investigate and determine the chemical composition of the oxidized structures. Raman spectroscopy was used for further analysis of the oxidized and metallic structures.

The above research is supported by the National Science Center under the project no. 2019/35/B/ST5/03956.

Research is also supported by the University of Lodz as part of the competition UniLodz IDUB- "Doctoral Research Grants" - 2022 edition, as part of project no. B2310009000186.07.

[1] P. J. Kowalczyk, O. Mahapatra, D. N. McCarthy, et al. Surf Sci, **605**, 659–667, 2011.
[2] S. Pinilla, J. Coelho, K. Li, et al. Nature Reviews Materials **7**, 717–735, 2022.

Transport signatures of Van Hove singularities in mesoscopic twisted bilayer graphene

Aleksander Sanjuan Ciepielewski [1], Jakub Tworzydło [2], Timo Hyart [1,3,4] and Alexander Lau [1]

[1] *International Research Centre MagTop, Institute of Physics, Polish Academy of Sciences, al. Lotników 32/46, 02-668 Warsaw, Poland.*
[2] *Faculty of Physics, University of Warsaw, ul. Pasteura 5, 02-093 Warsaw, Poland.*
[3] *Department of Applied Physics, Aalto University, 00076 Aalto, Espoo, Finland.*
[4] *Computational Physics Laboratory, Physics Unit, Faculty of Engineering and Natural Sciences, Tampere University, FI-33014 Tampere, Finland.*

Magic-angle twisted bilayer graphene exhibits quasi-flat low-energy bands with Van Hove singularities close to the Fermi level. These singularities play an important role in the exotic phenomena observed in this material, such as superconductivity and magnetism, by amplifying electronic correlation effects. In this work, we study the correspondence of four-terminal conductance and the Fermi surface topology as a function of the twist angle, pressure, and energy in mesoscopic, ballistic samples of small-angle twisted bilayer graphene. We establish a correspondence between features in the wide-junction conductance and the presence of van Hove singularities in the density of states. Moreover, we identify additional transport features, such as a large, pressure-tunable minimal conductance, conductance peaks coinciding with non-singular band crossings, and unusually large conductance oscillations as a function of the system size. Our results suggest that twisted bilayer graphene close the magic angle is a unique system featuring simultaneously large conductance due to the quasi-flat bands, strong quantum nonlinearity due to the Van Hove singularities and high sensitivity to external parameters, which could be utilized in high-frequency device applications and sensitive detectors.

MBE grown heterostructures of ZnSe, CdSe, $MoSe_2$, and hBN

B. Tronowicz [1], J. Kucharek [1], R. Bożek[1], T. Taniguchi[2], K. Watanabe[2], W. Pacuski [1]

[1] *Institute of Experimental Physics, Faculty of Physics, University of Warsaw, Pasteura St. 5, 02-093 Warsaw, Poland*
[2] *National Institute for Materials Science, Tsukuba 305-0047, Ibaraki, Japan*

The best optical properties of exfoliated transition metal dichalcogenides (TMDs) are obtained for monolayer materials encapsulated in hBN, so mechanically stacked in heterostructure hBN/TMD/hBN [1]. Part of this heterostructure can be reproduced using epitaxial methods, and indeed TMD grown on hBN exhibits much better optical properties [2] than TMD grown on other substrates. Still, the top hBN layer is missing in such a procedure. To finish heterostructure using large-scale epitaxial methods, the growth of hBN on TMD would be an ideal option. This however seems to be not accessible nowadays, because the very high growth temperature of hBN (over 1200C) makes it impossible to grow it on TMDs without destroying the previously deposited material. Consequently, other cap materials should be considered as candidates for protection of epitaxial TMDs.

In this work, we experimentally verify the possibility of covering TMDs with II-VI compounds based on selenides: ZnSe and CdSe. Materials are chosen due to chemical similarity to TMDs based on selenium, e.g $MoSe_2$, therefore there should be no risk of substitution of Se in TMD by other elements. Moreover, ZnSe is chosen due to its wide band gap and its transparency in the $MoSe_2$ emission spectrum. We expect that for TMDs, ZnSe will be just an isolator, similar to hBN. On the contrary, CdSe emission spectrum is close to the one of $MoSe_2$, so one can expect interactions in a formed heterostructure. Importantly, both ZnSe and CdSe can be grown at low temperatures (typically 300C) compared to temperatures used during the preparation of $MoSe_2$ (300-800C).

Heterostructures ZnSe/$MoSe_2$ and CdSe/$MoSe_2$ were grown using Molecular Beam Epitaxy (MBE) on exfoliated hBN deposited on SiO_2/Si substrates. Atomic force microscopy (AFM) and optical microscopy reveal the rich morphology of grown structures indicating the polycrystalline nature of II-VI material grown on $MoSe_2$. The results of low-temperature photoluminescence show that both ZnSe and CdSe strongly affect the optical spectra of $MoSe_2$. Moreover, the photoluminescence of CdSe is much stronger than the photoluminescence of MBE $MoSe_2$. Therefore research on $MoSe_2$ with II-VI layer present on top seems to be difficult. Still, we checked that the good optical properties of $MoSe_2$ grown on hBN can be restored by desorption of II-VI material from the surface of the heterostructure.

[1] F. Cadiz, E. Courtade, C. Robert, G. Wang, Y. Shen, H. Cai, T. Taniguchi, K. Watanabe, H. Carrere, D. Lagarde, M. Manca, T. Amand, P. Renucci, S. Tongay, X. Marie, and B. Urbaszek, Phys. Rev. X 7, 021026 (2017).
[2] W. Pacuski, M. Grzeszczyk, K. Nogajewski, A. Bogucki, K. Oreszczuk, J. Kucharek, K.E. Połczyńska, B. Seredyński, A. Rodek, R. Bożek, T. Taniguchi, K. Watanabe, S. Kret, J. Sadowski, T. Kazimierczuk, M. Potemski, P. Kossacki, Nano Letters 20, 3058 (2020).

Structural, Optical and Electrical Properites of Quaternary Hafnium-Aluminium Zinc Oxide Films Grown by Atomic Layer Deposition for Transparent Conductive Oxide Applications

M. Krajewski[1], M. Tokarczyk[1], P. Wróbel[1], A. Drabińska[1], M. Kamińska[1]

[1] *University of Warsaw, Faculty of Physics, Pasteura 5, Warsaw, Poland*

Transparent Conductive Oxide (TCO) films are characterized by having simultaneously exceptional electrical conductivity and high transmission in the visible range. Among many TCO materials, doped zinc oxide (ZnO) is one of the foremost candidates for next generation electronic devices, since it exhibits several desirable optoelectrical properties, in particular direct and wide bandgap (~3.37 eV), high carrier concentration exceeding 10^{19} cm^{-3} and very low resistivity in the range of 10^{-3} Ωcm. These properties may be finely tuned and enhanced by doping elements to create an oxide alloy. Despite the vast range of papers covering the properties of singly-doped ZnO, there is still undiscovered potential of simultaneous doping ZnO with two elements, creating a quaternary material. During our studies we fabricated a co-doped ZnO films with both aluminum and hafnium atoms (HAZO), utilizing atomic layer deposition technique (ALD). This method offers a precise control of the film thickness due to self-limiting character of the reactions during every half-cycle along with unraveled conformality and uniformity of the grown films. The optical, electrical and structural properties of the samples were investigated for varying Hf and Al concentrations to establish a comprehensive image of the studied material. The co-doped samples exhibit extremely low resistivity, close to 1×10^{-3} Ωcm – outperforming commonly used aluminum doped zinc oxide (AZO). We assume that the enhancement in carrier concentration after hafnium addition originates from the passivation of the deep oxygen vacancies, that act as electron trapping states along with decreasing the grain boundaries. Besides enhancing electronic properties, the co-doping opens a new possibilities of tuning both optical band gap and electrical properties. The proposed co-doped zinc oxide can found applications in the future electronic devices utilizing TCO materials such as flat panels, solar cells and variety of sensors.

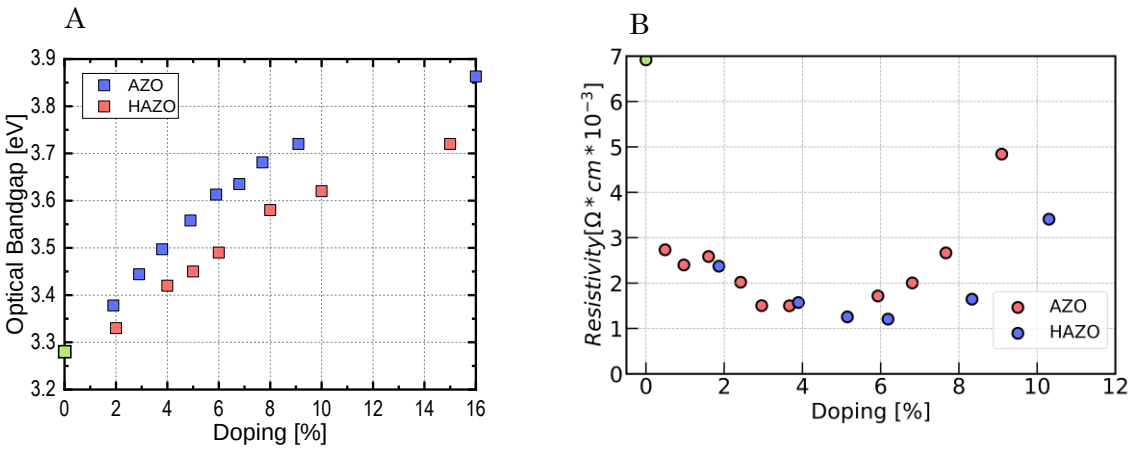

Figure 1. A) Optical bandgap widening with doping steadily increases, mainly due to Bernstein-Moss effect. B) Resistivity for differently doped samples shows a minimum around 4% and 6% for AZO and HAZO respectively.

ALD Grown ZnMgO:Al on Si for Photovoltaic Applications: Effect of High Mg Alloying and Al Doping.

R. Schifano[1], J. Kurek[1,2], S. Gierałtowska[1], Ł. Wachnicki[1], U. Rehman[1], D. Budiakivska[1,2], S. Chusnutdinow[1], K. Kopalko[1], R. Minikayew[1], B. Witkowski[1], M Godlewski[1], M. Pawłowski[2], C. Jastrzebski[2]

[1] *Institute of Physics, Polish Academy of Sciences, Al. Lotników 32/46, PL-02 668 Warsaw, Poland*

[2]*Faculty of Physics, Warsaw University of Technnology, Al. Koszykowa 75, PL-00 662 Warsaw, Poland*

Heterojunction solar cells based on ZnO/Si employed as an emitter and absorber, present a high interfacial defect density due to the ~40% lattice mismatch between the two materials. Despite that, it has been predicted by simulations that a potential theoretical efficiency of ~24% can be achieved if the conduction band gap misalignment (ΔE_C) between ZnO and Si is eliminated by Mg alloying [1]. Experimentally an increase in efficiency from ~4% to ~7% can be achieved by following this route [2]. However, it has been also found that further improvement in efficiency is hindered by the increase in resistivity of the ZnO based layer when the Mg content overcomes ~2-3 at.%. In the present work it is found that by keeping the Al content equal to ~2 at.% and by increasing the Mg content up to ~12 at.% into the ZnO layers, the films still exhibit excellent electrical properties: carrier concentration and mobility equal to ~2×10^{20} cm^{-3} and ~2 cm^2 V^{-1} s^{-1} as displayed in Fig.1(a) (experimental point with x_{Mg} content < 5 are without Al). A constant increase of the open circuit voltage of the test solar cells from ~0.34 V (without Al doping) to ~0.44 V as a consequence of the Mg and Al introduction is observed as shown in Fig.1(b). The realized test solar cells with the optimized Mg and Al content exhibit an open circuit voltage, short circuit current density, efficiency, and fill factor equal to ~0.42 V, ~30 mA cm^{-2}, ~7.5%, and ~60%, respectively. A realized device and I-V curve under standard illumination are shown in Fig.1(c).

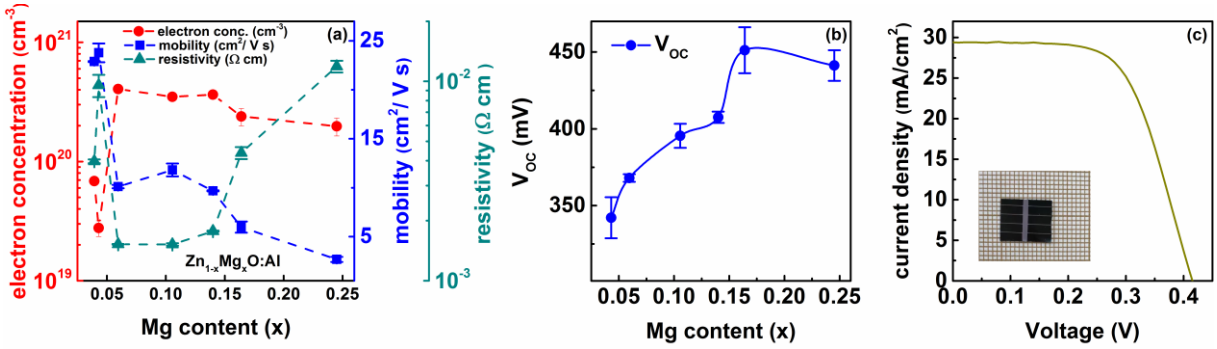

Fig1 (a) Carrier concentration, mobility, and resistivity vs Mg content **(b)** Open circuit voltage (V_{OC}) dependence on the Mg content **(c)** I-V curve under standard illumination of a test solar cell with Mg~12 at.%. (In **(a)** and **(c)** experimental data with $x_{Mg} < 5$ are without Al).

Acknowledgment
The work has been performed within the National Science Centre project UMO-2016/22/E/ST3/00553.

[1] K. E. Knutsen , R. Schifano et al. Phys. Status Solidi A **210**, No. 3, 585–588 (2013).
[2] R. Pietruszka, R. Schifano et al. Solar Energy Materials & Solar Cells **147**, 164 (2016).

Construction and studies of a cathode for photoelectrocatalytic hydrogen generation by water splitting

A. Bohdan[1], K. Korona[1], M. Krajewski[1], J. Kucharek[1], W. Pacuski[1], M. Tokarczyk[1], P.Podsadni[3], A. Czerwiński[2], K. Zarębska[2], M. Skompska[2], M. Kamińska[1]

[1]Faculty of Physics, University of Warsaw, Pasteura 5, 02-093 Warsaw, Poland
[2]Faculty of Chemistry, University of Warsaw, Pasteura 1, 02-093 Warsaw, Poland
[3]Faculty of Pharmacy, Medical University of Warsaw, Banacha 1, 02-097 Warsaw, Poland

Hydrogen is one of the most sustainable energy sources – it can be stored, transported, and used in fuel cells or combustion engines without the generation of any pollutants. Therefore, replacing fossil fuels with hydrogen has received intense attention in the last few years. However, hydrogen on Earth is mainly found as a component of molecules such as water and organic compounds. Today, it is produced mainly through steam reforming/gasification of fossil fuels, which not only consumes a large amount of natural gas, naphtha or coal, but also generates CO_2. In the pursuit of CO_2 – free hydrogen technology, electrolysis of water is a promising method.

In this work we present the results of the construction and studies of an innovative cathode for photoelectrocatalytic hydrogen production by water splitting. The oxides and $MoSe_2$ were selected so that the light-excited electrons had sufficient energy to ensure the hydrogen generation reaction. At the same time, the positions of the conduction bands of these materials relative to the vacuum level were such to ensure the transport of light-generated electrons to $MoSe_2$, which can thus act as a catalyst for the reaction.

Tuning the parameters of the oxide and $MoSe_2$ deposition processes allowed us to find a range of technological parameters for which a mechanically stable electrode with promising opto-electrical parameters was obtained. Wide structural and photoelectrical studies were performed. Raman scattering related to characteristic phonon vibrations and Energy-dispersive X-ray spectroscopy techniques were used to identify the deposited materials. SEM images proved successful deposition of the oxide and MoSe2 on the electrode. Photocurrent resulting from the excitation of the constructed cathode immersed in an aqueous solution with radiation from the solar spectrum was also observed. The research carried out so far shows that the constructed electrode is promising in terms of the possibility of using it for photoelectrocatalytic water splitting.

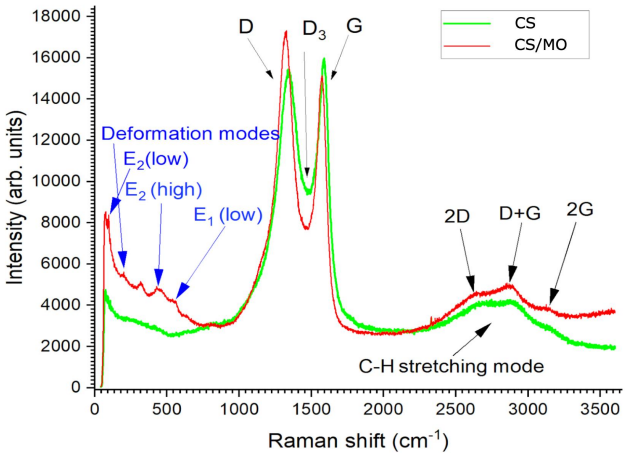

Fig.1. Raman spectra of an electrode (green curve) and carbon/MO structure (red curve). In the low-energy part of the spectrum, peaks from MO are visible.

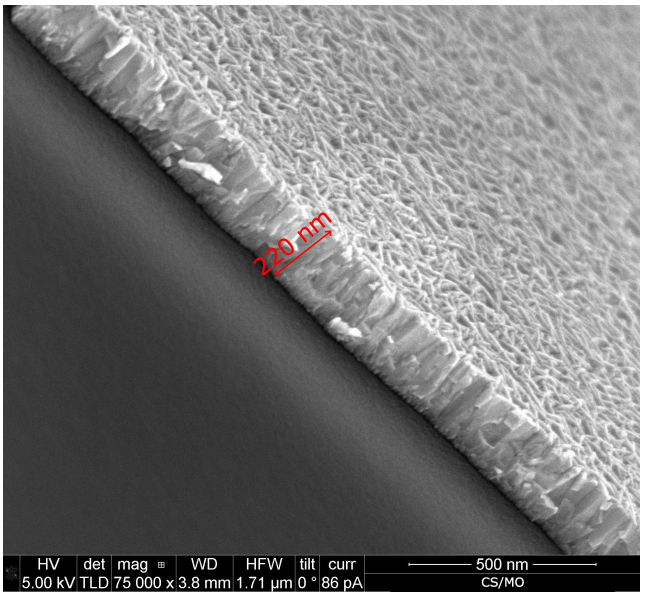

Fig.2 SEM image of the deposited metal oxide layer onto a carbon.

Degradation studies of $MAPbI_3$ perovskite using cathodoluminescence and microscopy techniques

Sara Piotrowska[1], Anna Reszka[2], Adam Wincukiewicz[1], Mateusz Tokarczyk[1], Bogdan J. Kowalski [2], Maria Kamińska[1]

[1] *Institute of Experimental Physics, Faculty of Physics, University of Warsaw, Ludwika Pasteura 5, Warsaw, Poland*
[2] *Institute of Physics, Polish Academy of Sciences, Al. Lotników 32/46, Warsaw, POLAND*

In modern times, considering climate change, we desperately look for sustainable energy sources. Photovoltaic cells are one of the most popular solutions to this problem. The widely used type of solar cells are those made of silicon, however, they are not without drawbacks - they are still too expensive and close to their efficiency limit. Moreover, their production is not as ecological as one could wish. In recent years, there has been a strong development of new generations of solar cells made with various materials acting as active layers. One of the most promising candidates for future applications in photovoltaics are hybrid organic-inorganic perovskites. The research shows that they can outperform Si cells in terms of efficiency, the cost of their production is much lower, and there are many ways to produce them in a more eco-friendly way[1].

The biggest problem with perovskites is that they can easily deteriorate under exposure to oxygen, water, and light. It is speculated that the degradation process depends on the size of the crystallites and the number of grain boundaries. In this study, we examined the effect of the perovskite (MAPbI3, where MA stands for methylammonium) synthesis process, carried out at different rates, on the surface morphology of $MAPbI_3$, in order to obtain the largest possible grains, and we followed the degradation process. Scanning electron microscopy and cathodoluminescence (CL) techniques were applied for the study. CL allowed the tracking of the degradation process at a spatial resolution of tens of nanometers, as the luminescence of $MAPbI_3$ and its degradation product PbI_2 are spectrally well separated (710 nm versus 490 nm). In the preliminary studies, it was shown that indeed the degradation is preferential at grain boundaries (Fig. 1).

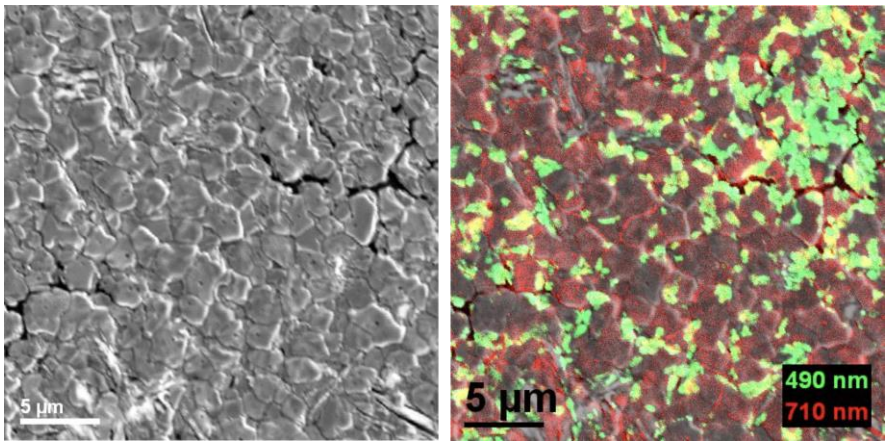

Fig. 1. (left) SEM image and (right) SEM-CL image detected at 490 nm (maximum of PbI_2 luminescence) and 710 nm (maximum of $MAPbI_3$ perovskite luminescence).

[1] X. Fan et al., Perovskite Solar Cells toward Eco-Friendly Printing, *Research 2021**(4)**:1-11* (2021)

Polymer solar cells thermal annealing of active layers – impact of annealing temperature on efficiency and ageing rate

W. Mech, M. Kamińska, K. P. Korona

Faculty of Physics, University of Warsaw, Pasteura 5, 02-093 Warsaw, Poland

Polymer solar cells are a third-generation photovoltaic cells that attract a great research interest in the last years. Their most important part is an active layer responsible for solar light absorption and exciton separation. The active layer is a nanoscale blend of organic semiconductors: donor and acceptor materials forming of bulk heterojunction. Typically, it is polymer (e.g. PTB7-Th) and fullerene derivative (e.g. $PC_{70}BM$). Polymer solar cells have some advantages comparing to silicon solar cells: low cost and ecological production, low weight, flexibility, possible semi-transparency and ease of production of multi-junction cells.

There are also some important disadvantages: lower efficiency and weaker air stability. One of these cons, lower efficiency, has been improved by application of a non-fullerene acceptor materials in form of low band-gap organic molecules e.g. BTP-4Cl-12 [1]. Such new acceptors have higher absorption near maximum of solar light spectrum than regular organic acceptor e.g. $PC_{70}BM$ with maintaining the same or better electron mobility. For the new acceptor with lower band-gap there were developed new donor materials like PBDB-T-2F with matching band-gap and energy levels what increased efficiency to over 17% in 2019 [1].

We present our results of research on two active layers of polymer solar cells: well known PTB7-Th:PC70BM and state-of-art PBDB-T-2F:BTP-4Cl-12. We tested annealing temperature impact on crucial parameters of the cells and on their long time stability. Thermal annealing not only removes solvents residues but also improves carrier mobility. The effects of annealing on the cell efficiency were showed in Fig.1. We obtained maximum cells efficiency 5.1% for PTB7-Th:$PC_{70}BM$ annealed at 50°C and 8.1% for PBDB-T-2F:BTP-4Cl-12 annealed at 130°C. Optical absorbance spectroscopy was carried out to check influence of thermal annealing on excitonic transitions. We observed clear BTP-4Cl-12 absorbance peak redshift after annealing (Fig. 2). The photocurrent spectra confirmed efficient current generation in both donor and acceptor materials. To investigate long-time stability of the cells a 4 months ageing measurements were performed. We have found out that optimal thermal annealing significantly improved cell stability.

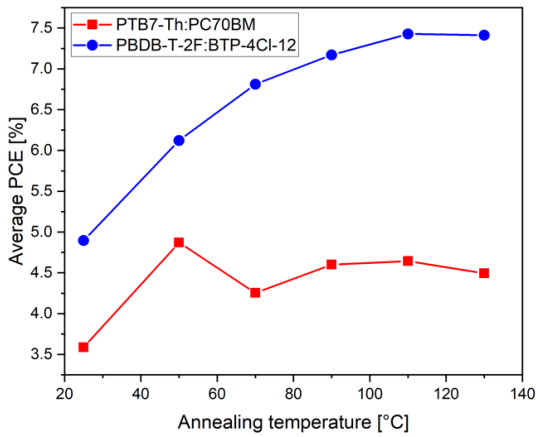

Fig. 1. Average power conversion efficiency (PCE) vs. annealing temperature.

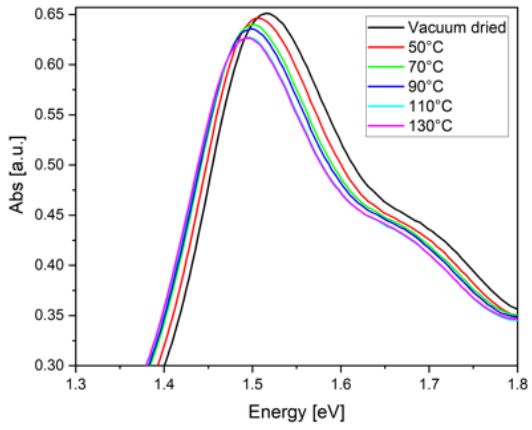

Fig. 2. Absorbance spectra of BTP-4Cl-12 annealed at different temperatures

[1] Y. Cui, *et al., National Science Review* **7**, 1239 (2020)

Towards Electrostatically Gated Perovskite Thin Films

Alexander Szoła, Wojciech Kolesiński, Mateusz Kędziora, Mateusz Goryca

University of Warsaw, Faculty of Physics, Pasteura 5, Warsaw 02-093, Poland

Perovskite semiconductors are widely studied in the context of solar light harvesting used for photovoltaic applications, but less in the context of their fundamental physical properties. As a medium exhibiting strong light-matter coupling, they may constitute an interesting platform for optoelectronics and opto-spintronics in particular.

Our long-term goal is to study spin dynamics in those materials to explore their potential applications in opto-spintronics. For that, we need to control the charge density in studied structures in a reliable way.

Here we present our efforts in the fabrication of electrostatically gated perovskite thin film encapsulated in hexagonal boron nitride - needed for the protection of the perovskite material from contamination and degradation. The electrostatic gating in the proposed van der Waals heterostructure is performed with the use of a graphene flake making and electrical contact with the perovskite film, as shown in Figure 1.

In our approach we modify the methods widely applied for the fabrication of transition metal dichalcogenide (TMD) structures, not only to obtain perovskite structures of high optical quality, but also to exploit the possibility to combine them with TMD materials in the future.

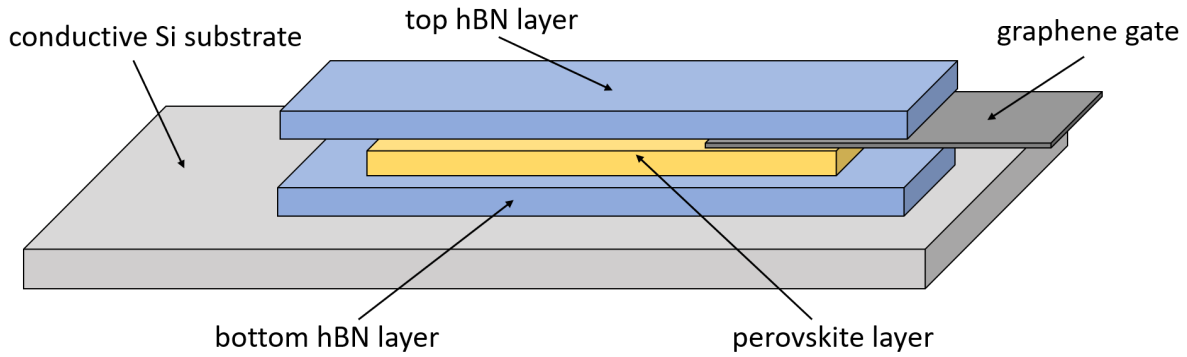

Figure 1: A schematic of perovskite thin film encapsulated between hexagonal boron nitride (hBN) slabs, electrostatically gated via graphene flake.

The structure and properties of bilayer borophene

Subrata Rakshit and Nevill Gonzalez Szwacki

Institute of Experimental Physics, Faculty of Physics, University of Warsaw, Pasteura 5, PL-02093 Warsaw, Poland

Borophene is a crystalline atomic monolayer of boron that exhibits several polymorphic forms [1]. In recent years, borophene has been identified as a rising star in materials science for the development of sensors, energy storage devices, and batteries.

Very recently it was experimentally demonstrated [2] the synthesis of an atomically well-defined borophene polymorph beyond the single-atomic-layer limit. The structure of the bilayer borophene is consistent with two covalently bonded α-sheets. While these sheets retained the highly desirable electrical and mechanical properties of single-layer borophene, it is proposed that the space between the layers could be used for energy or chemical storage. For example, the inclusion of a layer of lithium ions could enable the manufacture of 2D batteries.

In this work, we present the results of first-principles calculations for double-layer boron structures consisting of hexagonal, α-sheet, or honeycomb boron layers (see Fig. 1). Different arrangements between the layers have been considered. For the most stable structures, the electronic, elastic, and transport properties are studied. According to our calculations, the high metallic character of borophenes is, in most cases, preserved also for the double-layer structures. Also, the structural stability of the single layers is reinforced by the presence of interlayer bonds.

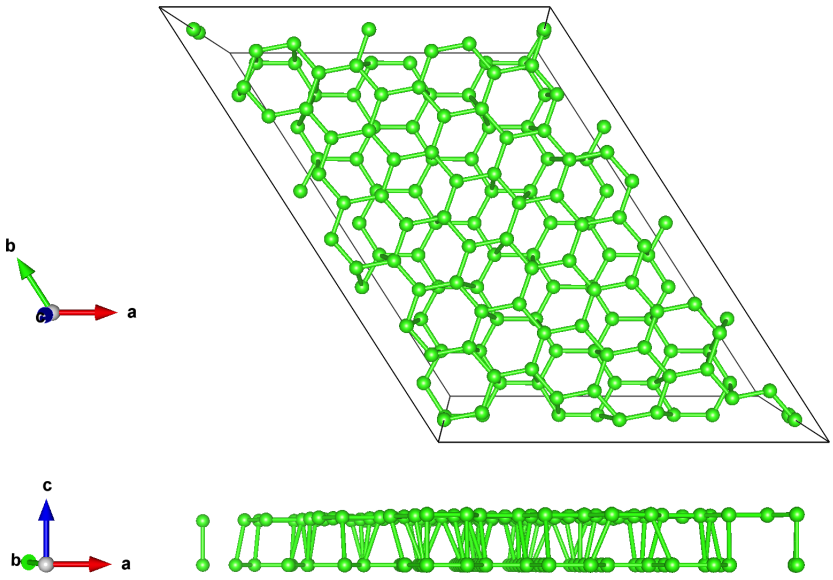

Figure 1: The atomic structure of double layer borophene. The single layers are boron honeycomb (*hc*) structures. The bottom panel shows the bonding between the layers.

[1] T. Tarkowski, N. Gonzalez Szwacki, and M. Marchwiany, *Phys. Rev. B* **104**, 195423 (2021).

[2] X. Liu et al., *Nat. Mater.* **21**, 35 (2022).

Towards Strain Engineering of High Quality 2D Perovskite Flakes

K. Zalewska[1], K. Posmyk[1], M. Śmiertka[1], M. Mączka[2], K. Watanabe[3], T. Taniguchi[4], M. Dyksik[1], M. Baranowski[1], P. Płochocka[1,5], A. Surrente[1]

[1] *Wrocław University of Science and Technology, Wrocław, Poland*
[2] *Inst. of Low Temp. and Structure Research, PAN, Wrocław, Poland*
[3] *Research Center for Functional Materials, NIMS, Tsukuba, Japan*
[4] *International Center for Materials Nanoarchitectonics, NIMS, Tsukuba, Japan*
[5] *Laboratoire National des Champs Magnétiques Intenses, CNRS Toulouse, France*

While strain engineering is a well-established tool to tune the optoelectronic properties of graphene and transition metal dichalcogenides [1], this approach is still at its infancy for two-dimensional (2D) metal halide perovskites. Before systematically applying uniaxial or biaxial stresses to 2D perovskites, it is essential to introduce an exfoliation strategy which enables to obtain flakes of optical quality comparable to that of the parent crystal.

Here, starting from $(PEA)_2PbI_4$ 2D perovskite crystals shown in Fig. 1(a), we exfoliate and encapsulate in hBN thin perovskite flakes [see Fig. 1(b)]. The high quality of both crystal and exfoliated flakes is demonstrated by the sharp resonances visible in the reflectance spectra of Fig. 1(c,d), attributed to bright, fine-structure split excitons. To test the response to external mechanical stimuli, we transferred $(PEA)_2PbI_4$ flakes to the non-planar substrates shown in Fig. 1(e) [2], and measured the room temperature PL spectrum as a function of the strain. The variation of the PL energy with increasing strain suggests the presence of an effect of the mechanical deformation on the electronic properties of these flakes.

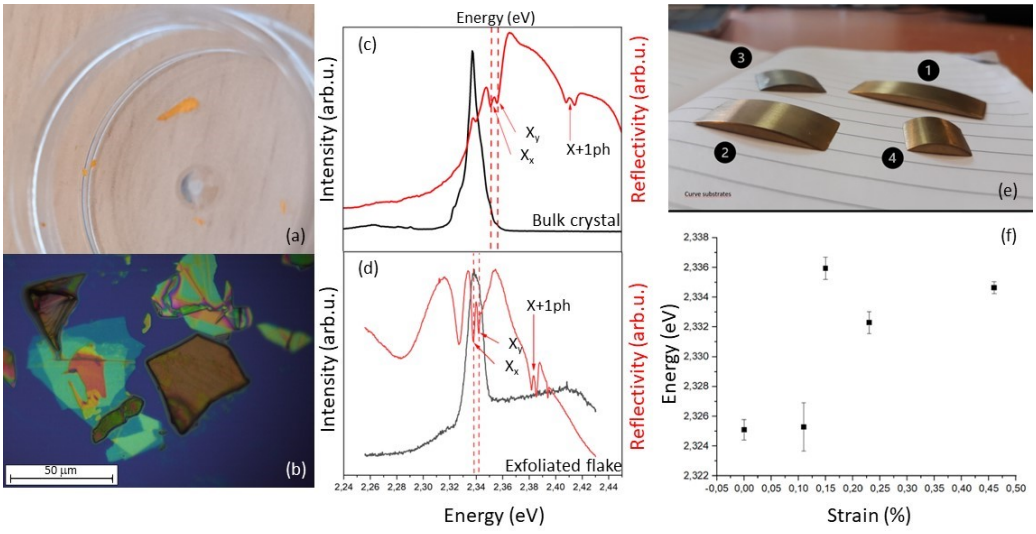

Figure 1: (a) Bulk $(PEA)_2PbI_4$ crystals used for the exfoliation of thin perovskite flakes. (b) hBN-encapsulated $(PEA)_2PbI_4$ flakes. Low temperature PL and reflectance spectrum of (c) the parent bulk $(PEA)_2PbI_4$ crystal and the exfoliated flakes. Relevant excitonic resonances are indicated. (e) Photograph of the curved substrates on which some flakes were transferred. (f) Room temperature PL energy of a flake transferred on substrates of different radii of curvatures.

[1] E. Blundo, *et al.*, Appl. Phys. Rev. **8**, 021318 (2021).
[2] Q. Tu, *et al.*, ACS Energy Lett. **4**, 796 (2019).

Solutions for spectroscopy and imaging

Markus Krause

Quantum Design GmbH, Im Tiefen See 58, 64-293 Darmstadt, Germany

The manufacturer Andor Technology provides a range of spectral instruments suitable for a wide range of spectroscopy applications. Czerny-Turner with different focal lengths and echelle spectrographs come pre-aligned and pre-calibrated for ease of operation.

Our modular spectroscopy systems are individual configurations. The range of spectrographs is complemented by detector technology for wavelength regions from the UV to the near-IR.
The Shamrock and Kymera series from Andor offer a wide range of spectrographs to find a solution for every application. The main difference of the three models is the focal length: 328, 500 and 750 mm, respectively. All models are based on the optical design according to Czerny-Turner. We offer:

-Pre-aligned, pre-calibrated spectrograph
-Large choice of light coupling interfaces
-Wide range of interchangeable gratings
-Monochromator capabilities
-Third party software support.

As mentioned above we also offer suitable detectors e.g. low-noise slow scanning CCD detectors for standard spectroscopy applications and high-performance CCD detectors for faster acquisitions. The EMCCD sensors are dedicated for measurements limited by read noise. The InGaAs photo diode arrays are ideal for wavelengths over 1000 nm.

Common features are their high-sensitivity in the UV and visible range. Thermo-electric cooling and high-quality AD converters reduce noise to allow application even in extreme low-light conditions.

Van der Waals materials for nanophotonic applications

Panaiot G. Zotev[1], Yue Wang[2], Daniel Andres-Penares[3], Toby Severs Millard[1], Luca Sortino[4], Nic Mullin[1], Donato Conteduca[2], Xuerong Hu[1], Charalambos Louca[1], Mauro Brotons-Gisbert[3], Sam Randerson[1], Armando Genco[1], Jamie Hobbs[1], Brian Gerardot[3], Thomas F. Krauss[2], A.I. Tartakovskii[1]

[1]*Department of Physics and Astronomy, University of Sheffield, Sheffield S3 7RH, UK*
[2]*Department of Physics, University of York, York, YO10 5DD, UK*
[3]*School of Engineering and Physical Sciences, Heriot-Watt University, Edinburgh, EH144AS, UK*
[4]*Nanoinstitute Munich, Faculty of Physics, Ludwig-Maximilians-Universität, München, 80539, Munich, Germany*

Nanophotonic structures enable a range of applications including optical waveguiding, Purcell enhancement of emission, low-threshold lasing and higher harmonic generation enhancement. Many research fields and technologies have benefited from nano-scale resonators and waveguides previously fabricated from noble metals [1] or high refractive index dielectrics such as silicon [2] and III-V materials [3]. While these offer a large range of opportunities for both research and technology, van der Waals materials may expand the possibilities of nanophotonics in the visible and near-infrared portion of the spectrum due to high, super-Mossian refractive indices ($n \approx 4$) [4], a large range of transparency windows, and numerous advantages due to their weak van der Waals attractive forces. In order to inspire and facilitate nanophotonic structures fabricated from these layered materials, we extract the dielectric constants of a diverse set including transition metal dichalcogenides (TMDs), III-VI semiconductors, and magnetic layered materials. Employing well established techniques, we fabricate nanoresonators with a range of geometries from these materials and observe Mie resonances as well as strong coupling between the excitonic features of TMDs and anapole modes with Rabi splittings up to 140 meV. After the transfer of a monolayer of WSe_2 onto WS_2 nanoantennas, we observe room temperature Purcell enhancement of emission [5] and low temperature formation of single photon emitters with enhanced quantum efficiencies within a system fabricated entirely from layered materials. Due to the weak van der Waals interactions of the nanoresonators and the substrate, we were able to employ an atomic force microscopy (AFM) cantilever in the repositioning of double-pillar nanoantennas to achieve ultra-small gaps ($\approx$10 nm) [5]. This post-fabrication technique enables applications such as stable, low-power optical trapping of quantum emitters with Purcell enhancement factors above 150.

[1] Y. Luo et al, *Nature Nanotechnology* **13**, 1137-1142 (2018).
[2] Y. Li et al, *Nature Nanotechnology* **12**, 987-992 (2017).
[3] L. Sortino et al, *Nature Communications* **12**, 6063 (2021).
[4] R. Verre et al, *Nature Nanotechnology* **14**, 679-683 (2019).
[5] P. Zotev et al, *ACS Nano* **16**, 6493-6505 (2022).

Excitation Dependent Energy Transfer in 2D Heterostructure

Arka Karmakar [1], Tomasz Kazimierczuk [1], Igor Antoniazzi [1], Mateusz Raczyński [1], Takashi Taniguchi [2], Kenji Watanabe [3], Adam Babiński [1], Abdullah Al-Mahboob [4], and Maciej R Molas [1]

[1] *Division of Solid State Physics, Institute of Experimental Physics, Faculty of Physics, University of Warsaw, Pasteura 5, 02-093 Warsaw, Poland*
[2] *International Center for Materials Nanoarchitectonics, National Institute for Materials Science, 1-1 Namiki, Tsukuba, Ibaraki 305-0044, Japan*
[3] *Research Center for Functional Materials, National Institute for Materials Science, 1-1 Namiki, Tsukuba, Ibaraki 305-0044, Japan*
[4] *Center for Functional Nanomaterials, Brookhaven National Laboratory, Upton, NY 11973, USA*

Monolayer (1L) thick two-dimensional (2D) transition metal dichalcogenides (TMDs) exhibit strong light-matter interaction [1]. Vertical heterostructures (HSs) made by the stacking of different TMDs have already shown promises for future optoelectronic device applications [2]. Interlayer charge (CT) and energy transfer (ET) are the two main photocarrier relaxation pathways in the TMD HSs. The interlayer CT process mainly occurs due to the energy level offset between the two materials, which survives only up to few nm distance [3]. Whereas, the long-distance interlayer ET process can survive up to several tens of nm [4]. Our previous work [5] has shown that due to the strong *overlap* between the *optical bandgaps* of the two TMDs, interlayer ET process dominates over the traditional CT process. In the present work [6], we explore the effect of resonant *overlap* between the *high-lying* excitonic resonances in the long-distance ET process in HS made by the 1Ls of molybdenum disulfide (MoS_2) and tungsten diselenide (WSe_2). At, low temperature (8 K) resonant excitations from the lower bandgap WSe_2 B and D excitonic levels create more photocarriers at the higher bandgap MoS_2 layer, resulting an enhanced (~2×) MoS_2 PL emission from the HS area. With the increasing temperature the enhanced PL emission starts to destroy due to the increased electron-phonon scattering. Our work provides a new insight into the long-distance interlayer ET process from the *lower-to-higher* bandgap TMD material, which will be beneficial in developing TMD-based future optoelectronic device applications.

References:

[1] U. Wurstbauer, B. Miller, E. Parzinger, and A. W. Holleitner, *J. Phys. D: Appl. Phys.* 50 (2017) 173001.
[2] N. Huo, Y. Yang, and J. Li, *J. Semicond.* 2017, 38 031002.
[3] L. Britnell, R. V. Gorbachev, R. Jalil, B. D. Belle, F. Schedin, M. I. Katsnelson, L. Eaves, S. V. Morozov, A. S. Mayorov, N. M. R. Peres, A. H. C. Neto, J. Leist, A. K. Geim, L. A. Ponomarenko, and K. S. Novoselov, *Nano Lett.* 2012, 12, 3, 1707–1710.
[4] F. Federspiel, G. Froehlicher, M. Nasilowski, S. Pedetti, A. Mahmood, B. Doudin, S. Park, J-O Lee, D. Halley, B. Dubertret, P. Gilliot, and S. Berciaud, *Nano Lett.* 2015, 15, 2, 1252–1258.
[5] A. Karmakar, A. Al-Mahboob, C. E. Petoukhoff, O. Kravchyna, N. S. Chan, T. Taniguchi, K. Watanabe, and K. M. Dani, *ACS Nano* 2022, 16, 3, 3861–3869.
[6] A. Karmakar, T. Kazimierczuk, I. Antoniazzi, M. Raczyński, T. Taniguchi, K. Watanabe, A. Babiński, A. Al-Mahboob, and M. R Molas, *arXiv*:2301.05644.

Dexter induced inverted valley polarization in monolayer WSe_2

J. Jasiński[1], S. Palai[2], M. Śmiertka[1], F. Gucci[3], A. Genco[3], S. Dal Conte[3], K. Watanabe[4], T. Taniguchi[5], M. Baranowski[1], P. Plochocka[1,2], A. Surrente[1]

[1] *Wrocław University of Science and Technology, Wrocław, Poland*
[2] *Laboratoire National des Champs Magnétiques Intenses, CNRS Toulouse, France*
[3] *Dipartimento di Fisica, Politecnico di Milano, Milano, Italy*
[4] *Research Center for Functional Materials, NIMS, Tsukuba, Japan*
[5] *International Center for Materials Nanoarchitectonics, NIMS, Tsukuba, Japan*

A highly efficient, but not particularly explored, intervalley scattering mechanism in transition metal dichalogenides resembles a Dexter coupling in the reciprocal space. This mechanism couples exciton states with the same spin in different valleys [1].

Here, we demonstrate that the Dexter-type intervalley scattering affects not only the neutral exciton [1], but also other excitonic complexes of a monolayer WSe_2. While the photoluminescence (PL) spectrum is co-polarized with the excitation laser when this is tuned far-off resonance with either A or B exciton, its degree of circular polarization (DCP) becomes negative when the laser light is tuned resonant with B exciton, as shown in Fig. 1(a). This vanishing or negative polarization of the exciton and biexciton complexes is confirmed by the polarization-resolved PL excitation (PLE) of Fig. 1(b,c,d). Pump-probe measurements shown in Fig. 1(e,f) demonstrate that immediately after an excitation pulse resonant with A exciton is absorbed, the DCP is negative, thus supporting the Dexter coupling as main mechanism driving the exciton dynamics in this condition.

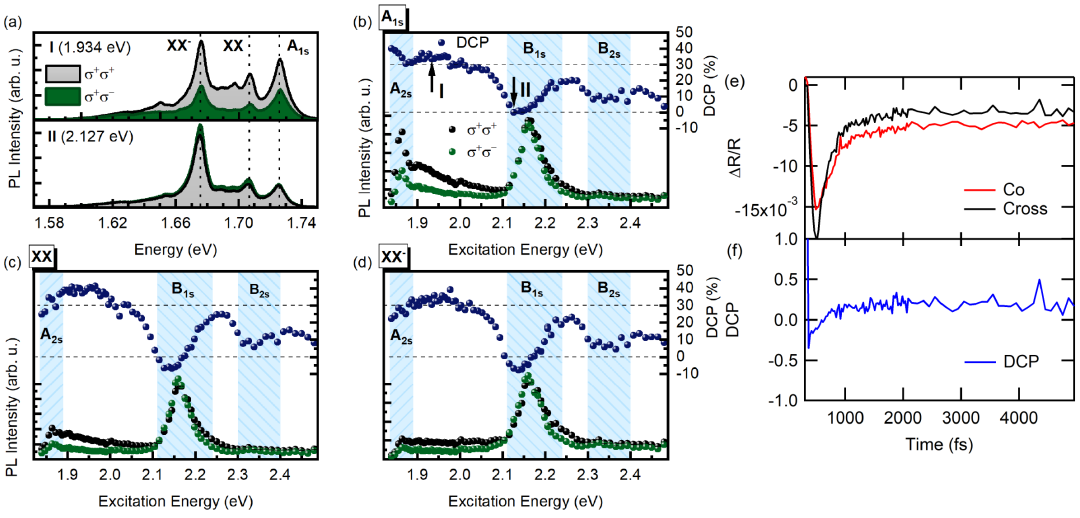

Figure 1: (a) PL spectra of encapsulated monolayer WSe_2 with detection of the light co-polarised ($\sigma^+\sigma^+$) and cross-polarised ($\sigma^+\sigma^-$) to excitation. Excitation energy between A_{2s} and B_{1s} in top panel and resonant with B_{1s} exciton in the bottom panel. (b,c,d) Excitation energy dependent PL intensity of the co- and cross-polarised emission and calculated degree of circular polarisation (DCP) for A_{1s}, XX and XX^-, respectively. (e) Photoinduced absorption of the B_{1s} exciton and (f) degree of circular polarization for an excitation resonant to A_{1s} exciton.

[1] G. Berghäuser, *et al.*, Nature Communications **9**, 971 (2018).

Hot luminescence or Raman scattering in monolayers of $MoSi_2N_4$

Maciej R. Molas[1], **Tomasz Woźniak**[2], **Łucja Kipczak**[1], **Adam Babiński**[1], **Su Sun**[3], **Chuan Xu**[3] **and Wencai Ren**[3]

[1] *Institute of Experimental Physics, Faculty of Physics, University of Warsaw, Warsaw, Poland*
[2] *Department of Semiconductor Materials Engineering, Wrocław University of Science and Technology, Wrocław, Poland*
[3] *Shenyang National Laboratory for Materials Science, Institute of Metal Research, Chinese Academy of Sciences, Shenyang, P. R. China*

Monolayers (MLs) of semiconducting transition metal dichalcogenides (S-TMDs), *e.g.* MoS_2 and WSe_2, have been demonstrated to carry the spin-like degree of freedom known as valley pseudospin due to the optical bandgap located at the $K^{\pm}$ points of their hexagonal Brillouin zone [1]. Recently, MLs of the MSi_2Z_4 family (M = Mo, W; Z = N, P, As, Sb), which form a new class of hexagonal non-centrosymmetric materials hosting extraordinary spin-valley physics, have been discovered [2].

In this work, we investigate the optical response of the $MoSi_2N_4$ ML, grown using chemical vapor deposition on Si/SiO_2 substrate [3], with the aid of photoluminescence (PL) performed in a wide range of temperature (5 – 300 K) and first principles calculations.

The relative PL spectra, calculated as the difference between the PL spectra measured on the ML and on the Si/SiO_2 substrate, as shown in the Figure. $MoSi_2N_4$ MLs are semiconductors with an indirect band gap of about 1.94 eV at 300 K. However, the excitation of the PL spectra with high energies of 3.06 eV or near to the band gap of 1.96 eV does not give rise to a measurable signal either at 300 K or at 5 K. Nevertheless, a significant PL is apparent under excitation close to the so-called A and B direct transitions in the $K^{\pm}$ valleys [3]. The obtained relative spectra are combined of two types of emission, *i.e.* a broad band with linewidths of ~200 meV, on top of which a series of narrow peaks emerges. Consequently, it is difficult to decompose this emission to Raman scattering or hot luminescence, since the ratio between the resonantly enhanced Raman signal and the optical recombination at the $K^{\pm}$ points is unknown. At T=5 K, only the Raman peaks are seen, which were ascribed to phonon modes using the calculated phonon dispersion spectrum.

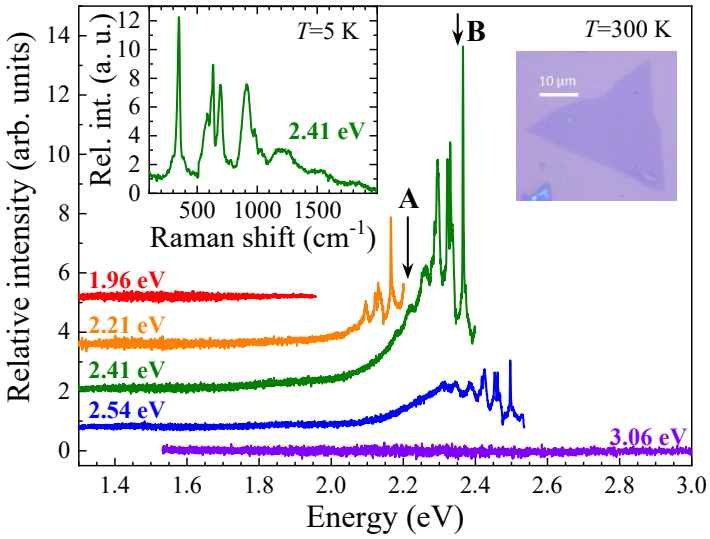

Figure Relative PL spectra of $MoSi_2N_4$ ML under different excitations. The insets show the spectrum at 5 K and the optical image of the studied ML.

Our results are the spore of research devoted to the MLs of the $MoSi_2N_4$ family, which properties locates them as ideal candidates for valleytronics, in line with S-TMD MLs.

[1] M. Koperski, *et al.*, *Nanophotonics* **6**, 1289 (2017).
[2] T. Woźniak, *et al.*, *Small* 2206444 (2023).
[3] Y.-L. Hong, *et al.*, *Science* **369**, 670 (2022).

Surface and Structural Analysis of (110)-oriented $Pb_{1-x}Sn_xTe$ Topological Crystalline Insulator

Sania Dad, Piotr Dziawa, Maciej Wójcik, Sławomir Kret, Jarosław Z. Domagała, Elżbieta Łusakowska, Piotr Wojnar, Janusz Sadowski

Institute of Physics, Polish Academy of Sciences, Aleja Lotnikow 32/46, PL-02-668 Warsaw, Poland

The novel class of semiconductors namely topological crystalline insulators (TCIs) is a rapidly developing research area of modern solid state physics. In these materials, surface electron states with Dirac dispersion relation are formed on certain high symmetry surfaces. $Pb_{1-x}Sn_xTe$ alloy has been experimentally discovered as a member of TCIs family in the previous decade. It exhibits topological phase transition above a critical concentration of Sn ($x \geq 0.36$ at LHe temperature) [1]. Theoretical predictions of band inversion at high symmetry L point in the Brillouin zone, and experimental evidence for topologically protected states on (001) [2] and (111) surfaces [3] of $Pb_{1-x}Sn_xTe$ alloy have already been proclaimed in literature. However, (110)-oriented $Pb_{1-x}Sn_xTe$ has not been studied experimentally in this context yet. We have grown thin layers of $Pb_{1-x}Sn_xTe$ solid solution by molecular beam epitaxy (MBE). To our knowledge the growth of $Pb_{1-x}Sn_xTe$ in the (110) orientation has not been reported so far. We have found that direct growth on epi-ready GaAs(110) substrates resulted in non-uniform layers with mixed (100) and (111) orientations. To get around this problem we have used hybrid substrates with thick CdTe(110) buffer grown in separate MBE system. The layers have been investigated by several characterization techniques such as energy dispersive X-ray fluorescence, atomic force microscope, X-ray diffraction and, high resolution transmission electron microscopy which reveals the (110)-orientation of $Pb_{1-x}Sn_xTe$. Angle-resolved photoemission experiments are underway to identify topologically protected surface states on the $Pb_{1-x}Sn_xTe$(110) surface.

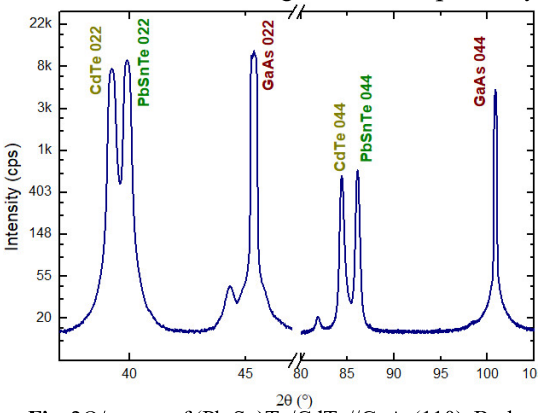

Fig. 2Θ/ω scan of (Pb,Sn)Te/CdTe//GaAs(110). Both (Pb,Sn)Te layer and CdTe buffer show same out of plane <011> growth

The authors acknowledge funding from the National Science Centre Poland, through projects No: 2019/35/B/ST3/03381, 2019/35/B/ST5/03434 and 2017/27/B/ST3/02470

[1] V.V. Volobuev, P.S. Mandal, M. Galicka, O. Caha, J. Sánchez-Barriga, D. Di Sante, A. Varykhalov, A. Khiar, S. Picozzi, G. Bauer. *Advanced Materials*.29.(**3**), 1604185**,** (2017).
[2] S.-Y. Xu, C. Liu, N. Alidoust, M. Neupane, D. Qian, I. Belopolski, J. Denlinger, Y. Wang, H. Lin, L.a. Wray. *Nature communications*.3.(**1**), 1-11**,** (2012).
[3] C. Yan, J. Liu, Y. Zang, J. Wang, Z. Wang, P. Wang, Z.-D. Zhang, L. Wang, X. Ma, S. Ji. *Physical review letters*.112.(**18**), 186801**,** (2014).

Ferromagnetic topological crystalline insulator $Sn_{1-x}Mn_xTe$ in an inhomogeneous magnetic field

A. Kazakov[1], V.V. Volobuev[1], M. Chojnacki[1,2], T. Wojciechowski[1,2], T. Wojtowicz[1]

[1] *International Research Centre MagTop, Institute of Physics, Polish Academy of Sciences, al. Lotników 32/46, 02-668 Warsaw, Poland*
[2] *Institute of Physics, Polish Academy of Sciences, al. Lotników 32/46, 02-668 Warsaw, Poland*

The archetypical topological crystalline insulator (TCI) SnTe doped with manganese becomes ferromagnetic at low temperatures. In the ferromagnetic state, there is an additional contribution to the Hall resistance, the anomalous Hall effect (AHE, R_{xy}^{a}), which depends on the magnetization of the material. An inhomogeneous external magnetic field modifies the spin texture of the magnetic material and can lead to the so-called topological Hall effect. The inhomogeneous magnetic field can be created by placing magnetic or superconducting (SC) structures on top of the layer under investigation. In the case of an SC layer made of type II superconductor, the inhomogeneity is caused by a vortex lattice formed in the magnetic field.

Previously, the effect of an inhomogeneous magnetic field on magnetotransport was studied mainly in non-magnetic materials. In this work, we extend this approach to ferromagnetic topological insulators. We grew 30-50 nm thin layers of $Sn_{1-x}Mn_xTe$ with a Curie temperature of around 5 K by molecular beam epitaxy. These layers were then processed in two-section Hallbars. One of the sections was covered with a SC Nb separated from the epilayer by a thin (~20 nm) oxide layer. The other section of the Hall bar was left bare for comparison. The influence of the SC layer on the magnetotransport of TCI ferromagnet was probed by measuring AHE in the $Sn_{1-x}Mn_xTe$ layer. We found that the AHE hysteresis loop in the covered area, $R_{xy}^{a,c}$, was wider than in the uncovered area, $R_{xy}^{a,u}$, as seen in Fig. a,b. This widening is caused by the Meissner effect and is a direct consequence of the modulation of the magnetic field by the SC layer. The difference between AHE curves in the uncovered and covered areas gives profiles that strongly resemble the magnetization curves of a superconductor (Fig. c). We also observed that additional peaks appear on a $R_{xy}^{a,g} - R_{xy}^{a,u}$ curve, indicating the emergence of the topological Hall effect caused by a SC flux inhomogeneity.

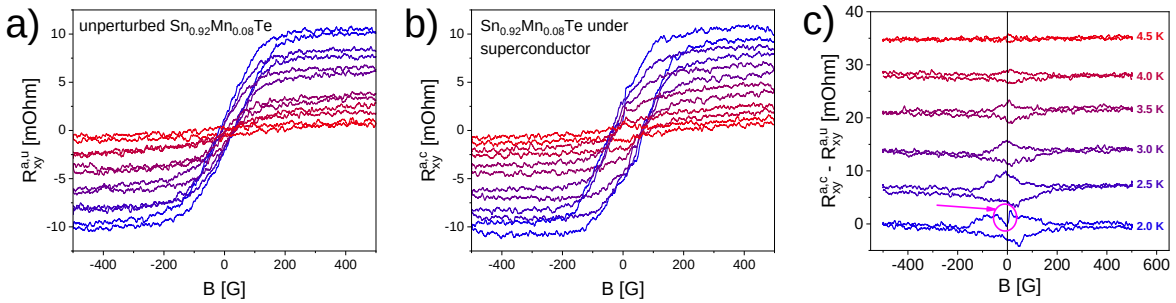

(a,b) AHE contribution to the Hall resistance R_{xy}^{a} in $Sn_{0.92}Mn_{0.08}Te$ measured as a function of the magnetic field B for various temperatures. AHE hysteresis in the Hallbar under the SC is much wider than in the bare epilayer. (c) The difference between AHE curves in covered and uncovered areas ($R_{xy}^{a,g} - R_{xy}^{a,u}$ resembles magnetization hysteresis. However, under certain conditions additional spike (marked with a magenta circle) appears, which can be considered as a signature of the topological Hall effect.

This research was partially supported by the Foundation for Polish Science through the IRA Programme co-financed by EU within SG OP.

Signatures of Weyl Fermions in Magnetotransport of Topological Semimetal α-Sn

Jakub Polaczyński [1], Alexandr Kazakov[1], Wojciech Zaleszczyk[1], Bartłomiej Turowski[1], Chang-woo Cho[2], Benjamin A. Piot[2], Rafał Rudniewski[1] Tomasz Wojciechowski[1], Tomasz Wojtowicz[1] and Valentine V. Volobuev[1,3]

[1] *International Research Centre MagTop, Institute of Physics, Polish Academy of Science, Al. Lotników 32/46, PL-02668 Warsaw, Poland*
[2] *Laboratoire National des Champs Magnétiques Intenses, CNRS, LNCMI, Université Grenoble Alpes, Université Toulouse 3, INSA Toulouse, EMFL, F-38042 Grenoble, France*
[3] *National Technical University "KhPI", Kyrpychova Str. 2, Kharkiv 61002, Ukraine*

Topological semimetals have emerged as an attractive platform for both applied and fundamental research. This has been stimulated by their unique electronic properties, namely the presence of topological surface states (TSSs) and a linear, Dirac-like band structure in the bulk. Among the many compounds studied, α-Sn (grey tin) is of particular interest as a rare example of an elementary material with an inverted band structure. Nominally a zero-gap semiconductor, it can be turned into both Dirac semimetal (DSM) and topological insulator (TI) phases by strain [1]. Despite its rich topological phase diagram, most of reports focus on the properties of TSSs in the TI phase of grey tin.

Successful molecular beam epitaxy (MBE) on a hybrid, insulating CdTe/GaAs(001) substrates allows us to address a weakly explored part of the grey tin topological phase diagram of gray tin. With film thicknesses up to 200 nm and compressive in-plane strain introduced by the substrate, we ensure that our α-Sn layers are in the DSM phase. Here we will present the results of a thorough magnetotransport studies of our structures, focusing on signatures of 3D Dirac and Weyl fermions.

The π-Berry phase of Shubnikov-de Haas oscillations is found in magnetic fields both perpendicular (B_{perp}) and parallel (B_{paral}) to the current, which is a signature of the 3D nature of the observed carriers and their non-trivial topology. The low effective mass derived from the temperature-dependent amplitude of the oscillations, $m^* \approx m_0$, is consistent with previous reports. Importantly, we perform a detailed study of the negative longitudinal magnetoresistance (NLMR), present in B_{paral} up to 30 T. By ruling out alternative sources of NLMR, we are able to relate it to the chiral anomaly – a phenomenon expected for Dirac and Weyl semimetals. Finally, we analyse the anisotropic magnetoresistance (AMR) and the planar Hall effect (PHE), observed when the sample is rotated in a constant, in-plane magnetic field. We show that these effects exhibit an angular dependence consistent with anomaly-related magnetoresistance. Altogether, our work establishes the electronic properties of α-Sn as consistent with the 3D DSM phase, confirming previous theoretical predictions [1] and laying a solid foundation for further research.

[1] Huaquing Huang and Feng Liu, Phys. Rev. B **95** (2017), 201101(R)

The research was partially supported by the Foundation for Polish Science through the IRA Programme co-financed by EU within SG OP (Grant No. MAB/2017/1). J.P. and A.K. acknowledge support of LNCMI-CNRS, member of the European Magnetic Field Laboratory (EMFL) and of the Ministry of Education and Science, Poland (grant no. DIR/WK/2018/07) via its membership to the EMFL.

Magnetic Circular Dichroism from Exchange Splitting in Intrinsic Magnetic Topological Insulator MnBi2Te4

S.-K. Bac [1], F. Le Mardelé [2], J. Wang [1], L. Riney [1], K. Yoshimura [1], I. Mohelsky [2], M. Ozerov [3], M. Zhukovskyi [4], T. Orlova [4], M. Orlita [2,5], X. Liu [1], and B. A. Assaf [1]

[1] *Department of Physics and Astronomy, University of Notre Dame, Notre Dame, IN 46556, USA*
[2] *LNCMI-EMFL, CNRS UPR3228, Univ. Grenoble Alpes, Univ. Toulouse 3, INSA-T, Grenoble and Toulouse, France*
[3] *National High Magnetic Field Laboratory, Florida State University, Tallahassee, FL 32310, USA*
[4] *Notre Dame Integrated Imaging Facility, University of Notre Dame, Notre Dame, IN 46556, USA*
[5] *Institute of Physics, Charles University, CZ-12116 Prague, Czech Republic*

MnBi2Te4 has attracted significant attention due to exhibit both its non-trivial topology and its magnetism, which give rise to interesting phenomena such as the quantum anomalous Hall effect [1-3] and the axion insulator effect [4]. However, most studies have focused on the properties of its surface states while its bulk-originated bands have remained relatively understudied. In this study, we report recent magnetooptical infrared spectroscopy measurements conducted on the intrinsic magnetic topological insulator MnBi2Te4. We carried out infrared absorption measurements under magnetic fields up to 34 T and observed an optical absorption in the mid-infrared that shifts to higher energy as the magnetic field increases. The energy of the transition versus magnetic field reflects the behavior of the anomalous Hall effect.The transition energy increases through the canted magnetic state of MnBi2Te4 and then saturates at 8 T when the system enters a ferromagnetic state. Then, the transition energy further increases when the magnetic field is above 25 T, where the magnetization of Mn antisite defects is likely to start flipping. Additionally, this absorption displays a strong magnetic circular dichroism, which likely originates from band splitting under the effect of magnetic exchange. Our studies not only reveal the infrared response of MnBi2Te4 but also provide insight into how the electronic structure changes through the phase diagram of this material, consistently following the behavior of the magnetization.

[1] Chang, C.-Z. et al. Sci. (80-.). **340**, 167–170, (2013)
[2] Chang, C.-Z. et al. Nat. Mater. **14**, 473–477, (2015)
[3] Checkelsky, J. G. et al. Nat. Phys. **10**, 731–736, (2014)
[4] Liu, C. et al. Nat. Mater. **19**, 522–527, (2020)

Non-trivial topological phases in transition metal rich half-Heusler Oxides

Bhautik R. Dhori [1], Raghottam M. Sattigeri [2] and Prafulla K. Jha [1]

[1] *Department of Physics, Faculty of Science, The Maharaja Sayajirao University of Baroda, Sayajigunj, Vadodara, Gujarat – 390 002, India*
[2] *International Research Centre MagTop, Institute of Physics, Polish Academy of Sciences, aleja Lotników 32/46, Warsaw 02 – 668, Poland*

Topological Insulators with gapless surface states and insulating bulk in non-centrosymmetric cubic systems have been extensively explored following the discovery of two-dimensional quantum spin hall effect in zincblende HgTe.[1,2] In such systems the negative band inversion strength function E_{BIS} (= $E_{\Gamma 6}$ - $E_{\Gamma 8}$ < 0) governs the robustness of the non-trivial topological states at ambient conditions.[3] Hence, realizing large negative values of E_{BIS} has been a guiding motivation of several investigations reported in literature. Here, we present a material design approach which can be employed to realize large negative values of E_{BIS} in cubic materials such as Half-Heusler (HH) oxides with 18 valence electron configurations.[4] We explore, α-, β-, and γ-phase (by placing transition metal atom at different Wyckoff positions) in HH oxides XYO (X = Li, K, Rb; Y = Cu, Ag, Au) for their non-trivial topological phases. Off these three phases, we observed that, the α-phase of nine HH oxides (wherein the transition metal atoms occupy 4a Wyckoff positions in the crystal structure) is the most promising with non-trivial topological phase, governed by the Mass-Darwin relativistic effects which enhances the E_{BIS} function. Whereas the other phases are either trivial semi-conductors or conductors. We find that the E_{BIS} in the α-phase is as high as – 2.37 eV which would remain robust under ambient conditions. We also find that under modest strain fields, the band inversion strength is robust retaining the non-trivial character. The non-trivial character of these compounds is further verified by analyzing the orbital characters across the Fermi level, ARPES-like surface state spectra, slab band structures and the Z_2 invariants. We believe that the α-phase of HH oxides presented here can be synthesized experimentally for diverse room temperature applications.

[1] Bernevig, B. A., Hughes, T. L., & Zhang, S. C., *Science*, **314**(5806), 1757-1761, (2006)
[2] Konig, M., Wiedmann, S., Brune, C., et.al., *Science*, **318**(5851), 766-770, (2007).
[3] Zhang, X. M., Xu, G. Z., Du, Y., et.al., *J. Appl. Phys.*, **115**(8), 083704, (2014).
[4] Casper, F., Graf, T., Chadov, S., et.al., *Semicond. Sci. Technol.*, **27**(6), 063001, (2012).

Topological phase transition in SnTe topological crystalline insulator thin films

Saeed Samadi, Rafał Rechciński and Ryszard Buczko

Institute of Physics, Polish Academy of Sciences, Aleja Lotników 32/46, 02-668 Warsaw, Poland

The quantum spin Hall (QSH) phase was theoretically predicted in (111)-oriented thin films in a certain range of thicknesses in the SnTe class of topological crystalline insulators (TCIs). The energy gap changes sign and oscillates with increasing the number of layers due to intersurface hybridization. This leads to the emergence of the two-dimensional (2D) topological insulator phase classified by a $\mathbb{Z}_2$ invariant protected by time-reversal symmetry [1,2].

We study topological properties of symmetric (111)-oriented films with a twin plane (TP) in the middle of the structure. The TP forms a (111) mirror symmetry plane and can be either cationic or anionic type. Recently, we have shown that both a cationic and an anionic TP defines a 2D TCI with mirror Chern number $C_m = 2$ and $C_m = 1$, respectively [3]. Using tight binding approximation we calculate mirror Chern number and $\mathbb{Z}_2$ invariant for thin films with TPs for a wide range of thicknesses. We show that TP topology combined with finite-size effects can influence how the topological invariants change with growing film thickness.

In addition, we investigate phase transitions in (001) films by calculating the mirror Chern number and find that it oscillates between $C_m = +2$ and $C_m = -2$ with growing thickness. Using a realistic tight binding model we uncover that the oscillation is made up of two components — a slow one described in Ref. [4], and a fast one, due to valley mixing, which changes the sign of C_m with every two added layers. Following Ref. [5] we consider films with atomic steps located symmetrically on the two surfaces. Such steps constitute boundaries between areas of different film thickness. In agreement with Ref. [5], we find that there appear gapless step-edge modes protected by (001) mirror symmetry, whenever the thicknesses on both sides of the step correspond to different values of C_m.

This work was supported by the Polish National Science Centre under project No. 2016/23/B/ST3/03725. Computations were carried out using the computers of Centre of Informatics Tricity Academic Supercomputer & Network.

[1] J. Liu et al., Phys. Rev. B **91**, 081407(R) (2015)
[2] S. Safaei et al., New J. Phys. **17**, 063041 (2015)
[3] S. Samadi et al., arXiv:-2212.14640 (2022)
[4] H. Ozawa et al., Phys. Rev. B **90**, 045309 (2014)
[5] W. Brzezicki et al., Phys. Rev. B **100**, 121107 (2019)

Scanning Gate Microscopy Probing of Electron-Hole Interference in a Normal-Superconductor Junction

Shalini Maji[1], Karol Sowa[2], Michał P. Nowak[1]

[1] *AGH University of Science and Technology, Academic Centre for Materials and Nanotechnology, al. A. Mickiewicza 30, 30-059 Krakow, Poland*
[2] *AGH University of Science and Technology, Faculty of Physics and Applied Computer Science, al. A. Mickiewicza 30, 30-059 Krakow, Poland*

We theoretically investigate Scanning Gate Microscopy (SGM) probing of electron and hole trajectories in a two-dimensional Normal-Superconductor (NS) junction embedding a Quantum Point Contact (QPC). SGM is a well-known technique that has been used to visualize branched electron flow from QPCs [1]. In our work, taking advantage of recent progress in the realization of NS junctions in gated heterostructures [2], we propose to use this method for probing the paths of electrons and Andreev-reflected holes. We find that in an NS junction the conductance probed by the SGM technique exhibits oscillations that are due to the self-interference of electrons and holes. In contrast to ordinary SGM measurements, the interference occurs not only between the QPC and the SGM tip, but also between the tip and the NS interface. Most importantly, we show that for the measurements performed at a non-zero bias, the oscillations exhibit beating with the two periods determined by the two Fermi wavelengths that correspond to the electron and the hole wave-vectors. Finally, we show that at non-zero energy, the hole does not retrace the electron path due to the difference in the incident and reflection angles at the NS interference which, in turn, leads to a pronounced interference pattern in the conductance map [see Fig. 1].

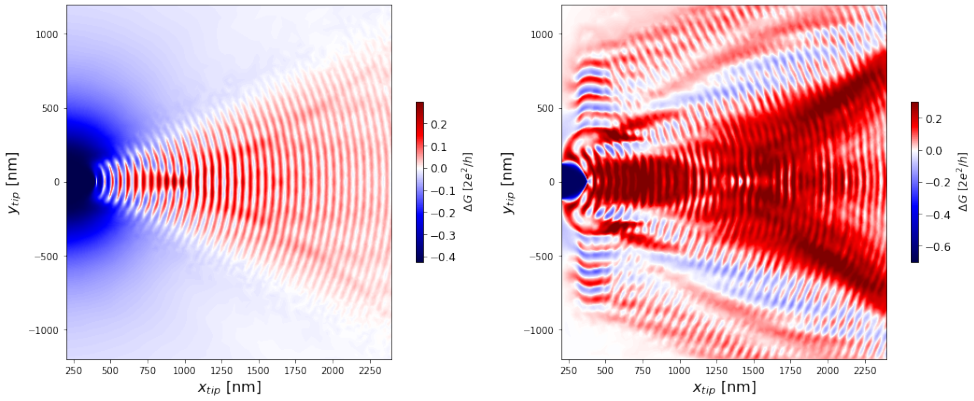

(a) Zero bias. (b) Non-zero bias.

Figure 1: Electron-hole interference in SGM conductance maps.

[1] M. A. Topinka, B. J. leRoy, S. E. J. Shaw, E. J. Heller, R. M. Westervelt, K. D. Maranowski, A. C. Cossard, *Science* 289 (2000)

[2] M. Kjaergaard, F. Nichele, H. J. Suominen, M. P. Nowak, M. Wimmer, A. R. Akhmerov, J. A. Folk, K. Flensberg, J. Shabani, C. J. Palmstrøm, C. M. Marcus, *Nat. Commun.* **7**, 12841 (2016).

Non-local Transport Signatures of Topological Superconductivity in Planar Josephson Junctions

Dibyendu Kuiri[1], **Michał P. Nowak**[1]

[1] *AGH University of Science and Technology, Academic Centre for Materials and Nanotechnology, Al. Mickiewicza 30, 30-059 Krakow, Poland.*

Finding signatures of topological superconductivity and the appearance of elusive Majorana-bound states has become one of the most significant challenges of modern solid-state physics. Josephson junctions, realized as hybrid nanostructures defined in a two-dimensional electron gas proximitized by a superconductor, have been considered promising candidates for the realization of well-controlled and scalable topological elements [1,2]. In this work, we propose and theoretically study a new method for probing the topological features of these systems. Instead of typical tunneling spectroscopy, which is sensitive only to states localized in the vicinity of the tunneling barrier [3] and prone to disorder-induced effects, we propose using a technique that probes the system in an open regime via non-local transport. In this configuration, the non-local conductance corresponds to the band structure of the system and enables elucidating the closing and reopening of the gap upon an increase in the phase difference, which is associated with the topological transition. This, however, happens only when the non-local signal reveres its sign when crossing zero energy and occurs due to the change of quasiparticle character of the bands at zero momentum. Moreover, we demonstrate that phase evolution is highly dependent on the strength of the indispensable Zeeman interaction, significantly changing the full phase diagram available for measurement in realistic experiments on hybrid Josephson junctions.

[1] F. Pientka, A. Keselman, E. Berg, A. Yacoby, A. Stern, and B. I. Halperin *Phys. Rev. X*, **7**, 123 (021032) (2017).
[2] M. Hell, M. Leijnse, and K. Flensberg, *Phys. Rev. Lett.* **118**, 107701 (2017).
[3] C. M. Moehle, P. K. Rout, N. A. Jainandunsing, D. Kuiri, C. Ting Ke, D. Xiao, C. Thomas, M. J. Manfra, M. P. Nowak, S. Goswami, *Nano Lett.* **22**, 8601 (2022).

Quantum Anomalous Hall effect and axion insulator phase in HgTe material class

G. Cuono [1], R. Islam [1], A. Lau[1], S. Mardanya[2], T.-R. Chang[2], B. Singh[3], C. M. Canali[4], T. Dietl[1] and C. Autieri [1]

[1] *International Research Centre Magtop, Institute of Physics,Polish Academy of Science, Aleja Lotników 32/46, PL-02668 Warsaw, Poland*
[2] *Department of Physics, National Cheng Kung University, Tainan 70101, Taiwan*
[3] *Department of Condensed Matter Physics and Materials Science, Tata Institute of Fundamental Research, Colaba, Mumbai 400005, India*
[4] *Department of Physics and Electrical Engineering, Linnaeus University, Kalmar, Sweden*

Dilute magnetic semiconductors have played a central role in the demonstrating and describing a strong and intricate sp-d exchange interactions, paving the way for the rise of magnetic topological insulators [1,2]. Recently, the exchange splittings of magneto-optical spectra in $Cd_{1-x}Mn_xTe$ and $Hg_{1-x}Mn_xTe$ have been described [3] and it has been demonstrated that superexchange dominates in magnetic topological insulators [4].

We study theoretically the interplay between magnetism and topology in HgTe-based systems in order to obtain the quantum anomalous Hall phase and the axion insulator phase.
To engineering the quantum anomalous Hall phase, we investigate the electronic and magnetic properties of the dilute magnetic semiconductors $Cd_{1-x}Cr_xTe$, $Hg_{1-x}Cr_xTe$, $Cd_{1-x}V_xTe$, $Hg_{1-x}V_xTe$ by using a density functional theory approach which goes beyond the standard functionals in order to correctly reproduce the topology and the band gap of these systems. We study the exchange couplings for all considered cases and we find that the coupling is ferromagnetic in case of doping with V, differently from the case of doping with Mn and Cr, where we find antiferromagnetic couplings. We conclude that the ferromagnetic coupling among V atoms in the insulating phase of topological HgTe can produce the quantum anomalous Hall phase[5].
To generate the axion insulator, we study the three-dimensional HgTe/MnTe superlattices stacked along the (001) axis. Our results show the evolution of the magnetic topological phases with respect to the magnetic configurations. An axion insulator phase is observed for the antiferromagnetic order with the out-of-plane Néel vector direction below a critical thickness of MnTe, which is the ground state amongst all magnetic configurations. Defining T as the time-reversal symmetry, this axion insulator phase is protected by a magnetic two-fold rotational symmetry $\mathbf{C_2 \cdot T}$. The axion insulator phase evolves into a trivial insulator as we increase the thickness of the magnetic layers. By switching the Néel vector direction into the ab plane, the system realizes different antiferromagnetic topological insulators depending on the thickness of MnTe. These phases feature gapless surface Dirac cones shifted away from high-symmetry points on surfaces perpendicular to the Néel vector direction of the magnetic layers[6].

[1] T. Dietl and H. Ohno, Rev. Mod. Phys. **86**, 187 (2014).
[2] Y. Tokura, K. Yasuda, and A. Tsukazaki, Nat. Rev. Phys. **1**, 126 (2019).
[3] C. Autieri, C. Śliwa, R. Islam, G. Cuono and T. Dietl, Phys. Rev. B **103**, 115209 (2021).
[4] C. Śliwa, C. Autieri, J. A. Majewski, and T. Dietl, Phys. Rev. B **104**, L220404 (2021).
[5] G. Cuono, C. Autieri and T. Dietl, unpublished.
[6] R. Islam, S. Mardanya, A. Lau, G. Cuono, T.-R. Chang, B. Singh, C. M. Canali, T. Dietl and C. Autieri, Phys. Rev. B **107**, 125102 (2023).

Geometry of the (001) surface and electron dispersion relations of topological IV-VI semiconductors.

A. Łusakowski[1], P. Bogusławski[1], and T. Story[1,2]

[1] *Institute of Physics, Polish Academy of Sciences, Al. Lotników 32/46, PL-02-668 Warszawa, Poland*

[2] *International Research Centre MagTop, Institute of Physics, PAS, Al. Lotników 32/46, PL-02-668, Warszawa, Poland*

In the electronic structure of topological crystalline insulators (TCI) from the IV-VI semiconductor family there are four Dirac points in the (001) surface Brillouin zone on $\bar{\Gamma} - \bar{X}$ directions. At these points, the energy band gap for surface states is zero due to mirror symmetries with respect to the (110) and $(\bar{1}10)$ planes. However, in the experimental works [1-3] it was discovered that there are two pairs of the surface states, one with zero gap and the other with nonzero gap. The opening of the gap suggests that one of the above mirror symmetries is broken. Scanning Tunneling Microscope measurements [2] revealed that the anion and cation sublattices at the surface are displaced relative to each other along the [110] direction by a vector (0.3, 0.3) Å. Such a displacement leads both to breaking the mirror symmetry with respect to the $(\bar{1}10)$ plane and the opening of the gap at two Dirac points.

Here, using the local density functional methods we analyse detailed atomic configurations at the (001) surfaces of PbTe, PbSe, SnTe and SnSe. Our results reveal rumpling, *i.e.* relative displacements of anion and cation sublattices in the [001] direction for the first few monolayers, and oscillatory character of interlayer distances between them. Both results are consistent with the previous theoretical and experimental data for the rock salt crystals. However, contrary to the claim of Ref. [2] we do not find any displacements of surface atoms in the (001) plane.

As expected, the rumpling does not open the band gap, because it does not break the mirror symmetry. We also show the dispersion relations for different Sn concentration in $Pb_{1-x}Sn_xSe$ slabs. The chemical disorder leads to the opening of the gap in TCI phase. For Sn concentrations corresponding to Weyl semimetal phase we observe an interval on the $\bar{\Gamma} - \bar{X}$ direction where the gap is vanishingly small.

Calculations are performed using a slab geometry. Optimization of atomic configuration is performed using OpenMX package [4]. Based on an initio results we construct a tight binding hamiltonian for thick slabs. Importantly, to obtain correct results it is necessary to take into account the dependence of tight binding parameters on the distance from the surfaces of the slab.

Acknowledgments

This work was partially supported by National Science Centre NCN (Poland) projects UMO- 2016/23/B/ST3/03725 (AŁ), UMO-2017/27/B/ST3/02470 (AŁ) as well as by the Foundation for Polish Science through the IRA Programme co-financed by EU within SG OP (TS).

[1] Y. Okada, *et al.*, *Science* **341**, 1496 (2013).

[2] I. Zeljkovic, *et al.*, *Nature Mater* **14**, 318 (2015).

[3] B.M. Wojek, *et al.*, Nat. Commun. **6**, 8463 (2015).

[4] see http://www.openmx-square.org

Magnetic and electrical properties of $CoRE_2W_2O_{10}$ ceramic materials

B. Sawicki[1], E. Tomaszewicz[2], T. Groń[1], M. Oboz[1], I. Gruszka[1], A. Guzik[1], P. Urbanowicz[1]

[1]*Institute of Physics, University of Silesia in Katowice, 40-007 Katowice, Poland*
[2]*Faculty of Chemical Technology and Engineering, Department of Inorganic and Analytical Chemistry, West Pomeranian University of Technology in Szczecin, 71-310 Szczecin, Poland*

Divalent metals tungstates, MWO_4 (M = Mn, Co, Zn, Cd and Pb), have been successfully used in spectroscopic and radiometric devices and as heavy and fast scintillators [1]. Many of them, *i.e.* when ionic radius of M^{2+} is relatively small, adopted monoclinic wolframite-type structure [2]. In turn, trivalent rare-earth metals tungstates (RE_2WO_6) exhibit many structural types including monoclinic symmetry with space group C2/c (where RE = Pr–Dy) [3]. They have been used in diode-pumped crystal lasers, new generation lighting in optical telecommunications, lidars and other applications requiring narrow spectral sources [4]. Our earlier studies on $MPr_2W_2O_{10}$ (M = Mn, Co and Cd) and $CdRE_2W_2O_{10}$ (RE = Y, Nd, Sm, Gd–Er) tungstates obtained by high-temperature sintering of adequate MWO_4/RE_2WO_6 mixtures showed that these new compounds crystallize with orthorhombic or monoclinic structure and exhibit generally non-conductive and paramagnetic properties [5,6].

Samples of other new $CoRE_2W_2O_{10}$ (RE = Y, Dy, Ho, Er) tungstates were obtained by high-temperature solid-state reaction method using $CoWO_4$ and RE_2WO_6 as the starting materials [7]. These materials were pressed and sintered at 1050°C to a ceramic form. Powder diffraction measurements of as-prepared sinters were carried out on a PANalytical PW1050 diffractometer. Static dc magnetic susceptibility was measured within the temperature range of 2–300 K in the zero-field cooled (ZFC) and field cooled (FC) mode. For these purposes a Quantum Design MPMS-XL-7AC SQUID magnetometer (Quantum Design, USA) was used. Electrical conductivity $\sigma(T)$ was measured by the dc method using a KEITHLEY 6517B Electrometer/High Resistance Meter within the temperature range of 77–400 K. Broadband dielectric spectroscopy measurements were carried out using pellets, polished and sputtered with (~80 nm) Ag electrodes within the frequency range of $2\cdot10^2$ – $2\cdot10^6$ Hz using a Hioki 3532-50 LCR HiTester and within the temperature range of 80–400 K.

The results of structural, magnetic and electrical measurements of $CoRE_2W_2O_{10}$ ceramics (RE=Y, Dy, Ho, Er) showed orthorhombic-type structure, paramagnetic state and insulating behaviour as well as a large value of relative permittivity above room temperature, which strongly depends on presence of 3*d* Co^{2+} ions, but not on the type of 4*f* RE^{3+} ones. The important property of ceramic samples is that they have a greater ability to accumulate charge in comparison with the micro-crystalline ones.

[1] V.G. Bodnar, S.F. Burachas, K.A. Katrunov, V.P. Martinov, V.D. Ryzhikov, V.I. Manko, H.H. Gutbrod, and G. Tamulaitis, *Nucl. Instrum. Methods Phys. Res. A* **411**, 376 (1998).
[2] A.W. Sleight, *Acta Crystallogr. B* **28**, 2899 (1972).
[3] A.A. Evdokimov, V.A. Efremov, and V.K. Trunov, Compounds of the Rare Earth Elements: Molybdates and Tungstates, Nauka, Moscow, 1991 (in Russian).
[4] G. Boulon, *Opt. Mater.* **34**, 499 (2012).
[5] Z. Kukuła, E. Tomaszewicz, S. Mazur, T. Groń, H. Duda, S. Pawlus, S.M. Kaczmarek, H. Fuks, and T. Mydlarz, *Philos. Mag.* **92**, 4167 (2012).
[6] Z. Kukuła, E. Tomaszewicz, S. Mazur, T. Groń, S. Pawlus, H. Duda, and T. Mydlarz, *J. Phys. Chem. Sol.* **74**, 86 (2013).
[7] E. Tomaszewicz, *J. Therm. Anal. Cal.* **93**, 711 (2008).

Magnetic properties of semiconducting $ZnCr_2Se_4$:Re single crystals

I. Jendrzejewska[1], T. Groń[2], B. Sawicki[2], J. Kusz[2], J. Goraus[2], Z. Stokłosa[3]

[1]*Institute of Chemistry, University of Silesia in Katowice, 40-007 Katowice, Poland*
[2]*Institute of Physics, University of Silesia in Katowice, 40-007 Katowice, Poland*
[3]*Institute of Material Science, University of Silesia in Katowice, 40-007 Katowice, Poland*

Seleno-spinels are promising compounds in the commercial use of thermoelectric devices [1] due to a fairly large cubic cell unit (~10 Å) and a strong covalent bond. Pure $ZnCr_2Se_4$, both in mono and polycrystalline form combines *p*-type semiconductor conductivity and helical antiferromagnetic (AFM) order below the Néel temperature T_N = 20 K with a strong ferromagnetic (FM) short-range interaction, as evidenced by the high positive Curie-Weiss temperature θ = 115 K [2,3]. The magnetic order at T_N is accompanied by structural transformation from cubic $Fd\bar{3}m$ to tetragonal $I4_1/amd$ symmetry with a small contraction along the *c* axis [4]. Rhenium is a conductor and paramagnetic, it has hexagonal symmetry and crystallizes in $P6_3mmc$ space group. The unit cell parameters of rhenium crystal are as follows: *a* = 276.0 and *c* = 445.8 pm [5].

$ZnCr_2Se_4$ single crystals doped with rhenium ions with the content of 0.06, 0.07, 0.08, 0.09. 0.10 and 0.11 located in the tetrahedral sites of the spinel structure were grown from binary selenide ZnSe, elemental rhenium and selenium by chemical vapor transport with anhydrous $CrCl_3$ as transport agent. Dynamic AC magnetic susceptibility, χ_{ac}, was measured in the temperature range 2-300 K and at an internal oscillating magnetic field H_{ac} = 1 Oe with an internal frequency *f* = 120 Hz taken at external static DC magnetic fields H_{dc} = 0, 10, 20, 30, 40 and 50 kOe. Magnetization isotherms, M(H), were measured at 2, 4, 10, 20, 40, 60, and 300 K and in the static DC magnetic field up to 70 kOe. Specific heat measurements were made in the temperature range of 2-300 K. For these purposes a Quantum Design MPMS-XL-7AC SQUID magnetometer was used. The electrical conductivity σ(T) was measured by the DC method using KEITHLEY 6517B Electrometer/High Resistance Meter in the temperature range of 77–400 K.

Magnetic (AC), specific heat, and electrical (DC) measurements showed semiconductor behavior, coupling of the phonon system and electron gas by a spin lattice determined by the Debye temperature of 295 K, two singularities on magnetization isotherms in critical fields of 12 and 60 kOe, AFM long-range order with the Néel temperature of T_N = 21.7 K, and a strong FM short-range interaction, as evidenced by an increase in the positive Curie–Weiss temperature, θ, from 75 to 83 K with increasing Re content in the sample. With the increase of the external DC magnetic field, a shift of T_N towards lower temperatures and θ towards higher ones was observed, as well as the appearance of broad peaks in the paramagnetic region at H_{dc} = 40 and 50 kOe, characteristic of spin fluctuations. Similar behavior was found in $ZnCr_2Se_4$:Ta single crystals [6].

[1] G.J. Snyder, T. Caillat, and J.P. Fleurial, *Mat. Res. Innov.* **5**, 67 (2001).
[2] R. Plumier, *J. Phys. Paris* **27**, 213 (1966).
[3] F.K. Lotgering, in: Proceedings of the International Conference on Magnetism, Nottingham, 1964 (Institute of Physics and the Physical Society, London, 1965), p. 533.
[4] R. Kleinberger, and R. de Kouchkovsky, *C.R. Acad. Sci. Paris, Ser. B* **262**, 628 (1966).
[5] N.N. Greenwood, A. Earnshaw, Chemistry of the Elements (Butterworth-Heinemann, Oxford–Boston, 1997), p. 1043.
[6] I. Jendrzejewska, T. Groń, P. Kwapuliński, J. Kusz, E. Pietrasik, T. Goryczka, B. Sawicki, A. Ślebarski, M. Fijałkowski, J. Jampilek, H. Duda, *Materials* **14**. 2749 (2021).

Magnetic and electrical properties of $CuCr_2Se_4$ nanoparticles

E. Malicka[1], T. Groń[2], A. Gudwański[1], B. Sawicki[2], M. Oboz[2], M. Karolus[3]

[1]*Institute of Chemistry, University of Silesia in Katowice, 40-00, Katowice, Poland*
[2]*Institute of Physics, University of Silesia in Katowice, 40-007 Katowice, Poland*
[3]*Institute of Materials Science, University of Silesia in Katowice, 40-007 Katowice, Poland*

Magnetic spinels with general formula $CuCr_2X_4$ (where X = S, Se and Te) are ferromagnetic [1] and metallic conductor at room temperature [2]. For this reason, these spinels have been extensively studied in terms of their potential applications in thermoelectric devices [3]. $CuCr_2Se_4$ obtained by solid phase synthesis has a normal cubic type structure with the symmetry of the $Fd\bar{3}m$ space group and the zero magnetic moment of the Cu ion in the tetrahedral site, whereas the three Bohr magnetons, corresponding with Cr^{3+} ions in the octahedral site [4]. Pure $CuCr_2Se_4$, both in mono and polycrystalline form has strong ferromagnetic long-range interactions below the Curie temperature of T_C = 460 K with strong ferromagnetic short-range interactions evidenced by a large positive Curie-Weiss temperature of θ = 465 K [1] as well as the electrical resistivity of $3.8 \cdot 10^{-6}$ Ωm and the positive Seebeck coefficient of 20.5 μV/K at room temperature [2] .

Spinel nanocrystallites of $CuCr_2Se_4$ with a size of 32 nm were obtained as a result of five-hour grinding of single crystals of this compound (in order to avoid phase impurities) by high-energy ball milling. The static magnetic susceptibility was recorded both in zero-field-cooled and field-cooled mode. Dynamic magnetic susceptibility was measured at an internal oscillating magnetic field H_{ac} = 3.9 Oe with an internal frequency f = 1 kHz in the temperature range of 5–300 K. Magnetization isotherms were measured at 5, 20, 40, 60, and 300 K using a SQUID magnetometer in applied external fields up to 70 kOe. Electrical conductivity σ(T) and thermoelectric power S(T) of the nanoparticles under study were measured by the DC method using a KEITHLEY 6517B Electrometer/High Resistance Meter and a Seebeck Effect Measurement System, respectively, within the temperature range of 77–400 K.

Magnetic and electrical studies have shown that the reduction of $CuCr_2Se_4$ single crystals to the size of nanoparticles leads to: 1) weakening of the long-range ferromagnetic interactions visible in the decrease of the Curie temperature from 460 to 196 K, 2) weakening of the short-range ferromagnetic interactions visible in the decrease of the paramagnetic Curie-Weiss temperature from 465 to 231 K, 3) lack of saturation of magnetization at 5 K and 70 kOe, 4) change of electrical conductivity from metallic to semiconductor, and 5) reducing the thermoelectric power factor σS^2 by three orders of magnitude at 400 K. The above results were considered in terms of magnetic interactions and their exchange integrals, derived from the high-temperature expansion of magnetic susceptibility. Calculations of the exchange integrals and the band width of the mixed valency of chromium ions [Cr^{3+}, Cr^{4+}] showed that the decrease in the size of the crystallites causes a significant weakening of the mechanism of the double exchange magnetic interactions, without changing the strength of the superexchange magnetic ones, and the reduction of the band width [Cr^{3+}, Cr^{4+}] from 0.76 to 0.19 eV. Similar behavior was found for $CuCr_2S_4$ nanoparticles [5].

[1] F.K. Lotgering, *Solid State Commun.* **2**, 55 (1964).
[2] M. Robbins, H.W. Lehmann, and J.G. White, *J. Phys. Chem. Sol.* **28**, 897 (1964).
[3] G.J. Snyder, T. Caillat, and J.P. Fleurial, *Mater. Res. Innov.* **5**, 67 (2001).
[4] C. Colominas, *Phys. Rev.* **153**, 558 (1967).
[5] E. Malicka, M. Karolus, J. Panek, Z. Stokłosa, T. Groń, A. Gudwański, B. Sawicki, and J. Goraus, *Physica B* **581**, 411829 (2020).

Magnetic and electric properties of Nd^{3+} and Mn^{2+}-co-doped calcium molybdato-tungstate single crystals

T. Groń[1], E. Tomaszewicz[2], B. Sawicki[1], M. Oboz [1], J. Kusz[1], M. Berkowski[3]

[1]*Institute of Physics, University of Silesia in Katowice, 40-007 Katowice, Poland*
[2]*Faculty of Chemical Technology and Engineering, Department of Inorganic and Analytical Chemistry, West Pomeranian University of Technology in Szczecin, 71-310 Szczecin, Poland*
[3]*Institute of Physics, Polish Academy of Sciences, 02-668 Warszawa, Poland*

Divalent metal molybdates and tungstates with tetragonal scheelite-type structure (space group $I4_1/a$, No. 88) both un-doped as well as activated with di- or/and trivalent ions are very interesting materials because of their excellent properties. Micro-/nanocrystalline as well as single crystals samples of these materials could be widely applied as efficient phosphors [1], solid state lasers [2], scintillators [3], and microwave dielectrics [4]. Calcium molybdate ($CaMoO_4$) and calcium tungstate ($CaWO_4$) as members of scheelite family are highly ionic compounds with a small contribution of a covalent bonding. Band gaps determined from the band dispersion calculations [5] indicated that both compounds are direct band gap insulators with the E_g values of: 3.41 eV for $CaMoO_4$, and 4.09 eV for $CaWO_4$. Our earlier magnetic and electric research of microcrystalline $Ca_{1-3x-y}Mn_y\square_xNd_{2x}(MoO_4)_{1-3x}(WO_4)_{3x}$ solid solution (when $0.0050 \leq x \leq 0.2000$ and $y = 0.0200$, where $\square$ denotes vacant sites) obtained by high-temperature annealing of ternary $MnMoO_4/Nd_2(WO_4)_3/CaMoO_4$ mixtures showed a paramagnetic behavior with long-range ferrimagnetic and short-range antiferromagnetic interactions in these materials as well as a weak *n*-type electrical conductivity with stronger activation of 1.0 eV above 300 K in the intrinsic region [6].

In this work, $Ca_{1-3x-y}Mn_y\square_xNd_{2x}(MoO_4)_{1-3x}(WO_4)_{3x}$ molybdato-tungstate single crystals ($x = 0.005$ or $x = 0.0099$ and with constant Mn^{2+} ions concentration, *i.e.* $y = 0.005$) have been grown by the Czochralski method in an inert atmosphere and subjected to structural, magnetic and electrical studies. The static magnetic susceptibility of as-grown single crystals was measured in the temperature range of 2–300 K and recorded both in zero-field-cooled and field-cooled mode using a Quantum Design SQUID magnetometer. Electrical conductivity σ(T) of doped single crystals was measured by the dc method using a KEITHLEY 6517B Electrometer/High Resistance Meter. Thermoelectric power S(T) was measured within the temperature range of 77–400 K using a Seebeck Effect Measurement System (MMR Technologies). Our studies have shown that replacing diamagnetic Ca^{2+} ions with paramagnetic Nd^{3+} ones with the content not exceeding of 0.02 and having a screened 4*f*-shell revealed a significant effect of orbital diamagnetism and Van Vleck's paramagnetism, residual electrical conductivity without intrinsic region and a change of sign of the Seebeck coefficient at ~230 K as well as the Fermi energy (~0.04 eV) and the Fermi temperature (~500 K), determined from the diffusion component of thermopower suggesting the presence of shallow acceptor and donor levels.

[1] C.R. Ronda, T. Jüstel, and H. Nikol, *J. Alloy Compd.* **277**, 669 (1998).
[2] G. Boulon, *Opt. Mat.* **34**, 499 (2012.
[3] V.B. Mikhailik, S. Henry, H. Kraus, and I. Solskii, *Nucl Instrum Methods Phys. Res. A* **583**, 350 (2007).
[4] E.S. Kim, S.H. Kim, and I.B. Lee, *J. Eur. Ceram. Soc.* **26**, 2101 (2006).
[5] Y. Zhang, N.A.W. Holzwarth, and R.T. Williams, *Phys. Rev. B* **57**, 12738 (1998).
[6] B. Sawicki, E. Tomaszewicz, M. Guzik, T. Groń, M. Oboz, H. Duda, S. Pawlus, and P. Urbanowicz, *Ceram. Int.* **49**, 944 (2023).

High-Quality MBE-grown Aluminum Layers for Experimental Realization of Majorana Bound States

A. Elbaroudy[1], B. Khromets[1,3,4], E. Bergeron[3,4], T. Blaikie[1], Y. Shi[1], M.C.A. Tam[1], S. Sadeghi[4], F. Sfigakis[3,4], J. Baugh[2,3,4,5], and Z.R. Wasilewski[1,2,4,5]

[1]Department of Electrical and Computer Engineering,
[2]Department of Physics and Astronomy, [3]Department of Chemistry,
[4]Institute for Quantum Computing (IQC), [5]Waterloo Institute for Nanotechnology (WIN),
University of Waterloo, Waterloo N2L 3G1, Canada

The small effective mass, large Landé g-factor, and strong spin-orbit interactions (SOI) make high-quality InAs, and InSb quantum well (QW) structures particularly appealing for the experimental realization of Majorana bound states (MBS) in the pursuit of topological quantum computing. Besides such near-surface QWs, an essential element of the MBS device is a layer of superconductive material with a very large coherence length at low temperatures and sufficiently high critical value of the in-plane magnetic field. A natural choice for such a material is aluminum. Even though the critical magnetic field of bulk Al is only 0.01 T, this is substantially increased for very thin layers. However, the high surface mobility of Al in a UHV environment, even at room temperature, and its tendency for 3D nucleation make the deposition of thin (~10 nm) continuous layers challenging. Growth of smooth layers has been typically done in dedicated UHV chambers with the substrate actively cooled with liquid nitrogen during Al deposition. Here we report on the growth of high-quality continuous Al layers directly inside the standard Veeco GEN10 MBE reactor at temperatures above 0 °C. We (i) show that at sufficiently high Al flux, the transition from 3D to 2D growth mode takes place, (ii) discuss the possible origin of such transition, and (iii) show results of an extensive in-situ and ex-situ characterization.

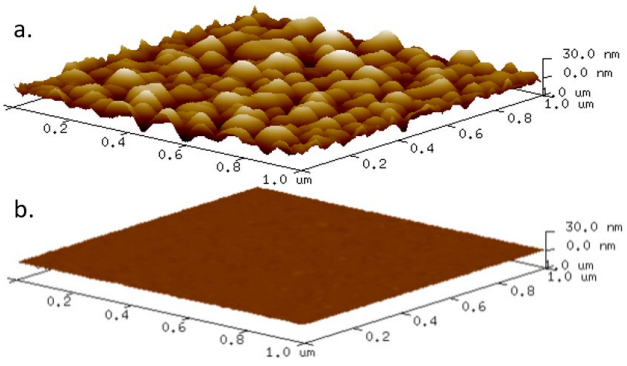

AFM scans of two aluminum layers grown on $In_{0.75}Ga_{0.25}As/In_{0.53}Ga_{0.47}As$ (6nm/100nm) on the InP(001) substrate. In both cases, the nominal thickness of the Al layer was 10 nm.
a. The layer was deposited at 0.5 Å/s.
b. The layer was deposited at 3.0 Å/s.

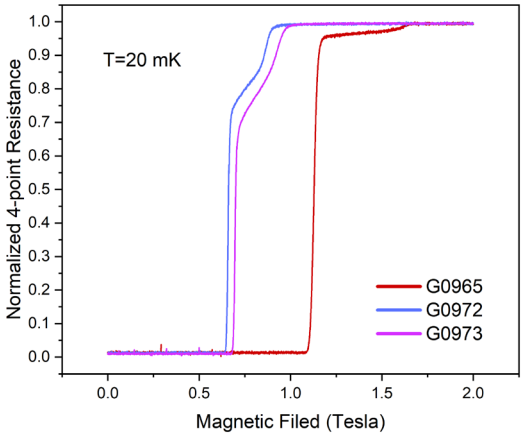

Superconducting to normal phase transition signatures for three Al layers:
G0972 was deposited at 3.0 Å/s (10 nm thick)
G0973 was deposited at 2.0 Å/s (10 nm thick)
G0965 growth rate decreased from 2.0 Å/s to approximately 1.3 Å/s during the deposition and is thinner.

Layers deposited at lower growth rates did not show superconductive behavior.

Majorana-Magnon Interactions in Topological Shiba Chains

Pei-Xin Shen[1], Vivien Perrin[2], Pascal Simon[2], and Mircea Trif[1]

[1] *International Research Centre MagTop, Institute of Physics, Polish Academy of Sciences, Aleja Lotnikow 32/46, PL-02668 Warsaw, Poland*
[2] *Université Paris-Saclay, CNRS, Laboratoire de Physique des Solides, 91405, Orsay, France*

A chain of magnetic impurities deposited on the surface of a superconductor can form a topological Shiba band that supports Majorana zero modes and hold a promise for topological quantum computing. Yet, most experiments scrutinizing these zero modes rely on transport measurements, which only capture local properties. Here we propose to leverage the intrinsic dynamics of the magnetic impurities to access their non-local character. Specifically, we calculate the spin susceptibility of the magnetic chain and show that the uniform magnonic mode, which spreads over the entire chain, becomes imprinted with the parity of the ground state. We find that the visibility of the spin susceptibility associated with the two parities oscillates between -1 and 1 in the topological regime as a function of the magnon frequency, while it is arbitrary in the trivial regime. These two distinct patterns originate from interference effects and are robust against moderate disorder. Our approach offers non-invasive alternative to the scanning tunnelling microscopy techniques used to probe Majorana zero modes. Conversely, the magnons could facilitate the manipulation of Shiba states and the Majorana zero modes.

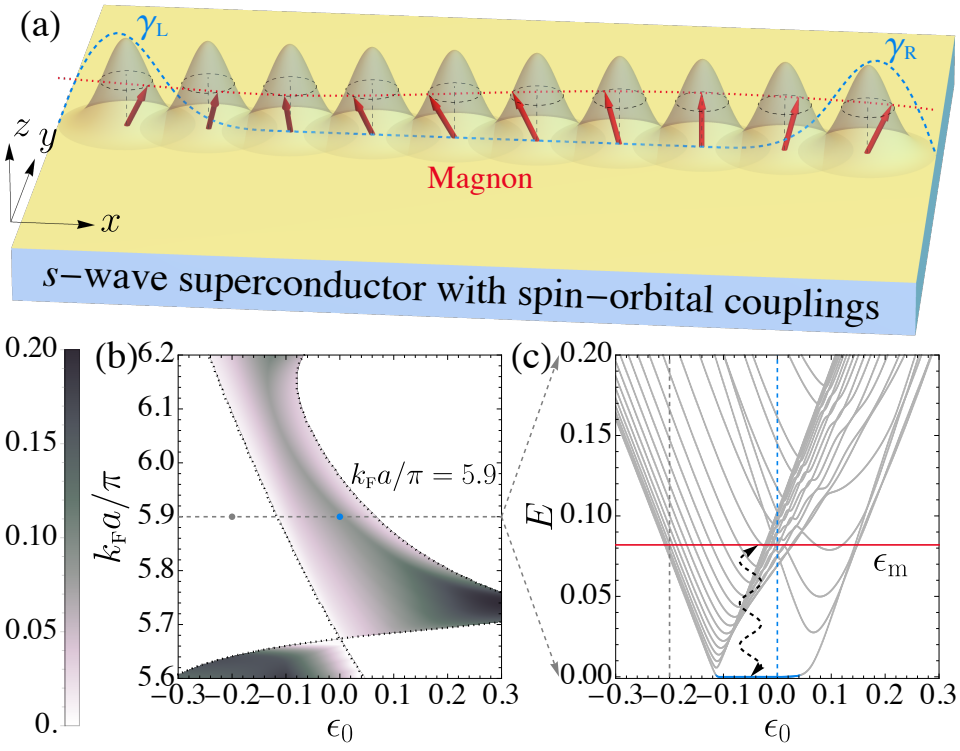

Figure 1: (a) A Sketch of the topological Shiba chain in the presence of magnons. (b) The phase diagram. (c) The spectrum and the Majorana zero mode.

Temperature Dependence of Spin Pumping in $Y_3Fe_5O_{12}$/Pt, $Ni_{81}Fe_{19}$/Pt and SnTe/$Ni_{81}Fe_{19}$ Thin Films

A. Moosarikandy, [1] M. Chojnacki,[2] K. Fronc,[1] W. Wolkanowicz,[2] T. Story,[1, 2] P. Sahoo,[1] S. Karuvanveettil,[1] and V. Bhat[1]

1 International Research Centre MagTop, Institute of Physics, Polish Academy of Sciences, Warsaw, Poland
2 Institute of Physics, Polish Academy of Sciences, Warsaw, Poland

Magnons(quanta of spin waves) are collective excitations in magnetic material and allow information processing without transferring charge [1]. Such no-charge-based devices are in great demand owing to information transfer without Joule heat loss. One of the crucial components of a magnonic device is the detection of a magnon signal by transferring it to an electrical signal. One prominent way to accomplish the goal of electric detection of magnon spin current is via a method called spin pumping [2] using inverse spin hall effect (ISHE) phenomena. When the heavy metal (e.g. Pt) or topological material is interfaced with the magnetic materials (FM), the spin current can be injected into the HM from FM via spin pumping. Precessing magnetic material transfer angular momentum from the FM to the FM/HM interface via coupling of the local magnetic moments of the FM with the conduction electrons of the HM. Recently, it has been reported via ferromagnetic resonance experiments that induced spin currents can be amplified instead of suppressed by adding a strong spin orbit coupled spin sink layers in a superconductor/ferromagnet hybrid structure [3] and is key for superconducting spintronics. Therefore, it is essential to study the low temperature spin pumping in Pt and topological materials, such as SnTe. We report broadband spin-wave spectroscopy and spin pumping experiments on $Y_3Fe_5O_{12}$/Pt, $Ni_{81}Fe_{19}$ (with Pt thickness varied from 7 nm to 75 nm), and SnTe/ $Ni_{81}Fe_{19}$ bilayer thin films for temperatures ranging from 300 K to 4 K. We observed a systematic shift in ferromagnetic resonance fields, amplitude, and linewidths as a function of frequency and temperature. For the in-plane and out-of-plane directions of the magnetic field, we observed distinct modes at lower temperatures. The spin mixing conductance, spin current density, and spin hall angle values showed strong temperature dependence. Our findings are key for the usage of Pt and SnTe as spin sink layers for the superconducting spintronics applications.

[1] A. V. Chumak, et al., Nature physics 11, 453 (2015)
[2] Y. Tserkovnyak, A. Brataas, and G. E. Bauer, Physical review letters 88, 117601 (2002)
[3] Jeon, KR., Ciccarelli, C., Ferguson, A.J. et al., Nature Mater 17, 499–503 (2018).

Size and curvature modulation of the magnetic properties of magnetite nanoshells

B. Camargo [1], B. Semenenko[2,3], M. Gorke[2], M. Barasinski[2,4], G. Garnweitner[2,4], J. Szczytko[1]

[1] *Faculty of Physics, University of Warsaw. Pasteura 5, 02-093 Warsaw, Poland.*
[2] *Institute for Particle Technology (iPAT), Technische Universität Braunschweig, Volkmaroder Str. 5, 38104 Braunschweig, Germany.*
[3] *Center of Pharmaceutical Engineering (PVZ), Technische Universität Braunschweig, Franz-Liszt Str. 35A, 38106 Braunschweig, Germany.*
[4] *Laboratory for Emerging Nanometrology (LENA), Technische Universität Braunschweig, Langer Kamp 6B, 38106 Braunschweig, Germany.*

Magnetic domains in bulk materials are defined as regions in space where spin correlations establish long-range order. Their occurrence is usually dictated by the structuro-chemical properties of the materials considered, whereas their dynamics, disposition and distribution can be related to extrinsic parameters such as disorder.

As the thickness of a magnetic material is reduced, shape anisotropy effects kick into play and progressively disrupt the magnetic ordering seen in bulk. In the limit of two dimensions (2D), no magnetic ordering is allowed in isotropic systems. This is the consequence of the well-known Mermin-Wagner theorem, which prohibits long-range ordering in low dimensional systems. One possibility to re-enable order in this case is to introduce strains, or otherwise break the systems in-plane isotropy.

A viable approach to induce such a break of isotropy, while not suppressing two-dimensionality, is to impose a curvature to an otherwise flat film. In doing so, magnetic centers confined to the plane still see their immediate surroundings as flat, but are actually canted in relation to farther neighbors. Such a canting between magnetic centers is akin to the introduction of an antisymmetric spin exchange coupling to the material, whose quantum mechanical equivalent is known as the “Dzyaloshinskii-Moriya Interaction” (DMI). The strength of such an interaction has the potential to trigger different spin textures, depending on the system considered. Formally, therefore, the careful control of the substrate curvature has also the potential to introduce different spin textures into the system under consideration, provided that the curvatures involved are steep enough.

Here, we employ magnetite nano-shells surrounding a non-magnetic silica core to explore the effects of curvature-induced magnetic textures in mesoscopic systems. Through a measurement of the magnetic response of nanoparticles of different sizes, we demonstrate the effective tuning of our samples with particle diameter. Such an approach allows a selective control of the blocking temperature of our devices, as well as the induction or suppression of vortex and onion states in the material. We compare the results of the core/shell system proposed with those of bulk magnetic nanoparticles, which are often described within the framework of a core/shell structure with a superparamagnetic core and a magnetically-active shell.

Towards Spintronics of Antiferromagnetic Semiconductors - Characterization of MnSe on GaAs

C. J. Krasucki[1], J. Z. Domagala[2], M. Gryglas-Borysiewicz[1], W. Pacuski[1], and M. J. Grzybowski[1]

[1]*Institute of Experimental Physics, Faculty of Physics, University of Warsaw, Warsaw, Poland*
[2]*Institute of Physics, Polish Academy of Sciences, Warsaw, Poland*

Antiferromagnets are materials that have become popular in the field of spintronics due to their ability to control the spin axis orientation with electrical current. As a result, several magnetic imaging techniques have been developed to detect the reorientation of antiferromagnetic spins. The research on antiferromagnetic spintronics has mainly focused on semimetallic systems or insulating oxides, leaving optical band-gap semiconductors unexplored. In this study, we investigate manganese selenide (MnSe), which has rocksalt structure and potentially uncompensated (111) planes, making it an attractive material for spin axis detection sensitive to uncompesated surfaces. In addition, since it is a wide gap semiconductor, it can be interfaced with a heavy-metal layer with strong spin-orbit interaction (i.e. platinum) to take advantage of the spin Hall magnetoresistance.

In this work, we study the quality of the MBE grown MnSe/GaAs structures with respect to a key factor - temperature of growth. The main tool to determine the quality of the samples was X-ray diffraction (XRD). We measured samples of MnSe/GaAs(001) and MnSe/GaAs(111).

From $2\theta/\omega$ scan of MnSe/GaAs(111) we obtained a lattice constant $a \approx 5.46$ Å, what indicate to rocksalt crystal structure of grown MnSe layers. We compared FWHM of RC scans of MnSe, where the lowest value, indicating the best quality of layer, was $\Delta = 0.6°$ for MnSe/GaAs(111) grown at T = 300 °C, and $\Delta = 0.3°$ for MnSe/GaAs(001) grown at T = 350 °C. We observe crystal twinning of MnSe layer on the MnSe/GaAs(111) samples. Sample grown at T $\geq$ 450 °C degrade which appears in unreliable values of FWHM using XRD.

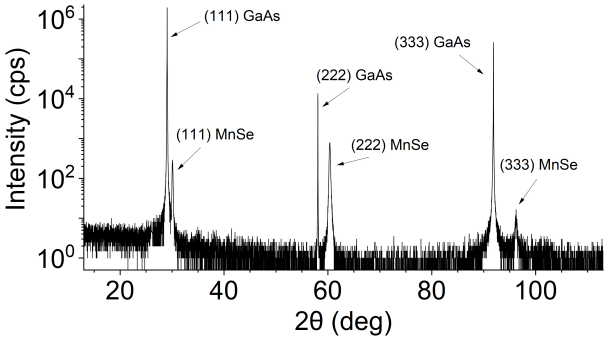

Figure 1: Long range $2\theta/\omega$ scan of MnSe/GaAs(111) sample grown at T = 300 °C.

MnSe/GaAs structures are a good base for the studies of the growth of more complex structures with quantum well having one barrier made of MnSe, which is interesting both in terms of optical experiments as well as magnetotransport when thin layer of platinum is added on the top.

The research was funded by National Science Centre (NCN), Poland under Grant 2021/40/C/ST3/00168.

Raman spectroscopy as an indicator of antiferromagnetic to paramagnetic phase transition in transition metal thiophosphates

M. Peter[1], J. Kopaczek[1], M. Rybak[1], Z. Sofer[2], and R. Kudrawiec[1]

[1] *Department of Semiconductor Materials Engineering, Wrocław University of Science and Technology, Wybrzeże Wyspiańskiego 27, 50-370 Wrocław, Poland*

[2] *Department of Inorganic Chemistry, University of Chemistry and Technology, Technická 5,166 28 Prague 6, Czech Republic*

Over the years, while electronic and optical properties of two-dimensional (2D) semiconductors were extensively studied experimentally, magnetic properties have remained neglected. That situation was related to the view that ferromagnetic order could not survive in a 2D regime due to increased thermal fluctuations [1]. However, a few years ago, Lado and Fernández-Rossier experimentally showed for CrI_3 crystal that magnetic order could be stabilized and survive in a low-dimensional regime [2]. Since then, 2D magnets are drawing growing interest, but plenty of phenomena still require extensive studies. Among 2D magnets, transition metal thiophosphates (MPS_3 - where M is transition metal) are a large family of van der Waals crystals exhibiting various types of intrinsic magnetic ordering.

In this work, we focused on correlating changes in Raman modes behavior with phase transition from antiferromagnetic to paramagnetic order for $MnPs_3$, $FePS_3$, $CoPS_3$, and $NiPs_3$. Moreover, we have elucidated how the replacement of transition metal influences the position of a given vibrational mode and its coupling to the antiferromagnetic phase. It can be seen in fig. 1 that around Néel temperature, one of the Raman modes loses its intensity and disappears completely while a new one of different symmetry emerges. The mentioned changes in symmetry were confirmed by angle-resolved Raman spectroscopy measurements fig. 1 (c). Furthermore, our experimental findings were supported by density functional theory that let us identify vibrational modes.

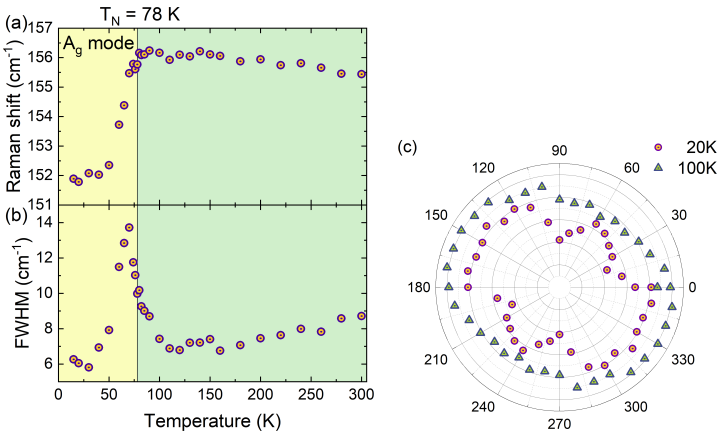

Figure 1: The analysis of A_g Raman mode behaviour with (a,b) temperature and (c) polarization for $MnPS_3$ with a Néel temperature of 78 K.

[1] N. D. Mermin, and H. Wagner, Phys. Rev. Lett. **17**, 1133 (1966)
[2] J. L. Lado, and J. Fernández-Rossier, 2D Mater. **4**, 035002 (2017)

Resonant Raman scattering of few-layers $CrBr_3$

Ł. Kipczak[1], A. Karmakar[1], M. Grzeszczyk[2,3], J. Pawłowski [1], A. Babiński[1], M. Koperski[2,3], M. R. Molas[1]

[1] *Faculty of Physics, University of Warsaw, Warsaw, Poland*
[2] *Dep. of Materials Science and Engineering, National University of Singapore, Singapore*
[3] *Inst. for Functional Intelligent Materials, National University of Singapore, Singapore*

Chromium bromide belongs to the family of magnetic layered materials with the general formula CrX_3 (X = Br, Cl and I). In bulk form, the intralayer and interlayer exchange couplings in CrB_3 are ferromagnetic, in contrast to $CrCl_3$ and CrI_3 characterized by the antiferromagnetic interlayer orders [1, 2].

In this work, we performed the Raman scattering (RS) experiment on thin $CrBr_3$ flake with thicknesses from 4 to 7 layers at low (T=5 K) and room (T=300 K) temperatures using 5 different excitation energies, *i.e.* 1.96 eV, 2.21 eV, 2.41 eV, 2.54 eV, and 3.06 eV. The thickness of the flakes was confirmed by atomic force microscopy.

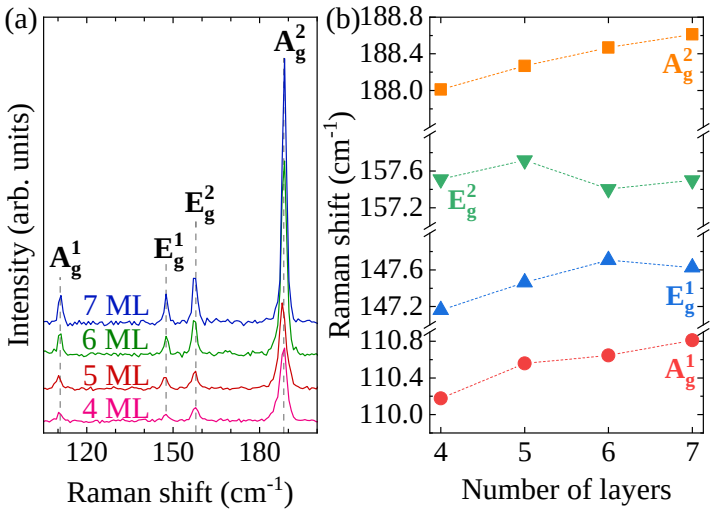

Figure 1: (a) Raman scattering spectra of thin flakes of $CrBr_3$ with thickness ranging from 4 to 7 layers. (b) Thickness dependence of the energies of the RS peaks.

In order to find the best resonant conditions for RS, we compared the intensities of the Raman peaks of $CrBr_3$ measured under different excitations. We found that the most intense Raman signal is observed under 2.41 eV excitation at room temperature. However, a substantial enhancement of the RS signal of about 3 times as compared to the aforementioned case was obtained under 3.06 eV excitation at T=5 K. The latter laser energy was chosen to investigate the thickness evolution of the Raman spectra, see Fig. 1(a).

As was reported in Ref. [1], four phonon modes, assigned as A_g^1, E_g^1, E_g^2, A_g^2, are Raman-active in $CrBr_3$. Note that the top indexes are additional numbering to resolve the peaks sharing the same notation. The thickness dependence of the observed phonon energies is presented in Fig. 1(b). A clear monotonic blueshift of the A_g^1 and A_g^2 peaks is seen when the number of layers increases with the relative energy difference between 4 and 7 layers of about 0.6 cm^{-1}. The corresponding evolutions of the E_g^1, E_g^2 energies reveal a more complex behavior with the relative difference of around 0.4 cm^{-1}. Our results confirm that the Raman technique can also be very useful in determining the thicknesses of the flakes in magnetic layered materials.

[1] D. P. Kozlenko, et al., *npj Quantum Materials* **6**, 2397-4668, (2021).
[2] M. Gilbertini, M. Koperski, et el., *Nat. Nanotechnol.* **14**, 408-419, (2019).

Nagaoka ferromagnetism in phosphorene quantum dots

Tanmay Thakur and Bartłomiej Szafran

AGH University of Science and Technology,
Faculty of Physics and Applied Computer Science,
al. Mickiewicza 30, 30-059 Kraków, Poland

Phosphorene, a monolayer form of black phosphorus, is a 2D material with strong anisotropy of the effective masses [1,2] that has been investigated in recent years. We consider a 2x2 array of quantum dots in phosphorene to investigate Nagaoka ferromagnetism - a magnetic ordering promoted in a system where number of electrons are one less than the number of sites. Although the ordering of spins in such system was proved by Nagaoka earlier, an experimental demonstration of this physical phenomenon was shown only recently by Ref. [3] for quantum dots arranged in square array in GaAs. Given than the electrons in phosphorene have large masses as well as large anisotropy, it is not obvious that the magnetic ordering will persist for the square array system in the material. We investigate the robustness of Nagaoka ferromagnetism against the geometry of the arranged dots using a single-band effective mass Hamiltonian [4] to extract the ground state of the system. An exact phase diagram of magnetic ordering as a function of the rectangle parameters is shown and we find the accurate geometry for which the Nagaoka energy gap is the largest. We also discuss the robustness of this ground state against potential detuning and shifting of one quantum dot. We demonstrate that shifting the dot has different impact on the ground state in different directions due to anisotropy, and thus Lieb-Mattis theorem, not Nagaoka theorem, now describes the deformed configuration.

[1] Li, L., Yu, Y., Ye, G. et al., *Nature Nanotech* **9**, 372–377 (2014).
[2] Xia, F., Wang, H. & Jia, Y., *Nat Commun.* **5**, 4458 (2014).
[3] Dehollain, Juan P., et al., *Nature* **579** (7800), 528-533 (2020).
[4] B. Szafran, *Phys. Rev. B* **101**, 23, 235313 (2020).

Magneto-phonon interaction in layered $Cr_2Ge_2Te_6$ ferromagnet

Grzegorz Krasucki[1] , **Katarzyna Olkowska-Pucko**[1], **Mihai I. Sturza**[2], **Holger Kohlmann**[2], **Adam Babiński**[1] **and Maciej R. Molas**[1]

[1] *Institute of Experimental Physics, Faculty of Physics, University of Warsaw, Warsaw, Poland*
[2] *Inorganic Chemistry, Leipzig University, Leipzig, Germany*

Two-dimensional magnets with van der Waals (vdW) structures have recently been revisited due to their potential uses. This fascinating group of materials gives high hopes to improve our spintronics nanotechnology and understanding of magnetic effects in two dimensional structures. Among magnetic vdW materials, $Cr_2Ge_2Te_6$ is a particularly interesting material, as it is in the very rare class of ferromagnetic semiconductors with a Curie temperature (T_c) of about 61 K and exhibits thickness-dependent ferromagnetic transition [1].

In this work, we examine Raman scattering (RS) measured on 10-nm-thick $Cr_2Ge_2Te_6$ flake using an excitation energy of 1.96~eV in a wide temperature range (5-300 K) and with polarization resolution.

The low-temperature (T=5 K) Raman spectrum of the studied $Cr_2Ge_2Te_6$ flake is composed of 7 Raman peaks, see the Figure. Their assignment to two groups of symmetries (E_g and A_g) was confirmed using polarization-resolved Raman experiments. Although most of the Raman peaks experience redshifts with increasing temperature, there are two Raman modes, E_g^2 and E_g^4, marked by red arrows in the Figure, which are sensitive to the transition through the T_c temperature. The E_g^2 peak disappears from the spectra above the T_c temperature, while E_g^2 one experiences nontrivial temperature evolution. Interestingly, the temperature dependence of the E_g^4 mode was already reported in Ref. [2]. In our case, the E_g^4 peak disappears from the Raman spectra above the T_c temperature, while its opposite behavior is observed under excitation energy of 2.41 eV.

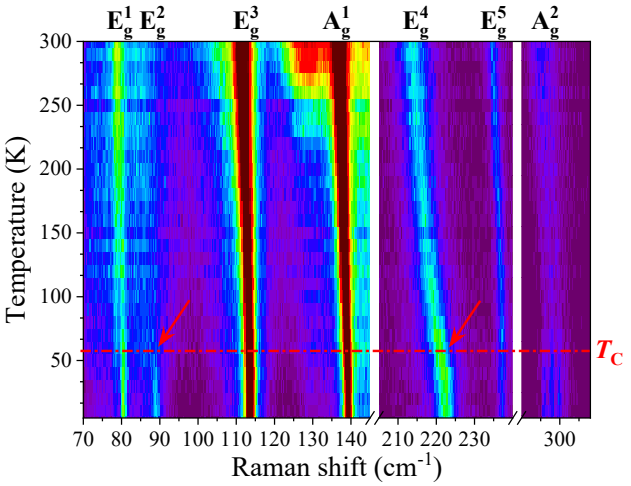

Figure False-colour map of temperature evolution of the RS spectra measured on $Cr_2Ge_2Te_6$ flake. The T_c value is indicated by horizontal red line, while the red arrows point abrupt transition for two peaks around T_c.

Our results demonstrate that the electron-phonon interaction, i.e. interplay between resonant and non-resonant conditions of Raman scattering, may be also important for the magneto-elastic coupling in the magnetic layered materials.

[1] C. Gong, *et al.*, *Nature* **546,** 265 (2017)
[2] Y. Tian, *et al.*, *2D Materials* **3,** 025035 (2016)

Investigating the Proximity Effect in h-BN/ 2D Magnet Heterostructures

Katarzyna Ludwiczak[1], Johannes Binder[1], Aleksandra Krystyna Dąbrowska[1], Piotr Tatarczak[1], Joanna Sitnicka[1], Jacek Jasiński[2], Roman Stępniewski[1], Andrzej Wysmołek[1]

[1]University of Warsaw, Pasteura 5, 02-093 Warsaw, Poland;
[2]University of Louisville, 2301 S 3rd St, Louisville, KY 40292, United States of America

Hexagonal boron nitride (h-BN) is a two-dimensional crystal widely used in layered materials research due to its flat surface, high chemical stability, and lack of dangling bonds. Recent advances in the study of color centers in h-BN have made it an excellent platform for investigating basic physical phenomena, including optically addressable spin defects, rendering it a promising candidate for quantum technologies [1].

We focus on the growth of high quality h-BN samples using Metalorganic Vapour Phase Epitaxy (MOVPE) technique. The samples are grown on large (~2 inches) sapphire substrates and cover them uniformly [2,3]. This method allows us to engineer material parameters such as its thickness, structure and consequently - type and concentration of defects. We observe emission from colour centres in epitaxially grown h-BN at different energies, indicating the presence of various defects, like boron vacancies or carbon-related defect complexes.

In this study, we explore the proximity effect between h-BN and 2D magnets (e.g. chromium trihalides). Such an approach enables the investigation of paramagnetic centres in h-BN using locally applied magnetic fields. We studied the photoluminescence of h-BN/$CrBr_3$/h-BN heterostructures and found an additional peak in the spectrum at low (liquid helium) temperature. We believe that the optical response is correlated with the magnetic ordering in $CrBr_3$ crystals (Fig 1).

In the future, the creation of such heterostructures can become feasible using a subsequential growth of 2D magnets on top of the h-BN epitaxial layers [3]. Such an approach could be a reliable solution for scaling up ultrathin heterostructures and allowing their future development for real-life applications.

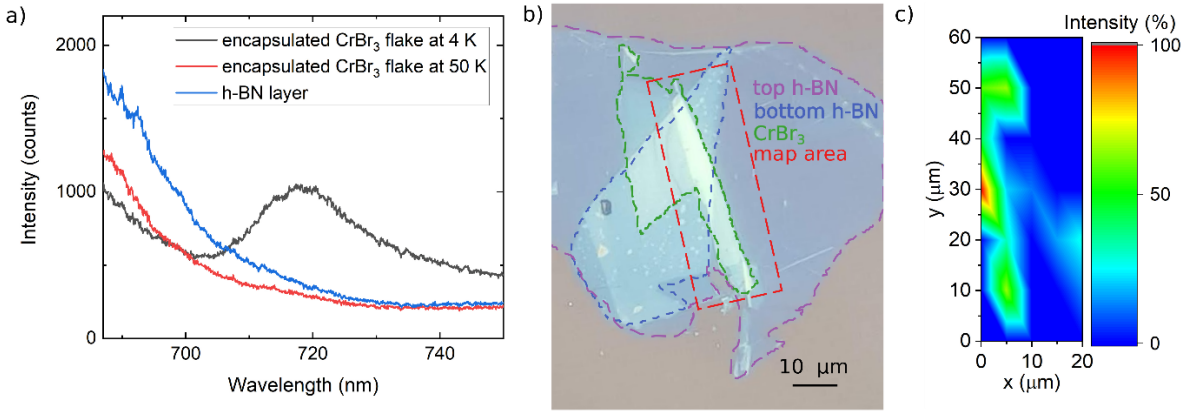

Fig. 1. a) Photoluminescence spectra of a h-BN/$CrBr_3$/h-BN heterostructure. b) Optical microscope image of the studied heterostructure. c) Intensity (peak area) map of the additional photoluminescence peak of the studied heterostructure.

This work was supported by the National Science Centre, Poland under decisions 2019/33/B/ST5/02766, 2020/39/D/ST7/02811 and 2021/41/N/ST3/03579.

[1] A. Gottscholl, et al., *Nature Materials* **19,** 540 (2020)
[2] A.K. Dąbrowska et al. *2D Mater.*, **8**, 015017 (2021)
[3] K. Ludwiczak et al., *ACS Appl. Mater. Interfaces* (2021), **13(40):** 47904–47911

Thermoelectric properties of $Pb_{1-x}Sn_xTe$ crystals doped with vanadium deep donors

T. Andrearczyk[1], A. Królicka[1], J. Korczak[1,2], M. Szot[1,2], R. Minikayev[1], P. Dziawa[1], E. Łusakowska[1], A. Szczerbakow[1], K. Dybko[1,2], T. Story[1,2]

[1]*Institute of Physics, Polish Academy of Sciences, Al. Lotników 32/46, 02-668 Warsaw, Poland*
[2]*International Research Centre MagTop, Institute of Physics, Polish Academy of Sciences, Al. Lotników 32/46, 02-668 Warsaw, Poland*

PbTe and SnTe as well as their substitutional alloys $Pb_{1-x}Sn_xTe$ are IV-VI semiconductor materials well known for topological crystalline insulator (TCI) properties as well as for their applications in mid-infrared devices and thermoelectric generators. Optimal application of these materials requires controlling of both type and concentration of conducting carriers: from almost semi-insulating bulk materials desired in TCIs to heavily doped (n,p=10^{19} - 10^{20} cm^{-3}) thermoelectric elements. In $Pb_{1-x}Sn_xTe$ the electrically active native defects (metal vacancies) determine very high background hole concentration (p=10^{18} - 10^{19} cm^{-3}). Controlling electrical properties requires doping with extrinsic donors (Bi, J) or acceptors (Na, Ag) and/or thermal annealing. Thermoelectric properties of $Pb_{1-x}Sn_xTe$ can also be controlled by incorporation of 3d transition metals, like Cr, Fe or V. The solubility of these transition metals in IV-VI semiconductors is limited to heavily doping regime (typically below 0.5 at.%) but they form a special class of resonant donor centers with the mixed valence 3+/2+ charge state depending on Sn content and Fermi level position.

In this work, we examine $Pb_{1-x}Sn_xTe$:V bulk crystals with nominal Sn content of x=0.2 and V content of 1 at.% grown by the Bridgman method under varying thermal regime and doping procedure. The crystals studied cover the composition range corresponding to the expected in-gap position of $V^{2+/3+}$ donor level [1]. Electron microscopy SEM-EDX analysis of chemical composition confirmed the Sn concentration smoothly varying along an ingot from x=0.13 to x=0.3 and an indication for very small V content (below 0.5 at. %) increasing towards the end of an ingot. To examine electrical properties, we measured the electrical conductivity and the Hall effect in the temperature range T=5-300 K revealing only p-type metallic conductivity with carrier concentration $p\approx 7*10^{18}$ cm^{-3} and resistivity ratio $\rho(300K)/\rho(5K)\approx 10$ due to the temperature dependence of mobility. We also measured, at room temperature, the thermoelectric power α and determined the key applicational parameter - thermoelectric power factor $P_\sigma=\alpha^2/\rho\approx 8\mu W/K^2cm$ (comparable to observed in good PbTe-based thermoelectric materials). No in-gap pinning of Fermi level by $V^{2+/3+}$ donors and semi-insulating state was experimentally found, presumably because only small part of V centers introduced into $Pb_{1-x}Sn_xTe$ (estimated 0.1 at.%) becomes electrically active. As a result, the electrical conductivity of our $Pb_{1-x}Sn_xTe$:V bulk crystals still remains dominated by native defects. This balance can be changed by further doping with V or reduction of vacancies concentration by annealing.

This research has been partially supported by the Foundation for Polish Science through the IRA Programme co-financed by EU within SG OP and by TechMatStrateg2/408569/5/NCBR/2019 project TERMOD of NCBR.

[1] E.P. Skipetrov et al., Semiconductors **46**, 741 (2012); Low Temp. Phys. **37**, 210 (2011).

Effect of Ni and Mn dopant on thermoelectric power generation performance of ZnO nanostructures synthesized via hydrothermal method

Ubaid ur Rehman[1], Khalid Mahmood[2], Arslan Ashfaq[2], Muhammad Faisal Iqbal[3], Kashaf ul Sahar[4], Abbas Ahmad Khan[5], Ejaz Hussain[4]*

[1]*Institute of Physics, Polish Academy of Sciences, Al. Lotników 32/46, 02-668 Warsaw, Poland*
[2]*Department of Physics, Government College University Faisalabad, Pakistan*
[3]*Department of Physics, Riphah International University Faisalabad, Pakistan*
[4]*Department of Chemistry, The Islamia University of Bahawalpur, Pakistan*
[5]*Department of Electronic Engineering, Hanyang University, Seoul 04763, South Korea*

**Ubaid.hsp@gmail.com*

Abstract

In this article, we have presented a low-cost hydrothermal approach to enhance the thermoelectric performance of ZnO nanostructures via modulation doping. For this purpose, we have prepared a series of pure and X:ZnO (X= Ni & Mn) samples. The Seebeck value of the Mn-doped samples possesses the maximum Seebeck coefficient of -36 $\mu V/^oC$ compared to the pure and Ni-doped samples (-22 $\mu V/^oC$ & -27 $\mu V/^oC$) at room temperature. The highest value of the Seebeck coefficient for the Mn-doped samples is related to the formation of mid-gap energy band states due to the substitution of Mn^{2+} with Zn^{2+}. These mid-band states induce an imbalance in the DOS, by producing a spin polarization effect that leads to a high Seebeck value. In terms of electrical conductivity, the Ni-doped ZnO sample exhibits the highest electrical conductivity of about 122 S/cm, due to the incorporation of Ni metal ions inside the ZnO matrix (confirmed by XRD) and leads to a high carrier concentration. However, the highest Seebeck value for the Mn-doped sample results in the maximum thermoelectric power factor $\sim 1.12\times10^{-5}$ $Wm^{-1}C^{-2}$ at room temperature.

Keywords; ZnO, doping, XRD, Seebeck coefficient, Electrical conductivity, Power factor

Acknowledgment

The author would like to acknowledge the funding from Polish National Science Centre (NCN) Project No. UMO-2016/22/E/ST3/00553 for the accomplishment of this research work.

Outstanding Thermoelectric Properties (ZT ≈ 5 – 6) of Functionalized 2D Molybdenum Nitrides (MXenes)

Jan Kołodziejczyk and Jacek A. Majewski

Faculty of Physics, University of Warsaw, ul. Pasteura 5, Warsaw, Poland

MXenes are relatively new family of low dimensional materials, which has been gaining more and more popularity in recent years. MXenes are mainly carbides and nitrides of early transition metals and they combine the properties of both components. Bare MXenes typically exhibit metallic behaviour and, therefore, are known to be good electric conductors. Interestingly, this property changes with functionalization of their surfaces. It occurs that functionalizing groups can change metallic MXenes into semiconducting ones, and not only open the band gap but also influence other properties, just opening the path towards many potential applications, e.g., in electronics, optoelectronics, and thermoelectricity.

In this communication, we present probably the first reported studies of geometry, stability, electronic structure and transport properties of bare and functionalized molybdenum nitrides Mo_2N (MXenes). The studies are based on first-principles calculations in the framework of density functional theory (DFT) employing pseudo-potentials and plane-wave basis as implemented in the QUANTUM ESPRESSO package. Here, we discuss the results for the bare, and functionalized with oxygen and fluorine Mo_2N layers. The bare Mo_2N is metallic with good electric conductivity. Functionalization of Mo_2N with F leads to opening of the band gap of 0.09 eV below the Fermi level, whereas the Mo_2N functionalization with O creates p-type semiconductor with energy gap of 0.49 eV.

The electronic transport properties were calculated using BoltzTraP2 code and the phonon transport properties were obtained by the Phono3py. It occurs that functionalization has significant impact on Seebeck coefficient and lattice thermal conductivity of these materials, quantities strongly determining the thermoelectric performance. The Seebeck coefficient is increased to $2.5*10^{-4}$ VK^{-1} for Mo_2NF_2 and $1.2*10^{-3}$ VK^{-1} for Mo_2NO_2. Functionalization decreases lattice thermal conductivity by about 6.5 times for Mo_2NF_2 and 10 times for Mo_2NO_2. These effects lead to the impressive thermoelectric properties of studied MXenes - with thermoelectric figure of merit in the range of $0.3 < ZT < 0.78$ for Mo_2NF_2 and $2.25 < ZT < 5.65$ for Mo_2NO_2, what outperforms all currently known materials.

Acknowledgement: This research has been supported by the NCN grant OPUS-16 (UMO2018/31/B/ST3/03758).

Photoemission study of the thermoelectric group IV-VI van der Waals crystals (GeS, SnS, and SnSe)

Agata K. Tołłoczko[1], Szymon J. Zelewski[1], Michał Błaszczak[1], Natalia Olszowska[2], Marcin Rosmus[2], Sefaattin Tongay[3], and Robert Kudrawiec[1]

[1] *Department of Semiconductor Materials Engineering, Wrocław University of Science and Technology, Wybrzeże Wyspiańskiego 27, 50-370 Wrocław, Poland*

[2] *Solaris National Synchrotron Radiation Centre, Jagiellonian University, Czerwone Maki 98, 30-392 Kraków, Poland*

[3] *School for Engineering of Matter, Transport and Energy, Arizona State University, Tempe, Arizona 85287, USA*

Semiconducting group IV-VI van der Waals crystals (MX, where M = Ge, Sn, and X = S, Se) are receiving increasing attention as environmentally-friendly thermoelectric materials. Among them, SnSe is considered the most promising as it exhibits a remarkably high thermoelectric figure of merit (ZT), initially attributed to its low lattice thermal conductivity [1]. However, it has been shown that the electronic band structure plays an equally important role in thermoelectric performance [2,3]. A certain band shape, described as a "pudding mold" and characteristic for all MXs, has been predicted to significantly improve ZT by combining good electrical conductivity with high Seebeck coefficient [4]. We explore this subtle feature experimentally for GeS, SnS, and SnSe by means of angle-resolved photoemission spectroscopy. The technique also allowed us to determine the effective mass and Fermi level position of as-grown undoped crystals. Our findings are supported by *ab initio* calculations of the electronic band structure. The results greatly contribute to the general understanding of the valence band dispersion of MXs and reinforce their potential as high-performance thermoelectric materials, additionally giving prospect for designing systems consisting of van der Waals heterostructures.

[1] L.-D. Zhao *et al*., Nature **508**, 7496 (2014).
[2] I. Pletikosić *et al*., Phys. Rev. Lett. **120**, 156403 (2018).
[3] Z. Wang et al., Nat Commun **9**, 1 (2018).
[4] K. Kuroki and R. Arita, J. Phys. Soc. Jpn. **76**, 083707 (2007).

Extension of rapid estimation of the flake thickness by color for a magnetic van der Waals 2D material

R. Komar, M. Raczyński, T. Kazimierczuk and P. Kossacki

Institute of Experimental Physics, Faculty of Physics, University of Warsaw, Pasteura 5, PL-02-093 Warsaw, Poland

The color analysis of thin flakes exfoliated on Si/SiO_2 substrates is an efficient method for identification of flakes of a given thickness. It is well known since the beginning of studies on graphene and related thin materials (especially hexagonal boron nitride[1]). With this method, we can bypass the need of using atomic force microscopy (AFM) to measure the thickness, significantly increasing the speed of the assembly of more complex structures. Thus, we greatly reduce the exposure time of the sample to potentially degrading external agents, which would be especially beneficial for rapidly oxidizing materials, one of which is chromium sulfide bromide (CrSBr).

CrSBr is an example of a layered van der Waals material that combines both optical and magnetic properties. Such a combination usually requires stacking of two different materials, while here it is realized within a single flake. The coupling of magnetic and optical properties makes this material a potential system for spintronics applications. Additionally, the magnetic properties of these materials vary with the number of atomic layers, which can help tailor them for technological applications.

Have we extended the well known methods of fast optical estimation of the layer thickness on the group of magnetic materials. By careful comparison of optical color images and AFM scans, we calibrate this technique for such materials as CrSBr. An example of a flake snapshot from the optical microscope and AFM scan with thickness readings for CrSBr is shown in Fig. 1. Importantly, most of the steps within this procedure can be done in a glovebox within a very high purity inert atmosphere, reducing the chance of material degradation.

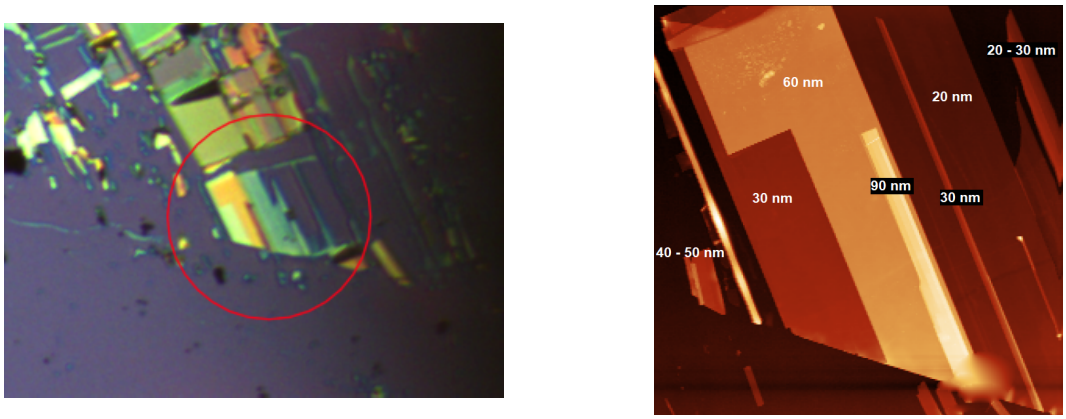

a) b)

Figure 1: Snapshot and AFM scan (with thickness labels) of CrSBr flake.

The obtained data allowed us to map the range of the thicknesses corresponding to selected colors. We discuss also enhancement of the sensitivity possible with use of narrow color filters.

[1] Yuto Anzai, et al, 2019, *Appl. Phys. Express* **12** 055007

Coherent shuttling of spins between silicon-based quantum dots

Łukasz Cywiński[1]

[1] *Institute of Physics, Polish Academy of Sciences, al. Lotników 32/46, PL 02-668 Warsaw, Poland*

Coherent communication between quantum registers separated by ~ 10 μm distances is one of the requirements for scalability of architectures based on gated quantum dots [1]. Moving a spin qubit across this distance, e.g. along a chain of tunnel-coupled dots [2], is one of possible solutions. I will discuss our recent theoretical work [3,4] on such a dot-to-dot adiabatic charge transfer in presence of realistic amount of charge noise and electron-phonon coupling in Si/SiGe QDs, which are currently the best candidates for a scalable semiconductor qubit architecture. I will discuss the close relationship between non-adiabatic (and thus non-deterministic) character of charge transfer, and spin dephasing caused by dot- and state-specific g-factors. Finally, I will describe an alternative qubit shuttling scheme in which gates are used to create a moving quantum dot [5,6]. I will argue that this scheme is more robust to electrostatic disorder compared to the one based on pre-existing tunnel coupled quantum dots, and I will discuss how the valley-orbit coupling in presence of interface roughness will be the main source of spin qubit dephasing in this scheme [6].

This work has been funded by the National Science Centre (NCN), Poland under QuantERA program, Grant No. 2017/25/Z/ST3/03044. Project Si-QuBus has received funding from the QuantERA ERA-NET Cofund in Quantum Technologies implemented within the European Union's Horizon 2020 program.

[1] L.M.K. Vandersypen, H. Bluhm, J. S. Clarke, A. S. Dzurak, R. Ishihara, A. Morello, D. J. Reilly, L. R. Schreiber, and M. Veldhorst, *Interfacing spin qubits in quantum dots and donors—hot, dense, and coherent*, npj Quantum Inf. **3**, 1 (2017); J. M. Boter et al, *The spider-web array–a sparse spin qubit array*, preprint arXiv:2110.00189 (2021).

[2] A.R. Mills, D.M. Zajac, M.J. Gullans, F.J. Schupp, T.M. Hazard, and J.R. Petta, *Shuttling a single charge across a one-dimensional array of silicon quantum dots*, Nat. Commun. **10**, 1063 (2019).

[3] J.A. Krzywda and Ł. Cywiński, *Adiabatic electron charge transfer between two quantum dots in presence of* $1/f$ *noise*, Phys. Rev. B **101**, 035303 (2020).

[4] J.A. Krzywda and Ł. Cywiński, *Interplay of charge noise and coupling to phonons in adiabatic electron transfer between quantum dots*, Phys. Rev. B **104**, 075439 (2021).

[5] I. Seidler, T. Struck, R. Xue, N. Focke, S. Trellenkamp, H. Bluhm, and L. R. Schreiber, *Conveyor-mode single electron shuttling in Si/SiGe for a scalable quantum computing architecture*, npj Quantum Inf. **8**, 100 (2022).

[6] V. Langrock, J.A. Krzywda, N. Focke, I. Seidler, L.R. Schreiber, and Ł. Cywiński, *Blueprint of a scalable spin qubit shuttle device for coherent mid-range qubit transfer in disordered Si/SiGe/*SiO_2, preprint arXiv:2202.11793, accepted to Phys. Rev. X Quantum.

Spin valley qubits in gated quantum dots in 2D

Maciej Bieniek [1,2]

[1] *Institut für Theoretische Physik und Astrophysik, Universität Würzburg, 97074 Würzburg, Germany,* [2] *Institute of Theoretical Physics, Wrocław University of Science and Technology, Wybrzeże Wyspiańskiego 27, 50-370 Wrocław, Poland*

With the development of advanced methods for fabricating 2D materials heterostructures, devices based on atomically thin semiconducting transition metal dichalcogenides (TMDs) are emerging as a promising platform in the field of quantum information science. Semiconducting TMDs typically exhibit a direct bandgap at the K-point in the hexagonal Brillouin zone. They have potential for realizing spin qubits with long coherence time due to spin-valley locking, caused by the strong spin–orbit interaction and the symmetries of their 2D lattice. These promising properties motivate our recent efforts to understand quantum dots in 2D materials [1-7]. In the first part of the talk I will review experimental progress in the field of gated TMD's quantum dots [6,7].

In the second part, I will present our theoretical approach to electronic structure of TMD's. Starting from general properties obtained using ab initio methods, I will discuss construction of the tight-binding model [1]. Then, I will describe an atomistic theory of electrons confined by metallic gates computed using a computational box with periodic boundary conditions including up to millions of atoms [2]. I will show twofold degenerate energy spectrum of electrons confined in the two nonequivalent K valleys as well as sixfold degenerate spectrum associated with Q valleys, the role of spin splitting and topological moments on valley electronic states. Next, I will focus on the strongly interacting system of electrons [3], where we predict the existence of valley- and spin-polarized broken-symmetry states tunable by the parabolic confining potential. The ground state in such system is formed by one of two phases, both spin and valley polarized or valley unpolarized but spin intervalley antiferromagnetic, which compete as a function of electronic shell spacing.

In the third part, I will focus on the theory of electron-spin-based qubits [4]. The qubits are identified with two degenerate spin and valley locked states in a gated quantum dot. I will describe the qubit operations necessary to rotate the spin-valley qubit as a combination of the applied vertical electric field, enabling spin-orbit coupling in a single valley, with a lateral strongly localized valley-mixing gate. I will also discuss the two-qubit system defined on valley isospins [5] of two electrons confined in a gate-defined double quantum dot, focusing on how to initialize, control, interact, and read out such valley qubits by only electrical means.

[1] M. Bieniek, M. Korkusiński, L. Szulakowska, P. Potasz, I. Ozfidan, P. Hawrylak, Phys. Rev. B 97, 085153 (2018),
[2] M. Bieniek, L. Szulakowska, and P. Hawrylak, Phys. Rev. B 101, 035401 (2020),
[3] L. Szulakowska, M. Cygorek, M. Bieniek, P. Hawrylak, Phys. Rev. B 102, 245410 (2020),
[4] A. Altintas, M. Bieniek, A. Dusko, M. Korkusiński, J. Pawłowski, P. Hawrylak, Phys. Rev. B 104, 195412 (2021),
[5] J. Pawłowski, M. Bieniek, T. Woźniak, Phys. Rev. Applied 15, 054025 (2021),
[6] J. Boddison-Chouinard, A. Bogan, N. Fong, K. Watanabe, T. Taniguchi, S. Studenikin, A. Sachrajda, M. Korkusiński, A. Altintas, M. Bieniek, P. Hawrylak, A. Luican-Mayer, L. Gaudreau, Appl. Phys. Lett. 119, 133104 (2021),
[7] A. Luican-Mayer, J. Boddison-Chouinard, A. Bogan, P. Barrios, J. Lapointe, K. Watanabe, T. Taniguchi, J. Pawłowski, D. Miravet, M. Bieniek, P. Hawrylak, L. Gaudreau, https://doi.org/10.21203/rs.3.rs-2133454/v1, preprint (2023).

Longitudinal coupling between electrically driven spin-qubits and a resonator

Sarath Prem, Marcin M. Wysokiński, Mircea Trif

International Research Centre MagTop, Institute of Physics, Polish Academy of Sciences, Aleja Lotników 32/46, PL-02668 Warsaw, Poland

At the core of the semiconducting spin qubits success is the ability to manipulate them electrically, enabled by the spin-orbit interactions. However, most implementations require external magnetic fields to define the spin qubit, which in turn activate various charge noise mechanisms. Here we study spin qubits confined in quantum dots at zero magnetic fields, that are driven periodically by electrical fields and are coupled to a microwave resonator. Using Floquet theory, we identify a well-defined Floquet spin-qubit originating from the lowest degenerate spin states in the absence of driving. We find both transverse and longitudinal couplings between the Floquet spin qubit and the resonator, which can be selectively activated by modifying the driving frequency. We show how these couplings can facilitate fast qubit readout and the implementation of a two-qubit CPHASE gate. Finally, we use adiabatic perturbation theory to demonstrate that the spin-photon couplings originate from the non-Abelian geometry of states endowed by the spin-orbit interactions, rendering these findings general and applicable to a wide range of solid-state spin qubits.

[1] S. Prem, M. M. Wysokiński, and M. Trif, arXiv: 2301.10163 (2023).

Optical control of solid-state quantum emitters

Doris E. Reiter

Condensed Matter Theory, TU Dortmund, 44221 Dortmund, Germany

Solid-state quantum emitters play a vital role in quantum technologies as photon sources. To make them viable for actual applications, the emitted photons need to have close to perfect properties. This includes a high brightness, high purity, high indistinguishability and, in case of entangled photons, a high concurrence. Semiconductor quantum dots are at the moment the most promising candidates to fulfil these requirements as astonishing good values for such quantities have been reported in the last few years. However, there is still room for improvement.

One aspect is the preparation of the excited state, which then leads to the emission of the photons. The straight forward method of resonant excitation, making use of the Rabi scheme, suffers from the influence of phonons [1]. Furthermore, because the exciting frequency is the same as the frequency of the emitted photons, sophisticated polarization filtering results in a loss of half the photons. Off-resonant schemes like the phonon-assisted state preparation [1] are incoherent, which can be disadvantageous depending on the target state. Accordingly, new protocols are proposed to optimize the excitation of quantum emitters.

In this talk, I will review different optical preparation schemes to excite the quantum emitter. In addition to well established schemes like Rabi or phonon-assisted processes, I will introduce the Swing-UP of EmitteR Population (SUPER) scheme that uses two red-detuned pulses to excite a quantum emitter [2]. Besides displaying interesting physics, the SUPER scheme is coherent and truly off-resonant and, thus, spectral filtering can be applied [3]. This could boost the photon rate up to a factor of two, making the SUPER scheme highly interesting for applications in quantum technology.

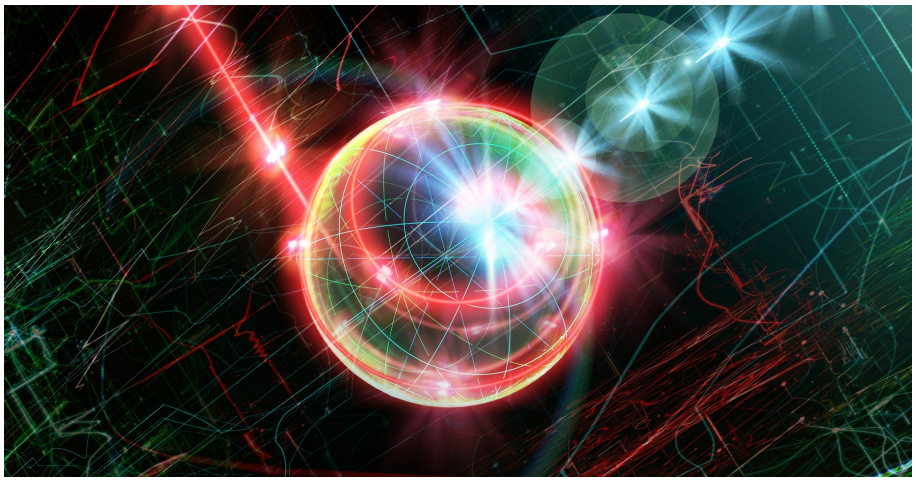

Figure 1: Artistic view of the Bloch sphere under the SUPER scheme

[1] D. E. Reiter, Acta Phys. Pol. A 122,1065 (2012).
[2] T. K. Bracht, D. E. Reiter et al., PRX Quantum 2, 040354 (2021).
[3] Y. Karli et al., Nano Lett. 16, 6567 (2022).

Epitaxial InAs/InP quantum dots as emitters of single photons and entangled photon pairs for fiber-based quantum communication

A. Musiał[1], M. Wasiluk[1], K. Roszak[2], M. Gawełczyk[3], P. Holewa[1], P. Wyborski[1], P. Podemski[1], M. Burakowski[1], H. Salamon[1], P. Mrowiński[1], M. Mikulicz[1], T. Smołka[1], K. Posmyk[1], A. Zielińska[1], J. P. Reithmaier[4], M. Benyoucef[4], G. Sęk[1] and W. Rudno-Rudziński[1]

[1] *Department of Experimental Physics, Politechnika Wrocławska, Wrocław, Poland*
[2] *Institute of Physics, Czech Academy of Sciences, Prague, Czech Republic*
[3] *Institute of Theoretical Physics, Politechnika Wrocławska, Wrocław, Poland*
[4] *Institute of Nanostructure Technologies and Analytics (INA), Center for Interdisciplinary Nanostructure Science and Technology (CINSaT), University of Kassel, Kassel, Germany*

Quantum dots (QDs) are an important resource for quantum communication, because of their capability of generating various non-classical light states. Compared to other physical systems, QDs provide high single-photon purity independent of the source brightness. They offer the possibility for on-chip integration and compatibility with well-established semiconductor technology, including deterministic fabrication of photonic devices. To fully exploit their application potential, emission in the telecom bands is required. InAs/InP material system is one alternative to provide emission in the telecom C-band [1].

Our work concerns InAs/InP QDs grown using ripening assisted molecular beam epitaxy technique [2]. They have been proven to be efficient sources of (triggered) single photons, with multiphoton emission probability below 1% [3] and spectrally broad (~60 nm) extraction efficiency for the QDs placed inside simple cylindrical photonic structures, at the maximum exceeding 13% [4]. Their thermal stability is better than for GaAs-based QDs emitting in this spectral range due to deeper confining potential, and it is mainly limited by escape of holes via the ladder of QD's excited states [5,6]. It enables maintaining single QD emission for temperatures as high as 150 K, which makes this system suitable for simple and cost-effective cooling methods, thus considerably increasing its application potential.

Additionally, these dots feature spin memory effects allowing for preferential initialization of electron spin state [6]. However, identification of trions is not straightforward and requires magnetooptical investigations [7], due to high in-plane symmetry of these dots, manifesting in low exciton fine structure splitting [2]. This, on the other hand, allowed achieving emission of entangled photon pairs (fidelity exceeding 0.55) generated from biexciton-exciton cascade at telecom C-band. It was realized under non-resonant excitation of a QD in a simple mesa structure and it can be improved by selected excitation of target states and placing QDs deterministically in microcavity structures. This enables application of such InAs/InP QDs in implementation of quantum teleportation schemes or quantum repeater architecture.

[1] M. Benyoucef and A. Musiał, *Chapter 18* in *Photonic Quantum Technologies: Science and Applications*, in press, WILEY-VCH GmbH (2023).
[2] A. Kors et al., *Applied Physics Letters* **112**, 172102 (2018).
[3] A. Musiał et al., *Advanced Quantum Technologies* **3(2)**, 1900082 (2020).
[4] A. Musiał et al., *Applied Physics Letters* **118**, 221101 (2021).
[5] T. Smołka et al., *Materials* **14**, 6270 (2021).
[6] P. Podemski et al., *Optics Express* **29**, 34024 (2021).
[7] W. Rudno-Rudziński et al., *Materials* **14**, 942 (2020).

State-of-the-art Quantum Dot-based Single-photon Sources for Quantum Key Distribution in Silica Fiber Networks at 1550 nm

Paweł Holewa [1,2,3], Emilia Ostój-Zięba[1], Daniel A. Vajner[4], Timm Gao[4], Mareike Lach[4], Maja Wasiluk[1], Benedek Gaal[2], Aurimas Sakansas[2], Marek Burakowski[1], Paweł Mrowiński[1], Bartosz Krajnik[1], Meng Xiong[2,3], Aleksander Huck[5], Kresten Yvind[2,3], Niels Gregersen[2], Anna Musiał[1], Tobias Heindel[4], Elizaveta Semenova[2,3] and Marcin Syperek[1]

[1] *Department of Experimental Physics, Faculty of Fundamental Problems of Technology, Wrocław University of Science and Technology, 50-370 Wrocław, Poland*
[2] *DTU Electro, Technical University of Denmark, Kongens Lyngby 2800, Denmark*
[3] *NanoPhoton-Center for Nanophotonics, Technical University of Denmark, 2800 Kongens Lyngby, Denmark*
[4] *Institute of Solid State Physics, Technical University of Berlin, 10623 Berlin, German*
[5] *Center for Macroscopic Quantum States (bigQ), Department of Physics, Technical University of Denmark, 2800 Kgs. Lyngby, Denmark*

Optical fiber-based quantum network connecting remote nodes forms the backbone to implement ultra-secure data exchange protocols and schemes, utilizing a quantum state of a single photon. Notably, for such quantum networks existing silica-fiber-based infrastructure can be used, where the spectral window around 1550 nm provides a low-loss photon transmission channel for long-haul communication. Moreover, one can benefit from existing devices and classical signal management protocols, simplifying the preparation, encoding and transfer of quantum states. Devices producing single photon states on demand are considered key building blocks of future quantum networks. While several single-photon sources (SPS) operating in the telecom C-band, including sources based on non-linear frequency conversion or emerging materials, have been demonstrated to date, semiconductor quantum dots (QDs) are among the most promising candidates, enabling exceptional performance and engineered photonic devices.

In this presentation, we show a deterministically-fabricated optically-triggered SPS emitting in the telecom spectral range near 1550 nm. The SPS consists of a single pre-selected self-assembled InAs/InP QD embedded in a circular Bragg grating cavity for Purcell-enhanced emission of the embedded quantum emitter. The applied deterministic fabrication technique results in a high device yield in combination with excellent quantum-optical properties, paving the way for scalable applications in photonic quantum information technologies. The high Purcell enhancement with $F_p = 5$ realized in our device, shows potential for single photon generation at GHz rates. Moreover, the cavity's far-field emission pattern allows for efficient photon extraction close to 17% at the numerical aperture 0.4, which can be further optimized for the coupling to single-mode fibers. The device provides high single photon emission purity with $g^{(2)}(0) = 3.2\times10^{-3}$ at $T = 4.2$ K, while still supporting a good performance ($g^{(2)}(0) = 0.2$) at elevated temperatures ($T = 50$ K) accessible with compact Stirling-type cryocoolers. Finally, Hong-Ou-Mandel-type two-photon interference (TPI) experiments reveal record-high photon indistinguishabilities of 19% in the as-measured case and 99.8% with temporal post-selection.

Finally, we evaluated our SPS in a test environment for its potential implementation in polarization-encoded BB84 quantum key distribution (QKD) in silica fiber networks. A careful benchmarking of the performance of our source compared with previous single-photon QKD experiments reveals that transmission distances in excess of 100 km can be expected in full implementations.

Heterogeneously Integrated InAs/InP Quantum Dot Single-photon Emitter with the Si Platform for On-chip Quantum Photonics

Marek Burakowski[1], Paweł Mrowiński[1], Paweł Holewa[1,2,3], Aurimas Sakanas[2], Elizaveta Semenova[2,3], Grzegorz Sęk[1] and Marcin Syperek[1]

[1] *Department of Experimental Physics, Faculty of Fundamental Problems of Technology, Wrocław University of Science and Technology, Wybrzeże Wyspiańskiego 27, 50-370 Wrocław, Poland*
[2] *DTU Electro, Technical University of Denmark, Kongens Lyngby 2800, Denmark*
[3] *NanoPhoton-Center for Nanophotonics, Technical University of Denmark, 2800 Kongens Lyngby, Denmark*

Photonics-based quantum technologies would remarkably advance the processing and transfer of information. Photonic integrated circuits (PIC) in which semiconductor-based components, like emitters, waveguides (WGs), and detectors, can all be integrated on a compact photonic chip, provide a better performance, and increase their functionality when assembled with silicon-based electronics.

We present modelling, fabrication, and experimental studies on a hybridized InP/Si WG system with InAs/InP quantum dots (QDs) as single photon emitters [1]. The structure is fabricated via the direct wafer bonding technique of InP and silicon-on-insulator chips, followed by the e-beam lithography and inductively coupled plasma etching steps resulting in the InP WGs formation. Before fabrication, the structure was optimized numerically, revealing the optimal architecture for the most efficient coupling between QDs and propagating modes in the InP/Si WG and, further, along the the Si/SiO_2 WG. A linear taper structure achieves the efficient light field coupling between the InP/Si and Si/SiO_2 WGs [2]. We demonstrate the light coupling between InP and Si parts and examine the quantum nature of photons generated by a QD and propagating through WGs. The Hanburry-Brown and Twiss interferometric experiment on photons emitted by a QD and collected at the cleaved facet of the Si/SiO_2 WG revealed a good suppression of multiphoton emission events with $g^{(2)}(0) < 0.2$. The outcomes of our study underscore the potential benefits of this technological approach for advancing the development of quantum on-chip photonics using single-photon sources which can be easily combined with external fiber optics networks.

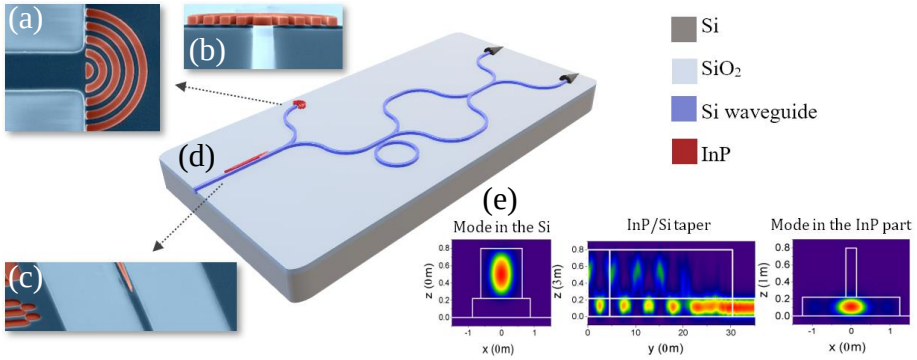

Scanning electron microscope images of the fabricated outcoupler (a, b) and taper (c). Conceptual illustration of the PIC with a heterogeneously integrated QD emitter (d). Modes of transmission for the calculated waveguide (e).

[1] P. Holewa *et al.*, *Phys. Rev. B* ***101***, 195304 (2020).
[2] P. Mrowiński *et al.*, *Opt. Express* **31**, 1541-1556 (2023)

Electrically gated single photon emitters in monolayer transition metal dichalcogenides

K. Oreszczuk[1], A. Rodek[1], Ł. Zinkiewicz[1], J. Howarth[2], T. Taniguchi[3], K. Watanabe[3], and P. Kossacki[1]

[1] *University of Warsaw, Poland*
[2] *University of Manchester, United Kingdom*
[3] *National Institute for Materials Science, Tsukuba, Japan*

Monolayers of transition metal dichalcogenides (TMDs) draw much attention as semiconducting materials with robust optical properties, strong Coulomb interaction, and an optically accessible valley degree of freedom. While some of the questions related to excitation dynamics and other electronic properties of the pristine TMDs are still to be answered, much attention is drawn to the more specific system based on ultrathin layers of TMDs. In recent years, significant research efforts have been directed to quantum emitters formed on various carrier localization centers in TMDs. Such objects are characterized by small linewidth, long luminescence lifetime, and single-photon emission. Related sharp emission lines are visible among or energetically below the band of relatively broad non-localized excitonic states. Such objects can be observed in monolayers or bilayers of several different TMDs. Single photon emitters (SPEs) are interesting from the point of view of photonics. Their properties, combined with the extraordinary properties of the free excitonic states in atomically thin TMDs, can open up perspectives for many advances in photonics and optoelectronics. However, these possibilities are currently hindered by a need for a more thorough understanding of the excitonic structure of the SPEs.

In this work, we identify and study SPEs created on different types of localized centers, particularly point defects and strain centers. Following Ref. [1], we expect that the Zeeman shift amplitudes should strongly depend on the nature of the trapping state, allowing identification of the SPEs localized on different types of defects. We investigate the SPE states in the TMD monolayers and determine the statistically most prevalent mechanism of carrier localization. We find, that in case of the WSe_2 monolayer the hole trapping is the most prevailing mechanism, although emitters based on electron trapping can also be observed. Furthermore, control over the Fermi level facilitated by the electrical gating in the sample allows for estimating the energy of the doping states responsible for the localizing center in the TMD layer.

[1] J. Dang et. al., *Npj 2D Mater. Appl.* **4**, 1 (2020).

Epitaxial Boron Nitride Processing and Conductivity

J. Rogoża, B. Furtak, J Binder, A. K. Dąbrowska, R. Stępniewski, A. Wysmołek

Faculty of Physics, University of Warsaw, Pasteura 5, 02 – 093 Warsaw, Poland

Hexagonal boron nitride (h-BN) is a very promising candidate for optoelectronic applications in the deep ultraviolet spectral range due to its exceptional physical properties, such as high chemical stability, thermal conductivity and wide bandgap energy. A large cross section for neutron capture renders BN an outstanding candidate for neutron detectors.

In our experiments, we used h-BN grown on two inch sapphire wafers. Growth was performed via metalorganic vapour-phase epitaxy (MOVPE) [1,2]. High-resolution SEM images, X-ray and Raman studies indicate a very good quality of the obtained hBN layers. However, obtaining micro-scale devices on epitaxial h-BN layers is a challenge due to wet delamination that may occur during typical processing stages.

To address this issue, we present a novel preparation method of as grown h-BN layers prior to optical lithography. Our technique relies on the controlled delamination and deposition of the epitaxial layer that prevents unwanted delamination from the sapphire substrate during etching and metal coating processes and produces fewer wrinkles in the processed h-BN.

It enables multiple-stage processes, including etching and sputtering, on thin layers of epitaxial h-BN. Fig. 1 shows an example of a h-BN Hall bar processed with reactive ion etching and coated with metallic contacts made of an AuPd alloy.

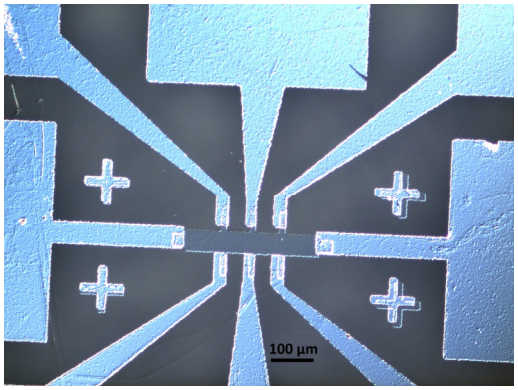

Fig 1. Optical image of a h-BN Hall bar structure with AuPd electrodes. The structure was created with a 2-stage lithographic process.

This novel preparation method allowed to study the effect of annealing of epitaxial h-BN layers in nitrogen atmosphere in the MOVPE reactor as well as the effect of irradiation with electrons in a scanning electron microscope (SEM). The electrical conductivity was measured before and after annealing and electron irradiation. The results show a significant increase in electrical conductivity after both treatments. These findings demonstrate the potential for controlling the electrical properties of h-BN, which is crucial for electronic and optoelectronic applications of epitaxial h-BN.

This work was partially supported by the National Science Center of Poland, grants no 2019/33/B/ST5/02766, 2021/41/N/ST7/04326.

[1] A. Dąbrowska, et al. 2D Materials 8, 015017 (2020)
[2] M. Tokarczyk, et al, 2D Materials 10, 025010 (2023)

Direct MOVPE growth of high-quality h-BN on the wafer-scale: the role of substrate off-cut

M. Tokarczyk, A. K. Dąbrowska, G. Kowalski, R. Bożek, J. Iwański, J. Binder, R. Stępniewski and A. Wysmołek

Faculty of Physics, University of Warsaw, Pasteura 5, 02-093 Warsaw, Poland

Hexagonal boron nitride (h-BN) is an attractive 2D material for possible applications in electronic and optoelectronic devices based on van der Waals heterostructures, but direct growth of high-quality hBN on the wafer-scale is still the bottleneck for future successful implementation of hBN in industry. Although the growth of h-BN by MOVPE has already been reported [1, 2], there is a fundamental lack in understanding of many basic aspects of growth. In particular, the role of the substrate off-cut, although known to be of major importance for the growth of other materials, has not been fully addressed so far.

In this communication, we present a study that addresses the influence of the sapphire substrate off-cut angle on the final growth of h-BN obtained in a two-step growth procedure [2]. The main process starts with a self-limiting continuous growth (CFG) of a BN buffer followed by flow-modulated epitaxy (FME) in the second step and is used to study substrates with different off-cuts angles for three different CFG times.

Based on results obtained x-ray diffraction and reflectometry, Raman and Fourier-transform spectroscopy, atomic force microscopy and scanning electron microscopy (SEM), we find that a substrate with off-cut angle of 1° clearly yields the highest quality of h-BN layers. Samples with this off-cut have the lowest amount of debris on the surface (see fig. 1), most intense x-ray diffraction signal, minimal Raman phonon linewidth and thinnest amorphous BN part.

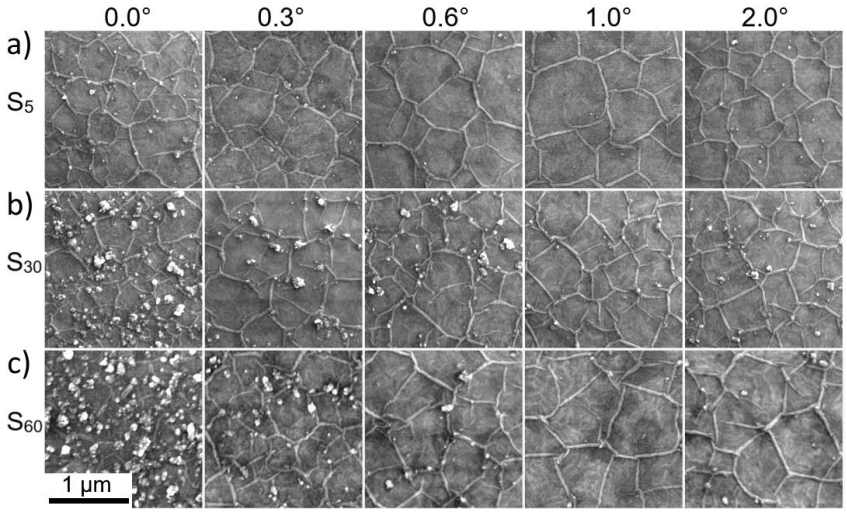

Figure 1. SEM images of the two stage samples grown with 5 min, 30 min and 60 min of the CFG buffer and with a similar 60 min FME final process. a) S_5 sample with five off-cuts, b) S_{30} sample with five off-cuts, c) S_{60} sample with five off-cuts.

A detailed analysis of the crystallographic structure of the hBN layers and mechanisms responsible for the existence of an optimal off-cut angle will be discussed.

Acknowledgments: This work was supported by the National Science Centre, Poland, under decisions 2019/33/B/ST5/02766 and 2020/39/D/ST7/02811.

[1] Y. Kobayashi, T. Akasaka, J. Cryst. Growth **310**, 5044 (2008).
[2] A. K. Dąbrowska, et al. 2D Materials **8**, 015017 (2020).
[3] M. Tokarczyk, et al. 2D Materials **10**, 025010 (2023).

Manipulating hBN Bandgap Properties With Aluminum

Jakub Iwański, Mateusz Tokarczyk, Krzysztof P. Korona, Piotr Tatarczak, Jan Pawłowski, Aleksandra K. Dąbrowska, Johannes Binder, Roman Stępniewski and Andrzej Wysmołek

Faculty of Physics, University of Warsaw, Pasteura 5, 02-093 Warsaw, Poland

Research on artificial light sources led to the development of semiconductor emitters that have a number of advantages, e.g. small size, long lifetime, high efficiency. To obtain shorter-wavelength emitters one usually alloys GaN-based structures with aluminum to increase the bandgap of the material (to 6.2 eV for pure AlN). However, by using this technology one can so far obtain only low luminescence efficiencies in the deep UV (DUV, 4.4-6.2 eV). This spectral region is of high importance for the sterilization of water, air and surfaces since light in the DUV can distrupt DNA of pathogenes.

In our research we focus on filling the efficiency gap in the DUV spectral range. We test an approach based on hexagonal boron nitride which despite of an indirect bandgap has a photoluminescence (PL) intensity of the band-edge transition that is more than two orders of magnitude higher than that of an AlN epilayer which has a direct bandgap [1]. Because the conduction band minima responsible for direct and indirect emission are close to each other in hBN, the emission efficiency can be potentially further enhanced when electronic states are properly manipulated [2].

In this work we study boron nitride layers grown with metalorganic vapor phase epitaxy (MOVPE) on 2-inch sapphire substrates [3-4]. The studied samples were alloyed with aluminum using different flows of trimethylaluminium (TMAl). Based on results obtained by UV-Vis, Raman and Fourier-transform spectroscopies, X-ray diffraction, scanning electron microscopy, atomic force microscopy and photoluminescence we will discuss how different flows of aluminum precursor affect the properties of the final epitaxial hBN layer.

As presented in figure 1, the absorbance spectra change with the amount of TMAl. The spectra revealed two peaks which energies coincide with direct (higher energy) and indirect (lower energy) transitions in hBN. The intensity ratio and the position of those peaks vary between the samples. This observation suggests that we are capable of manipulating the boron nitride bandgap by alloying with aluminum. The possible reasons and consequences of such a behavior will be discussed.

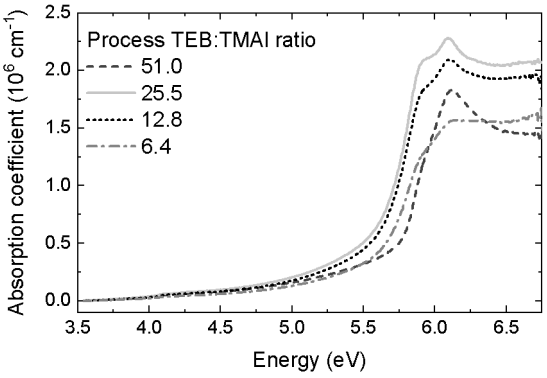

Figure 1: Absorption coefficient measured at room temperature for the samples grown with different TEB:TMAl ratio. Absorption coefficient uncertainty is estimated to be 10^5 cm^{-1}.

Acknowledgment: This work was supported by the National Science Centre, Poland, under decisions 2019/33/B/ST5/02766, 2020/39/D/ST7/02811 and 2022/45/N/ST5/03396.

[1] Maity, A., et al. *Progress in Quantum Electronics* 76 (2021): 100302
[2] Henck, H., et al. *Physical Review B* 95.8 (2017): 085410
[3] Dąbrowska, A. K., et al. *2D Materials* 8.1 (2020): 015017
[4] Tokarczyk, M., et al. *2D Materials* 10 (2023): 025010

MBE growth of CdTe on hBN

A. Szczerba[1], J. Kucharek[1], J. Pawłowski[1], T. Taniguchi[2], K. Watanabe[2], W. Pacuski[1]

[1] *Faculty of Physics, University of Warsaw, Pasteura St. 5, 02-093 Warsaw, Poland*
[2] *National Institute for Materials Science, Tsukuba 305-0047, Ibaraki, Japan*

Hexagonal boron nitride (hBN) has been shown to be a perfect substrate for the growth of high optical quality 2-dimensional materials such as $MoSe_2$ [1]. The main advantages of hBN compared to other semiconductor materials is a very high energy gap (5.9 eV) and ultra-low roughness in the case of exfoliated hBN. The motivation of the present work is based on the observation that such properties of hBN could be also useful for the epitaxy of 2D structures formed from 3D materials, such as e.g. CdTe quantum wells (QWs). In such a case hBN could act both as a flat substrate and barrier material with a high energy gap.

The growth was realized by Molecular Beam Epitaxy on exfoliated hBN flakes deposited on Si (100) substrates covered by 90 nm of SiO_2. Despite the use of relatively small hBN flakes, the Reflection High-Energy Electron Diffraction (RHEED) was applied in order to observe the evolution of the surface during the growth of the structure. We tested the growth of various tellurides: CdTe, ZnTe, (Cd,Mg)Te, and their heterostructures. After the growth, samples were examined with Atomic Force Microscopy (AFM) and low-temperature photoluminescence (PL) was investigated.

Several samples were grown in various temperatures of the substrate during growth. For typical growth temperatures of tellurides (250-350°C) there was no observable deposition of material on hBN. The best results were obtained for the lowest temperatures, below 200°C. The AFM scans of hBN covered by II-VI materials revealed a polycrystalline structure with two different areas: with and without the influence of the electrons from RHEED. In the photoluminescence spectrum of samples with CdTe quantum wells with (Cd,Mg)Te barrier a sharp peak of a CdTe quantum well was observed in the area influenced by RHEED. Interestingly, in the area without the influence of RHEED PL of quantum wells was not observed by far. Also presence of hBN for the formation of high optical quality QWs is important, because areas where CdTe was deposited directly on SiO_2 (no on hBN flakes) revelaed only PL of (Cd,Mg)Te barriers, not CdTe quantum wells.

[1] W. Pacuski, M. Grzeszczyk, K. Nogajewski, A. Bogucki, K. Oreszczuk, J. Kucharek, K.E. Połczyńska, B. Seredyński, A. Rodek, R. Bożek, T. Taniguchi, K. Watanabe, S. Kret, J. Sadowski, T. Kazimierczuk, M. Potemski, P. Kossacki, *Nano Letters* **20**, 3058 (2020).

Carbon-enriched Epitaxial Boron Nitride Layers as Contact Material for h-BN Devices

B. Furtak[1], J. Rogoża[1], J. Binder [1], A. Ciesielski [1], M. Tokarczyk [1], R. Stępniewski [1], A. Wysmołek[1]

[1]*Faculty of Physics, University of Warsaw, Pasteura 5, 02-093 Warsaw, Poland*

One of the most prominent members of the 2D materials, hexagonal boron nitride (h-BN), is the subject of extensive research thanks to their wide potential use in optoelectronics. However, the difficulty in producing high quality layers as well as the lack of ohmic contacts limits its practical use, despite excellent properties such as chemical stability, thermal conductivity and wide bandgap.

In this communication we study the effect of variable carbon content in h-BN layers, grown by Metaloorganic Vapor Phase Epitaxy (MOVPE)[1], on its optical and electrical properties in attempt to obtain a conductive contact material. Using nitrogen instead of hydrogen as carrier gas, as well as adjusting the ratio of gaseous precursors and temperature allows for the manipulation of carbon content in the grown layers.

The differences in sample compositions were estimated using EDX spectroscopy. Optical and electrical measurements were also performed. Raman and UV-Vis spectra confirm differences in both structure and bandgap.

Electrical measurements were performed on a Hall-bar structure, manufactured by plasma etching and photolithography processes. Results show a reduction in resistivity in samples with high carbon content in comparison to pure h-BN.

Optimizing the growth process in order to obtain high quality conductive layers is a promising step towards finding suitable contacts for future h-BN devices.

[1]A. K. Dąbrowska et al 2021 2D Mater. 8 015017

Acknowledgments: This work was partially supported by the National Science Centre of Poland, grants no 2019/33/B/ST5/02766, 2021/41/N/ST7/04326.

Determining Strain Components in a Diamond Waveguide from Asymmetric ODMR Spectra of NV^- Center Ensembles

M. S. Alam [1], D. Wigger [2], M. Gawełczyk[1], P. Machnikowski[1]

[1] *Institute of Theoretical Physics, Wroclaw University of Science and Technology, Wroclaw, Poland*
[2] *School of Physics, Trinity College Dublin, Dublin 2, Ireland*

The negatively charged nitrogen-vacancy center in diamond (NV^-) has shown great potential in nanoscale sensing and quantum information based on their rich spin physics. Efficient fluorescence detection and interface with light, in general, is crucial for realizing these applications in experiments. Laser-written waveguides in diamond have recently been used to improve the coupling between NV^- centers and light [1]. The NV^- spin states are detected by the optically detected magnetic resonance (ODMR) spectra. However, in the waveguides, these ODMR spectra are found to be consistently asymmetric.

Here, we theoretically simulate the experimentally obtained ODMR signals and find that strain, that could have been introduced in the process of laser writing, can explain the ODMR asymmetry even without invoking built-in electric fields, which differs from previous studies [2-3]. By fitting the theory to experimental signals gathered from different positions on the sample, we quantify all three relevant strain tensor components for full profiles across the waveguide.

Our model consists of NV^- centers interacting with a resonant or near-resonant microwave and the static strain field. We exploit the translational symmetry of the waveguide, which reduces the number of relevant strain components to three. Since yellow diamond samples have a high density of NV^- centers with a uniform distribution along all four possible defect orientations in the crystal, our modeled signal comprises equal contributions from all four possible NV^- center orientations. We numerically calculate individual NV^- centers' eigenstates and corresponding excitation probabilities for microwave-driven transitions. Based on this, we compose the simulated ODMR spectrum from pairs of weighted Lorentzians for each NV^- orientation. Finally, we extract the strain components by fitting the model to the experimental data.

Our results provide reasonable predictions for quantifying the strain distribution in the studied waveguide structures.

Acknowledgements:
We are grateful for support from the H2020 Marie Curie ITN project LasIonDef (GA no. 956387).

References:
[1]. M. Hoese et al., *Phys. Rev. Applied* **15**, 054059 (2021).
[2]. T. Mittiga et al., *Phys. Rev. Lett.* **121**, 246402 (2018).
[3]. J. Kölbl et al., *New J. Phys.* **21**, 113039 (2019).

Post-implantation Defect Accumulation in Crystal Lattice of β-Ga_2O_3 Implanted with Yb ion

Mahwish Sarwar[1], Renata Ratajczak[2] and Elżbieta Guziewicz[1]

[1]*Institute of Physics, Polish Academy of Sciences, Al. Lotnikow 32/46, 02-668 Warsaw, Poland*
[2]*National Centre for Nuclear Research, Soltana 7, 05–400 Otwock, Poland*

Gallium oxide (Ga_2O_3) is an ultra-wide bandgap semiconductor of interest for many applications, including optoelectronics. Undoped Ga_2O_3 emits light in the UV range, that can be tuned to the visible region of the spectrum by rare earth dopants. Ytterbium may further enhance the span of applications due to emission in the infrared region of the spectrum. Ion implantation is a renowned doping technology used for the alteration of material properties. Despite of many advantages of this technique, it could lead to lattice damage and defect accumulation which need to be studied thoroughly as these factors strongly influence the material properties.

Our previous work, where we studied structural defects and recovery of the crystal lattice of β-Ga_2O_3 after Sm implantation and post-implantation annealing, indicates that the damage of the crystal lattice after implantation is not typical and needs further investigations [1]. In the present study, the (-201) orientated β-Ga_2O_3 single crystals were implanted with Yb ions fluences ranging from $5x10^{11}$ to $5x10^{15}$ at./cm^2. Channeling Rutherford backscattering spectrometry (RBS/c) was used to study modification of the crystal lattice induced by ion implantation and annealing. The RE depth profile was analyzed by the SIMNRA calculations, while the McChasy simulations were used to quantify the defect distributions. The obtained accumulation curve reveals the two-step damage process. From the fluence of $5x10^{13}$ /cm^2, the damage of the Ga_2O_3 lattice starts to increase very fast, reaching the amorphization level for the Yb ion fluence of $1x10^{14}$ /cm^2. The new form of defect that is created on the highest level is found to be annealing resistant.

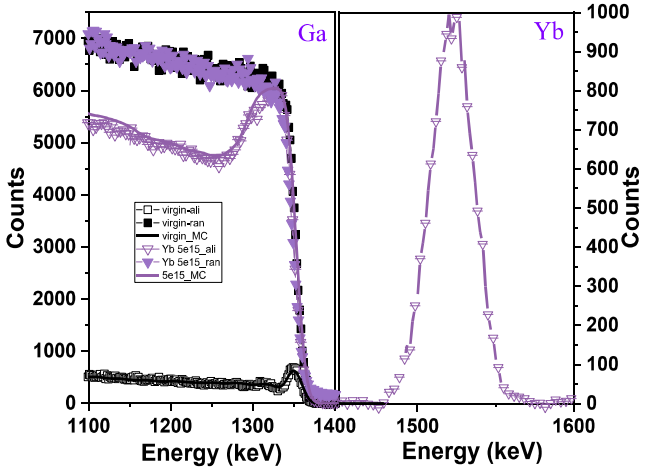

Random and aligned RBS/c spectra for β-Ga_2O_3 implanted with Yb. The solid line represents the McChasy simulations.

Acknowledgements
The work was supported by the international project co-financed by the funds of the Minister of Science and Higher Education in years 2021-2023; contract No. 5177/HZDR/2021/0 and Helmholtz-Zentrum Dresden-Rossendorf (20002208-ST).

References

[1] M. Sarwar et al., *Adv. in Sci. and Tech. Research Journal* 2022, 16(5), 147–154

The structural properties anisotropy of β-Ga_2O_3 implanted with Yb

Renata Ratajczak[1], Mahwish Sarwar[2], Cyprian Mieszczynski[1], Przemysław Jozwik[1], Wojciech Wozniak[2], Ulrich Kentsch[3], René Heller[3] and Elzbieta Guziewicz[2].

[1] National Centre for Nuclear Research, ul. Soltana 7, 05-400 Otwock, Poland
[2]Inst. of Physics, Polish Acad. of Sciences, Aleja Lotnikow 32/46, PL-02668 Warsaw, Poland
[3]Helmholtz-Zentrum Dresden-Rossendorf, Bautzner Landstrasse 400
D-01328 Dresden, Germany
[*]presenting author, e-mail: Renata.Ratajczak@ncbj.gov.pl

Nowadays doped and un-doped gallium oxide is one of the most exciting materials in research and technology, and one of the most important tasks in this issue is the development of controlled methods of doping this material. Rare earth-doped Ga_2O_3 seems to be attractive for future optoelectronic devices such as phosphors, displays, and LEDs with emission in the visible spectral range. The ion implantation technique is one of the attractive ways to produce such systems. However, even though ion implantation is the most common semiconductor doping method, the studies of this process for Ga_2O_3 with RE are still at the initial stage.

In our recent research, we paid particular attention to the issue of the Ga_2O_3 anisotropy (in its thermodynamically stable β-Ga_2O_3 phase), which has not been theoretically predicted, but experimentally observed in optical and electrical investigations. In this work, the studies on the structural properties of β-Ga_2O_3 crystals, (010) and (-201) oriented, irradiated with different fluencies of Yb ions and subsequently annealed, have been performed. The crystal lattice damage, structure recovery, as well as Yb depth profiles, and Yb ions location in the β-Ga_2O_3 crystal lattice, were studied by Rutherford Backscattering Spectrometry in the channeling direction (RBS/c) and supported by computer simulations. Our studies reveal the strong influence of anisotropy on structural properties, with a significantly lower damage level for (010) oriented β-Ga_2O_3 crystals, and a small number of substitutions of gallium sites by Yb atoms as well. Interestingly, contrary to the common opinion, ~~is~~ that the β-Ga_2O_3 has strong radiation resistance, our results show that it is very easy to make this material amorphous. However, the crystal lattice recovery is also much easier than in other wide bandgap materials.

Acknowledgments *The work was supported by the NCN project UMO-2022/45/B/ST5/02810 and RADIATE projects 21002661-ST, 21002663-ST realized at IBC, Helmholtz Zentrum Dresden Rossendorf.*

Electron Paramagnetic Resonance of Beta-Gallium Oxide Modified by High-Energy Electron Irradiation

Agnieszka Wołoś, [1] **Joanna Sitnicka,**[1] **Romain Grasset,**[2] **and Marcin Konczykowski** [2]

[1] *University of Warsaw, Faculty of Physics, Pasteura 5, 02-093 Warszawa, Poland*
[2] *Laboratoire des Solides Irradiés, Ecole Polytechnique, CEA/DRF/IRAMIS, CNRS, Institut Polytechnique de Paris, 91128 Palaiseau, France*

Several electron paramagnetic resonance (EPR) signals have been identified in β−Ga_2O_3, among which there is an intrinsic acceptor – gallium vacancy, both doubly ionized V^{2-}_{Ga} with spin ½ and singly ionized V^{-}_{Ga} with spin 1 [1, 2] and an intrinsic donor – oxygen vacancy O^{2-} trapping single electrons and exhibiting strong motional narrowing [3]. These EPR signals can be used to monitor defect formation and evolution of electronic properties of β−Ga_2O_3 modified by high-energy electron irradiation.

β−Ga_2O_3 single crystals doped with Sn were irradiated by a 2.5 MeV electron beam at 20 K at the Sirius facility, Ecole Polytechnique, Palaiseau. The electron irradiation produces a spread of Frenkel pairs, vacancy-interstitial. Interstitials are typically highly mobile at room temperature and annihilate at the surface, thus the expected effect of irradiation comes usually from vacancy-type induced defects. Indeed, in the EPR experiment after the irradiation, a signal characteristic to doubly ionized gallium vacancy, V^{2-}_{Ga}, is observed (Figure1), indicating a lowering of the Fermi level to the band gap. In contrast, pristine samples show the presence of shallow donor signal specific for conducting samples. The characteristic parameters of the resonance line, its linewidth, g-factor, and amplitude, evolve with temperature indicating a transition from states localized at donors to the delocalized states in the conduction band. The evolution of signals after subsequent annealing, thus removing the irradiation defects, is also discussed.

The presented study aims to shed light on the possibility of tuning the Fermi level towards the β−Ga_2O_3 valence band. This still unsolved issue is crucial for the practical implementation of this ultra-wide band gap material in electronics and opto-electronics.

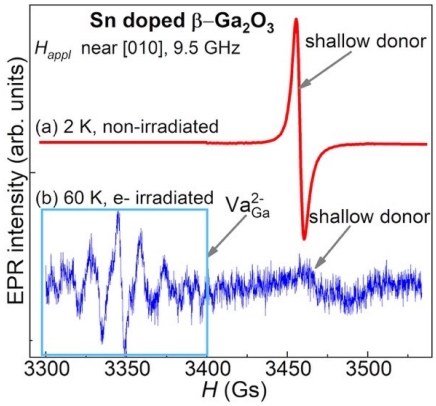

Figure 1. EPR spectra of pristine β−Ga_2O_3 doped with Sn (a) and irradiated with 2.5 MeV electrons (b).

[1] E. Kananen, L. E. Halliburton, K. T. Stevens, G. K. Foundos, and N. C. Giles, *Appl. Phys. Lett.* **110**, 202104 (2017).
[2] D. Skachkov , W. R. L. Lambrecht , H. J. von Bardeleben , U. Gerstmann, Quoc Duy Ho, and P. Deák , *J. Appl. Phys*. **125**, 185701 (2019).
[3] M. Yamaga, E. G. Villora, K. Shimamura, and N. Ichinose, Phys. Rev. B **68**, 155207 (2003).

Effects of Si/N Ion Implantation on Defect formation and Doping of Gallium Oxide

Iraida N. Demchenko [1], Yevgen Syryanyy [1,2], Asiyeh Shokri [1], Yevgen Melikhov [3] and Maryna Chernyshova [1]

[1] *Institute of Plasma Physics and Laser Microfusion, ul. Hery 23, 01-497 Warsaw, Poland*
[2] *Warsaw University of Technology, Faculty of Electronics and Information Technology, Nowowiejska 15/19, 00-665 Warsaw, Poland*
[3] *Institute of Fundamental Technological Research Polish Academy of Sciences, ul. Pawinskiego 5b, 02-106 Warsaw, Poland*

A new generation of power devices based on the wide-bandgap (WBG) semiconductor, Ga_2O_3, is expected to revolutionize the power electronics industry. Many promising β-Ga_2O_3-based devices have already been reported, such as Schottky barrier diodes, MOSFETs, and various solar-blind photodetectors [1 - 4]. So far, the development of Ga_2O_3-based transistors has been focused mainly on utilizing lateral geometry. On the other hand, the vertical geometry would allow for higher current drives without having to enlarge the chip size, simplified thermal management, and far superior field termination. However, for this geometry to be realized, both *n*-type and *p*-type doping should be achieved in Ga_2O_3, with *n*-type readily available [5, 6]. Contrarily, *p*-type doping in Ga_2O_3 is fundamentally challenging to be achieved due to the very flat valence band maximum (VBM) of O 2*p* in nature and self-compensation [7 - 9].

It was recently shown that *p*-type conductivity can be achieved even in undoped Ga_2O_3 layers with annealing in an oxygen atmosphere due to the β-Ga_2O_3 particular point defect chemistry and the large formation energy of oxygen vacancies [10, 11]. Such annealing increases the free hole concentration by three orders of magnitude due to the formation of VGa(-) - Vo (++) complexes, being a shallow acceptor center. However, the mobility was found to reduce, probably due to a greater number of acceptor scattering centers compared to the as-grown sample.

Another approach would be to use nitrogen as *p*-type dopant with subsequent post-annealing treatment as was shown in [6] where nitrogen and silicon were used to engineer a Ga_2O_3 transistor using ion implantation. Consequently, there is a need for a better understanding of the origin of the observed complicated behavior of Si and N elements in the Ga_2O_3 matrix, which results in different transport properties.

In this work, we aimed to identify structural defects caused by Si(N) implanted into the Ga_2O_3 matrix, their transformations and possible interaction with host intrinsic defects employing various experimental techniques: RBS/c, PIXE, HR XDR, XANES, TEM. The crucial task is the identification of the local surrounding of the mentioned above dopants and understanding the driving forces for phase transformations taking place upon implantation and subsequent annealing.

[1] S. J. Pearton et al., *Appl. Phys. Rev.* **5**, 011301 (2018).
[2] M. Higashiwaki et al., *Appl. Phys. Lett.* **112**, 060401 (2018).
[3] A. M. Armstrong et al., *J. Appl. Phys.* **119**, 103102 (2016).
[4] J. Kim et al., *Appl. Phys. Lett.* **113**, 102103 (2018).
[6] M.H. Wong et al., *IEEE Electron Device Lett.* **40**, 431 (2019).
[7] A. Kyrtsos et al., *Appl. Phys. Lett.* **112**, 032108 (2018).
[8] A. T. Neal et al., *Appl. Phys. Lett.* **113**, 062101 (2018).
[9] S. B. Zhang et al., *Phys. Rev. B* **63**, 075205 (2001).
[10] E. Chikoidze et al., *Mater Today Phys.* **3**, 118 (2017).
[11] E. Chikoidze et al., *J. Mater. Chem. C* **7**, 10231 (2019).

PA-MBE Grown CdMgO:Eu Ternary Alloy on m- and c-Oriented Al_2O_3 Substrates

J. K. Jadoon [1], A. Adhikari [1], A. Lysak[1], A. Wierzbicka[1], W. Lisowski[2], M. Stachowicz[1], A. Kozanecki[1], and E. Przezdziecka[1]

[1] Institute of Physics, Polish Academy of Sciences, Al. Lotników 32/46,02-668 Warsaw, Poland
[2] Institute of Physical Chemistry, Polish Academy of Sciences, Marcina Kasprzaka 44/52, 01-224 Warsaw, Poland

Oxides based on cadmium (Cd) and magnesium (Mg) due to their properties can find an extensive range of potential applications in photovoltaics, light-emitting diodes, and other optoelectronic devices. In this work, a series of CdMgO:Eu ternary alloys were grown on *m*- and *c*-oriented Al_2O_3 with varying Mg concentrations using plasma-assisted molecular beam epitaxy. The crystal structure and topographical features of grown ternary alloys were analyzed using X-ray diffraction and atomic force microscopy (AFM). X-ray photoelectron spectroscopy (XPS) was used to determine the chemical state and composition of Eu and it confirmed Eu^{3+} europium oxidation states. The optical properties of as-grown and annealed samples were examined with UV-visible spectrometry, PL, and CL measurements. Transmission spectra revealed that the alloys are highly transparent in the visible region, where transmittance increases with incident wavelength (**λ**) and over 500 nm approaches nearly 90% for all samples **Fig. 1. (a-b).** Utilizing diffuse reflectance spectra, the dielectric constants, refractive index, and extension coefficient were also evaluated. The band gap energy (E_g) was estimated using the standard Tauc plot and the Kubellka-Munk model. The increasing trend was observed in (E_g) under Mg-rich conditions. From transmittance spectra, the highest energy gap values for *m*- and *c*-oriented alloys are estimated to be 2.866 eV and 3.011 eV, which are due to the high Mg concentration as consistent with literature [1]. CL confirmed the presence of Eu-related peaks in the red spectral range for annealed samples. The surface topography of CdMgO:Eu alloys are homogeneous and uniform; rms values are at the level below 1 nm and increase with Mg concentration.

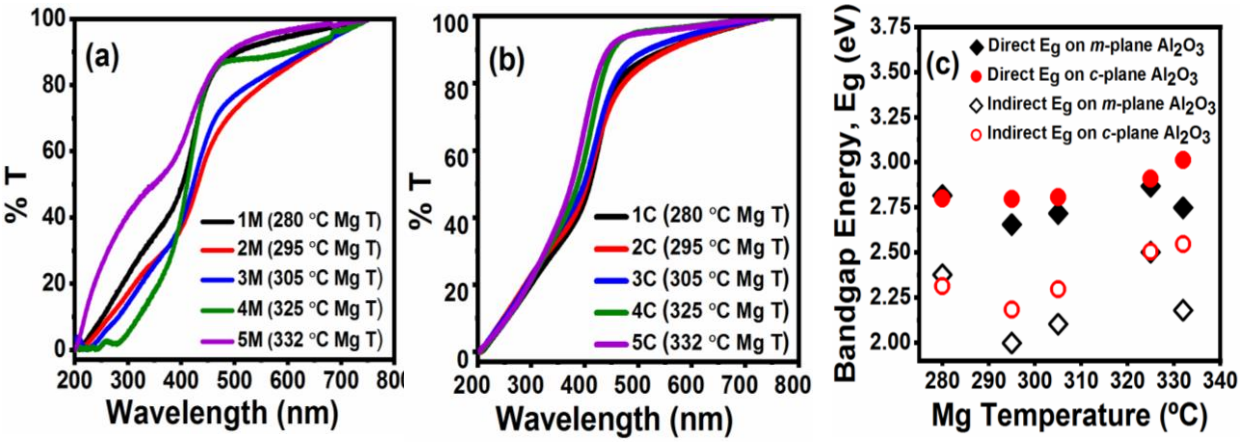

Fig. 1. (a-b) Transmittance vs **λ** for *m*- (1M-5M) and *c*-oriented (1C-5C) alloys samples, **(c)** Direct and indirect bandgap energy (E_g) of CdMgO:Eu alloys on *m*- and *c*-oriented Al_2O_3 from transmittance spectra.

Acknowledgement. The work is supported by the Polish NCN project DEC-2021/41/B/ST5/00216.

[1] A. Adhikari, A. Lysak, A. Wierzbicka, P. Sybilski, A. Reszka, B.S. Witkowski, & E. Przezdziecka, *Materials Science in Semiconductor Processing*. *144*, 106608 (2022).

MBE growth of wide band gap wurtzite MgZnO superlattices doped with Eu for effective visible emission

M. Stachowicz [1], J.A. Mathew [1], J.M. Sajkowski[1], R. Jakiela[1], Y. Zhydachevskyy[1], S. Magalhaes[2], E. Alves[2], A. Kozanecki[1]

[1]*Institute of Physics, Polish Academy of Sciences, Al. Lotników 32/46 PL-02-668 Warsaw, Poland*
2 Centro Tecnológico Nuclear, Instituto Superior Técnico, Universidade de Lisboa, P-2686953 Sacavém, Portugal

Zinc oxide became of increasing technological importance, in particular for the development of light emitting diodes and lasers operating in the visible and ultraviolet region. Such devices contain heterojunctions and active areas based on quantum structures. Rare earth elements can be introduced into semiconductors either via ion implantation or by in-situ doping for extension of spectral range of emission of those. Epitaxial growth and in-situ doping allows to avoid problems with incomplete reconstruction of the crystal lattice which are common problems in the case of implantation method. Molecular Beam Epitaxy is perfectly suited for the production of thin crystalline layers, complex multilayer structures and for selective doping of carefully chosen layers, such as quantum wells. It can also be expected that some RE dopants can be stabilized in various oxidation states, including less common states like for example Ce^{4+}, Yb^{2+}, Eu^{2+} and other lanthanide ions [1]. Such a possibility is particularly interesting in the case of Eu, which when incorporated into the same host material, often coexists in two ionic states: 2+ and 3+ [2].

Wurtzite MgZnO alloys in form of superlattice structures have been grown by molecular beam epitaxy on variously oriented sapphire substrates on high-quality ZnO buffer layers. The widened band gap energy of utilized MgZnO layers was large enough to play a role whether as a barrier or quantum well selectively doped with Eu ions. The concentrations and distributions of Eu atoms in the respective hosts were analysed using Secondary Ion Mass Spectrometry, which confirmed successful doping around the level of similar to 1%. Optical properties of the samples were investigated by room temperature photoluminescence and Photoluminescence excitation measurements. The results obtained with Secondary Ion Mass Spectrometry were verified with Rutherford Backscattering spectrometry, which included not only random spectra but also angular measurements of main channels in order to shed light on eventual strains present in the structures and acting upon Eu ions. All performed analysis suggest the co-existence of 2+ and 3+ ionic states of Eu in the SL structures, and only 3+ ionic state after thermal treatment. Futhermore, optical measurements revealed strong enhancement of $^5D_0 \rightarrow {}^7F_J$ intra-4f-shell transitions of Eu^{3+} in MgZnO based superlattices.

[1] K.A. Gschneidner Jr., J.-C.G. Bünzli, V.K. Pecharsky (Eds.), Handbook on the Physics and Chemistry of Rare Earths, vol. 1, Elsevier Science, Amsterdam (2010).

[2] L. Zhou, P. Du, L. Li, Sci. Rep., 10, 20180 (2020).

Acknowledgements:

The work was partly supported by the NCN project No. 2019/35/B/ST8/01937.

Initial optimization of the growth conditions of GaAs homo-epitaxial layers after cleaning and restarting the MBE reactor.

D. Jarosz[1, 2], M. Stachowicz[3], P. Krzeminski[1], M. Ruszala[1], A. Jus[1], P. Sliz[1], D. Ploch[1], M. Marchewka[1].

[1] *University of Rzeszow, Institute of Materials Science and Engineering, Center of Microelectronics and Nanotechnology, Al. Rejtana 16c, PL-35-959 Rzeszow, Poland,*
[2] *International Research Centre MagTop, Institute of Physics, Polish Academy of Sciences, PL-02-668 Warsaw, Poland,*
[3] *Institute of Physics, Polish Academy of Sciences, Al. Lotnikow 32/46 PL-02-668, Warsaw, Poland,*

The Molecular Beam Epitaxy (MBE) technique is renown as the most suitable for growth of high quality crystalline materials and nanostructures such as GaAs. Although, once established, optimal growth parameters required for repeatability of top quality structures may be easily lost as MBE is highly sensitive to any changes in the system. Especially, routine servicing procedures, which include any activity which requires unsealing of the growth chamber are devastating for developed growth parameters and force the necessity of recalibration. In this work, we present the process of growth parameters pre-optimization for obtaining homoepitaxial GaAs layers after servicing and restarting MBE system. Namely we present, how each step of reestablishing optimal growth condition influence various characteristics of obtained GaAs layers. Those include in situ, structural, and spectral measurement techniques.

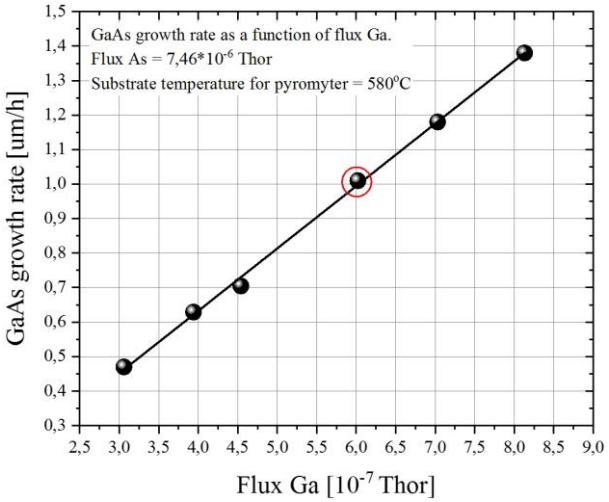

Diagram 1. *The dependence of the growth rate of GaAs layers on the gallium flux for the constant arsenic flux 7.46e^{-6} Thor and the substrate temperature of 580 °C.*

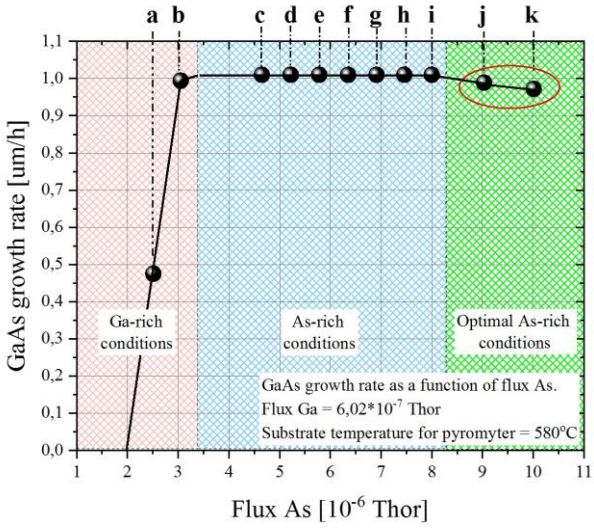

Diagram 2. *The dependence of the growth rate of GaAs layers on the arsenic flux for the constant gallium flux 6.02e^{-6} Thor and the substrate temperature of 580 °C. 3 areas are marked in the diagram:*
Red - gallium rich condition,
Blue - arsenic rich condition,
Green - arsenic rich optimal condition.

Acknowledgments. The project was partly supported by grants:

•Foundation for Polish Science Through the IRA Programme cofinanced by EU within SG OP(Grant No. MAB/2017/1)
•National Centre for Research and Development (NCBR), under project No. TECHMATSTRATEG-III/0038/2019-00

Geometrical selection during MBE growth of nanowires on polycrystalline substrates

K. Olszewski, M. Sobanska, A. Wierzbicka, and Z.R. Zytkiewicz

Institute of Physics, Polish Academy of Sciences, Al. Lotnikow 32/46, 02-668 Warsaw, Poland

If semiconductor nanowires (NWs) are to be applied in electrically driven devices they should be well-oriented relative to the substrate normal. This requirement is easily fulfilled if NWs are formed by self-assembly on amorphous substrate. Then there are no epitaxial constraints and NWs grow perpendicular to the substrate surface. If, however, NWs are strongly linked to a polycrystalline substrate, their random orientation is expected due to an arbitrary arrangement of substrate grains, eventually impeding application of such NW array.

In this work we show that unidirectional supply of material fluxes in molecular beam epitaxy (MBE) favors growth of well-oriented NWs even despite random orientation of grains on which epitaxially linked NWs nucleate. We present a geometrical model describing an impact of MBE system geometry on the orientation of the NWs. Specifically, we calculated effective area of the nanowire's top facet S_{eff} that is in the line of sight of an effusion cell as a function of nanowire tilt relative to substrate normal (α) and substrate rotation angle (ω) (see Fig. a). The S_{eff} value is equivalent to the number of atoms incorporated on the NW top facet which, in the framework of the model, controls axial growth rate of the NW. For example, this is the case of metal-limited MBE growth of A_3B_5 NWs. Fig. b shows normalized value of S_{eff} as a function of α and ω. As seen, the maximum of S_{eff} corresponds to the NW facing directly in the direction of the effusion cell (α = 40°, ω = 0°) as expected. However, during rotation of the substrate the fastest growing nanowires are the ones that are perpendicular to the surface (Fig. c). To verify the model we grew GaN NWs on ZrN polycrystalline buffers. Without substrate rotation the NWs grew uniformly arranged at α = 40°, ω = 0° (Fig. d), i.e. exactly as predicted by our model. Standard growth with rotation of the substrate led to densely packed NWs with significantly limited tilt dispersion (Fig. e). We attribute this behavior to the shadowing of strongly tilted NWs by preferentially grown perpendicular ones.

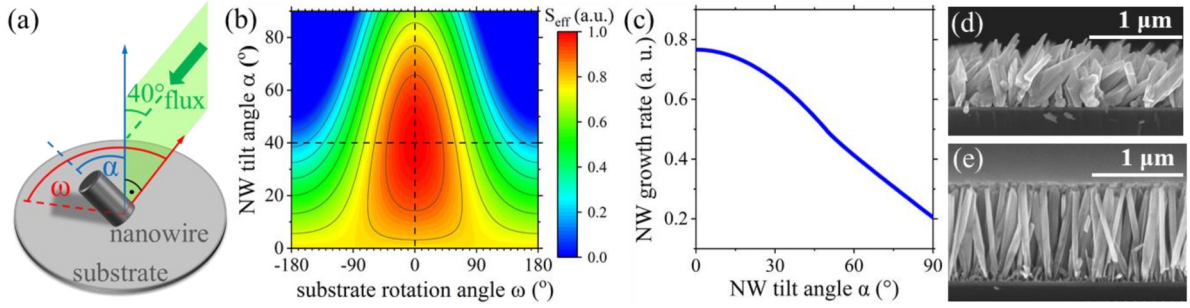

Fig. (a) geometry of the system; (b) effective area S_{eff} of the NW top facet as a function of α and ω angles; (c) average NW growth rate after entire substrate rotation as a function of the NW tilt α. SEM images of GaN NWs grown on ZrN buffer without (d) and with (e) substrate rotation.

This work was partially supported by the NCN grant 2021/43/D/ST7/01936. The authors thank Z. Szopniewski for depositing ZrN layers, and A. Reszka and A. Lysak for SEM measurements.

Insights into Raman spectra and doping concentration profiles of Eu-doped {ZnCdO/ZnO} superlattices

Igor Perlikowski[1], Eunika Zielony[1], Anastasiia Lysak[2], Ewa Przeździecka[2]

[1] *Department of Quantum Technologies, Wrocław University of Science and Technology, Wybrzeże Wyspiańskiego 27, 50-370, Wrocław, Poland*
[2] *Institute of Physics, Polish Academy of Sciences, Al. Lotników 32/46, 02-668, Warsaw, Poland*

ZnO is a commonly known semiconductor compound that has found application in various types of optoelectronic devices, such as lasers, diodes, and photodetectors. In photovoltaic cells it is used as a transparent conducting film, due to its wide band gap (ca. 3.37 eV at room temperature [1]) and low resistivity [2].

In high-efficiency thin film solar cells absorber layer can consist of several layers, each of them suited to absorbing a specific energy range of photons. In this case, ZnO could be in control of UV light conversion. To expand its possibilities towards shorter wavelengths, we propose ZnCdO alloy, as CdO has an energy gap of 2.24 eV [3]. The remaining key component of the presented samples is europium (Eu). Both ZnO and CdO has been successfully doped with this rare-earth metal, giving rise to a huge improvement in carrier concentration and mobility, which is desirable in terms of future applications [4, 5].

Eventually, we decided to use superlattice (SL) structure type grown by molecular beam epitaxy to strictly control composition of the final material. Moreover, in SLs it is possible to modulate the energy gap simply by changing thickness of a sublayer, which is also a promising feature [6]. Thus, in this work we would like to present first Eu-doped {ZnCdO/ZnO} SL structures. Raman spectroscopy (Fig. 1.) has revealed additional modes, dopant-related ones, forbidden in bulk ZnO, that occur in doped ZnO films. Furthermore, post-growth treatment analysis showed that annealing cause significant modifications in Raman spectra associated with changes of impurity content. Additionally, p-n junctions with the aforementioned SL structures were prepared on silicon substrates to be able to perform electrical measurements. Current-voltage characteristics shown the obtained samples are functioning diodes with a rectifying p-n junction. Capacitance-voltage measurements helped to determine dopant concentration and its distribution within the junction depletion region. To the best of our knowledge, there are no results of studies reporting observation of Eu dopants in Raman spectra and doping concentration profiles of Eu-doped {ZnCdO/ZnO} superlattice structures.

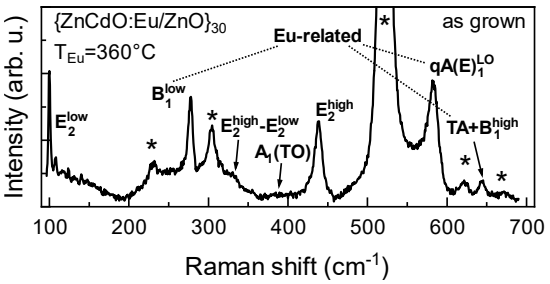

Fig. 1. Raman spectrum of one of the samples with various ZnO modes. Si substrate modes are marked with an asterisk.

The work was supported by the Polish NCN projects DEC-2021/41/B/ST5/00216.

[1] G.-C. Yi et al., *Semicond. Sci. Technol.* **20**, S22 (2005).
[2] K. Matsubara et al., *Thin Solid Films* **431**, 369 (2003).
[3] A. Ashrafi, 2015, doi: 10.13140/RG.2.1.3726.2881.
[4] R. Swapna et al., *Procedia Materials Science* **10**, 723 (2015).
[5] A.A. Dakhel, *Opt. Mater.* **31**, 691 (2009).
[6] E. Przeździecka et al., *Nanoscale Res. Lett.* **16**, 59 (2021).

Electrical and thermal transport properties of CdO and CdMgO alloys grown using plasma-assisted MBE technique

A. Adhikari[1], Z. Adamus[1,2], M. Pawlak[3], A. Lysak[1], and E. Przezdziecka[1]

[1]*Institute of Physics, Polish Academy of Sciences, Al. Lotnikow, 32/46, 02-668, Warsaw, Poland*
[2]*International Research Centre MagTop, Institute of Physics, Polish Academy of Sciences, 02-668 Warsaw, Poland*
[3]*Institute of Physics, Faculty of Physics, Astronomy, and Informatics, Nicolaus Copernicus University, Grudziadzka 5, 87-100, Torun, Poland*

CdO is one of the oldest transparent conducting oxides (TCOs) that attracts considerable attention for optoelectronic applications because of its high electron concentration, high electron mobility, and high transparency in the visible spectrum. Our recent reports on MBE-grown CdMgO alloys show that the lower optical bandgap of CdO (E_g=2.3 eV) can be overcome by alloying with wide bandgap MgO (E_g=7.5 eV) which is useful for light detection from visible to deep UV regimes [1,2]. However, to obtain maximum energy absorption, it is important to understand the relation between Cd and O_2 parameters during the growth process which influences the stoichiometry of the CdO and related ternary alloys. In the present studies, we investigated plasma-assisted molecular beam epitaxy (PA-MBE) grown CdO and CdMgO ternary alloys. Temperature-dependent Hall measurement revealed the maximum mobility of 352 $cm^2V^{-1}s^{-1}$ achieved at room temperature with a carrier concentration of about 4.5 x 10^{19} cm^{-3}. The thermal transport properties, such as thermal conductivity, thermal diffusivity, and thermal boundary resistance, were measured using photothermal infrared radiometry. We believe that our findings may provide valuable insight for a better understanding of CdMgO alloys which can open up new prospects for designing novel optoelectronic devices.

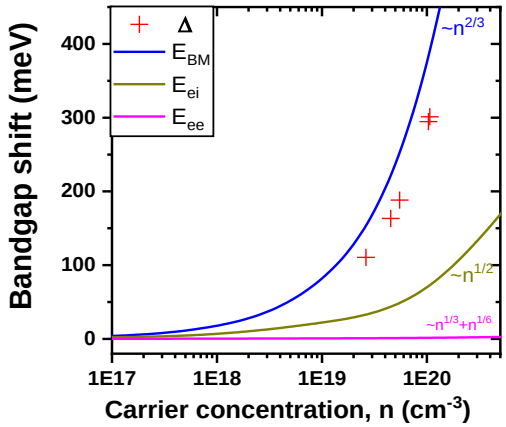

Figure 1. Bandgap shift as a function of carrier concentration
(Total shift $\Delta = \Delta E_{BM} - \Delta E_{BGN}$ is denoted by + sign)

The work was supported by the Polish NCN project DEC-2021/41/N/ST5/00812 and DEC-2021/41/B/ST5/00216.

[1] A. Adhikari, A. Lysak, A. Wierzbicka, P. Sybilski, A. Reszka, B.S. Witkowski, and E. Przezdziecka, *Mater. Sci. Semicond. Process.* 144, 106608 (2022).
[2] A. Adhikari, A. Wierzbicka, A. Lysak, P. Sybilski, B. S. Witkowski, and E. Przezdziecka. arXiv preprint arXiv:2210.11785 (2022).

Characterization of MBE grown {Zn(Mg)O/ZnCdO}$_m$ superlattices doped in-situ with Eu

A. Lysak [1,2], E. Przeździecka [1], A. Wierzbicka [1], A. Reszka [1], M. Stachowicz [1], R. Jakiela [1], P. Dłużewski [1], A. Adhikari [1] and A. Kozanecki [1]

[1] *I Institute of Physics, Polish Academy of Sciences, Al. Lotnikow 32/46, Warsaw, Poland*
[2] *Berdyansk State Pedagogical University, Berdyansk, Ukraine*

Zinc oxide (ZnO) is a well-known n-type semiconductor with a wide, direct bandgap - 3.37 eV at room temperature and a high exciton binding energy (60 meV) and potentially has wide applications in optoelectronics [1]. The synthesis of Zn(Cd,Mg)O ternary alloys and quantum structures (heterostructures, multiquantum wells and superlattices) enables bandgap engineering in a wide spectral range from ultraviolet to green [2]. The red luminescence can be obtained in oxide structures by doping with Eu. ZnO nanostructures doped with rare earth elements are synthesized by various techniques, however, a method for obtaining quantum structures with a predetermined location of Eu has not yet been developed. The molecular beam epitaxy (MBE) technology makes it possible to place Eu either in barriers or/and in quantum wells.

In this work we present the properties of in situ Eu-doped {Zn(Mg)O/ZnCdO}$_m$ short-period superlattices (SLs) grown on sapphire substrates (Al_2O_3) by MBE. The thicknesses of the ZnMgO and ZnCdO:Eu layers are 15±3 nm and 2±1 nm, respectively. Eu impurity was introduced into quantum wells. The obtained structures were characterized by X-ray diffraction (XRD), scanning electron microscopy (SEM), transmission electron microscopy (TEM) and secondary-ion mass spectrometry (SIMS). The optical properties were tested by photo- / cathodoluminesence (PL/CL) measuments and UV-Vis spectroscopy. The XRD pattern of Eu-doped {Zn(Mg)O/ZnCdO}$_m$ SLs indicated hexagonal crystal structure. The formation of good quality SLs were confirmed by TEM and XRD measurements. Studies of the CL spectra for as grown in situ Eu-doped {Zn(Mg)O/ZnCdO}$_m$ SLs showed at room temperature emission bands at ~617 nm, due to the $^5D_0 - {}^7F_2$ intra-4f-shell transition of Eu^{3+} ions (Fig. 1). We have determined the optimal conditions for amplifying the red emission. All structures were annealed for 1 minute in an O_2 environment at various temperatures. The highest intensity of the $^5D_0 - {}^7F_2$ peak was observed after annealing at 700°C. The decrease in intensity after annealing at high temperatures can be associated with the destruction of the superlattice structure due to Cd and Mg diffusion [3].

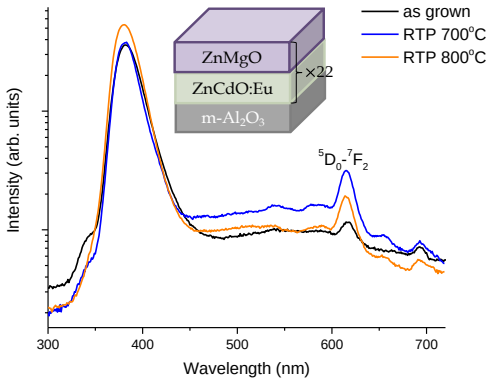

Fig. 1. RT-CL spectra of as-grown and annealed {ZnMgO/ZnCdO:Eu}$_{22}$ SLs.

This work was supported in part by the Polish National Science Center, Grants No. 2019/35/B/ST8/01937, and 2021/41/B/ST5/00216.

[1] S. Vyas, *Johnson Matthey Technol. Rev.*, ***64***(2), 202-218 (2020).
[2] P. L. Liu and P. T. Shao, *Molecular Simulation*, **39**(12), 1007-1012 (2013).
[3] M. Stachowicz, et al. *Applied Surface Science* **587** 152830 (2022).

n-ZnO/ZnCdO/p-Si and n-ZnCdO/ZnO/p-Si diodes: studies on the influence of the junction interlayer on electrical properties and structural defects

R. Szymon [1], E. Zielony [1], M. A. Pietrzyk[2] and A. Lysak[2]

[1] *Department of Quantum Technologies, Wroclaw University of Science and Technology, Wybrzeze Wyspianskiego 27, 50-370 Wroclaw, Poland*
[2] *Institute of Physics, Polish Academy of Sciences, Al. Lotnikow 32/46, PL-02668 Warsaw, Poland*

Zinc oxide (ZnO) remains competitive in the wide-bandgap semiconductor family, convenient for ultraviolet and blue optoelectronics: light-emitting diodes (LEDs) and lasers. Among others, its advantages are low price and ability for bandgap engineering. Indeed, the zinc-cadmium-oxide alloy (ZnCdO) is an example of such technology, providing bandgap narrowing [1]. However, alloying ZnO with CdO is problematic in the full composition range due to the solid solubility of Cd which is limited to ~40%, as well as different stable crystal structures - wurtzite (ZnO) and rock salt (CdO). Therefore, optimisation of ZnO and ZnCdO-based structures is still challenging at hand, as well as their n-type conductivity nature is discussed.

In our work [2], we studied the pair of bilayers of n-ZnO/ZnCdO and n-ZnCdO/ZnO on a p-Si substrate grown by molecular beam epitaxy. We carried out an in-depth investigation of these heterojunctions with their electrical properties based on: current-voltage (IV) and capacitance-voltage (CV) measurements in the broad temperature range of 40 to 300 K, as well as deep-level transient spectroscopy (DLTS). Research was supported by the micro-Raman scattering for study of their structural properties and lattice dynamics.

The IV characteristics confirmed the rectifying properties of the heterojunctions, with the electrical parameters obtained: rectifying factor, ideality factor, built-in voltage, series and junction resistance. The further study of IV plots in log-log scale gave insight into the current transport mechanisms of diodes, pointing out the multi-tunneling capture-emission process and space charge limited current, which are a consequence of the presence of defects. Next, the dopant concentrations were calculated from CV characteristics with their dependences on temperature and junction depletion region width. Finally, the DLTS results confirmed the presence of typical donor-like traps (see Fig.). It was noticed that cadmium atoms affected the electrical properties and energies of trap present in the studied junctions.

Our research let us suppose that the Cd-related defect complexes, such as: Zn_i-Cd_{Zn}-V_O or Cd_{Zn}-V_O, are the most appropriate candidates for n-type conductivity of ZnCdO alloys.

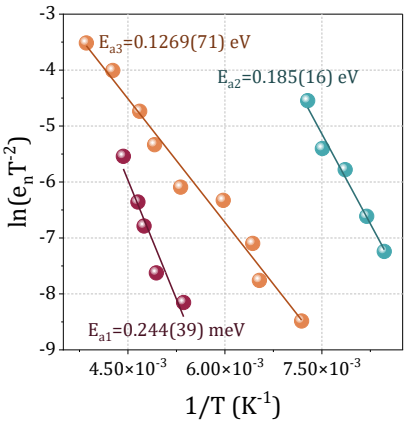

Fig. Arrhenius plot for n-ZnCdO/ZnO/p-Si junction (red and blue) and n-ZnO/ZnCdO/p-Si diode (orange).

[1] M.A. Pietrzyk, A. Wierzbicka, E. Zielony, A. Pieniazek, R. Szymon, E. Placzek-Popko, Sens. Actuator A Phys. **315**, 112305 (2020).

[2] R. Szymon, E. Zielony, A. Lysak, M.A. Pietrzyk, *Influence of the type of interlayer on current transport mechanisms and defects in n-ZnO/ZnCdO/p-Si and n-ZnCdO/ZnO/p-Si heterojunctions grown by molecular beam epitaxy*, J. All. Compd. (2023) (under review).

An insight into the optical properties of GaN nanowires with Al_2O_3 and HfO_2 shells

R. Szymon [1], E. Zielony [1], M. Sobanska[2], A. Wierzbicka[2], A. Reszka[2], S. Gieraltowska[2] and Z.R. Zytkiewicz[2]

[1] *Department of Quantum Technologies, Wroclaw University of Science and Technology, Wybrzeze Wyspianskiego 27, 50-370 Wroclaw, Poland*
[2] *Institute of Physics, Polish Academy of Sciences, Al. Lotnikow 32/46, PL-02668 Warsaw, Poland*

Recent development of gallium nitride-based heterostructures to a great extent is based on nanostructures, which help to overcome the limits of heteroepitaxy. Among others, nanowires (NWs) arrays bring many advantages since they eliminate global stress, increase the photoluminescence efficiency, and provide new opportunities for the construction of modern devices by changing the NWs composition, architecture or dimensions. This may lead to the next generation of ecological and highly efficient light emitters and detectors.

In this work, we have studied self-assembled GaN nanowires of ~90 nm diameter and 2 μm height, grown by plasma-assisted molecular beam epitaxy on a Si(111) substrate. The NWs were covered with oxide shells of Al_2O_3 and HfO_2 prepared by atomic layer deposition process. The nominal thicknesses of the shells were 5, 10 and 20 nm. The structural parameters of the NWs, such as diameters and fill factors, were derived from SEM images. The core-shell architecture was verified in the SEM transmission mode.

The influence of shells on the optical properties of GaN NWs was studied in optical reflectance and photoluminescence measurements. First, the reflectance spectra were measured and examined within the wavelength range of 300-1800 nm at room temperature. The effective medium approximation model was used to fit the observed interference patterns [1] (Fig. (a)). Based on the reflectance measurements, spectral dependence of effective refractive index was calculated. It has been shown that the experimental data precisely follow the theoretical model. Moreover, the fill factors were estimated with the Bruggeman model [1]. Their values were found to agree very well with those obtained from SEM images.

Finally, the optical properties of the NW samples were studied in the temperature range of 10 to 300 K. The photoluminescence signal (Fig. (b)) was observed in the ultraviolet region with strong emission bands around 3.45 eV, 3.42 eV and 3.18 eV [2, 3]. Their origin and dependence on oxide shell thickness will be discussed.

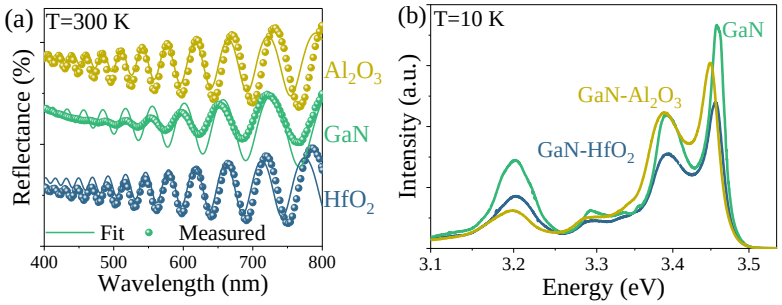

Fig. (a) Reflectance spectra (points) with theoretical fits (lines), and (b) PL spectra at 10 K of GaN/Si NWs with various oxide shells.

[1] H. Y. Chen, et al., Opt. Express **16**, 8106 (2008)
[2] K. P. Korona et al., J. Phys.: Condens. Matter **30**, 315301 (2018)
[3] K.P. Korona et al., J. Luminescence **155**, 293 (2014)

This work was partially supported by the Polish NCN grants 2021/43/D/ST7/01936 and 2022/45/B/ST5/02876.

Effect of strain and surface proximity on the acceptor grouping in ZnO:N

O. Volnianska, S. Mishra, and E. Guziewicz

Institute of Physics, Polish Academy of Sciences, Al. Lotnikow 32/46, 02-668 Warsaw, Poland

The experimentally observed two types of photoelectron spectra of different crystallites in ZnO:N indicate the grouping of acceptor and donor complexes in separate domains [1]. Density Functional Theory (DFT) studies suggest that the acceptor domains can involve zinc vacancy (V_{Zn}) and -$(NHx)_O$ groups and provide complexes-related acceptor states near the valence band maximum. However, the formation energies of these complexes are relatively high, and the acceptor-related sample properties in general depend on a number of factors such as growth or annealing conditions [2]. As the formation of defects involves distortion of the crystal lattice, it may be assumed that micro-strain plays an important role here.

DFT study of the effect of strain and surface proximity on the formation of (V_{Zn}) -$(NHx)_O$ complexes was performed using QUANTUM-ESPRESSO package [3] within the generalized gradient approximation (GGA) with the Hubbard-like +U term describing the on-site Coulomb interactions. The formation of complexes require the migration of the constituent defects and was computed using the Nudged Elastic Band (NBE) approach under (a) tensile and compressive biaxial strains in planar plane and along z-axis, (b) hydrostatic pressure, (c) local lattice distortion provoked by uncontrolled impurities as CH_x groups, and finally (d) surface proximity. In the last case, defects were introduced into the 0D nanocrystal object, as quantum dot (QD). DFT results indicates a strong strain effect on the electronic structure and activation of migration energy (E_A). In particular, 4% compressive biaxial strain reduced migration barrier of zinc vacancy moving around $(NH)_O$ from 0.65 eV to 0.24 eV. Moreover, the presence of a CH_x group near the complex lowers this value to zero. The effect of strain explains lowering of acceptor formation energy and might be also responsible for grouping of acceptors which can be formed only in crystallites showing compressive strain. In support to the DFT results, low-temperature cathodoluminescent CL maps reveal more intensive acceptor CL for the higher average micro-strain values.

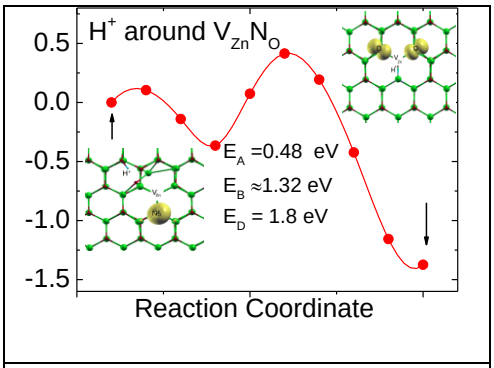

Fig. 1 The calculated energy profiles of the migrating H^+ along VN. The energy zero is set to the initial configurations. E_A, E_B, and E_D are activation, binding, and dissociation energies, respectively.

Acknowledgement. The work was supported by the project No. 2018/31/B/ST3/03576, founded by the National Science Centre. Calculations were done at the Interdisciplinary Center for Mathematical and Computational Modeling, University of Warsaw.

[1] E. Guziewicz, *et al*., Phys. Rev. Appl. 18, 044021 (2022).
[2] S. Mishra, *et al*., Phys. Status Solidi A, 2200466 (2022).
[3] P. Giannozzi *et al*.: *J. Phys.: Condens. Matter*. **21**, 395502 (2009).
[4] H. Jonsson, G. Mills, and K. W. Jacobsen, ‘‘Nudged elastic band method for finding minimum energy paths of transitions,’’ in Classical and Quantum Dynamics in Condensed Phase Simulations, edited by B. J. Berne, G. Ciccotti, and D. F. Coker , World Scientific, Singapore, 1998, p. 385.

Tailoring of the optical and electrical characteristics of ZnO: Ga heterostructures by a metallic buffer layer

Ali Hassan[1,2*], Abbas Ahmad Khan[3], Muhammad Azam[4] , Umar Farooq[5], Muhammad Zubair[6], Yu Cao[1,2]

[1]*China International Science & Technology Cooperation Base for Laser Processing Robotics, Wenzhou University, Wenzhou 325035, PR China*

[2]*Zhejiang provincial Key laboratory of Laser Processing Robotics, College of Mechanical and Electrical Engineering, Wenzhou University, Wenzhou 325035, PR China*

[3]*Department of Physics and Department of Energy Systems Research, Ajou University, Suwon 16499, Korea*

[4]*Department of Physics, Faculty of Sciences, University of Central Punjab, Lahore 54000, Pakistan*

[5]*Key Laboratory of the Ministry of Education for Advanced Catalysis Materials, Department of Chemistry, Zhejiang Normal University, Jinhua 321004, Zhejiang, PR China*

[6]*Centre for Advanced Material Application CEMEA, Slovak Academy of Sciences, Dúbravska´ Cesta 5807/9 845 11, Bratislava, Slovak Republic*

Corresponding Author: alirao@wzu.edu.cn

Abstract:

Due to its excellent transmittance, high UV emission, higher environmental and thermal stability, abundance of resources, and inexpensive cost for use in many sophisticated applications, nano-dimensional ZnO has received a lot of attention. In this regard, we present information on the photoluminescence and structural characteristics of thin films of Ga-doped ZnO made using pulsed laser deposition. A methodical presentation of the significant impact of Au and Ag as an interlayer on Ga-doped ZnO thin films has been made. According to X-ray diffraction examination, the generated films' crystalline microstructure was correctly aligned along (002) lattice planes with a hexagonal wurtzite structure. A surface analysis using a field emission scanning electron microscope revealed the films' surfaces to have very little surface roughness. With the addition of metallic interlayers, these films demonstrate an improvement of twofold photoluminescence behavior in the vicinity of band edge emission. Using an IR spectrophotometer, the resulting films' band gap energies ranged from 3.29 to 3.52 eV. Ga-doped ZnO offers a novel technique to replace other UV and IR photodetectors since reflection spectra show less reflectance (16%) and increased absorption in the UV-NIR region.

Ferromagnetic Resonance Studies of (Ga,Mn)N

Y.K. Edathumkandy[1], K. Gas[1], D. Sztenkiel[1], K. Das[1], D. Hommel[2,3], H. Przybylińska[1], M. Sawicki[1]

[1] *Institute of Physics, Polish Academy of Sciences, Warsaw, Poland*
[2] *Lukasiewicz Research Network–PORT, Polish Center for Technology Development, Wrocław, Poland*
[3] *Institute of Low Temperature and Structure Research, PAS, Wrocław, Poland*

Dilute ferromagnetic semiconductors, in particular (Ga,Mn)N predicted to have an exceptionally high Curie temperature (T_C), have attained great research importance due to their unique ability to combine the properties of semiconductors and magnetic materials [1]. Moreover, GaN being a wide band gap semiconductor has been dominating the photonics [2] and high power electronics. So it is important to make an effort to understand the underling magnetic properties of (Ga,Mn)N.

We report ferromagnetic resonance (FMR) studies of a series of (Ga,Mn)N layers grown by molecular beam epitaxy [3,4]. All investigated samples showed ferromagnetic signatures, as evidenced by SQUID magnetometry, with T_C ranging from 3 to 12 K. A broad angularly dependent FMR signal appears only at higher temperatures, closer to and above T_C, with intensities roughly scaling with magnetic susceptibility of the material, as shown in Fig, 1. However, apart from a very weak paramagnetic signal of Mn^{2+}, no ferromagnetic resonance is observed below 7 K, *i.e.*, where such ferromagnetic features as the hysteresis of magnetization curves and the remnant moment are the strongest. We relate this counterintuitive lack of low temperature FMR signal to inhomogeneous broadening caused by non-uniform distribution of magnetic ions and thus inhomogeneities in coupling strengths influencing the local magnetic anisotropies of Mn^{3+} ions.

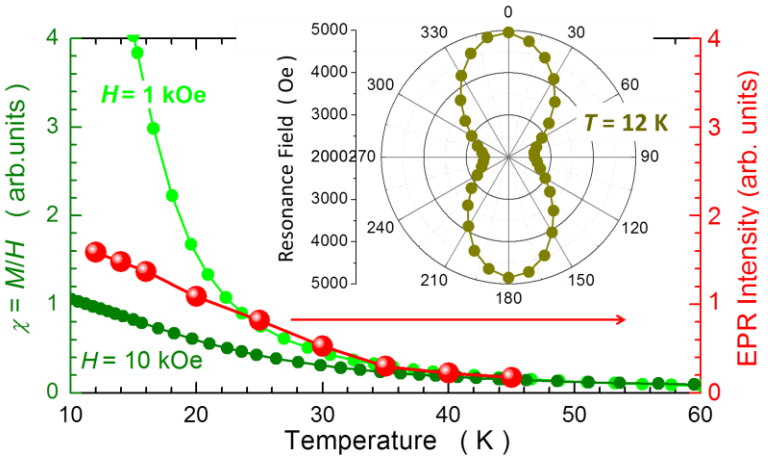

Fig.1 Comparison of magnetic susceptibilities determined by SQUID at fields of 1 and 10 kOe with that determined from FMR signal intensity at fields about 2 kOe. The inset shows the angular dependence of the resonance fields at 12 K

This study has been supported by the National Science Centre (Poland) through OPUS (UMO - 2018/31/B/ST3/03438) project.

[1] T. Dietl, H. Ohno, Rev. Mod. Phys. **86**, 1 (2000).
[2] S. Nakamura, T, Mukai, M. Senoh, App. Phy. Lett., **64**, 13 (1994).
[3] G. Kunert et al., Appl. Phys. Lett. **100**, 155321 (2012).
[4] K. Gas *et al.* J. Alloys Compd. **747**, 946 (2018).

Impact of current flow direction on the distribution of carriers in multiple, color-coded InGaN quantum wells

M. Chlipała, H. Turski, K. Nowakowski-Szkudlarek, A. Feduniewicz-Żmuda, C. Skierbiszewski

Institute of High-Pressure Physics PAS, ul. Sokołowska 29/37, 01-142 Warsaw, Poland

Unique properties of group III-nitride semiconductors allow for the design of high-efficiency and high-power optoelectronic devices. However, not all of these properties are advantageous. The fact that the internal quantum efficiency (IQE) tends to drop for high current densities, caused by significant Auger recombination and decreased injection efficiency is one of its negative characteristics [1]. The straightforward solution to this problem is to increase the number of quantum wells (QW), but III-nitrides pose strong built-in, spontaneous and piezoelectric fields ($\overrightarrow{F_P}$). This, together with the low mobility of holes in comparison to electrons, leads to the asymmetric carrier distribution and injection in the active region with multiple QWs, where in standard structures the QW closes to the p-type region tends to dominate [2].

To assess this implication, two LEDs with current flow direction ($\vec{J}$) parallel to built-in polarization (Fig. 1 c-d), and two with $\vec{J}$ anti-parallel to $\overrightarrow{F_P}$ (Fig1. a-b) are compared. This is achieved on bulk Ga polar substrate by using the buried tunnel junction (TJ) [3,4]. In addition, all LEDs consist of double 2.6nm QW where the position of the blue- and green-emitting active region was varied with respect to the p-type region, resulting in structures where electrons firstly flow to the shallow blue QW, for LEDs in Fig. 1 a, d, or deeper, green QW, for LEDs in Fig. 1 b, c.

By measuring the relation between emission peaks from green- and blue-emitting QW in a wide range of current densities we investigated the impact of the polarization on the carrier distribution in double, color-coded InGaN-based QW LEDs.

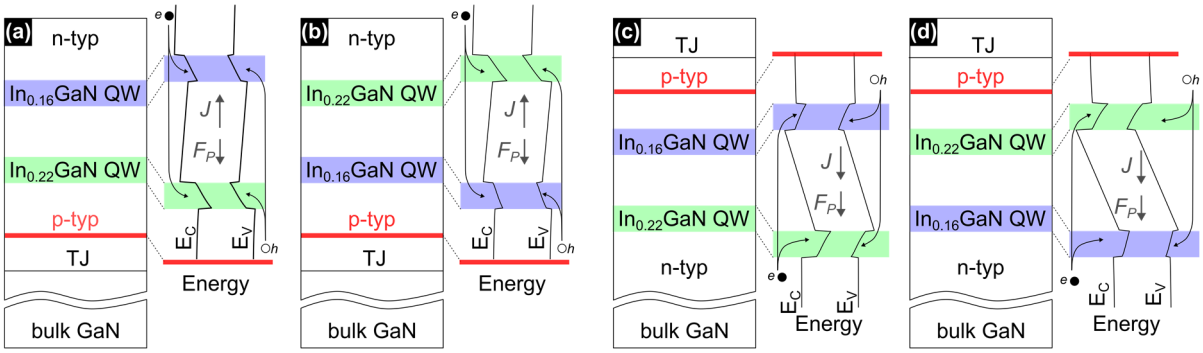

Fig. 1 Schematic structures and band structures at ~100 A/cm² for LEDs with (a-b) p-type down, (c-d) p-type up.

Acknowledgments: This work is carried out within National Science Centre Grant, UMO-2018/31/B/ST5/03719, UMO-2019/35/N/ST7/04182, and project of the Foundation for Polish Science co-financed by the European Union under the European Regional Development Fund TEAM-TECH POIR.04.04.00-00-210C/16-00.

[1] Li, X., et al. *Superlattices and Microstructures*, *47*(1), 118–122 (2010)
[2] David A., et al. *Applied Physics Letters*, *92*(5), (2008).
[3] Turski, H., et al. *Journal of Applied. Physics,* 125, 1–23 (2019)
[4] Chlipała M., et al. *Applied Physics Letters*, 120, 171104 (2022

Extreme InGaN growth conditions by plasma assisted molecular beam epitaxy

M. Siekacz[1], M. Żak[1], K. Gołyga[1], M. Kryśko[1], A. Feduniewicz-Żmuda[1], H. Turski[1], C. Skierbiszewski[1], G. Muziol[1].

[1]*Institute of High Pressure Physics, PAS, Sokolowska 29/37, 01-142 Warsaw, Poland.*

The crucial challenge in high quantum efficiency nitride based devices like light emitting diodes (LEDs) or laser diodes is the growth of InGaN layers. In this work we study properties of InGaN layers grown by plasma assisted MBE (PAMBE) for very high nitrogen fluxes – 2.8 µm/h. These conditions are unusual for PAMBE technology since available high N flux is limited by e.g. MBE pumping speed to maintain enough high vcuum (less than 10^{-4} torr) during process. The high nitrogen flux prevents InGaN decomposition. This allows us to explore growth conditions of InGaN that were previously not achievable in PAMBE – growth at high temperatures. The InGaN layers were grown in In-rich conditions, with different Ga fluxes with constant N flux (2.8 um/h) and a very high growth temperature T_g=710 C.

The obtained results are analyzed within phenomenological model of InGaN growth assuming growth on nonequivalent atomic steps [1]. In Figure 1(c) the InGaN content as a function of Ga flux is shown according this model prediction. As the Ga flux is reduced, we observe saturation of In content due to the decomposition of InGaN (Nitrogen loss) - it is observed as stabilization of photoluminescence emission wavelength (around 430 nm). The behavior of emission wavelength for low (0.04 um/h) and high (2.5 um/h) Ga fluxes also follows model prediction of In content.

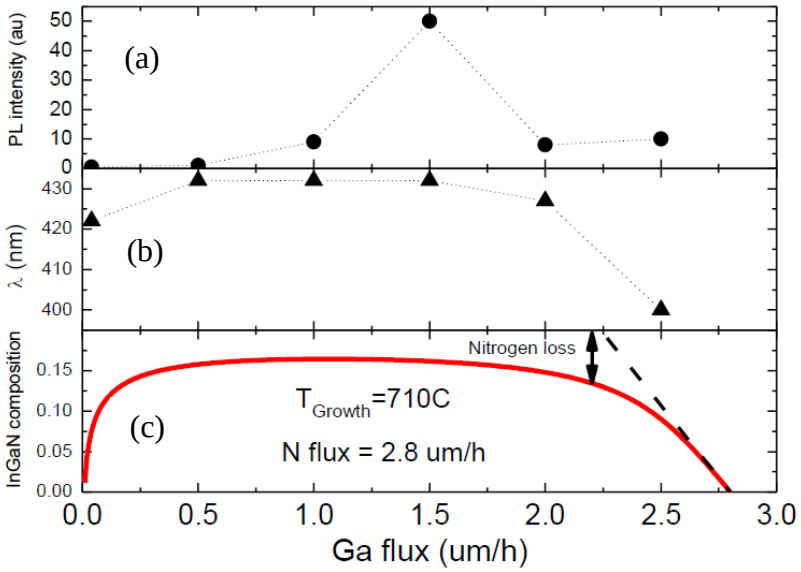

Fig. 1. The intensity of photoluminescence from InGaN layers (a), the wavelength (b) and the indium composition as a function of Ga flux (In content calculated from theoretical model [1]).

We found that the photoluminescence intensity strongly depends on the Ga flux (see Fig.1 (a)). It can be correlated with the surface morphology. We will discuss the photoluminescence efficiency, surface morphology and indium content of InGaN layers.

[1] H. Turski, M. Siekacz, Z.R. Wasilewski, M. Sawicka, S. Porowski, C. Skierbiszewski, Nonequivalent atomic step edges—Role of gallium and nitrogen atoms in the growth of InGaN layers, Journal of Crystal Growth 367 (2013) 115-121.

Doping inhomogeneity at the nanoscale in GaN:Si studied by electrochemical etching

A. Feduniewicz-Żmuda [1], M. Siekacz [1], N. Fiuczek [1], O. Gołyga [1], M. Sawicka [1], K. Sobczak[,2] and C. Skierbiszewski [2]

[1] *Institute of High Pressure Physics, PAS, Sokołowska 29/37, 01-142 Warsaw, Poland.*
[2] *Faculty of Chemistry, Biological and Chemical Research Center, University of Warsaw, Żwirki i Wigury 101, 02-089 Warsaw, Poland.*

Electrochemical etching (ECE) has recently emerged as a very useful method to fabricate porous GaN of a decreased refractive index [1] e.g. for cladding layers in laser diodes [2] or for removal of sacrificial layers and structure lift-off [3]. Due to high selectivity against n-type doping, ECE technique can also serve as a tool to detect inhomogeneity in Si doping in GaN grown by plasma-assisted molecular beam epitaxy (PAMBE) [4]. We showed that surface morphology – atomically flat or step-bunched – impacts the Si incorporation and leads to doping inhomogeneity at the nanoscale.

In this work we focus on the extremely high Si doping of GaN up to $1 \cdot 10^{20}$ cm^{-3} and its consequences for the surface morphology and the electrical properties within the layer. We study GaN:Si^{++} layers grown by PAMBE on GaN/Sapphire templates. First, we observe the enhanced growth rate along the a-direction $\langle 11\bar{2}0 \rangle$ that causes the emergence of the hillocks with star-shaped arms, that we call "nanostars", see Figure 1(a). Second, we investigate local Si content and measure only a 10% Si composition decrease in the nanostar by energy-dispersive X-ray spectroscopy (EDX) and third, we use ECE to study electrical properties at the nanoscale. Because the nanostars are less conductive than the surrounding layer, they are not etched during ECE, see Figure 1(b). We discuss the origins of the decreased nanostar conductivity and attribute it to an increased compensation that is most likely caused by the complexes of Si substitutional and vacancies.

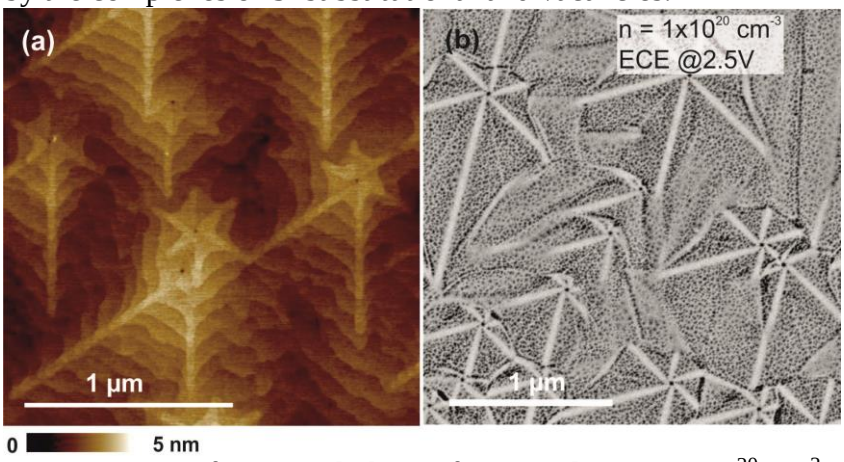

Figure 1 (a) Surface morphology of GaN:Si layer n=$1 \cdot 10^{20}$ cm^{-3}, (b) SEM after ECE at 2.5V.

[1] C. Zhang et al., (Invited) New Directions in GaN Photonics Enabled by Electrochemical Processes. *ECS Transactions* 72, 47-56 (2016).
[2] M. Sawicka et al, Electrically pumped blue laser diodes with nanoporous bottom cladding, *Optics Express* **30**, 10709-10722 (2022).
[3] S. H. Park et al., Wide bandgap III-nitride nanomembranes for optoelectronic applications. Nano Lett 14, 4293-4298 (2014).
[4] M. Sawicka et al., Revealing inhomogeneous Si incorporation into GaN at the nanometer scale by electrochemical etching. Nanoscale 12, 6137-6143 (2020).

Acknowledgements: This work was also financially supported by National Science Centre Poland within grants SONATA no. 2019/35/D/ST5/02950 and 2019/35/D/ST3/03008. The research leading to these results has also received funding from the Norway Grants 2014-2021 via the National Centre for Research and Development grant no. NOR/SGS/BANANO/0164/2020

Visible luminescence of BGaN-based structures: towards defects-related LEDs

M. Guziewicz [1], E. B. Możdżynska[1,2], P. Ciepielewski [1], E. Dumiszewska[1], B. Stańczyk[1], M. Wzorek[1], and K. Kościewicz [1]

[1] *Łukasiewicz Research Network-Institute of Microelectronics and Photonics, Al. Lotników 32/46, 02-668 Warsaw, Poland*
[2] *Faculty of Materials Science and Engineering, Warsaw University of Technology, Wołoska 141, 02-507 Warsaw, Poland*

Boron containing $Me^{III}N$ nitrides are currently of interest because boron can affect the physical properties of GaN-based ternary (BGaN, BAlN) and quaternary (BInGaN, BAlGaN) alloys. Theoretical studies indicate that boron can provide the ability to tune the bandgap width, lattice parameters and dielectric constant of the compounds. Therefore, $BMe^{III}N$ compounds can be useful be useful for production of new electronic or optoelectronic devices.

We fabricated and characterized BGaN-based epitaxial structures on sapphire substrates with various buffer and active layers grown by MOCVD for LED applications. Photoluminescence and Raman spectra were measured to demonstrate red lighting and the residual stress within the LED structures. Crystals structure and morphology of the layers were characterized by XRD and TEM methods, and electrical parameters by Hall measurements. As was recently revealed, the B concentration in BGaN depends on growth temperature [1]. It was shown that the B concentration in BGaN determined to be about 2.5% at., decreases with increasing growth temperature. Such layers are highly insulating with a sheet resistance of 8×10^{10} Ω/sq. A typical photoluminescence appears in the broad red range, which can be attributed to a defect center with an activation energy of 1,35 eV [2]. In this work, we intentionally doped BGaN layers with Si or Mg, using appropriate precursors, to form n- or p-type semiconductor. Additionally, p-n junctions with BGaN were produced in the form of multilayer epitaxial stacks. Because of many structural defects formed in BGaN grown at temperature close to 900°C or higher, indium was incorporated into the layer to attenuate the contraction of the BGaN lattice parameters. Such an In-induced contraction can lead to lattice-matched crystal growth. Fig.1 shows the PL spectra with red luminescence over a wide range, including the yellow component, while the bandgap edge emission is almost eliminated. The yield of red luminescence is higher for B-rich BGaN:Mg grown at 800°C, but for BGaN:Si the yield is higher for samples grown at 1050°C. Comparative studies of BGaN and BInGaN layers suggest next steps to improve structural and electrical parameters of the layers required for red defect- related LEDs.

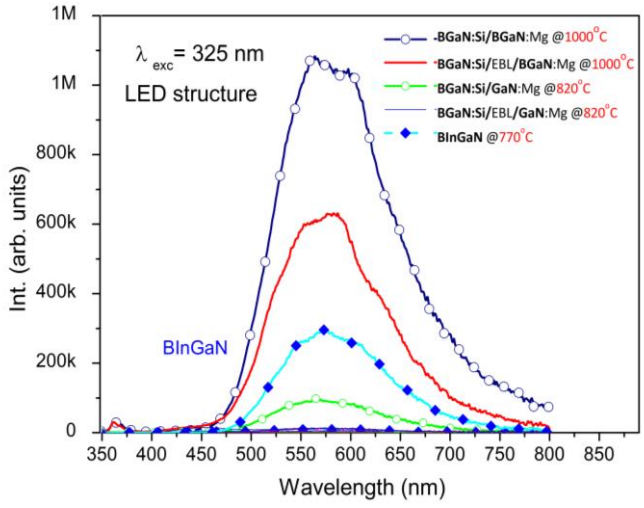

Fig. 1. PL spectra of LED structures with BGaN or BInGaN epilayers grown on sapphire (0001).

[1] E. B. Mozdzynska, S. Złotnik, P. Ciepielewski, at al., J. Mater. Sci. **57**, 7265 (2022)
[2] E. B. Mozdzynska, P. Kaminski,, R. Kozłowski, at al., J. Mater. Sci. **57**, 17347 (2022)

Modification of luminescence of the nitride nanowires by chemical treatment of their surface

Bogdan J. Kowalski, Anna Reszka, Marcin Klepka, Anna Wolska, Marta Sobanska, Zbigniew R. Zytkiewicz

Institute of Physics, Polish Academy of Sciences, Aleja Lotników 32/46, PL-02-668 Warsaw, Poland

Although the influence of surface conditions on transport and optical properties of semiconductor nanowires (NWs) has been identified, the methods of controlling it and inhibiting its detrimental impact on the NW characteristics still remain an important subject of research. As the depth of the depletion or accumulation layer induced by surface band bending may become comparable with the diameter of the NW, its part available for transport, charge carrier injection and light generation can be markedly reduced. This applies also to NWs made of the group III nitrides. Therefore, we carry out complementary studies of luminescence of GaN NWs vs. chemical and electronic conditions on their surfaces.

The NWs are grown catalyst-free on in-situ nitradated Si (111) substrates by plasma-assisted molecular beam epitaxy (MBE). The morphology of the samples is assessed by scanning electron microscopy (SEM). The luminescence of individual NWs is investigated by SEM-based cathodoluminescence spectroscopy and mapping. X-ray photoelectron spectroscopy (XPS) enables us to measure the shifts of the valence band maximum with respect to the Fermi level (i.e. to deduce changes in surface band bending) as well as assess changes in the chemical composition of the surface.

We report the results of CL and XPS experiments on the GaN NWs modified by etching their surfaces in KOH and HCl solutions. Both substances are used as media that etch, deoxidize or passivate nitride surfaces [1-3]. Therefore we applied them to modify surface chemical composition and charge accumulation in view to optimize luminescence of the GaN NWs.

The CL technique enabled us to reveal changes induced in luminescence of individual NWs as well as of the ensemble of them. Cathodoluminescence line-scans helped us to follow changes in the intensity and spectrum of luminescence along the NW. The XPS experiments, carried out in an oblique configuration to probe a substantial part of the side NW surface, allowed us to follow the changes in the emission from the GaN atoms, surface contaminants (oxygen and carbon) and residues of the etching solutions. So, changes in the surface chemical composition could be assessed. Shifts of the valence band edge vs. the Fermi level showed the changes in the surface band bending. The correlation of the results acquired by both techniques evidenced the possibility to control GaN NW luminescence by surface etching.

This work was partially supported by the Polish NCN grants 2022/45/B/ST5/02876 and 2021/43/D/ST7/01936.

[1] D. Priante, M. Tangi, J.-W. Min, N. Alfaraj, J.W. Liang, H. Sun, H.H. Alhashim, X. Li, A.M. Albadri, A.Y. Alyamani, T.K. Ng, B.S. Ooi, Optic.Mat.Express **9**, 203 (2019)
[2] M. Biswas, V. Chavan, S. Zhao, Z. Mi, S. Chakrabarti, ACS Appl. Nano Mater. **1**, 1968 (2018)
[3] C.Y. Lee, H. Sekiguchi, H. Okada and A. Wakahara, Jpn. J. Appl. Phys 51, 076503 (2012)

Strain relation in GaN nanowires with HfO_2 and Al_2O_3 shells examined by X-ray diffraction and Raman spectroscopy techniques

A. Wierzbicka[1], R. Szymon[2], E. Zielony[2], A. Reszka[1], M. Sobanska[1], S. Gieraltowska[1], P. Sybilski[1], and Z. R. Zytkiewicz[1]

[1] *Institute of Physics, Polish Academy of Sciences, Al. Lotnikow 32/46, PL-02668 Warsaw, Poland*
[2] *Department of Quantum Technologies, Wroclaw University of Science and Technology, Wybrzeze Wyspianskiego 27, 50-370 Wroclaw, Poland*

Recent years have exhibit the dynamic development of integration photonics with electronics on a single platform. GaN nanowires (NWs) are often studied as a potential building blocks of such systems since NWs grow virtually free of strain and defects even on substrates with large lattice mismatch [1, 2]. Usually side surfaces of NWs are passivated by oxide shells. Thus, the question arises about the strain induced by such shells.

In this work we studied self-assembled GaN nanowires of ~100 nm diameter and 2 μm height, grown by plasma-assisted molecular beam epitaxy on Si(111) substrates. The NWs were covered with shells of HfO_2 and Al_2O_3 using atomic layer deposition. The nominal thicknesses of the shells were 5, 10 and 20 nm. The dimensions of the NWs, such as diameters and shell thicknesses, were measured from SEM images. The uniformity of shells covering GaN NWs was analyzed in the SEM transmission mode.

Structural properties of GaN core-shell NWs were examined using X-ray diffraction (XRD) and Raman spectroscopy techniques. In particular, the values and the type of strain were investigated, together with their dependence on the shell thickness. First, the XRD curves and high resolution XRD maps were measured to calculate the accurate values of lattice parameters of GaN core parts. $2\theta/\omega$ scans of 0002 GaN reflections (see Fig. 1(a)) revealed changes in interplanar distances in the GaN core with the magnitude depending on the thicknesses of shell parts. Calculations of *a* and *c* lattice parameters allowed to find the in-plane (ε_{xx}) and out-of-plane (ε_{zz}) strain values for the studied samples. Next, the Raman spectroscopy was used to study the lattice vibration mechanisms, crystalline quality and strain in GaN/HfO_2 and GaN/Al_2O_3 core-shell structures. The comparison of in-plane strain values (ε_{xx}) obtained by these two techniques is presented in Figure 1 (b). The origin of strain and influence of oxide shell thickness on strain distribution in GaN/oxide core-shell nanowires will be discussed within this work.

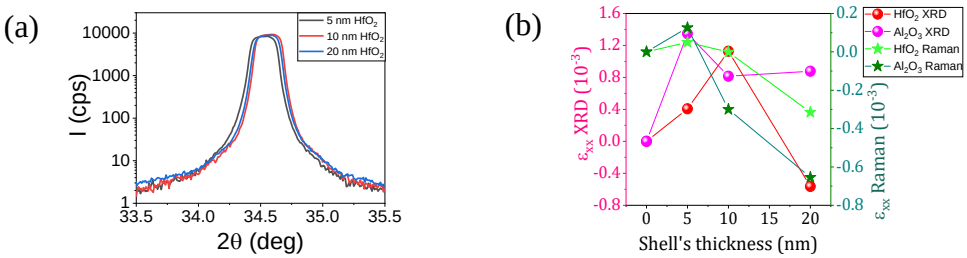

Figure 1. (a) XRD $2\theta/\omega$ scans of 0002 GaN reflection for GaN NWs with HfO_2 shell of different thickness, and (b) the values of ε_{xx} strain component calculated from XRD and Raman measurements of GaN/oxide NWs of various shell thickness.

[1] W. Guo, M. Zhang, P. Bhattacharya and J. Heo, *Nano Lett.* **11,** 1434 (2011).
[2] S. Li and A. Waag, *J. Appl. Phys.* **111**, 071101 (2012).
This work was partially supported by the Polish NCN grants 2021/43/D/ST7/01936 and 2022/45/B/ST5/02876.

Investigation of strain relation and lattice dynamics in {CdO/MgO} superlattices grown by plasma-assisted molecular beam epitaxy

A. Wierzbicka[1], E. Przezdziecka[1], I. Perlikowski[2], E. Zielony[2]

[1] *Institute of Physics, Polish Academy of Sciences, Al. Lotnikow 32/46, PL-02668 Warsaw, Poland*
[2] *Department of Quantum Technologies, Wroclaw University of Science and Technology, Wybrzeze Wyspianskiego 27, 50-370 Wroclaw, Poland*

Cadmium oxide (CdO) is a promising material for transparent conducting oxide (TCO) thin films due to its excellent performance regarding conduction [1]. It is characterized by high transparency in the visible spectrum, low resistivity and high carrier mobility [1]. In the TCO family, II-VI ternary oxide alloys have attracted considerable interest due to the possibility of modulating their band gaps in a wide range of values [1], what opens up the possibility of new applications in modern optoelectronic devices.

In this work we have studied a series of {CdO/MgO} superlattices (SLs) grown on *a*-, *c*-, *m*- and *r*-plane sapphire substrates by plasma-assisted molecular beam epitaxy (PA-MBE). The samples were measured by X-ray diffraction (XRD) and Raman spectroscopy techniques to obtain the strain distribution in SLs system as well as to study the lattice dynamics in the fabricated structures.

Figure 1 (a) shows the high resolution X-ray diffraction map (HRXRD) for selected sample grown on *r*-plane sapphire. It clearly reveals the periodic structure of the superlattice. Moreover, HRXRD maps allow to designate the accurate values of *a* and *c* lattice parameters for the series of samples. Furthermore, we can calculate the in-plane (ε_{xx}) and the out-of-plane (ε_{zz}) strain values.

Next, the Raman measurements were performed to examine lattice vibration mechanisms and crystalline quality of {CdO/MgO} SLs. The typical spectrum is shown in Figure 1 (b). First-order Raman modes are forbidden in the case of rocksalt compounds such as CdO and MgO. However, lattice mismatch between layers it the SLs induce strain in the structure. Disorder introduced by the strain may be the reason of the appearance of TO MgO mode.

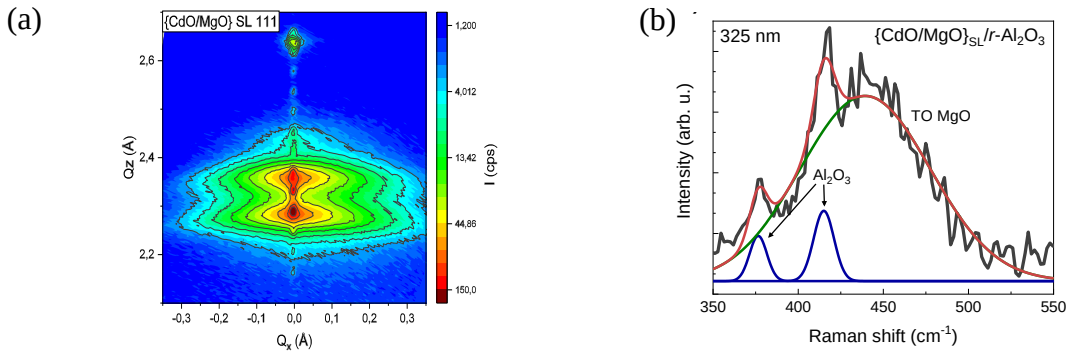

Figure 1. High resolution XRD maps measured for 111 CdO/MgO SL peak (a) and Raman spectra with an analysis of selected spectrum range carried out by fitting the data with Lorenz function (b) obtained for SLs on *r*-plane sapphire.

[1] U. Ozgur, Y.I. Alivov, C. Liu, A. Teke, M.A. Reshchikov, S. Dogan, V. Avrutin, S.J. Cho and H. Moroc, *J. Appl. Phys.***98**, 1 (2005).

The work was supported by the Polish NCN project DEC-2021/41/B/ST5/00216.

Band parameters of group IV semiconductors in wurtzite structure

Jakub Ziembicki[1], Paweł Scharoch[1], Maciej P. Polak[2], Michał Wiśniewski[3], Robert Kudrawiec[1]

[1]*Department of Semiconductor Materials Engineering, Wrocław University of Science and Technology, Wybrzeże Wyspiańskiego 27, 50-370 Wrocław, Poland*
[2]*Department of Materials Science and Engineering, University of Wisconsin-Madison, 1509 University Ave., Madison, WI 53706, United States*
[3]*Department of Experimental Physics, Wrocław University of Science and Technology, Wybrzeże Wyspiańskiego 27, 50-370 Wrocław, Poland*

Metastable crystal phases of group IV semiconductors present in low aspect ratio nanostructures exhibit great potential to overcome current limitations in semiconductor industry. Their chemical and structural similarity to diamond structure is a key factor in incorporation such structures in current group IV technology, at the same time leaving much room for tailoring physical properties by means of size effect and polytypes mixing. Usual pathway for modeling heterostructures and low dimensional systems are **kp** and tight binding models which are computationally efficient and require minimal set of parameters. It is known however, that the accuracy of these models relies strongly on their parametrization and the stable phase values, present in the literature, cannot be transferred to other crystal phases. On the other hand *ab initio* methods provide great accuracy without empirical parameters but are computationally more expensive which limits their use in complex systems modeling.

The goal of presented work is the parametrization of six band **kp** model for lonsdaleite crystal phase which is the second most common phase after diamond. We use high accuracy *ab initio* methods to derive physical properties of group IV materials and then transfer our results to **kp** model. In particular the effects of strains on crystal and band structures are investigated in detail and described by elastic tensor and absolute deformation potentials respectively. Our parameters set together with already known parameters for diamond structure allows for efficient modeling of heterostructures containing different polytypes.

Solutions for spectroscopy and imaging

Markus Krause

Quantum Design GmbH, Im Tiefen See 58, 64-293 Darmstadt, Germany

The manufacturer Andor Technology provides a range of spectral instruments suitable for a wide range of spectroscopy applications. Czerny-Turner with different focal lengths and echelle spectrographs come pre-aligned and pre-calibrated for ease of operation.

Our modular spectroscopy systems are individual configurations. The range of spectrographs is complemented by detector technology for wavelength regions from the UV to the near-IR.
The Shamrock and Kymera series from Andor offer a wide range of spectrographs to find a solution for every application. The main difference of the three models is the focal length: 328, 500 and 750 mm, respectively. All models are based on the optical design according to Czerny-Turner. We offer:

-Pre-aligned, pre-calibrated spectrograph
-Large choice of light coupling interfaces
-Wide range of interchangeable gratings
-Monochromator capabilities
-Third party software support.

As mentioned above we also offer suitable detectors e.g. low-noise slow scanning CCD detectors for standard spectroscopy applications and high-performance CCD detectors for faster acquisitions. The EMCCD sensors are dedicated for measurements limited by read noise. The InGaAs photo diode arrays are ideal for wavelengths over 1000 nm.

Common features are their high-sensitivity in the UV and visible range. Thermo-electric cooling and high-quality AD converters reduce noise to allow application even in extreme low-light conditions.

Realization of a High-Finesse Cavity Platform for Functionalization of Emitters

N. Dalla[1], P. Kulboka[1], P. Sojewski[1], K. Oreszczuk[1], T. Kazimierczuk[1], P. Kossacki[1], R. J. Warburton[2], and T. Jakubczyk[1]*

[1]*University of Warsaw, Ludwika Pasteura 5, Warsaw, 02-093, Poland*
[2]*Department of Physics, University of Basel, Basel CH-4056, Switzerland*
*corresponding author: *tomasz.jakubczyk@fuw.edu.pl*

The race for the idealization of a quantum-computing device has led to the demand for an efficient single-photon generation device with optimized attributes of purity, indistinguishability, and brightness. The two latter parameters can be improved by incorporating single-photon emitters inside a photonic cavity. Here, we present a cavity platform, where the top mirror consists of a concave Gaussian-like shape, while the bottom mirror is planar. This cavity geometry achieves high finesse values since the upper wavefront of the Hermite-Gaussian beam matches the mirror geometry and is reflected into the cavity mode with minimal losses. It also facilitates achieving low-mode volume since the beam waist rests at the bottom mirror. Both factors are crucial for high-Purcell Factors. The bottom mirror rests on a piezo stage while the top rests on a tunable kinematic mount. The elements are connected by a stiff and lightweight cage mount to shift the mechanical resonance frequencies above the typical acoustic and seismic environmental noise frequencies.

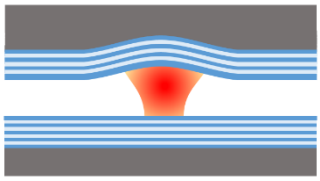

Figure 1. Schematics of the cavity design.

The cavity length was scanned to characterize the cavity setup with an oscillating voltage applied to the piezo, which holds the bottom mirror. Two lasers, one acting as a reference and the other tunable, were shined upon the cavity. The resulting distance between the two corresponding peaks for a cavity mode was utilized to provide information about the slopes of the cavity modes. With that, we could determine the broadening of the cavity modes in the wavelength domain, which led to the information about the Q-factors of the cavity. Since, for a cavity without internal losses, the Q-factor varies linearly with the mode numbers thus, we were able to calculate the finesse parameter. For our mirrors with 500 ppm transmission, we were able to achieve Q-Factors up to 10^5 and Finesse of $6 \cdot 10^3$, which is comparable to the theoretical values for the mirrors.

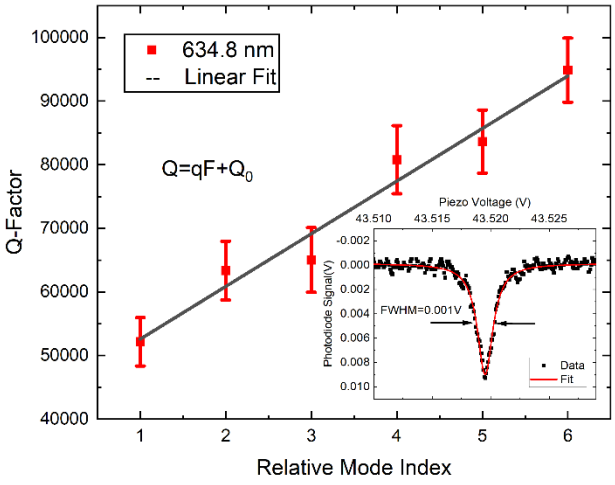

Figure 2. Q-Factors for different modes. In subset, photodiode voltage with cavity length detuning.

[1] Tomm, N., Javadi, A., Antoniadis, N.O. et al. A bright and fast source of coherent single photons. *Nat. Nanotechnol*. 16, 399–403 (2021).

Electrical switching of a chiral lasing from polariton condensate in a Rashba-Dresselhaus regime

K. Łempicka-Mirek[1], M. Król[1], L. De Marco[2], A. Coriolano[2,3], L. Polimeno[2], I. Viola[4], M. Kędziora[1], M. Muszyński[1], P. Morawiak[5], R. Mazur[5], P. Kula[6], W. Piecek[5], P. Fita[1], D. Sanvitto[2], J. Szczytko[1], B. Piętka[1]

[1] *Institute of Experimental Physics, Faculty of Physics, University of Warsaw, Poland*
[2] *CNR Nanotec, Institute of Nanotechnology, Lecce, Italy*
[3] *Dipartimento di Matematica e Fisica E. De Giorgi, Università del Salento, Campus Ecotekne, Via Monteroni, Lecce 73100, Italy*
[4] *CNR-NANOTEC, Institute of Nanotechnology, Rome, Italy*
[5] *Institute of Applied Physics, Military University of Technology, Warsaw, Poland*
[6] *Institute of Chemistry, Military University of Technology, Warsaw, Poland*

Efficient optical processing of classical and quantum information imposes on light novel requirements: chirality and low threshold non-linearities. In this work we demonstrate a chiral lasing from an optical modes due to emerging photonic Rashba-Dresselhaus spin-orbit coupling. For this purpose we developed a new electrically tunable device based on an optical cavity filled with birefringent liquid crystal (LC) and perovskite crystals [1]. Our novel method for the growth of single crystals of $CsPbBr_3$ inorganic perovskite in polymer templates allows us to obtain crystals with controlled size and thickness. Such crystals we place in a microcavity filled with bifefringent LC. We reach a strong light-matter coupling regime between perovskite excitons and cavity modes, and induce polariton condensation at room temperature on cavity chiral modes [2].

In our device, the emission from the condensate can be spectrally tuned by 29 meV, thanks to the sensitivity of the liquid crystal to an external voltage. We use birefringence of the liquid crystal to induce the Rashba-Dresselhaus spin-orbit coupling. We show chiral polaritonic modes below condensation threshold and simultaneous emission from the polariton condensate in two, tilted beams exhibiting polarization of opposite handedness above the threshold (Figure 1). We make use of different condensation thresholds for different regimes of spin-orbit interactions to create electrically controlled switch.

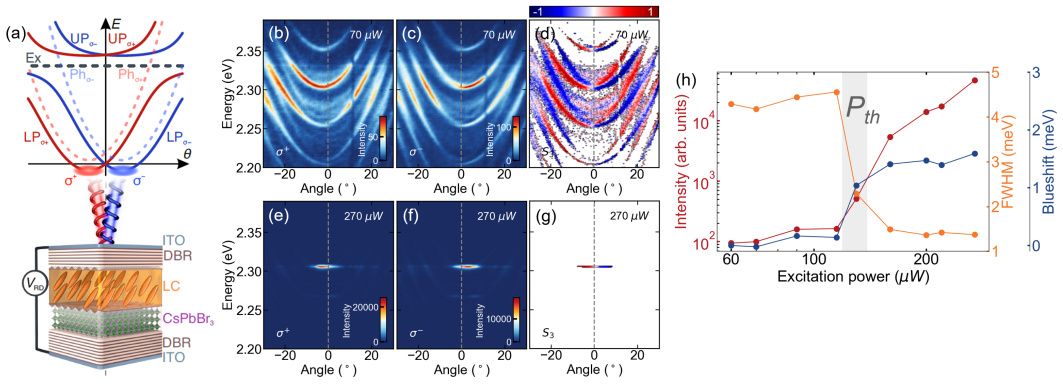

Figure 1. Polariton condensation in the Rashba-Dresselhaus regime. (a) Scheme of the sample and graph of a circularly polarized polariton condensation. Angle-resolved photoluminescence spectra in both circular polarizations and resulting the S_3 parameter: (b–d) below and (e–g) above the condensation threshold. (h) Emission intensity, spectral linewidth and energy blueshift for increasing excitation power.

[1] K. Łempicka-Mirek, et al., *Science Advances* **8**, 40 (2022).
[2] K. Łempicka-Mirek, et al., *arXiv:2211.11852* (2022).

Natural Exceptional Points Appearing in Semiconductor Microcavity Systems

M. Furman[1], A. Opala[1,2], M. Król[1], R. Mirek[1], K. Tyszka[1], B. Seredyński[1], W. Pacuski[1], J. Szczytko[1], M. Matuszewski[2], B. Piętka[1]

[1] *Institute of Experimental Physics, Faculty of Physics, University of Warsaw, Pasteura 5, 02-093 Warsaw, Poland*
[2] *Institute of Physics, Polish Academy of Sciences, Aleja Lotników 32/46, 02-668 Warsaw, Poland*

In quantum mechanics various systems can be represented within a Hermitian Hamiltonian description. In the case of a physical system in which gain and dissipation play a significant role, this description is no longer valid and the non-Hermitian character of the system must be taken into account.

An example of a phenomenon that can only occur in non-Hermitian systems is the appearance of the so-called exceptional points (EPs). These specific singularity points arise in parameter space, where at least two eigenvalues are degenerate (both the real and imaginary parts of the energies are equal). The EPs are characterized by an exotic topology of the eigenvalue surfaces near an exceptional point singularity [2], which can be demonstrated while encircling them in the parameter space in which they appear. Performing a full loop around the EP does not lead to the initial state, but results in switching to the second eigenstate. In this work, following the theoretical model, we observe such a behavior experimentally in a semiconductor microcavity.

In our work, we demonstrate the emergence of the exceptional points associated with the transition of the system from the strong to the weak light-matter coupling regime. We perform angle-resolved experiments in which we additionally vary the Rabi splitting by the power of the incident laser beam. Specifically, we encircle the EP in parameters space of a wave vector–coupling strength, as shown in the Figure. The presence of the EP is evidenced by the specific exchange between the eigenstates, which is in excellent agreement with the proposed theoretical model.

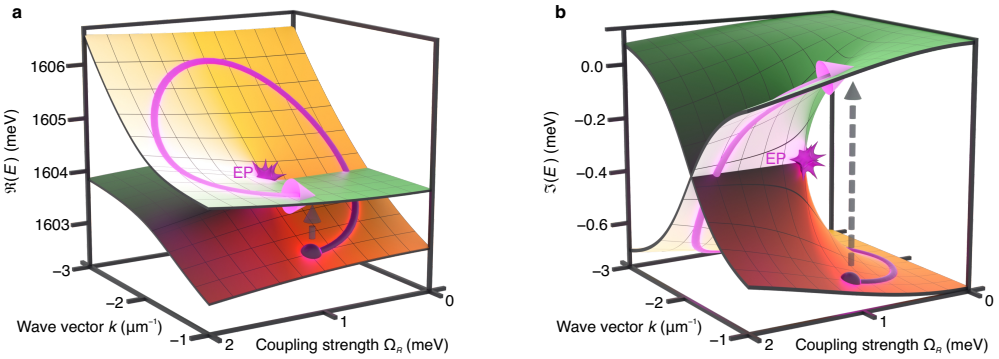

Figure: Encircling the exceptional point in a space of parameters: Rabi splitting and wave vector change, (a) real and (b) imaginary part of the energy.

[1] A. Opala, M. Furman, M. Król, R. Mirek, K. Tyszka, B. Seredyński, W. Pacuski, J. Szczytko, M. Matuszewski, B. Piętka, "Natural exceptional points in the collective excitation spectrum of a light-matter system", in review.

[2] M. Miri, A. Alù, "Exceptional points in optics and photonics", *Science* **363**, 6422, (2019).

Driven-dissipative Bose-Einstein condensation of photons in a VCSEL

Maciej Pieczarka[1], Marcin Gębski[2], Aleksandra N. Piasecka[1], Michał Wasiak[2], James A. Lott[3] and Tomasz Czyszanowski[2]

[1]*Department of Experimental Physics, Faculty of Fundamental Problems of Technology, Wrocław University of Science and Technology, Wrocław, Poland*

[2] *Photonics Group, Institute of Physics, Lodz University of Technology, Łódź, Poland*

[3] *Institute of Solid State Physics and Center of Nanophotonics, Technical University Berlin, Berlin, Germany*

Photons are the first ever particles considered in the Bose-Einstein statistics and the most abundant bosons in nature. Surprisingly, photonic gases were among the latest to demonstrate Bose-Einstein condensation (BEC) [1], despite many analogies developed over the years between laser physics and BEC. Recently, semiconductor lasers have been proposed to be a promising direction in photon BECs at room temperature [2].

Here, we observe signs of a driven-dissipative BEC phase transition in a broad-area oxide-confined vertical-cavity surface-emitting laser (VCSEL) designed for 980 nm optical data communication. We tested devices with different cavity mode-quantum well energy detunings, following the conclusions of the photon BEC physics based on Rhodamine 6G-filled cavities. For negative detuning, we observed ground-state condensation, followed by a thermalised distribution of excited states, in agreement with the Bose-Einstein distribution. Remarkably, the photon gas thermalises to effective temperatures much lower than those of the device. We also extract the effective chemical potential from the spectrum and compare it to the theory recently developed in the ultra-fast thermalisation limit [3], which suggests the driven dissipative nature of the nonequilibrium BEC in the semiconductor resonantor. In contrast, for a positively detuned device, we observed a standard broad-area VCSEL behaviour with multimode lasing above the threshold current, with an absence of Bose-Einstein distribution. Furthermore, we discuss the issue of an accurate description of the density of states of a realistic device and the actual shape of the confining potential under different driving conditions.

Our results show a new perspective on semiconductor VCSELs, which can be used to test the nonequilibrium BEC physics in table-top room-temperature devices. Moreover, it opens the possibility to observe effective photon-photon interactions and collective superfluid phenomena in photon BECs, using the well-known ultrafast semiconductor nonlinearities, which has been impossible in rhodamine-based photon BECs limited by the slow thermo-optical nonlinearity. This would eventually link the worlds of polariton and photon superfluid physics into one device.

[1] J. Klaers et al., Nature 468, 545 (2010)
[2] S. Barland et al., Opt. Express 29, 8368 (2021)
[3] V. Y. Shishkov et al., Phys. Rev. Lett. 128, 065301 (2022)

Topologically protected interface states induced by spin-orbit coupling in liquid crystal microcavity

A. Opala[1,2], P. Oliwa[1], M. Muszyński[1], B. Piętka[1], J. Szczytko[1], M. Matuszewski[2]

[1] *Institute of Experimental Physics, Faculty of Physics, University of Warsaw, ul. Pasteura 5, PL-02-093 Warsaw, Poland*
[2] *Institute of Physics, Polish Academy of Sciences, Aleja Lotników 32/46, PL-02-668 Warsaw, Poland*

Liquid crystal optical microcavities are a novel platform for achieving adjustable synthetic Hamiltonians with Rashba-Dresselhaus spin-orbit interactions [1].

In this work, we study the topological properties of light within a one-dimensional photonic lattice featuring spin-orbit coupling. To investigate the topological properties of our system, we propose a two-band tight-binding Hamiltonian in momentum space, treating spin-orbit coupling as a perturbation. We prove that topological properties of the considered system are characterised by a winding number $\mathcal{W}$. This topological invariant counts the number of times the eigenstates wind around the origin in momentum space when the wave vector runs through the Brillouin zone, $k = 0 \rightarrow 2\pi$. Compared to the well-known Su-Schrieffer-Heeger (SSH) model of a topological insulator, our one-dimensional lattice, allows for both negative and positive values of the topological invariant. This property enables us to investigate topologically protected states at the interface between lattices with a different sign of a winding number, schematically illustrated in Figure 1. We demonstrate that this leads to qualitatively new topological interface states that are absent in the SSH model.

Our theoretical analysis provides a promising perspective for realising a new class of topological lasers based on liquid-crystal optical microcavities. Furthermore, our results can be extended to a broad range of one-dimensional topological Hamiltonians with spin-orbit coupling or internal degrees of freedom [2].

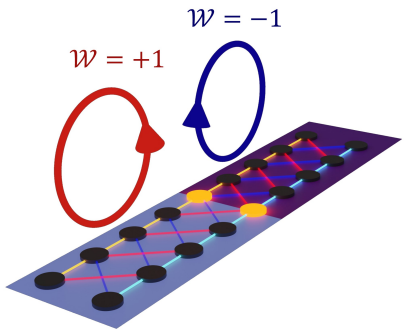

Figure 1 – Schematic illustration of a topologically protected interface state in the basis of vertical and horizontal polarization eigenstates.

[1] K. Rechcińska, M. Król, R. Mazur, P. Morawiak, R. Mirek, K. Łempicka, W. Bardyszewski, M. Matuszewski, P. Kula, W. Piecek, P. G. Lagoudakis, B. Pietka, J. Szczytko. *Science* **366**, 727-730 (2019).

[2] A. Manchon, H. C. Koo, J. Nitta, S. M. Frolov, R. A. Duine. *Nature Mater.* **14**, 871–882 (2015).

Quantum Mechanical-like Approach with Effective Hamiltonians Based on Resonant States in Optical Cavities

Przemysław Oliwa[1], Witold Bardyszewski[2], Barbara Piętka[1], and Jacek Szczytko[1]

[1] *Institute of Experimental Physics, Faculty of Physics, University of Warsaw, Pasteura 5, Warsaw, Poland*
[2] *Institute of Theoretical Physics, Faculty of Physics, University of Warsaw, Pasteura 5, Warsaw, Poland*

Optical microcavities are extensively studied in solid-state physics due to the interaction between confined photons and excitons in the active layer leading to a strong coupling regime and even a Bose-Einstein condensate. Alternatively, a cavity with birefringent and active material enables the creation of synthetic fields for photons, where light polarization acts as the spin for electrons. The interaction between orthogonally polarized modes leads to various effects of solid-state physics, including the Rashba-Dresselhaus interaction [1], merons and antimerons (Bloch and Neel skyrmions) [2], persistent spin helix [3], and annihilation of exceptional points [4]. Although the Berreman [5] and Schubert [6] transfer matrix methods are well established (though time-consuming), many researchers prefer to use a simpler 2×2 effective Hamiltonian based on ideal resonator (Fig. 1 (a)) to describe each of the aforementioned effects.

Our work introduces a method based on resonant state and perturbation theory to derive formulas for the 2×2 effective Hamiltonians for various types of cavity coupling. Firstly, we replace the standard stack of distributed Bragg reflectors with δ-mirrors (Fig. 1 (b)), and, using Green's function, we obtain a simplified formula for the electric field. We adopted the perturbation theory for Green's function to obtain the multimode Hamiltonian, which can then be further simplified to the 2×2 effective Hamiltonian (Fig. 1 (c)) via the next perturbation method, which includes interactions with other states (Fig. 1 (d)). In the last phase, we proposed a formula for polarization patterns, which is essential for their accurate determination, and relies on the rotation of basis via perturbation theory (Fig. 1 (e)). The application of a solid-state approach to solve optical problems not only simplifies calculations, but also allows better understanding of various problems like topological systems or non-hemritian physics.

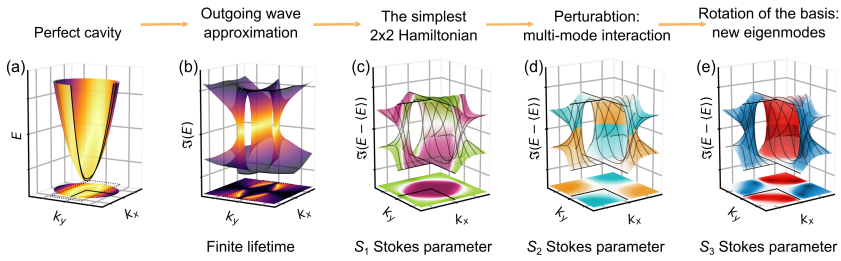

Figure 1: Schematic of the idea of presented theoretical approach. The imaginary part (i.e. finite lifetime) of polarized photons is presented.

[1] K. Rechcińska, et al. *Science* **366,** 727-730 (2019).
[2] M. Król, et al. *Optica* **8,** 255 (2021).
[3] M. Król et al. *Phys. Rev. Lett.* **127,** 190401 (2021).
[4] M. Król, et al. *Nat. Comm.* **13,** 5340 (2022).
[5] D. W. Berreman *J. Opt. Soc. Am.* **62**, 502-510 (1972).
[6] M. Schubert *Phys. Rev. B* **53**, 4265-4274 (1996).

Merons in Reciprocal Space as a Result of Photonic Spin-Orbit Interaction in Birefringent Microcavity

Maria Popławska[1], Przemysław Oliwa[1], Mateusz Król[1], Witold Bardyszewski[2], Barbara Piętka[1], Jacek Szczytko[1]

[1] *Institute of Experimental Physics, Faculty of Physics, University of Warsaw, Pasteura 5, Warsaw, Poland*
[2] *Institute of Theoretical Physics, Faculty of Physics, University of Warsaw, Pasteura 5, Warsaw, Poland*

Studies of light trapped in liquid crystal optical microcavities (LC MC) offer a possibility to observe a wide variety of quasiparticles and spin-related phenomena. In our work, we present analysis of experimental data and computational methods based on effective 2×2 Hamiltonians, that led to spotting in the system specific polarization patterns.

In this study, we investigate the microcavity filled with liquid crystal, which acts as tunable birefringent material. Different effective refractive indices for light polarized along and perpendicular to the LC anisotropy direction lead to splitting between the horizontally and vertically polarized cavity modes. Through applying external voltage to ITO electrodes across the microcavity, we were able to tilt the molecules around the chosen axis and, therefore, smoothly tune the energy of horizontal mode. For a certain value of applied voltage, we coupled two modes with orthogonal polarization and different parities, which resulted in an analog of the Rashba-Dresselhaus (RD) spin-orbit coupling [1]. We studied polarization of the cavity modes in reciprocal space at positive detuning with respect to RD resonance and observed the appearance of two points with purely circular polarization. Winding of the polarization states around those points in momentum space forms a pattern known as a meron [2,3].

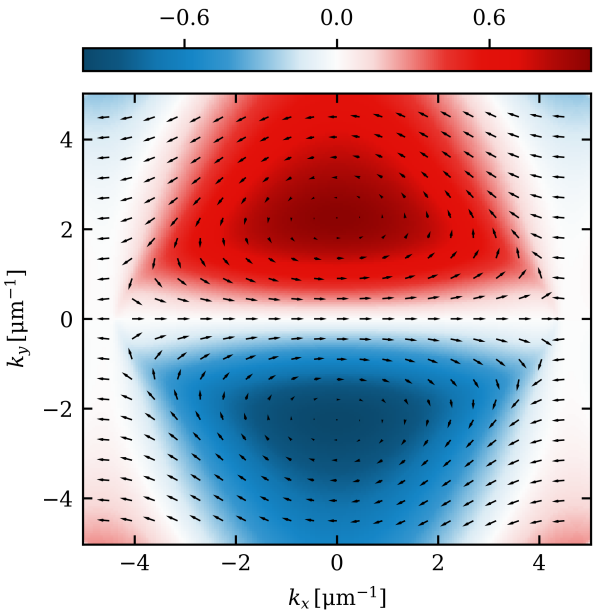

Figure 1: Theoretical results for polarization of light in momentum space calculated on resonant states in outgoing wave boundary condition for RD regime in LC MC. Parameters S_1 and S_2 are denoted as arrows $\vec{S} = [S_1, S_2]^{\mathrm{T}}$ and S_3 in a color scale.

Theoretical descriptions of these systems can be performed by well-known and highly time-consuming Berreman [4] and Schubert [5] methods, but in this work we use our simple theory, which allows us to describe these effects with satisfactory precision. Figure 1 shows the polarization structure in momentum space for the RD regime in LC MC obtained for the cavity with δ-mirrors in the outgoing wave boundary condition.

[1] K. Rechcińska et al. *Science* **366,** 727–730 (2019).
[2] C. Guo et al. *Phys. Rev. Lett.* **124,** 106103 (2020).
[3] M. Król et al. *Optica* **8,** 255–261 (2021).
[4] D. W. Berreman *J. Opt. Soc. Am.* **62,** 502–510 (1972).
[5] M. Schubert *Phys. Rev. B* **53,** 4265–4274 (1996).

Numerical Approach to Determine the Fourier Plane of Light Propagation Through Cartesian-Oval Shaped Microlenses

Zuzanna Werner, Jakub Lewandowski, Maria Popławska, Magdalena Furman, Przemysław Oliwa, Aleksander Bogucki, Łukasz Zinkiewicz, Bartłomiej Seredyński, Wojciech Pacuski, Jacek Szczytko, Barbara Piętka

Institute of Experimental Physics, Faculty of Physics, University of Warsaw, ul. Pasteura 5, Warsaw, Poland

Exciton-polaritons are quasiparticles emerging as a result of strong coupling between photons in optical microcavity and excitons confined in quantum wells. Exciton-polaritons, due to their bosonic nature, can undergo a non-equilibrium phase transition to the condensate state [1]. This process occurs as a result of the relaxation of excitons with high momentum to the minimum of the lower polariton branch. Unfortunately, the observation of the polariton relaxation processes is experimentally challenging due to the numerical aperture (NA) of the optical system that limits the observable range of in-plane momenta.

Our idea was to design a novel shape of oval microlenses with high numerical aperture that would allow for the detection of so far unavailable ranges of polariton in-plane momenta and the direct probing of the excitonic reservoir. Our idea is based on the recent realization of aspherical solid immersion microlenses that allowed to shape the light emitted form nanostructures into low-divergence beam [2]. Our design allow not only to extract high emission angles but additionally, the Fourier plane is formed into a flat surface that can be easily projected onto a planar surface of a CCD.

We considered microlenses with various sizes and shapes to optimize imaging of the reciprocal (Fourier) space. The simulations were based on geometrical optics. We started from setting three point sources of light within the cavity and propagated from them beams at a different emission angles. Fourier plane is plotted based on the positions where the beams were the closest to cross each other. Repeating the procedure for different emission angles, we could simulate the geometry of the full Fourier plane as shown in Figs. 1(a) and 1(b). We found out that Cartesian-oval shape of the microlens results in a plane which is approximately planar for a wide range of the emission angles [Fig. 1(a)]. In addition, we compared the typical dispersion relation of exciton-polaritons in planar microcavities [Fig. 1(c)] obtained by standard imaging optics composed of microscope objective of NA = 0.55 (green) with the dispersion relation that would be realized by our microlens (orange). We prove that our microlens allows to access much wider range of energies and in-plane momenta and enables the observation of excitonic reservoir.

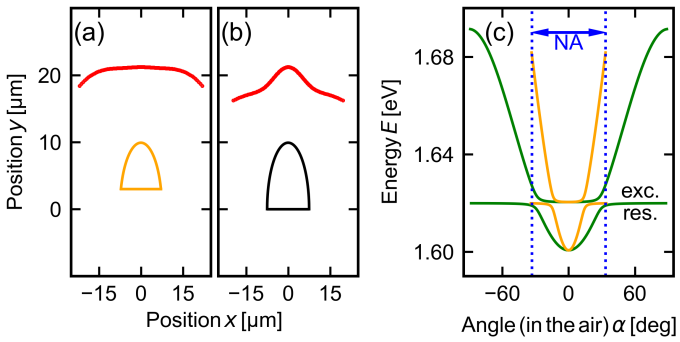

Figure 1: (a), (b) Fourier plane (red) determined for two different shapes of microlenses, (c) polariton dispersion relations obtained for the simulations of planar optical microcavity (green) and microcavity with printed microlens (orange) from (a).

[1] J. Kasprzak et al., *Nature* **443**, 409-414 (2006).
[2] A. Bogucki et al., *Light Sci. Appl.* **9**, 48 (2020).

Localization of light on defects in microcavities with built-in uniform lying helix

J. Czapiński [1], M. Muszyński [1], E. Otón [2], P. Oliwa [1], R. Mazur [2], P. Morawiak [2], W. Piecek [2], P. Kula [3], B. Piętka [1], J. Szczytko [1]

[1] *Institute of Experimental Physics, Faculty of Physics, University of Warsaw, ul. Pasteura 5, PL-02-093 Warsaw, Poland*
[2] *Institute of Applied Physics, Military University of Technology, ul. Gen. S. Kaliskiego 2, 00-908, Warsaw, Poland*
[3] *Institute of Chemistry, Military University of Technology, ul. Gen. S. Kaliskiego 2, 00-908, Warsaw, Poland*

Uniform lying helix (ULH) is a type of cholesteric liquid crystal arrangement, where the helix axis is oriented parallel to the substrate surface. The rotation of liquid crystal molecules results in the appearance of a periodic structure of refractive indices in the form of sripes (see Fig. 1). Molecules in each stripe are aligned parallel to each other, In our study, we placed such a structure inside a 3 micron optical microcavity made of two distributed Bragg reflectors (DBR), fabricated by the method of vapor deposition out of six-pairs of SiO_2 and TiO_2 grown on transparent Indium tin oxide electrodes. The center of the stop band of the DBRs was 530 nm.

The periodic modulation of refractive index of the ULH is responsible for the formation of photonic bands, similar to bands formed in a 1D photonic crystal. The introduced bandgaps are of around *40* meV, depending on period of the stripes, which slightly varied across the sample.

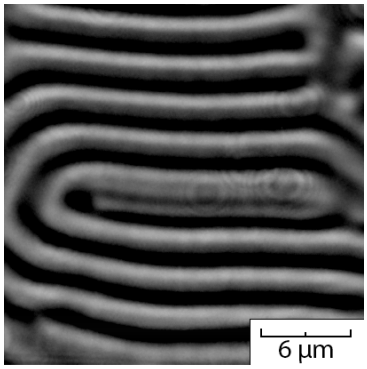

Figure 1. A defected state of ULH. The pitch of the stripe in the middle of the spiral is smaller than the pitch of the surrounding ULH.

In the study we focused mainly on on certain imperfections in the ULH periodicity, where the helix wound up on itself (see Fig. 1.) forming an elongated spiral. The optical defect state inside of this spiral was found to have a different energy compared to the regular ULH around it. We performed statistical analysis to determine a correlation between the energy of the optical defect state and its size. It was found that if the pitch of the defect was smaller than the pitch of the regular ULH, the energy of the defect state lay inside the energy bandgap generated by the regular ULH. If the helix pitch inside the spiral was bigger, the defect's energy lied beneath the minimum energy of ULH state.

By applying the electric field to electrodes built-inside the cavity we found that the pitches, as well as energy states of the optical defect and the regular ULH structure were tunable up to 3V of external voltage, above that level, the structure deteriorated into a nematic and periodic structure disappeared. The presented work introduces a new, interesting system, where the 1D photonic crystal can be controlled and tuned by external electric field.

Self-organizing photonic potential with tunable band structures coupled by spin-orbit interaction in birefringent optical cavity

M. Muszyński[1], P. Oliwa[1], E. Oton[2], R. Mazur[2], P. Morawiak[2], W. Piecek[2], P. Kula[3], B. Piętka[1], J. Szczytko[1]

[1] *Institute of Experimental Physics, Faculty of Physics, University of Warsaw, ul. Pasteura 5, PL-02-093 Warsaw, Poland*
[2] *Institute of Applied Physics, Military University of Technology, ul. Gen. S. Kaliskiego 2, 00-908, Warsaw, Poland*
[3] *Institute of Chemistry, Military University of Technology, ul. Gen. S. Kaliskiego 2, 00-908, Warsaw, Poland*

Photonic crystals with optical anisotropy possess degrees of freedom related to the polarization of light and specified directions allowed by dispersion. The coupling of photonic modes of different parity – which is possible due to birefringence – may introduce chirality [1]. If an additional periodic potential is present, the resulting photonic band gaps and eigenstates of light inherit the polazation properties of the whole system [2].

Here, we demonstrate a dye-doped optical microcavity with a built-in uniform lying helix (ULH) structure that was induced in a chiral nematic liquid crystal matrix. As a result of the presence of ULH, a one-dimensional self-organized periodic lattice of refractive index modulation was formed. We observed two separate photonic band structures with orthogonal linear polarizations of light (Figures a, b). The inclination of the helix with respect to the plane of the cavity additionally induced a Rashba-Dresselhaus spin-orbit interaction for light, which couples these two bands together. As a result of the spin-orbit coupling, new chiral states with distinct circular polarizations are formed (Figure c).

The proposed platform has several unique technological advantages. A self-assembled one-dimensional well-oriented photonic potential is formed over a macroscopic area. The period of ULH can be tuned by external electric field, thickness of the cavity and temperature. In addition, due to doping the structure with light emitters, the system can exhibit non-linear effects like the laser light emission from photonic bands, which opens new possibilities for the photonic control of light-emitting devices.

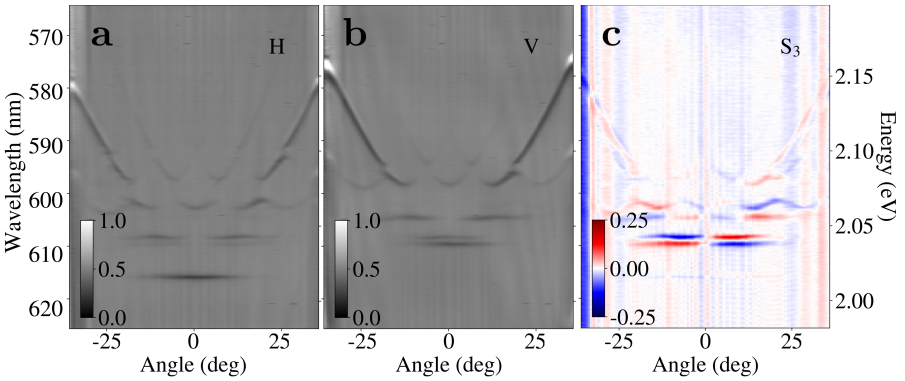

Figure 1 – Dispersion relation measured for the orthogonal linear (a) horizontal H and (b) vertical V polarization of the detected light. (c) The Stokes parameter S_3 shows circularly polarized states of light caused by Rashba-Dresselhaus spin-orbit coupling.

[1] K. Rechcińska, et al. *Science* **366**, 727-730 (2019).
[2] M. Muszyński, et al. "Band structures coupled by spin-orbit interaction in self-assembled photonic lattice in liquid crystal optical microcavities" (Manuscript in preparation)

Flow of an exciton-polariton condensate in optical microcavities with the natural structural disorder

S. Świerczewski[1], R. Mirek[1], M. Król[1], M. Furman[1], M. Matuszewski[2], A. Opala[1,2], J. Szczytko[1], B. Piętka[1]

[1] *Institute of Experimental Physics, Faculty of Physics, University of Warsaw, ul. Pasteura 5, PL-02-093 Warsaw, Poland*
[2] *Institute of Physics, Polish Academy of Sciences, Aleja Lotników 32/46, PL-02-668 Warsaw, Poland*

Exciton-polaritons are coherent quasiparticles that emerge from the strong interaction between cavity photons and quantum well excitons in semiconductor microcavities. The hybrid nature of these quasiparticles leads to strong nonlinear interparticle interactions and excellent transport properties. Recently, experimental studies have reported the observation of nontrivial dynamical effects in microcavities with a structural disorder, including relaxation oscillations and the generation of nonlinear waves [1]. The observed effects may be used in optical information processing in the future. Nevertheless, the precise control of polariton flow in a microcavity with inhomogeneous potential is still challenging.

Here, we investigate the formation of exciton-polariton condensate currents in a microcavity with a built-in structural disorder Fig. 1 a). We focus on forming polariton condensates under nonresonant excitation in an asymmetric potential trap. We demonstrate that the flow and counterflow of condensates inside a double quantum well can be precisely controlled by the intensity of laser sources acting on each potential minimum Fig. 1 b). This control is made possible by the optical anti-trapping potential created by an incoherent excitonic reservoir. Our theoretical model is based on the generalized open-dissipative Gross-Pitaevskii equation coupled with the exciton-polariton reservoir of excitons and hot carriers. Our analysis accurately reproduces the experimental results and provides insights into the fully optical, precise control of exciton-polariton networks. Our study can be helpful in the development of novel optoelectronic devices based on exciton-polaritons.

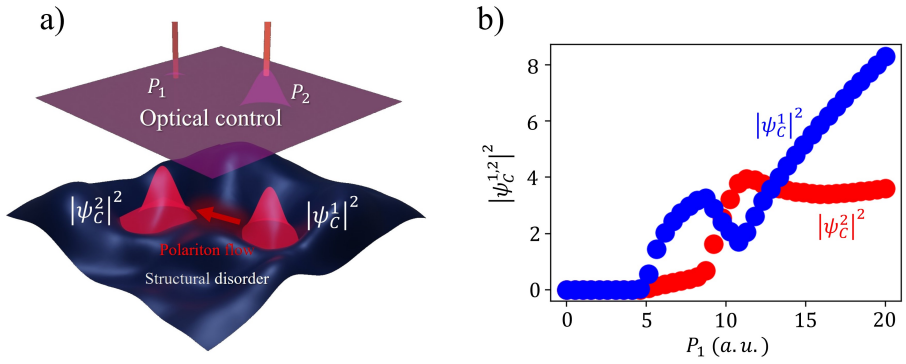

Fig. 1 – Optically controlled polariton condensate flow between two potential minima occurring due to natural structural disorder a). Emission intensity from simultaneously excited condensation sites when P_2 is constant b).

[1] M. Pieczarka, M. Syperek, Ł. Dusanowski, et al., *Sci Rep* **7**, 7094 (2017).

Experimental Evaluation of the Indistinguishability of Single Photons at 1.55 µm Generated by InAs(P)/InP Quantum Dots

D. A. Vajner [1], M. Wasiluk [2], P. Holewa [2,3,4], E. Zięba-Ostój [2], B. Gaál [3], A. Sakanas [3], B. Krajnik [2], M. Xiong [3,4], K. Yvind [3,4], N. Gregersen [3], M. Syperek [2], E. Semenova [3,4], A. Musiał [2], T. Heindel [1]

[1] *Institute of Solid State Physics, Technical University of Berlin, 10623 Berlin, Germany*
[2] *Laboratory for Optical Spectroscopy of Nanostructures, Department of Experimental Physics, Wrocław University of Science and Technology, 50-370 Wrocław, Poland*
[3] *DTU Electro, Technical University of Denmark, 2800 Kongens Lyngby, Denmark*
[4] *NanoPhoton-Center for Nanophotonics, Technical University of Denmark, 2800 Kongens Lyngby, Denmark*

Epitaxial quantum dots (QDs) have great potential as non-classical light sources in quantum technologies [1,2]. For advanced quantum cryptographic key exchange algorithms, single indistinguishable photons, generated on demand, are needed [3]. An appealing technology platform in this context are QDs emitting at 1.55 µm, showing prospects for long-haul low-loss optical transmission in a standard silica fiber [4,5].

In this contribution we investigate quantum optical properties of single photons emitted by InAs(P)/InP QDs heterogeneously integrated with silicon. The QDs are grown by metalorganic vapor-phase epitaxy in the Stranski-Krastanow mode and exhibit low areal density (3.1×10^8 cm^2) and emission at ~1.55 µm [6]. A metallic mirror beneath the QDs increases photon extraction efficiency to about 10% [7]. It enables imaging of the QD emission, letting localize a specific QD with ~50 nm accuracy, allowing for engineering of QD photonic environment.

In our study, we confirm single-photon emission from the QDs via measurements of the second-order autocorrelation function $g^{(2)}(\tau)$, revealing $g^{(2)}(0) = (3.2 \pm 0.6) \times 10^{-3}$ under quasi-resonant pulsed excitation. To investigate the degree of indistinguishability of emitted photons and gain insight into underlying dephasing mechanisms, Hong-Ou-Mandel-type two-photon interference (TPI) experiments are conducted as a function of the temporal delay δt between consecutively emitted photons. The TPI visibility, quantifying the degree of indistinguishability, was comparatively analyzed using both, integration of the raw experimental data and applying a fitting model, revealing the raw (i.e. 'as measured') and the post-selected TPI visibility. For $\delta t = 4$ ns, we determine the visibility by evaluating the coincidences around $\tau = 0$ for co- and cross-polarized photons and compare the result with the method based on evaluating the areas of adjacent coincidence maxima in a characteristic five-peak pattern [8]. We obtain raw (post-selected) TPI visibilities of up to 20% (99%) and comparatively discuss the experimental uncertainties.

In summary, our work provides important insights and shows progress in generating telecom C-band single indistinguishable photons for applications in quantum information technologies.

[1] X. Zhou, L. Zhai, and J. Liu, *Photon. Insights* **1**, 2 R07 (2023).
[2] P. Michler, Quantum Dots for Quantum Information Technologies Vol. 237, Springer (2017).
[3] D. A. Vajner, L. Rickert, T. Gao *et al.*, *Adv. Quantum Technol*. **5**, 2100116 (2022)
[4] Y. Arakawa and M. J. Holmes, *Appl. Phys. Rev.* **7**, 021309 (2020).
[5] M. Benyoucef and A. Musiał, Chapter 18 in Photonic Quantum Technologies: Science and Applications, in press, WILEY-VCH GmbH (2023).
[6] P. Holewa, M. Gawełczyk, C. Ciostek, *et al.*, *Phys. Rev. B* **101**, 195304 (2020).
[7] P. Holewa, A. Sakanas, U. M. Gür *et al.*, *ACS Photonics* **9**, 7, 2273–2279 (2022).
[8] A. Thoma, P. Schnauber, M. Gschrey, *et al.*, *Phys. Rev. Lett.* **116**, 033601 (2016).

Magneto-Optical Properties of Single Symmetric InAs/InP Quantum Dots Emitting in the Telecom C-band

Maja Wasiluk [1], Anna Musiał [1], Marek Burakowski [1], Johann P. Reithmaier [2], Mohamed Benyoucef [2], Wojciech Rudno-Rudziński [1]

[1] *Laboratory for Optical Spectroscopy of Nanostructures, Department of Experimental Physics, Wrocław University of Science and Technology, Wybrzeże Wyspiańskiego 27, 50-370, Wrocław, Poland*
[2] *Institute of Nanostructure Technologies and Analytics, CINSaT, University of Kassel, Heinrich-Plett-Str. 40, 34132 Kassel, Germany*

Self-assembled epitaxial semiconductor quantum dots (QDs) have been the subject of study due to both – their interesting fundamental properties and potential practical applications. Discrete atom-like energy structure makes them ideal as an active region for non-classical light sources, e.g., single photon sources or sources of polarization entangled photon pairs [1, 2]. The latter require high in-plane symmetry of the nanostructure and/or external tuning to minimize the exciton fine structure splitting. Such sources can be utilized in quantum communication, e.g., to exchange cryptographic key or as building blocks of quantum networks, in particular, quantum repeater architectures. In this case, emission in the telecommunication windows, compatible with existing optical fiber infrastructure, is needed. QDs have also potential in spintronic applications, where individual spins of electrons and holes confined in the dots are used to store information (quantum memory) or as an active part of switching devices depending on the carrier g-factor. In this case, spin coherence properties are of interest.

Magneto-optical polarization-resolved measurements in Faraday and Voigt configurations enable to understand the nature of excitonic complexes in QDs. In particular, extension of the wave function can be deduced from the diamagnetic coefficient, g-factor of carriers/excitonic complexes can be determined based on the Zeeman splitting allowing also for observation of the fine structure of excitonic complexes and identification of emission lines in the single QD spectrum as originating from certain carrier configurations [3]. Finally, spin coherence time can be determined based on depolarization (Hanle) curve obtained with quasi-resonant excitation with circularly polarized laser beam [4].

In this study, we determine experimentally the fundamental magneto-optical properties of the new generation of symmetric, and low-density (2×10^9 cm^{-2}) InAs/InP QDs grown by ripening process-assisted molecular beam epitaxy [5]. These QDs fulfill the requirement of telecom spectral range emission (1.55 μm). Photon extraction efficiency was enhanced by growing the QDs on top of a distributed Bragg reflector, resulting in 6.8% photon extraction efficiency for planar sample [6] and 13.3% for QDs in cylindrical mesas [7]. High single-photon purity ($g^{(2)}(0) < 0.01$) [8] and low fine structure splitting makes them promising candidates for generating non-classical light.

[1] Y. Arakawa and M. Holmes, *Appl. Phys. Rev.* **7**, 021309 (2020).
[2] X. Zhou, L. Zhai, and J. Liu, *Photon. Insights* **1**, 2 R07 (2023).
[3] W. Rudno-Rudziński, M. Burakowski, J. P. Reithmaier *et al.*, *Materials* **14**, 942 (2021).
[4] Y. Masumoto, S. Oguchi, B. Pal, and M. Ikezawa, *Phys. Rev. B* **74**, 205332 (2006).
[5] A. Kors, J. P. Reithmaier, and M. Benyoucef, *Appl. Phys. Lett*. **112**, 172102 (2018).
[6] T. Smołka, K. Posmyk, M. Wasiluk *et al.*, *Materials* **14**, 6270 (2021).
[7] A. Musiał, M. Mikulicz, P. Mrowiński *et al.*, *Appl. Phys. Lett.* **118**, 221101 (2021).
[8] A. Musiał, P. Holewa, P. Wyborski *et al.*, *Adv. Quantum Technol.* **3**, 1900082 (2020).

Optimization of on-chip photonic structures for a hybrid InP/Si platform via deep learning approach

Paweł Mrowiński[1], **Grzegorz Sęk**[1], **Marcin Syperek**[1]

[1] *OSN Laboratory, Department of Experimental Physics, Wrocław University of Science and Technology, Wybrzeże Wyspiańskiego 27, 50-370 Wrocław, Poland*

The range of desired on-chip photonic components performing particular tasks in integrated circuits based on a single material platform like silicon-on-insulator is broad and often infeasible when it contains a well-defined quantum emitter. However, a heterogeneous integration with other platforms offers to merge both utilities, those which are well known in silicon platform and those which offer efficient light sources at telecom wavelengths. We aim to study numerically the photonic structures realized in InP/Si combined systems such as a ridge waveguide nanobeam cavity, ring resonator, directional coupler, and multimode interference (MMI) beam splitter as vital components for future quantum-integrated photonic chips. We used finite-difference time-domain (FDTD) commercial software to study the photonic device's performance in a broad spectral range within a single-shot simulation. First, we study a ring resonator which can be used as an interference filter for the propagation along the waveguide resulting in a free spectral range of ~50 nm and finesse of 20. Such high performance is found using a specific taper system near the ring structure. Next, using a grating structure design of nanoholes along an InP waveguide, we designed various systems that can enhance the dipole emission by a Purcell factor of 25 and 75 % of bidirectional transmission using only 7 periods of the grating design. It also allows a directional enhanced emission for asymmetric configuration of 10/5 periods resulting in a Purcell factor of 14 and 90 % of transmission within a 5-nm-wide spectral window. Then, we optimized the directional coupler and MMI beam splitter to get the highest transmission and a splitting ratio close to 50 %. Both geometries require specific tapering along the propagation direction for efficient light transfer.

Last, we realized an optimization algorithm for a 1D nanobeam cavity based on deep learning (neural network) [1,2,3] to achieve the optimized transmission along the waveguide from a single dipole source at 1.55 μm photon wavelength. In this step, we used inversed, fully-connected network with 3 hidden layers, which can learn from our 3D FDTD results. The trained network can predict the exact geometry of a photonic system based on spectral data, which serves as an input set of parameters to maximize the device's performance.

[1] Tahersima, M. H., Kojima, K., Koike-Akino, T., Jha, D., Wang, B., Lin, C., & Parsons, K. (2019) *Scientific Reports*, *9*(1), 1368. 10.1038/s41598-018-37952-2.
[2] T. Asano and S. Noda, Opt. Express 26, 32704 (2018) 10.1364/OE.26.032704.
[3] Z. Liu, D. Zhu, L. Raju, and W. Cai, Adv. Sci. 8, 2002923 (2021) 10.1002/advs.202002923.

Optical Characteristics of Monolithic High-Contrast Gratings for Quantum-Dot Vertical-Cavity Surface-Emitting Lasers at 940 nm.

Bartosz Kamiński[1], Jakub Boniecki[1], Mikołaj Janczak[3], Niels Heermeier[2], Floriana Laudani[2], Sven Rodt[2], Stephan Reitzenstein[2], Marcin Gębski[3], Tomasz Czyszanowski[3], Grzegorz Sęk[1] and Anna Musiał[1]

[1] *Laboratory for Optical Spectroscopy of Nanostructures, Department of Experimental Physics, Wrocław University of Science and Technology, Wybrzeże Wyspiańskiego 27, 50-370 Wrocław, Poland*
[2] *Institute of Solid State Physics, Technical University of Berlin, Hardenbergstraße 36, D-10623 Berlin, Germany*
[3] *Photonics Group, Institute of Physics, Łódź University of Technology, ul. Żeromskiego 116, 90-924 Łódź, Poland*

Vertical-cavity surface-emitting lasers (VCSELs) have a wide range of unique properties that distinguish them from conventional semiconductor lasers [1]. However, they still face some challenges, for instance, they require innovations in reduction of the thickness of the cavity mirrors which are typically distributed Bragg reflectors (DBRs). Monolithic high-index contrast gratings (MHCGs) are a very attractive alternative for DBRs as well as externally-fabricated high-contrast gratings (HCGs). MHCGs has been already proven as efficient mirrors for VCSELs [2-5]. They bring unprecedented simplification of the device designs and offer flexibility in the material choice, opening new prospects for realization of VCSELs emitting at wavelengths hardly achievable in the past. MHCGs are able to reflect light, as well as can classical subwavelength HCGs, but without the requirement to be sandwiched between low-refractive-index layers [6].

In contrast to standard DBRs, the MHCG enables resonant wavelength setting of every laser in the on-chip array separately, by design of MHCG geometrical parameters. As a result, the MHCG VCSELs array chip can be fabricated in a cost-efficient way on a single wafer, reducing greatly the costs of production and device footprint.

In this work, we characterize optically MHCGs with different geometries by performing microreflectance measurements. Gratings design has been numerically optimized for high reflectivity (> 90%) in the 930-955 nm spectral range required for VCSELs in the optical water vapour detection systems. To achieve this, the grating period, filling factor and trench depth were varied. Three sets of gratings differing in etching depth have been fabricated by means of electron-beam lithography on a double-polished GaAs substrate. Within each set filling factor and trench width was varied to cover theoretically predicted high reflectivity area. The experimental characteristics are compared with numerical results to provide feedback for both fabrication and modelling. Obtained results are an important step in development of QD VCSELs with MHCGs as a top mirror.

This work is supported by the Investitionsbank Berlin and the Polish National Centre for Research and Development within the scope of project „QD-Sense: Cost-efficient gas sensing system based on wavelength tunable quantum-dot VCSEL arrays with nanogratings“.

[1] K. Iga, Jpn. J. Appl. Phys. **47**, 1 (2008).
[2] S. Kim , et al., ACS Photonics **6**, 18-22 (2019).
[3] M. Gębski, J. A. Lott, and T. Czyszanowski, Opt. Express **27**, 7139-7146 (2019).
[4] T-C. Chang, et al., ACS Photonics **7**, 861-866 (2020).
[5] T. Czyszanowski, et al., Nanophotonics **9**, 913-925 (2020).
[6] M. Dems, J. Light. Technol. **35**, 159-165 (2016).

Methods for Determining High Finesse in Open Cavity Systems

P. Kulboka[1], N. Dalla[1], T. Kazimierczuk[1] , P. Kossacki[1] and T. Jakubczyk[1]

[1]*University of Warsaw, Ludwika Pasteura 5, Warsaw, 02-093, Poland*

Open microcavities enhance the interaction of light and quantum emitters, which is used to obtain bright sources of indistinguishable on-demand single photons [1] and is expected to enable advanced measurements of emmiters' coherent and noncoherent dynamics [2]. Microcavities with low internal optical losses, characterized by several thousand and higher finesse factors, are of particular interest. Measuring such high finesse values is an experimental challenge that can be approached in several ways.

Traditionally, finesse is defined as $F = FSR/\delta\nu$ [3], where FSR (Free Spectral Range) is the frequency spacing to the next longitudinal mode, and $\delta\nu$ is the resonance linewidth. However, this definition is hard to use for high-finesse microcavities based on distributed Bragg reflectors (DBRs) as the FSR can be comparable to, or even larger, than the stopband of the DBR structure. Additionally, measuring the resonance linewidth requires very high mechanical stability of the cavity.

To overcome the challenges mentioned above, a dynamic setup[4] can be used in which the length of the cavity changes periodically in time, minimizing the influence of acoustic noise. In addition, this allows finesse measurements to be performed using single or multiple light wavelengths, and resonances are observed as the length of the cavity changes.

In this work, we applied several methods for determining high finesse values in a planar-concave open cavity system. We discuss the advantages and limitations of each method and compare the results.

[1] S. Flågan, D. Riedel, A. Javadi, T. Jakubczyk, P. Maletinsky, and R. J. Warburton, *J Appl Phys*, vol. **131**, no. 11 (2022).
[2] C. L. Smallwood, R. Ulbricht, M. W. Day, T. Schröder, K. M. Bates, T. M. Autry, G. Diederich, E. Bielejec, M. E. Siemens, and S. T. Cundiff, *Phys. Rev. Lett*. **126**, 213601 (2021).
[3] W. 'Nagourney, *Quantum Electronics for Atomic Physics*. Oxford University Press (2010).
[4] L. Greuter *et al.*, *Appl Phys Lett*, vol. **105**, no. 12 (2014)

Reflectivity spectra of GaAs/AlAs Distributed Bragg Reflector in the MIR Calculated by the Transfer Matrix Method

Helena Janowska[1], Agata Zielińska[1], Anna Musiał[1] and Grzegorz Sęk[1]

[1] *Department of Experimental Physics, Wrocław University of Science and Technology, Wybrzeże Wyspiańskiego 27, 50-370 Wrocław, Poland*

Photonic structures play an important role in tailoring the emission properties according to the requirements of a specific application. There are applications demanding vertically emitting lasers operating in mid-infrared (MIR), as e.g., some of the optical gas sensing schemes. In that context distributed Bragg reflectors (DBRs) are typically used. The DBRs constitute of many pairs of alternating layers of two high-refractive-index contrast dielectric/semiconductor materials, which in epitaxial structures need to be lattice matched to the substrate to avoid strain accumulation. For this purpose it has been proposed a standard and technologically mature material - GaAs/AlAs. It is technologically demanding as the DBR need to be much thicker than for the shorter wavelengths resulting in longer growth process during which precise control of layer thicknesses needs to be maintained. In this case, only the thickness of each layer needs to be up-scaled for the longer wavelengths.

Our work aims at calculating reflectivity spectra of DBR structures designed for the MIR range by employing the transfer matrix method. The structure contains GaAs/AlAs DBR. The transfer matrix method is based on considering the amplitudes of electric field during the propagation of an electromagnetic wave through the structure and includes propagation within a material of a given refractive index and thickness, as well as reflection and transmission at each of the interfaces. By using the common notation, the light propagation in the whole structure can be represented by a 2D array called a transfer matrix [1-4]. The method was implemented in Python and used to calculate the reflectivity spectra of the DBR. Through such simulation, we are able to match the values of thicknesses of layers and types of materials of such a structure before fabrication in order to optimize its design. This is a crucial contribution to the self-consistent design-fabrication-measurement of optical properties loop and allows for broad range parameter study to understand the sensitivity of the reflectivity spectrum on the structural parameters.

[1] A. Zielińska et al., *Optics Express* **30**, 20225 (2022).
[2] M. Pieczarka, *Badania kondensatów polarytonów ekscytonowych w półprzewodnikowych mikrownękach optycznych z wbudowanym nieporządkiem*, PhD thesis, Wrocław (2017).
[3] A. V. Kavokin et al., *Microcavities,* Oxford University Press (2007).
[4] M. A. Muriel and A. Carballar, *IEEE Photonics Technology Letters* **9**, 955 (1997).

Optimization of the polarization state of an ensemble of quantum dots for chiral emission

J. Rosiński[1], M. Gawełczyk[1], K. Tarnowski[2], P. Karwat[3], D. Wigger[3], and P. Machnikowski[1]

[1]*Institute of Theoretical Physics, Wrocław University of Science and Technology, Wrocław, 50-370, Poland*
[2]*Department of Optics and Photonicss, Wrocław University of Science and Technology, Wrocław, 50-370, Poland*
[3]*School of Physics, Trinity College Dublin, Dublin 2, Ireland*

Controlling the interaction of light and matter is the basis for many applications ranging from light technology to quantum information processing, many of which are based on nanophotonic structures. The confinement of light in such nanostructures imposes an inherent link between its local polarization and its propagation direction, known as spin-momentum locking of light [1]. This modifies the elementary processes of light-matter interaction: the emission and absorption of light of an appropriately polarized emitter becomes chiral, i.e., propagation direction-dependent. Placing a solid-state quantum emitter in a photonic crystal waveguide is promising for future applications because a very high fraction of the generated light can be injected into the waveguide guided mode [2]. Here, we focus on maximizing the directionality of chiral light emission from a quantum dots (QDs) placed within half core region of the photonic waveguide, as quantified by the fraction D of light emitted in the desired direction.

Most research so far has focused on placing the single emitter with circularly polarized transitions at a point of perfect circular polarization (a C point). These points are scarce. The photonic crystal structures support circular polarization at a few accessible locations, resulting in small area with high directional contrast D_{90} (top left panel in Fig. 1). That would require a precise embedding of QD in a waveguiding structure. To avoid this deposition requirement we consider ensemble of quantum dots and calculete net directionality. We find an optimal elliptical polarization of the QD transition dipole that maximizes the net directionality of the whole planar QD ensemble. We also calculate the Purcell factor and determine the area where $|D| \geq 0.9$ to explore the advantage of optimized elliptical polarization with respect to circular one. It is noticeable that optimizing the elliptical polarization state broadens the area of the waveguide core that may be used for unidirectional coupling with a single quantum emitter, while maintaining a high Purcell factor. We also perform $\mathbf{k} \cdot \mathbf{p}$ calculations to find geometrical parameters of the QD leading to the optimized polarization of the emission. This proves that optimal polarization is feasible if a small magnetic field of 0.2 T is applied.

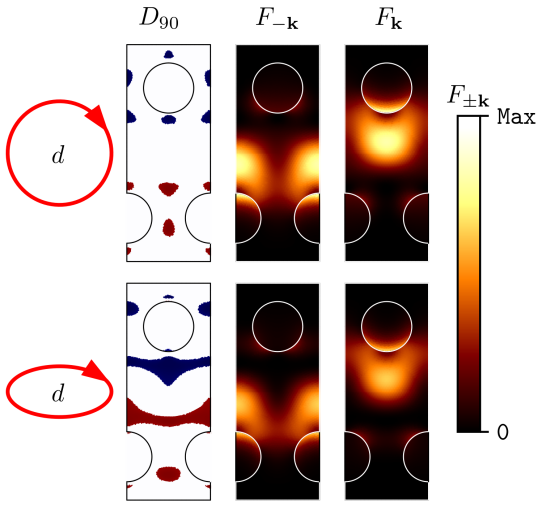

Figure 1: *The Purcell enhancement factor (right) and area where $|D| \geq 0.9$ (left) for an optimized elliptical polarization state (bottom) compared to the circular one (top) as a reference.*

[1] K. Bliokh et al., *Nat. Photonics* **9**, 796–808 (2015).
[2] A. Javad et al., *J. Opt. Soc. B* **35**, 514–522 (2018).

Controlled coherent coupling in a quantum dot molecule measured with nonlinear spectroscopy

D. Wigger[a,b], J. Schall[c], M. Deconinck[c], N. Bart[d], P. Mrowiński[a], M. Krzykowski[a], K. Gawarecki[a], M. von Helversen[c], R. Schmidt[c], L. Bremer[c], F. Bopp[e], D. Reuter[f], A. D. Wieck[d], S. Rodt[c], J. Renard[g], G. Nogues[g], A. Ludwig[d], P. Machnikowski[a], J. J. Finley[e], S. Reitzenstein[c], and J. Kasprzak[e,g]

[a] Institute of Theoretical Physics, Wrocław University of Science and Technology, 50-370 Wrocław, Poland, Poland
[b] School of Physics, Trinity College Dublin, Dublin 2, Ireland
[c] Institute of Solid State Physics, Technische Universität Berlin, 10623 Berlin, Germany
[d]Lehrstuhl für Angewandte Festkörperphysik Ruhr-Universität Bochum, Germany
[e] Walter Schottky Institut, TU München, 85748 Garching, Germany
[f] Department Physik, Universität Paderborn, 33098 Paderborn, Germany
[g] Univ. Grenoble Alpes, CNRS, Grenoble INP, Institut Néel, 38000 Grenoble, France

Semiconductor quantum dot molecules are considered as promising candidates for quantum technological applications due to their wide tunability of optical properties and coverage of different energy scales associated with charge and spin physics. While previous works have studied the tunnel-coupling of the different excitonic charge complexes shared by the two quantum dots by conventional optical spectroscopy, we here report on the first demonstration of a coherently controlled inter-dot tunnel-coupling focusing on the quantum coherence of the optically active trion transitions. We employ ultrafast four-wave mixing spectroscopy to resonantly generate a quantum coherence in one trion complex, transfer it to and probe it in another trion configuration. With the help of theoretical modelling on different levels of complexity we give an instructive explanation of the underlying coupling mechanism and dynamical processes.

Diffusion of quantum well excitons measured with nonlinear spectroscopy

K. Połczyńska[a], M. Raczyński[a], Z. Śnioch[a], G. Nogues[b], W. Langbein[c], W. Pacuski[a], P. Kossacki[a], J. Kasprzak[b]

[a] *Faculty of Physics, University of Warsaw, ul. Pasteura 5, 02-093 Warszawa, Poland*
[b] *Univ. Grenoble Alpes, CNRS, Grenoble INP, Institut Néel, 38000 Grenoble, France*
[c] *School of Physics and Astronomy, Cardiff University, The Parade Cardiff, UK*

Optical spectra of semiconductors display narrow resonances below the absorption edge, which are attributed to the excitons, i.e. pairs of electrons and holes, bound by the Coulomb interaction. We here perform coherent nonlinear spectroscopy of excitons in epitaxially grown CdTe-based quantum wells. By performing heterodyne four-wave mixing (FWM) microscopy, we find that the exciton absorption is dominated by homogeneous broadening on areas exceeding a few hundred microns squared. The photon-echo sequence of the FWM reveals no traces of the inhomogeneous broadening, indicating that excitons experience no localization due to the microscopic potential fluctuations. Under such conditions, the excitons with a large in-plane momentum of their center of mass (out of the light cone), can freely roam across the quantum well. After reaching mesoscopic distances, within 10 μm range, they can relax back to the radiative cone and recombine radiatively. In these novel experiments, we take advantage of the microscopic configuration of the FWM to probe the diffusion of the exciton density and coherence. This is achieved by measuring FWM as function of the spatial separation between pumps, inducing density or coherence of the excitons, respectively, and the probe converting them into the FWM. An extra care is taken to distinguish between FWM originating from diffusive excitons, i.e. those traveling between the pump and the probe, and the FWM signal created directly by the scattered light impinging the probe. This proof-of-principle experiment demonstrates that heterodyne FWM can be employed to infer propagative effects of excitons in semiconductor nanostructures.

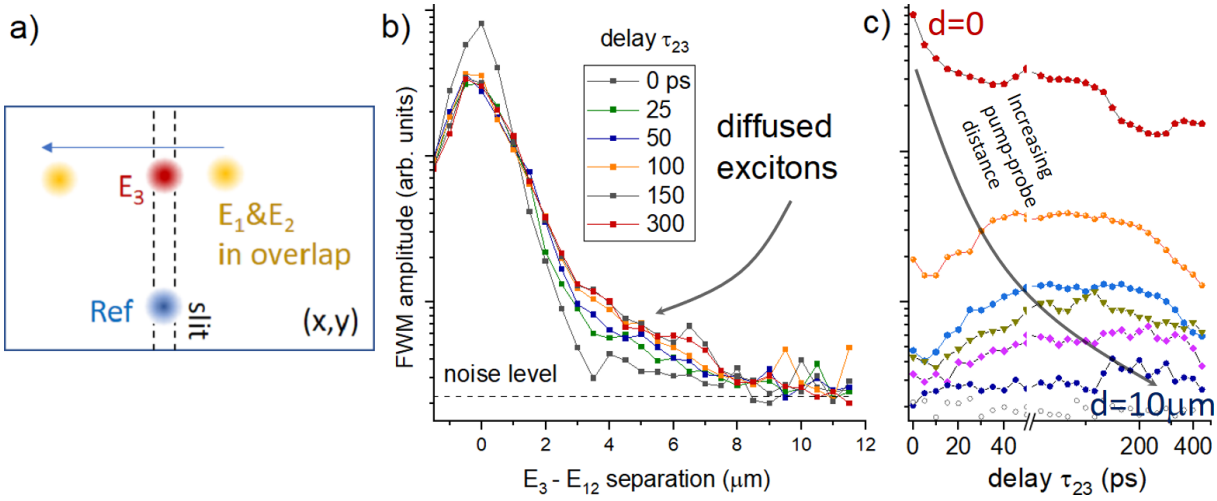

Figure 1: a) A geometry of the spatially-resolved FWM experiment, FWM generated at the probe position E_3, is detected via heterodyne spectral interference with the reference Ref. b) build up of the exiton diffusion with increasing the delay τ_{23}, c) signatures of the diffusive excitons in the delay dependence: with increasing the pump-probe the maximum of the FWM shifts to larger delays τ_{23}

Coherent imaging and dynamics of exciton complexes in $MoSe_2$ monolayers epitaxially grown on a hexagonal boron nitride

Karolina E. Połczyńska[1], Simon L. Denmat[2], Takashi Taniguchi[3], Kenji Watanabe[3], Marek Potemski[1,4], Piotr Kossacki[1], Wojciech Pacuski[1] and Jacek Kasprzak[1,2]

[1] *Faculty of Physics, University of Warsaw, ul. Pasteura 5, 02-093 Warsaw, Poland*
[2] *Univ. Grenoble Alpes, CNRS, Grenoble INP, Institut Néel, 25 rue des Martyrs, 38000 Grenoble, France*
[3] *International Center for Materials Nanoarchitectonics, National Institute for Materials Science, 1-1 Namiki, Tsukuba 305-0044, Japan*
[4] *Laboratoire National des Champs Magnétiques Intenses, CNRS-UGA-UPS-INSA-EMFL, 25 Av. des Martyrs, 38042 Grenoble, France*

Technology of preparing heterostructures made of semiconducting transition metal dichalcogenides (TMDs) is based on exfoliation of thin films from van der Waals bulk crystals. While the nonscalability of the exfoliation top-down approach is not an issue in the fundamental research, for which the proof-of-principle demonstrations are essential, it is a major roadblock on the academia-industry pathway of this field. In order to merge these novel materials with the semiconductor microelectronics, strainfree monolayer samples homogeneously covering wafers of a few inch diameter are required.

Here we present studies of $MoSe_2$ grown by molecular beam epitaxy on the silicon substrate with exfoliated hBN flakes. We performed four-wave-mixing (FWM) imaging and spatially correlated the obtained amplitude of the nonlinear optical response of the studied flakes with the layer thickness obtained from AFM measurements as shown in the fig. 1. It allowed us to precisely characterise the signal originating from the epitaxially-grown monolayers with respect to the surface morphology. Furthermore, by measuring the FWM signal in the temporal domain we were able to determine the dephasing dynamics of exciton complexes and ascertained its temperature dependence.

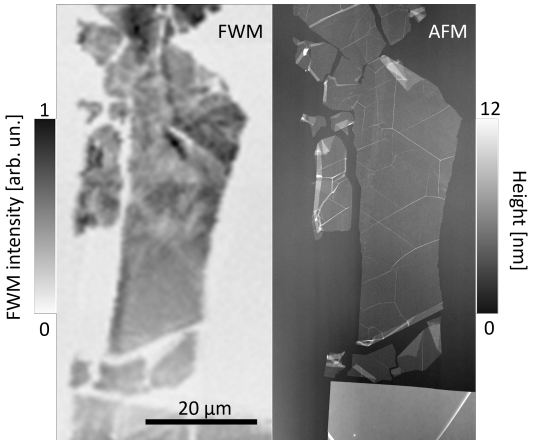

Figure 1: Epitaxial $MoSe_2$ monolayer grown on hBN flake at the SiO_2 on the silicon substrate. FWM imaging in comparison to AFM amplitude.

Our results show that these epitaxial monolayers, while opening the prospect of being compatible with the semiconductor optoelectronics industry, display excellent optical response, providing they cristalize on atomically flat surfaces, here provided by hBN flakes. The quality and intensity of the produced signal is comparable with their non-encapsulated counterparts obtained via exfoliation. As such, our findings fortify the viability of the MBE growth method for the production of high quality TMD monolayers. Furthermore, its inherent versatility opens up alluring new research venues for these particular family of 2D materials.

Probing the Local Temperature Distribution in Electrically Pumped Broad-Area VCSELs

Aleksandra N. Piasecka[1], Marcin Gębski[2], Michał Wasiak[2], James A. Lott[3], Tomasz Czyszanowski[2] and Maciej Pieczarka[1]

[1]Faculty of Fundamental Problems of Technology, University of Science and Technology, Wybrzeże Wyspiańskiego 27, 50-370 Wrocław, Poland
[2]Institute of Physics, Łódź University of Technology, ul. Wólczańska 219, 90-924 Łódź, Poland
[3]Institute of Solid State Physics and Center of Nanophotonics, Technical University Berlin, Hardenbergstraße 36, 10623 Berlin, Germany

Bose-Einstein condensation of photons in an optical microcavity filled with rhodamine 6G has been reported [1]. The following recent study showed that a photon gas in a state of thermal equilibrium with its surroundings trapped in semiconductor optical microcavity can display signatures of Bose-Einstein condensation [2]. However, the effects of ununiform local temperature on Bose-Einstein distribution in semiconductor lasers have not been examined yet.

The emission spectrum of semiconductor electrically pumped vertical-cavity surface-emitting lasers (VCSELs) is directly influenced by the local temperature and current density distribution. The effective inhomogeneous confining potential is the reflection of the effective local width changes in the cavity. This inhomogeneity effect changes the density of states function and influences extracted values of the Bose-Einstein distribution. The assumption that the density of states is purely 2D and has a fixed value over the whole VCSEL resonator may be an insufficient approximation. The most commonly used measurement method to characterize the thermally induced shift in the lasing wavelength provides only information on the average temperature distribution across the entire microcavity surface [3]. Here, we present a novel technique for measuring local spectral temperature distribution in wide aperture oxide-confined VCSELs by locally fitting the Boltzmann distribution to the high-energy tail of the spontaneous emission spectrum. Furthermore, we characterized the local potential change of the microresonator, measuring the local fundamental mode energy by filtering the spontaneous emission in the wavevector space close to the normal incidence $k_{\parallel} \approx 0$. The resulting data can be compared to theoretical simulations of the influence of current and temperature on the local potential shape.

Studies on the thermalised boson gas of trapped photons in electrically pumped VCSEL microresonators is a new promising direction in Bose-Einstein room-temperature condensation. Therefore, understanding the details of wide aperture semiconductor VCSELs may provide devices that act as Bose-Einstein condensate of photons, allowing for new research on Bose-Einstein photon condensation physics.

[1] J. Klaers et al., Nature 468, 545 (2010)
[2] S. Barland et al., Opt. Express 29, 8368 (2021)
[3] M. Farzaneh et al., IEEE Photon. Technol. Lett., vol. 19, no. 8, pp. 601-603, (2007)

Modeling InAs/GaSb Type-II Superlattices for Mid-Wavelength Infrared Photodetectors with the nextnano++ Software

Herbert A. Maczko[1]

[1] *nextnano GmbH, Konrad-Zuse-Platz 8, 81829 Munich, Germany*

Type-II superlattices (T2SLs) are characterized by: i) flexible tunability of the energy band gap by adjusting thicknesses of consisted layers without changing their content, ii) carrier separation suppressing nonradiative Auge recombination, and iii) high effective masses reducing band-to-band tunnelling current [1]. In contrast to type-I superlattices where effective mass approximation often is applied, modeling T2SL may cause additional difficulties originating in strong hybridization of S and P orbitals. Such conditions occur when T2SLs consist of thick layers resulting in small energy gap or even energies of some electron states lower than energy of first hole state, within the picture of effective mass approximation. As both electrons and holes are described in such cases by mutually overlapping wavefunctions, additional interaction is inevitable and hybridization effects must be considered. Eight-band k·p model can be applied for this purpose [2].

In this poster, I present a simple analysis of InAs/GaSb T2SL using the nextnano++ software [3-5]. The InAs/GaSb T2SLs are examples of promising heterostructures with potential to outperform currently state-of-the-art mercury cadmium telluride in applications for mid-wavelength infrared photodetectors [1]. I show how to effectively design these super lattices and how to obtain information about electronic band structures, relevant optical transitions, wavefunction envelopes, and hybridization effects. Presented approach can be easily applied and followed for basic analysis of any superlattices, that might come very helpful for groups focusing on optical spectroscopy or growth of numbers of such structures.

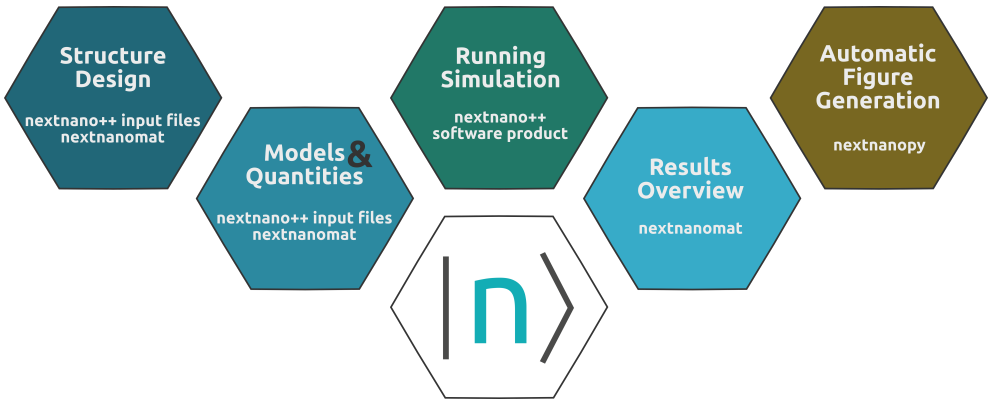

Figure 1: Basic design and analysis process of T2SL with the nextnano++ software

[1] D. O. Alshahrani, M. Kesaria, E. A. Anyebe, V. Srivastava and D. L. Huffaker, *Adv. Photonics Res.* **3**, 2100094 (2022).

[2] C. H. Grein, P. M. Young, M. E. Flatté and H. Ehrenreich, *J. Appl. Phys.* **78**, 12 (1995).

[3] A. Trellakis, T. Zibold, T. Andlauer, S. Birner, R. K. Smith, R. Morschl and P. Vogl, *J. Comput. Electron.* **5**, 285-289 (2006).

[4] https://www.nextnano.com

[5] https://github.com/nextnanopy

Applications of InAs/$InAs_{0.625}Sb_{0.375}$ Superlattice in Far-infrared Detection

Ghulam Hussain

International Research Centre MagTop, Institute of Physics, Polish Academy of Sciences, Aleja Lotników 32/46, PL-02668 Warsaw, Poland

E-mail: ghussain@magtop.ifpan.edu.pl

ABSTRACT

Using first-principles calculations, we calculate the electronic and optical properties of InAs/$InAs_{0.625}Sb_{0.375}$ superlattices (SL). To accurately approximate the electronic and optical properties, the modified Becke-Johnson exchange-correlation functional is pondered. After analyzing the electronic and optical characteristics of bulk InAs and InSb, we then investigated InAs/$InAs_{0.625}Sb_{0.375}$ SL. The electronic and optical properties of the InAs/$InAs_{0.625}Sb_{0.375}$ SL are studied with three lattice constants of the bulk InAs, GaSb and AlSb, respectively. It is observed that the electronic and optical properties strongly depend on the lattice constant. A considerable decrease in the energy gaps and the effective masses of the heavy-holes in the k_x-k_y plane compared to the bulk phases of the parent compounds can be obseved. We demonstrate that the electrons are s-orbitals delocalized in the entire superlattice, while the holes have mainly 5p-Sb character localized in the In(As,Sb) side of the superlattice. In the superlattice, the low-frequency absorption spectra greatly increase when the electric field is polarized orthogonal to the growth axis allowing the applicability of III-V compounds for the long-wavelength infrared detectors.

Magnetic properties of TRS broken ferrovalley semiconductors

Ghulam Hussain, Giuseppe Cuono, and Carmine Autieri

International Research Centre MagTop, Institute of Physics, Polish Academy of Sciences,
Aleja Lotników 32/46, PL-02668 Warsaw, Poland

E-mail: ghussain@magtop.ifpan.edu.pl

ABSTRACT

The intrinsic ferromagnetism in 2D materials and the magnetic anisotropy energy (MAE) are importants yardstick for nanoscale applications. We employed first-principles scheme to investigate the electronic band structures, the strain dependence of MAE in pristine VSi_2Z_4 (Z=P, As) and its Janus phase $VSiGeP_2As_2$ and the evolution of the topology as a function of the Coulomb interaction. It is observed that $MoSi_2P_4$ monolayer show equal bandgaps at K/K′ points of brillouine zone due to the the preserved time-reversal symmetery (TRS). On the other hand, all the vanadate based 2D structures exhibit unequal bandgaps at K/K′ with ferromagnetic ground state ordering owing to broken TRS, which is known as ferrovalley semiconductors. A large value of coupling J is obtained, and this, together with the magnetocrystalline anisotropy can produce a large critical temperature. We found an out-of-plane (in-plane) magnetization for VSi_2P_4 (VSi_2As_4), while in-plane magnetization in $VSiGeP_2As_2$. Furthermore, we observed a correlation-driven topological transition in the Janus $VSiGeP_2As_2$. These ferrovalley semiconductors possess inherent spontaneous valley polarization induced by intrinsic ferromagnetism and, thus offer the possibility to address the challenges of valleytronic materials.

Bulk And Contact Low Frequency Noise Investigated With Transmission-Line-Model: InAs case

Ł. Ciura [1], J. Wróbel[2], P. Martyniuk[2]
[1]*Rzeszow University of Technology, W. Pola 2, Rzeszow, Poland*
[2]*Institute of Applied Physics, Military University of Technology, 2 Kaliskiego Str.,Warsaw, Poland*

The Transmission-Line-Model (TLM) is a well-known technique that can be used for obtaining parameters of the material or device under consideration, i.e., the sheet resistance, the metal-semiconductor contact parameters, e.g. contact resistance, transfer length, etc. The method relies on resistance measurements between pairs of contacts separated by different distances L. This work reports experimental studies on TLM samples made from n-type InAs doped with Si (N_d=2×10^{16} cm^{-3}, N_d=2×10^{17} cm^{-3}, and N_d=2×10^{18} cm^{-3}) and with various metallization (Au, Ti/Au, Ti/Pt/Au) and contact formation procedure (annealing).

Besides the standard characteristics measured for a TLM, the low frequency noise was also measured. The preliminary results are shown in Fig. 1, where the resistance to TLM (inset) and the normalized low frequency noise S_U (f=1Hz)/U^2 are shown as functions of the spacing of the contacts L. From this characteristic, the origin of observed low frequency noise can be identified by comparing characteristics' slope with a theoretical slope for two different models that assume bulk or contact origin of low frequency noise.

The scientific goal of the work is to investigate the influence of InAs doping, contact metallization, and their formation (annealing) on the total noise and separate bulk and contact noise contributions.

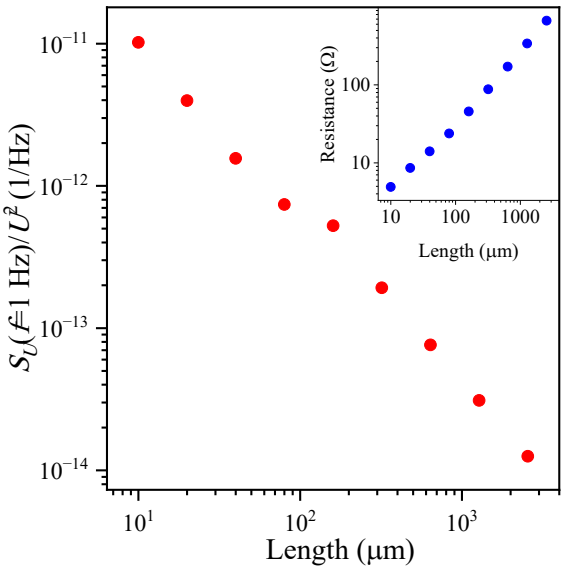

Fig. 1. Resistance and relative low frequency noise as a function of the distance between pairs of contacts for n-type InAs, doped with N_d=2×10^{16} cm^{-3}, transmission-line-model sample with Au contacts.

Optical characterization and pump-probe measurements of InAs/GaSb and InAs/InAsSb type-II superlattices

Michał Rygała[1], Andreas Bader[2], Tristan Smołka[1], Fabian Hartmann[2], Grzegorz Sęk[1], Sven Höfling[2] and Marcin Motyka[1]

[1] *Laboratory for Optical Spectroscopy of Nanostructures, Department of Experimental Physics, Faculty of Fundamental Problems of Technology, Wroclaw University of Science and Technology, wyb. Stanisława Wyspiańskiego 27, Wrocław, Poland*
[2] *Julius-Maximilians-Universität Würzburg, Physikalisches Institut and Würzburg-Dresden Cluster of Excellence ct.qmat, Lehrstuhl für Technische Physik, Am Hubland, 97074 Würzburg, Deutschland*

Modern optical gas detection systems utilize the technique of tunable diode laser absorption spectroscopy (TDLAS) for different applications in science, manufacture, or medicine. [1] Through tuning the emission wavelength, the presence and concentration of trace gases are possible to detect in real-time with their limit in single ppb range. Optical gas detection systems employing mid-infrared spectral range often comprise of active structures grown within so called 6.1 Å family of semiconductors, i.e. InAs, GaSb, AlSb alloys. Superlattice structures within this material system with type-II alignment have the potential to exceed the working parameters of widely used optoelectronic devices, such as HgCdTe infrared photodetector. [2]

Optically active type-II superlattices were obtained through molecular beam epitaxy and then characterized utilizing Fourier-transform infrared spectrometer (FTIR) and pump-probe system. The measurements were performed on two sets of structures – type-II InAs/GaSb superlattices and type-II Ga-free InAs/InAsSb superlattices. The parameter varying the samples within the first set was the approach to interface engineering – the samples were either "Sb-soaked" or an InSb monolayer was inserted between each SL period [3] which was also considered in our previous works. [4] Samples within the second set, on the other hand, varied through SL periodicity of 5, 6 and 8 nm which allowed to shift the main transition from 5 to 9 μm at room temperature. [5]

Photoluminescence spectra were obtained for all samples in 10 to 300K temperature range and then complemented with photoreflectance measurements for characteristic temperatures to increase the sensitivity of the measurement for less optically active transitions. In addition, pump-probe measurements were performed to investigate the dynamics of carrier relaxation and recombination processes in proximity of transition energies observed in previous experiments.

Presented findings could provide valid insights in the fundamental properties such as carrier lifetimes within InAs/GaSb and InAs/InAsSb SLs to further optimize and improve the working parameters of possible future applications in the field of infrared optoelectronics.

*This work was supported by Polish National Science Center (NCN) within OPUS-22 grant no. 2021/43/B/ST3/02473

[1] J. A. Nwaboh, et al., *Meas. Sci. Technol.*, **29**(9), 095010 (2018)
[2] C. H. Grein, et al., *Appl. Phys. Lett.*, **65**(20), 2530–2532 (1994)
[3] A. Bader et al., *Proc. SPIE,* **11830**, 118300E (2021)
[4] M. Rygała et al., *Phys. Rev. B*, **104**(8), 085410 (2021)
[5] A. Bader et al., *Proc SPIE,* **12233**, 122330F (2022)

Modelling of Band Structure and Optical Properties of InAsP/InP Quantum Dots in Nanowires

Jakub Boniecki[1], Giada Bucci[2], Valentina Zannier[2], Lucia Sorba[2], Anna Musiał[1] and Grzegorz Sęk[1]

[1] *Laboratory for Optical Spectroscopy of Nanostructures, Department of Experimental Physics, Wroclaw University of Science and Technology of Wroclaw, Wybrzeze Wyspianskiego 27, 50-370 Wroclaw, Poland*
[2] *NEST, Istituto Nanoscienze-CNR and Scuola Normale Superiore, I-56127 Pisa, Italy*

Chemical beam epitaxy (CBE) is known as efficient technological approach to grow quantum dots (QDs) in nanowires (NWs). In such a case the lateral size of the dot is limited by the width of the NW following the size of the seeding Au droplet, whereas the height of the nanostructure is controlled by the amount of deposited material. Compared to more common epitaxial self-assembled QDs embedded in a semiconductor matrix, CBE-grown QDs in NWs offer greater engineering capabilities for tailoring the energy levels and optical properties to meet requirements of specific application [1]. In addition, NWs geometry limits emission into the free-space modes in-plane and guide the emission in the vertical direction, which translates into increased light extraction efficiency resulting in brighter source with larger photon flux [2]. This is particularly important for nonclassical light sources, such as single photon emitters. However, a kind of drawback of this growth method is a deposition of a thin layer of QD material onto the bare substrate, i.e. in the areas beyond the NWs. This thin layer is expected to emit light which can overlap spectrally with emission from the QDs for certain thicknesses and compositions. Additionally, carriers could be trapped in it affecting overall carrier dynamics – both relaxation to the QDs and their emission. Therefore, it is crucial to better understand energy states of such a layer and its effect on QD emission.

The main objective of conducted research is to study theoretically the energy band structure of $InAs_xP_{1-x}$ QDs in InP NWs grown by CBE technique on InP substrate with different crystallographic orientations (1,0,0) and (1,1,1), which results in crystallization of the nanostructures in zinc blend or wurtzite structure, respectively. In particular, it is of interest if the thin $InAs_xP_{1-x}$ layer formed naturally during CBE growth of QDs, overlaps spectrally with QDs emission and what is the electronic structure of the system and its optical response. To calculate these properties versus various nanostructure geometries a commercial software Nextnano++ [3] is employed, i.e. an implementation of the 8-band $k \cdot p$ in three dimensions. Simulations are performed for realistic compositions and geometries following the structural data for several sets of samples: different QD heights and As content. As a result, the confined levels and probabilities of optical transitions are derived (without the excitonic effect) and compared with experimental results obtained from microphotoluminescence measurements.

[1] S. Battiato, S., et al, *Nanotechnology* **30**, 194004 (2019).
[2] J. Claudon, J. Bleuse, et al. *Nature Photon.* **4**, 174 (2010).
[3] https://nextnano.de/

Temperature Dependence of Refractive Indices of $In_{0.53}Ga_{0.47}As$ and InP in the Mid-Infrared Spectra Range Determined by Fourier Transform Spectroscopy

Monika Mikulicz[1], Michał Rygała[1], Tristan Smołka[1], Mikołaj Badura[2], Wojciech Kijaszek[2], Adriana Łozińska[2], Damian Radziewicz[2], Beata Ściana[2], Marcin Motyka[1*]

[1] Laboratory for Optical Spectroscopy of Nanostructures, Department of Experimental Physics, Faculty of Fundamental Problems of Technology, Wroclaw University of Science and Technology, Wybrzeże Wyspiańskiego 27, 50-370 Wrocław, Poland
[2] Department of Microelectronics and Nanotechnology, Faculty of Electronics, Photonics and Microsystems, Wrocław University of Science and Technology, Janiszewskiego 11/17, 50-372 Wrocław, Poland

The main motivation behind the determination of refractive indices of InP and InGaAs in mid-infrared spectral range is to enable more accurate and effective analysis and design of materials and optical components for a variety of applications e. g. growth of active regions for mid-infrared sources of light such as quantum cascade lasers (QCLs) and detectors. QCLs are semiconductor lasers that emit mid-infrared light, and have a wide range of applications in chemical sensing, medical diagnostics, and environmental monitoring [1]. InP substrates provide a suitable platform for the epitaxial growth of QCLs with high output power, high efficiency, and good thermal stability [2]. Moreover, it was shown, that InP and InGaAs can be used to grow efficient Distributed Bragg Reflector (DBR) designed for near-infrared spectral range [3]. By controlling the reflectivity and transmission of infrared light, DBRs can help improve the performance and functionality of infrared devices. In our case we will show that functionality of mentioned concept InGaAs/InP DBR can be further exploited for longer wavelengths i.e. 4 μm.

Refractive index of InP was determined by transmittance measurements of double sided polished undoped substrate in wide spectral range performed for temperatures ranging from 10 K to 300 K and through the analysis of measured interference pattern [4]. The result in near-infrared spectral range was verified by common spectroscopic method for measuring refractive index - ellipsometry, which measures the polarization of light reflected from a sample at various angles of incidence and allow us to adjust the curve for longer wavelength with high accuracy [5]. This knowledge was used to determine the refractive index of $In_{0.53}Ga_{0.47}As$ in the same wide range of temperatures by modelling the experimentally obtained spectra of reflectance measured on $In_{0.53}Ga_{0.47}As$/InP DBR with Lumerical software. The modelling of experimental spectra for 300 K required adjusting the nominal values for layer thicknesses of about 2% which finally made the refractive indices of $In_{0.53}Ga_{0.47}As$ only unknown parameter to generate DBR reflectance spectrum for lower temperatures. This approach provides an accurate and non-destructive means of refractive index determination for semiconductors in wide range of temperatures and broad mid-infrared spectral range.

[1] H.I. Schiff, et al., (Wiley, New York 1994).
[2] M. Razeghi, *IEEE Journal of Selected Topics in Quantum Electronics*, **15**, 3 (2009).
[3] S. Sprengel et al., *Appl. Phys. Lett.* **106**, 151102 (2015).
[4] M. Milosevic and S. W. King, *Appl. Opt.* **52**, 4477-4482 (2013).
[5] R. Gupta and S. G. Kaplan, *J. Res. Natl. Inst. Stand. Technol.* (2003).
* This work was supported by the Polish National Science Centre within Project No. 2019/33/B/ST7/02591

Carrier dynamics of type-II quantum wells emitting in mid-infrared

Tristan Smołka[1], Michał Rygała[1], Krzysztof Ryczko[1], Andreas Bader[2], Fabian Hartmann[2], Borislav Petrovic[2], Sven Höfling [2], Marcin Motyka[1]*

[1] Laboratory for Optical Spectroscopy of Nanostructures, Department of Experimental Physics, Faculty of Fundamental Problems of Technology, Wrocław University of Science and Technology, Wybrzeże Wyspiańskiego 27, 50-370 Wrocław, Poland
[2] Technische Physik, Wilhelm-Conrad-Röntgen-Research Center for Complex Material Systems, Universität Würzburg, Würzburg, Germany

Interband cascade lasers (ICLs) are a type of semiconductor lasers that operate in the mid-infrared region of the electromagnetic spectrum. They have unique properties that make them essential for a variety of applications, such as gas sensing, spectroscopy, medical diagnostics, and communication [1]. ICLs have a cascade structure of multiple quantum wells, which allows them to achieve high efficiency, low threshold current, and continuous-wave operation at room temperature [2,3]. Nevertheless, further optimization of the active region can be achieved. In this approach we will examine influence of tensile and compressive strain on the electronic structure [4] and carrier dynamics.

This study presents transient absorption (TA) pump-probe measurements of type-II WQW InAs/GaInSb/InAs and InAsSb/GaAsSb/InAsSb structures designed for mid-infrared interband cascade lasers emitting close to 3.5 μm. The aim of this study is to investigate the fundamental carrier dynamics in this material systems, which is essential for their further possible applications in e.g. mode-lock lasers. TA measurements were performed in order to determine influence of the compressive or tensile strain application in quantum wells on carrier lifetimes regarding fundamental transitions and other interface-related ones.

Additionally, photoreflectance (PR) and photoluminescence (PL) measurements were used to investigate the band structure and optical properties of the samples. Both the PR and PL spectra showed strong signals near 3.3 μm, which corresponds to the fundamental type-II transition of the QW and additional signals (observed in PL) related to possible interface-atom intermixing processes. The temperature-dependent PL measurements revealed a strong temperature dependence of the PL intensity, with a significant reduction in the intensity at higher temperatures. The energy shift of the transitions were also studied through temperature-dependent PR. Observed optical transitions and their energies were in good agreement with theoretical calculations realized within 8kp formalism.

*This work was supported by National Science Center of Poland within grant OPUS-22 no. 2021/43/B/ST3/02473

[1] Du, Z.; Zhang, S.; Li, J.; Gao, N.; Tong, K., *A Review. Appl. Sci.*, **9**, 338 (2019)
[2] I. Vurgaftman et al. IEEE Journal of Selected Topics in Quantum Electronics, **19**, 4, (2013)
[3] A. Bauer, F. Langer, M. Dallner, M. Kamp, M. Motyka, G. Sęk, K. Ryczko, J. Misiewicz, S. Höfling, and A. Forchel , Appl. Phys. Lett. **95**, 251103 (2009)
[4] M. Motyka, M. Dyksik, K. Ryczko, R. Weih, M. Dallner, S. Höfling, M. Kamp, G. Sęk, and J. Misiewicz , Appl. Phys. Lett. **108**, 101905 (2016)

Influence of Mg^{2+} codoping on excitation relaxation and emission properties of $(Lu,Gd)_3(Ga,Al)_5O_{12}$:Ce,Mg scintillators

A. Solovjovas [1], S. Nargelas [1] M. Kučera [2] and G. Tamulaitis [1]

[1] *Institute of Photonics and Nanotechnology, Saulėtekio al. 3, Vilnius, Lithuania*
[2] *Charles University, Faculty of Mathematics and Physics, Ke Karlovu 5, Prague, Czech Republic*

Scintillation materials have currently a very wide application field from medical imaging and high energy physics experiments to the homeland security systems and nuclear safety monitoring. The successful growth of Ce-doped gadolinium aluminum gallium garnet (GAGG) single crystals that are prospective for the detection of ionizing radiation due to their high density, high light yield, and the absence of intrinsic radioactivity encouraged an intensive development of mixed garnet-type scintillators for efficient and fast scintillation detectors. The codoping by small amounts of divalent alkali-earth ions was proved to be a successful method to achieve faster scintillation, whereas the influence of codoping on the emission properties at the codoping levels comparable to that of the activator ions still remains a subject for investigation [1].

In this work, we focus on Ce-doped and Mg-codoped $(Lu,Gd)_3(Ga,Al)_5O_{12}$:Ce,Mg (LuGGAG) multicomponent single crystalline epitaxial layers grown using liquid phase epitaxy (LPE) method. LPE technique has an advantage in the preparation of Ce-doped garnets at lower temperatures allowing noticeable reduction of the concentration of antisite and vacancy-related defects acting as effective traps for electrons. We report our results of a study of electronic excitation relaxation and emission properties in a set of Ce-doped LuGAGG films containing different content of Mg^{2+} ions (from 0 to 2200 ppm). The linear and transient absorption, steady-state and time-resolved photoluminescence spectroscopy have been used to study the influence of Mg^{2+} ions on excitation relaxation and emission properties of Ce^{3+} activator ions in the 80-600K temperature range.

The dominant excitation relaxation pathways were examined exploiting selective photoexcitation of the first and second excited levels of Ce^{3+} ions. The study of photoluminescence temperature dependence under selective excitation of the lowest excited Ce^{3+} level $5d_1$ revealed emission thermal quenching due to increasing thermal escape of electrons to the conduction band and subsequent nonradiative recombination. The slight increase of photoluminescence intensity from low-to-room temperature after the selective excitation of $5d_2$ level indicate the localization of electrons during their transfer to emitting $5d_1$ level due to bandgap fluctuations caused by compositional disorder of mixed garnet crystal matrix. The additional decrease of photoluminescence intensity and increased emission decay rate was found in the LuGAGG films containing more than 300 ppm of Mg. The later observation is in line with the formation of nonradiative activator-codopant related excitation relaxation route [2].

[1] D. Zhu, M. Nikl, W. Chewpraditkul, and J. Li, "Development and prospects of garnet ceramic scintillators: A review," *Journal of Advanced Ceramics*, vol. 11, no. 12, pp. 1825–1848, Nov. 2022.
[2] P. Schauer, O. Lalinský, M. Kučera, Z. Lučeničová, and M. Hanuš, "Effect of Mg co-doping on cathodoluminescence properties of LuGAGG:Ce single crystalline garnet films," *Optical Materials*, vol. 72, pp. 359–366, Oct. 2017.

Characterization of the Microwave Strip Antenna in the Experiment of Optically Detected Magnetic Resonance

Zuzanna Śnioch, Aleksandra Łopion, Aleksander Bogucki, Karolina E. Połczyńska, Wojciech Pacuski, Tomasz Kazimierczuk, Andrzej Golnik and Piotr Kossacki

Faculty of Physics, Institute of Experimental Physics, University of Warsaw, ul. Pasteura 5, 02-093 Warszawa, Poland

Optically Detected Magnetic Resonance (ODMR) is a powerful technique that allows for local and selective sampling of magnetic properties. The intensity of the measured ODMR signal crucially depends on how effectively microwave radiation is provided to the sample.

Typically, the magnetic resonance signal, e.g., in Electron Paramagnetic Resonance (EPR), is measured with a single specific frequency of the RF field. The single-frequency restriction is imposed by the resonant cavity employed to amplify the strength of the RF field. In order to perform measurements in a wide range of frequencies, a totally different approach is needed. Our research aimed to characterize a new type of broadband microwave antenna and its role as an element of the experimental system.

The microwave antenna is designed to act as a long line: a transmission line, which length is comparable to the wavelength of the propagating microwaves. The transmission lines are the metalized tracks on the dielectric support plates that encircle the sample. The antenna's construction allows it to work in low temperatures, such as 1.5 K, and with a wide range of microwave frequencies. The actual antenna is shown in the picture below.

In this research, the signal was measured on the reference sample – a quantum well (Cd, Mn)Te with manganese content of 0.3%. The characterization was made based on measurements of various microwave radiation power and various environmental conditions, such as the temperature and pressure of helium surrounding the sample, affecting its dielectric constant. Obtained results are compared with the results of numerical simulations.

[1] Bogucki A., et al., *Phys. Rev. B* **105**, 075412 (2022).
[2] Łopion A., et al., *Phys. Rev. B* **106**, 165309 (2022).
[3] Goryca M. i Bogucki A., Sample Holder for Measurements of Optically Detected Magnetic Resonance, "Sample holder patent WO2021064687A1" (2021).

Hybrid Acousto-Optic Driving of Rabi Oscillations of Electron Spin in a Quantum Dot

M. Kuniej, M. Gawełczyk, and P. Machnikowski

Institute of Theoretical Physics, Wrocław University of Science and Technology, 50-370 Wrocław, Poland

Performing coherent Rabi rotations is a necessary step toward complete control of a qubit. For a quantum bit based on spin states, it can be achieved with microwaves [1]. However, such control with macroscopically long waves causes problems when considering the miniaturization of integrated circuits. While for an electron confined in a semiconductor quantum dot (QD), state control has been achieved with optical pulses [2], such methods are unavailable for many other promising solid-state systems (like NV centers or superconducting qubits). A promising solution is to use acoustic waves that couple to all mentioned systems and allow chip miniaturization.

In this contribution, we propose a hybrid (acousto-optic) approach to controlling the spin state of an electron in a QD. We theoretically show Rabi oscillations for the Zeeman-split ground state of a QD-confined electron modulated using the acoustic field. The acoustic field amplitude sets the rotation axis, while spin rotations are controlled by pulsed off-resonant optical coupling to the trion state. Thus, we take advantage of orders of magnitude shorter lengths of acoustic fields compared to microwaves and rotate the spin with two nanoscale-compatible fields.

Although direct coupling between spin states and deformations is negligible in such systems, our hybrid control leads to controllable Rabi oscillations with a frequency that depends on the amplitudes of both acoustic and optical fields. The ground state doublet and the trion level form a configuration known as a Λ-system [3]. In our model, the acoustic field modulates the trion level, to which both spin states are coupled via optical pulses. This leads to the second-order coupling between the spin states.

To better understand the evolution of the system, we compare direct numerical calculations with the results of approximate analytical derivation. To this end, we model the system using a Hamiltonian in the dipole and rotating wave approximation. We derive an effective Hamiltonian of the ground state doublet by eliminating the trion level in the quasi-degenerate perturbation theory [4]. This effective description allows us to predict the evolution of the spin qubit. Importantly, due to the specific form of effective coupling, we find a way of varying the spin-rotation axis. Lastly, we study the destructive processes accompanying the evolution of the system. For this, we use the Lindblad master equation and show that trion recombination has negligible effects for short optical pulses.

We anticipate our work to be a starting point for designing and creating a controllable qubit and its extension to a two-qubit gate defined on tunnel-coupled QDs.

[1] F. H. L. Koppens, et al., *Nature* **442**, 766 (2006)
[2] D. Press, et al., *Nature* **456**, 218 (2008).
[3] M. Scully, and M. Zubairy. "*Quantum optics*" Cambridge: Cambridge University Press (1997).
[4] P.-O. Löwdin, *J. Chem. Phys.* **19**, 1396 (1951).

Noise effects on the resonance fluorescence from acoustically modulated quantum dots

Rafał A. Bogaczewicz, Paweł Machnikowski

Institute of Theoretical Physics, Wrocław University of Science and Technology, Wybrzeże Wyspiańskiego 27 50-370, Wrocław, Poland

In the field of quantum information processing, one of the current goals is the high scale integration of miniaturized devices. Photons are not always an ideal carrier of information, hence hybrid quantum acousto-optic systems have been proposed, which use surface phonons as the information carrier within the device [1]. A quantum dot (QD) can be used as a transducer between the acoustic and optical signals on the quantum level.

In this work we theoretically study the spectrum of the low-excitation resonance fluorescence (RF) for a single two-level QD, whose transition energy depends on time due to two simultaneous factors: First, the QD is modulated by a surface acoustic wave (SAW). Second, it is affected by environmental noise.

We iteratively solve the equations of motion for the density matrix of a two-level system driven by a weak, monochromatic, classical laser light. Then, the two-time correlation function is found using the quantum regression theorem. The time-integrated RF spectrum is obtained in the standard way as its Fourier transform, including a finite instrumental resolution. Thus, we extend our previous analysis of the noise effects in RF [2] to acoustically modulated systems [3,4].

The noise-free RF spectrum shows a series of unbroadened peaks from elastic scattering, shifted by a multiple of acoustic frequencies from the laser frequency [3,4]. White-noise environmental fluctuations leads to the appearance of additional peaks from inelastic scattering. They are located relative to the transition frequency and their width depends on the exciton decay rate and phase diffusion coefficient. We show that the environmental noise modifes the relative intensities of the spectral lines in the spectrum of a periodically modulated system. We study also the acoustic frequency mixing effect [4] and show that noise affects the quantum interference between various contributions to the scattering process, decreasing the contrast of spectral oscillations as a function of the relative phase of the two acoustic waves of different frequencies.

We consider also the case of telegraph noise environmental fluctuations, which differs from the white-noise case by the structure of spectral lines.

Our study presents a comprehensive characterization of noise effects on the resonance fluorescence spectra of acoustically modulated systems and may be useful both for interpreting experiments as well as for determining the limits of quantum acousto-optic transduction.

[1] Delsing P. *et al.*, *J. Phys. D: Appl. Phys.* **52**, 353001 (2019).
[2] Bogaczewicz R. A., Machnikowski P., arXiv:2303.01531v1 (2023).
[3] Wigger D. *et al.*, *Phys. Rev. Res.* **3**, 033197 (2021).
[4] Weiß M. *et al.*, *Optica* **8**, 291 (2021).

Energy gap determination from photoacoustic spectroscopy measurements

Kamil Misztal [1], Jan Kopaczek [1] and Robert Kudrawiec [1]

[1] *Wrocław University of Science and Technology, Wybrzeże Wyspiańskiego 27, 50-370, Wrocław, Poland*

Photoacoustic spectroscopy (PAS) is a powerful technique to investigate the basic physical properties of semiconducting materials, e.g., thermal diffusivity, heat capacity, electron-trapping sites, energy gap, and so on. Moreover, PAS is a method that allows obtaining an optical absorption based on a sound wave emitted by a semiconducting sample. That sound wave is formed due to a periodic heat generation in the sample, which subsequently causes pressure changes in a surrounding gas detected by an acoustic transducer [1]. This method does not require any special sample preparation and allows examining materials even in powdered form, which is not possible for other absorption-like methods. However, so far, no in-depth studies comprehensively approach such issues as how sample size and thickness influence the photoacoustic signal. Here we address the questions mentioned above. All the experiments were carried out on molybdenum disulfide (MoS_2) since its properties are well-known, and it is easy to exfoliate MoS_2 crystal to obtain thinner samples.

In the first step, we investigated how the thickness of MoS_2 influenced the photoacoustic signal. Surprisingly when the sample is thinner, more signal is generated during PAS measurements (see Fig. 1a). Moreover, it is clearly visible in Fig. 1a that the energy gap determined from the knee method (see gray lines) is blue-shifted, going from the thick to thin samples. For the thickest MoS_2 crystals, we observed that the obtained energy is close to the indirect band gap at 1.2 eV, while for the thinnest MoS_2, the energy is around the lowest direct optical transition (~1.8 eV). The second issue on which we focused is the sample size. In Fig. 1b, we showed photoacoustic amplitude for different sample sizes. All values of the PAS signal were taken at 1.9 eV (saturation area). It can be seen that signal slowly increases when reducing the sample size and then starts to drop quicker, following a linear trend as shown by a straight cyan line (inset of Fig. 1b). As mentioned, below certain sample size signal decreases, which is expected since the less light is absorbed and the signal from smaller volume is generated. In our studies, we will provide a tentative explanation for observed behavior.

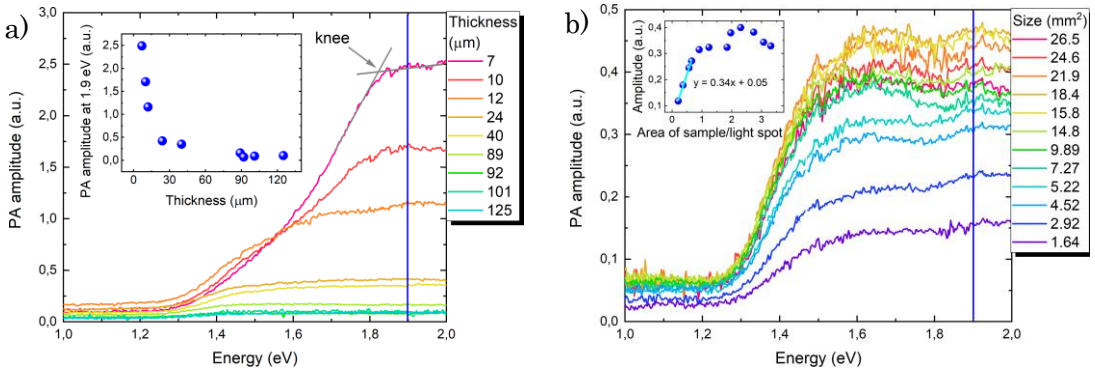

Figure 1. (a) PAS signal for MoS_2 of different thicknesses. Inset shows PA amplitude taken from 1.9 eV (blue line), gray lines shows knee, and (b) PAS signal for a samples of various size. Inset shows PA amplitude against area of sample/light spot taken at 1.9 eV (blue line). The Cyan line in inset represents linear fit.

[1] Tatsuki Shinoda, Yuichi Yamaguchi, Akihiko Kudo, and Naoya Murakami
The Journal of Physical Chemistry C **2022** *126* (49), 20975-20982

Magnetic field and temperature dependence of the Mn^{2+} spin relaxation rate in a (Cd, Mn)Te/(Cd, Mg)Te quantum well

A. Bogucki, Z. Śnioch, A. Łopion, K. E. Połczyńska, W. Pacuski, T. Kazimierczuk, A. Golnik and P. Kossacki

Institute of Experimental Physics, Faculty of Physics, University of Warsaw, ul. Pasteura 5, 02-093, Warszawa, Poland

The spin-lattice relaxation rate is an important parameter that determines whether a magnetic ion can be considered for information processing applications. More precisely, the dependence of the relaxation rate on parameters such as temperature and magnetic field can provide clues as to what type of mechanism is responsible for the energy dissipation.

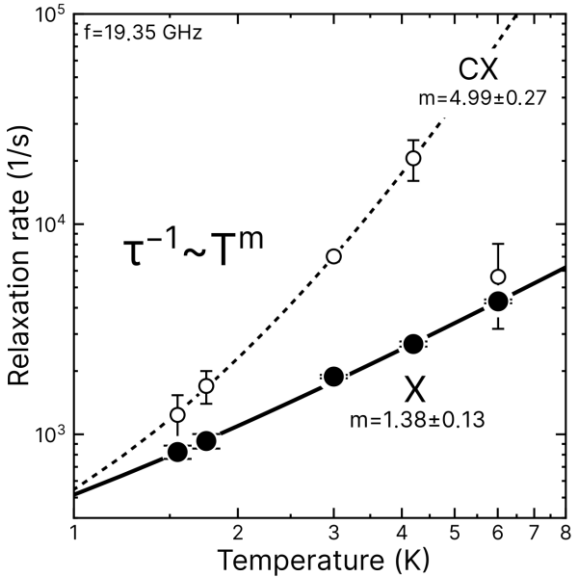

Figure 1 The spin-lattice relaxation rate of the Mn^{2+} ions in CdTe quantum well vs temperature can be described with the power function. The relaxation rate dependence of the neutral exciton (X) is dominated by the direct mechanism. In contrast, the charged exciton (CX) dependency suggests multi-phonon processes.

In this work we present the results of the spin-lattice relaxation rate measurements of a (Cd, Mn)Te/(Cd, Mg)Te quantum well. For this purpose we utilize the time-resolved optically detected magnetic resonance (ODMR) technique known for its sensitivity [1]. The spin-lattice relaxation time of Mn^{2+} ions in the (Cd, Mn)Te/(Cd,Mg)Te quantum well was measured as a function of magnetic field and temperature (see Fig. 1).

Obtained results can be explained in the frame of a modified model described in [2]. The modified model takes into account that energy levels of manganese are not equally spaced. The distance between the Mn^{2+} energy levels depends on the magnetic field and strain present in the sample. The observed temperature and magnetic field dependencies are well described by proposed model. Our results suggest that the dominant mechanism of energy dissipation in the measured system is the so-called 'direct process', in which a phonon is emitted or absorbed.

[1] A. Łopion, A. Bogucki, W. Kraśnicki, K. E. Połczyńska, W. Pacuski, T. Kazimierczuk, A. Golnik, and P. Kossacki, *Magnetic Ion Relaxation Time Distribution within a Quantum Well*, Phys. Rev. B 106, 165309 (2022)
[2] A. M. Witowski, *Numerical Studies of Magnetization Relaxation of Mn $^{2+}$ in Zinc Blende Crystals*, Acta Phys. Pol. A **82**, 876 (1992).

III-V-on-Silicon-Nitride Mode-Locked Lasers

Bart Kuyken

[1] *Ghent University – imec Department of Information Technology, Technologiepark-Zwijnaarde 126 9052, Ghent, Belgium*

In this work, we highlight our recent results on heterogeneously integrated III-V-on-silicon-nitride (Si3N4) modelocked lasers [1, 2]. In particular, we demonstrate a III-V-on-Si3N4 mode-locked laser with a sub-GHz repetition rate and unprecedented noise performance [1] as well as energetic pulsed lasers. In contrast to earlier reported III-V-on-Si mode-locked lasers [3], silicon nitride waveguides can routinely achieve ultra-low losses close to 1 dB/m and do not suffer from nonlinear absorption, paving the way for a new generation of improved on-chip mode-locked lasers

The low-noise comb laser employs a ring cavity and fabry-perot geometry, consisting of long silicon nitride spirals on top of a patterned silicon-on-insulator wafer, as shown in Fig. 1. Here, the 330 nm thick silicon nitride waveguides are defined using deep-UV lithography, permitting low-cost and high-volume wafer-scale manufacturing. We enable heterogeneous integration, by defining a recess locally defined in the 4.2 µm SiO2 top cladding using dry etching techniques. Furthermore, given the large refractive index difference between the silicon nitride waveguide and the III-V gain waveguide, an intermediate silicon taper is introduced to ensure efficient evanescent coupling.

This process relies on the kinetically controlled adhesion of an elastomeric stamp to pick devices from the source InP wafer and print them on the silicon nitride target chip. In contrast to bonding techniques, microtransfer printing allows for integrating a III/V coupon in a recess. Moreover, this approach supports massively parallel integration, enabling wafer-scale fabrication. After transfer printing, the coupon is post-processed to isolate a saturable absorber. Furthermore, vias are etched to access the n-InP layer and electrical contacts are added to enable biasing of the device.

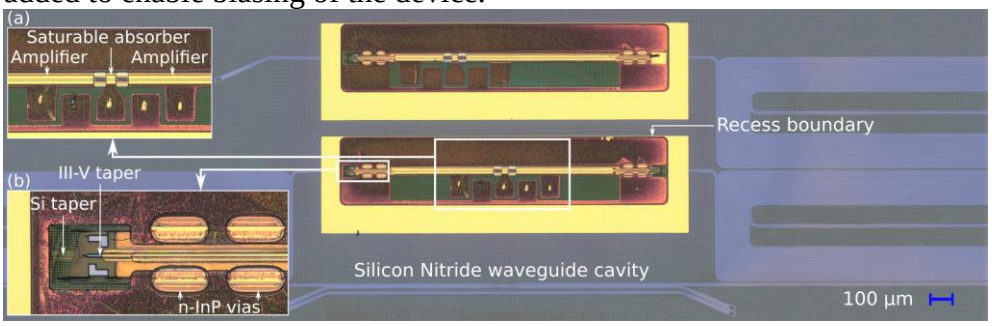

References

[1] S. Cuyvers et al., "Low Noise Heterogeneous III-V-on-Silicon-Nitride Mode-Locked Comb Laser," Laser & Photonics Reviews 15, 2000485 (2021).

[2] K. Van Gasse et al., "Recent advances in the photonic integration of mode-locked laser diodes," IEEE Photonics Technology Letters 31(23), 1870 - 1873 (2019).

[3] A. Hermans et al., "High-pulse-energy III-V-on-silicon-nitride mode-locked laser," APL Photonics 6, 096102 (2021).

[4] Z. Wang et al., "A III-V-on-Si ultra dense comb laser," Light: Science & Applications 6, p.e16260 (2017).

Recovering rectangular band profile in polar InGaN-based heterostructures utilizing junction field

R. Zdunek[1,2], M. Chlipała[2], G. Muziol[2], C. Skierbiszewski[2], J. Łusakowski[1,3], H. Turski[2,4]

[1] *Faculty of Physics, University of Warsaw, ul. Pasteura 5, 02-093 Warsaw, Poland*
[2] *Institute of High Pressure Physics, Polish Academy of Sciences, ul. Sokołowska 29, 01-142 Warsaw, Poland*
[3] *Centera Laboratories, IHPP, PAS, ul. Sokołowska 29, 01-142 Warsaw, Poland*
[4] *School of ECE, Cornell University, 14853 Ithaca, NY, USA*

III-nitride heterostructures are most commonly obtained along polar and semipolar directions. As a consequence built-in polarization, both spontaneous and piezoelectric, has to be taken into account when simulating and designing nitride devices.

We studied single InGaN quantum well (QW) heterostructures closely surrounded by p- and n-type layers with different doping levels. Band profiles of two exemplary structures simulated using 1D DDCC simulation software developed by Yuh-Renn Wu et. al [1] are shown in Fig 1.

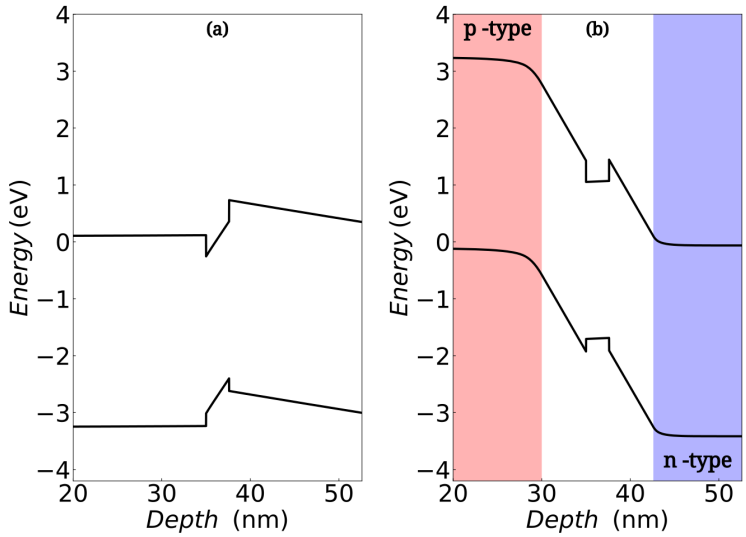

Figure 1: Conduction and valance band profile for $In_{0.17}Ga_{0.83}N/In_{0.03}Ga_{0.97}N$ QW surrounded by (a) no intentional doping and (b) $N_A = 6 \cdot 10^{19}$ atoms/cm^3, $N_D = 3 \cdot 10^{20}$ atoms/cm^3 .

We used plasma-assisted molecular beam epitaxy to obtain very sharp doping profile to investigate optical transitions in Ga-polar QWs with varied total electric field. Change in doping concentrations within the cladding layers affect the depletion width what results in different value of the total electric field in the QW (FQW) (see Fig 1.). By reaching doping concentrations above 10^{20} atoms/cm^3 we were able to obtain p-n junction field high enough to completely abolish built-in electric field and recover rectangular-like band profile typical to nonpolar heterostructures (Fig 1(b)).

We analyzed influence FQW on the photoluminescence (PL) spectra as a function of pumping power. As expected from simulations, for different doping levels we obtained substantially different shift of the emission peak. For structure without p-n junction we observed 9 nm shift, while for the highest used doping level the emission wavelength was independent of pumping power indicating total electric field in QW close to zero.

This research was funded in part by National Science Centre, Poland no.2021/43/D/ST3/03266 and UMO-2019/33/B/ST7/02858

[1] Y.-R. Wu, R. Shivaraman, K.-C. Wang and J.S. Speck, *Applied Physics Letters* **101**, (2012).

Deep-level traps in as-grown and electron-irradiated n-GaN layers grown by MOVPE on Ammono-GaN substrate

P. Kruszewski*[1], J. Plesiewicz[1], V. P. Markevich[2], P. Prystawko[1], S. Bulka[3], M. Hallsal[2], I. Crowe[2], L. Sun[2], A. R. Peaker[2]

[1] *Institute of High Pressure Physics, Polish Academy of Sciences, Sokolowska 29/37, 01-142 Warsaw, Poland*
[2] *Photon Science Institute and Department of Electrical and Electronic Engineering, the University of Manchester, Manchester, M13 9PL, UK*
[3] *Institute of Nuclear Chemistry and Technology, Dorodna 16, 03-195 Warsaw, Poland*

*Corresponding author: kruszew@unipress.waw.pl
Keywords: GaN, electron irradiation, defects, deep level, DLTS

In this paper, the results of junction spectroscopy measurements on deep-level defects in Metal–Organic Vapor-Phase Epitaxy n-GaN samples grown on highly doped Ammono-GaN and subjected to 1.5 MeV electron irradiation are compared. It is found that in addition to the commonly observed deep-level traps in n-type GaN, such as E1 (0.25 eV) and E3 (0.59 eV), 1.5-MeV electron irradiation introduces two other electron traps, EE1 and EE2, with electronic levels at about 0.14 and 0.98 eV below the conduction band edge (E_C), respectively. In the case of the EE1 level, a strong influence of the electric field (E) on the electron emission rate (e_{em}) is observed which suggests a donor type character of this trap level. Further, we have observed that strong electric field, as high as 2×10^5 V/cm, results in lowering the activation energy of electron emission from the EE1 level down to the value of 0.095 eV. The strong $e_{em}(E)$ dependence for the EE1 trap can explain the wide variation in electronic signatures of this trap reported in previously published publications. The analysis of the EE1 trap concentrations in the electron irradiated samples allowed us to estimate the average production rate of this trap by 1.5 MeV electrons as 0.125 cm^{-1} for n-GaN material grown on Ammono-GaN substrate. Possible origins of the detected deep-level traps are discussed.

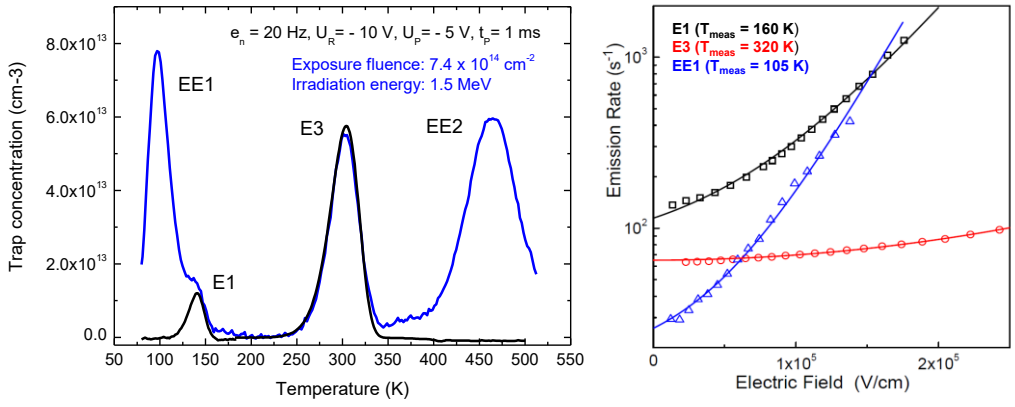

Fig. 1. On the left, the conventional DLTS spectra for both: reference sample (black curve) and 1.5 MeV electron-irradiated sample to dose of 7.4×10^{14} cm^{-2} (blue curve). On the right, the dependencies of the rate of electron emission from the E1, E3, and EE1 traps versus electric field strength in the depletion regions of reverse-biased Schottky diodes.

Acknowledgement
This work was financially supported by the National Science Centre, Poland through Project Number 2020/37/B/ST5/02593.

Bound states in continuum confined in GaN based subwavelength gratings

T. Fąs[1], D. Yavorskiy[2,3], E. Pruszyńska-Karbownik[1], M. Sawicka[4], J. Kacperski[4], J. Wróbel[3,5], P. Nowicki[3] A. Kazakov[6], J. Polaczyński[6] A. Feduniewicz-Żmuda[4] Cz. Skierbiszewski[4], D. Schiavon[4], P. Perlin[4], T. Czyszanowski[7], J. Suffczyński[1]

[1] *Faculty of Physics, University of Warsaw, Warsaw, Poland*
[2] *CENTERA Laboratories, Institute of High Pressure Physics PAS, Warsaw, Poland*
[3] *Institute of Physics, Polish Academy of Sciences, Poland*
[4] *Institute of High Pressure Physics, Polish Academy of Sciences, Warsaw, Poland*
[5] *Institute of Applied Physics, Military University of Technology, Poland*
[6] *Int. Research Centre MagTop, Institute of Physics, Polish Academy of Sciences, Poland*
[7] *Institute of Physics, Łódź University of Technology, Łódź, Poland*

Subwavelength gratings are photonic structures made of stripes of subwavelength thickness spaced periodically in one direction. They are a canonical example of an open optical system that can confine optical bound in the continuum (BIC) states. BIC arises from the symmetry of the system due to destructive interferences, resulting in the confinement of the mode. The quality (Q) factor of BIC states approaches infinity and they coexist with a continuous spectrum of unbound states. In real systems, due to finite dimensions, one observes so-called quasi-BIC, with a finite Q-factor. Use of gallium nitride (GaN) in photonics is highly advantageous due to its negligible absorption in visible spectrum and durability. Despite well established growth technology, nano-structuration still requires development.

We present two sets of GaN subwavelength gratings produced by e-beam lithography followed by dry-etching. One set was fabricated from MOVPE-grown GaN on sapphire substrate. The second one was etched in MBE-deposited GaN on porous GaN substrate made by electrochemical etching. Figure 1a) shows an example of the angle resolved reflectivity map of the grating on sapphire. Presence of vanishing reflectivity features at photon momentum $k = 0$ confirms the existence of quasi-BIC state. In addition, we detect a rarely observed interference based quasi-BIC for k at the border of the Brillouin zone. The Q-factors of quasi-BICs in both sets are determined to be above 10^4 and their linewidth goes below measurement resolution of 0.1 nm. Polarization resolved measurements reveal the presence of vortexes in reflected light, which further supports existence of quasi-BIC [1].

In summary, thanks to developed structuration technology we demonstrate modes of very high Q-factor in different types of GaN-based subwavelength gratings, as well as the existence of quasi-BIC states with non-zero wavevector values.

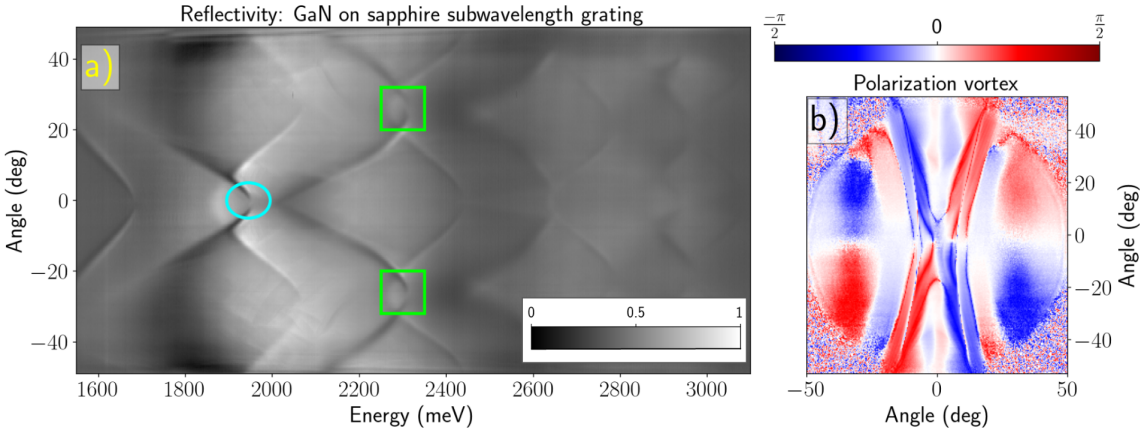

Figure 1: a) Angle resolved reflectivity measurements of GaN on sapphire subwavelength grating. BIC states are observed at $k = 0$ (blue circle) or $k \neq 0$ (green rectangle). b) Polarization vortex of a mode involving BIC at $k = 0$.

[1] H. M. Doeleman et al. *Nature Photonics*, 12(7):397–401, Jul 2018.

The research was partially supported by the Foundation for Polish Science through the IRA Programme co-financed by EU within SG OP (Grant No. MAB/2017/1)

Dynamics and Effective Interactions of a Photonic Condensate in an Optical Trap

Antonina Bieganowska [1], Christian Schneider [2], Sven Höfling [3], Sebastian Klembt [3], Marcin Syperek [1] and Maciej Pieczarka [1]

[1] *Department of Experimental Physics, Faculty of Fundamental Problems of Technology, Wrocław University of Science and Technology, Wyb. Wyspiańskiego 27, 50-370*
[2] *Institue of Physics, University of Oldenburg, Oldenburg 26129, Germany*
[2] *Technische Physik and Wilhelm-Conrad-Röntgen-Research Center for Complex Material Systems, Universität Würzburg, Am Hubland, 97074 Würzburg, Germany*

The bosonic nature of both polaritons and photons allows them to achieve Bose-Einstein condensation (BEC), forming a macroscopically coherent state. Polariton and photon condensates are intensively studied systems, where the nature of equilibrium and non-equilibrium BEC is explored. In high density regime, the strong coupling between excitons and photons is lost, and the system undergoes a crossover into the weak coupling, where one can observe a photonic condensate. On one hand, exciton polaritons interact with each other because of the excitonic component. On the other hand, interactions within the photonic condensate may originate from nonlinearities of the active material itself, e.g. via nonlinear refractive index, which has not been reported yet, especially using the geometry of an optical trap. These interactions are expected to manifest as collective Bogoliubov spectrum of excited states.

In this contribution, by using a GaAs-based microcavity sample, we experimentally study dynamics of photonic condensate in an optically induced trap and the effects of photon-photon interactions by measuring the momentum dispersion using the time-resolved spectral tomography on a streak camera. The sample is excited with the pumping pulsed laser shaped into a ring to obtain an effective potential created by the photo-excited reservoir. In the weak coupling regime, the effective potential results from local changes of the cavity's refractive index induced by excessive carriers, which act at the same time as the photon gain [1]. At strongest pumping powers - which correspond to the highest particle densities in the system - modification of the photon condensate dispersion is clearly visible, which can be a signature of effective photon-photon interactions. The photonic condensate is driven-dissipative in nature, hence in the experiment we observe a shape resembling the dissipative Bogoliubov spectrum, Figure 1 [2]. Our results are important in further understanding of the nature of photonic condensates as well as in their undiscovered dynamics.

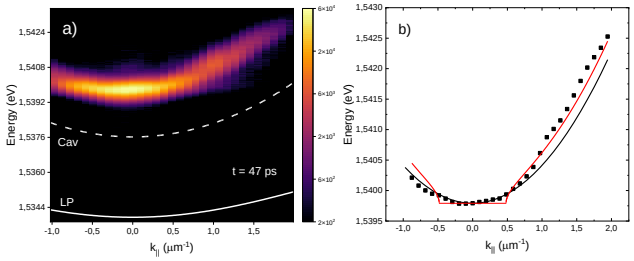

Figure 1. (a) Measured dispersion of a photonic condensate at highest pumping power at time after pulse corresponding to the highest photon density. Theoretical photon and polariton curves are marked with Cav and LP. (b) Extracted energies from (a) (squares), with blueshifted theoretical cavity mode (black line) and fit with the dissipative Bogoliubov dispersion (red line).

[1] M. Pieczarka et al., *Opt. Express* **30**, 17070 (2022).
[2] J. Bloch, I. Carusotto and M. Wouters, *Nat. Rev. Phys.* **4**, 470-488 (2022).

Advances and Prospects of Gallium Oxide Material and Device Technologies

Masataka Higashiwaki[1,2]

[1]*Department of Physics and Electronics, Osaka Metropolitan University, Sakai, Osaka 599-8531, Japan*
[2]*National Institute of Information and Communications Technology, Koganei, Tokyo 184-8795, Japan*

Gallium oxide (Ga_2O_3) is not a novel material and has a long history of more than 60 years. Especially, it has been well recognized as a native oxide formed on GaAs and GaN. However, as a semiconductor material, single-crystal Ga_2O_3 had been largely ignored by a great majority of researchers and engineers, even though it possesses attractive material properties such as an extremely large bandgap energy of 4.5 eV, a projected large critical electric field of over 7 MV/cm, and availability of large-diameter single-crystal wafers produced from melt-grown bulks. This situation changed in 2011, with our demonstration of first single-crystal Ga_2O_3 field-effect transistors (FETs) [1]. Since then, Ga_2O_3 has attracted much attention as an emerging semiconductor, especially due to high expectations for applications to future power switching and harsh environment electronics [2, 3]. Now, Ga_2O_3 has been widely recognized as a key material among ultrawide bandgap semiconductors, which are defined by bandgap energy exceeding those of SiC and GaN.

In this talk, after a brief introduction of material properties of Ga_2O_3, state-of-the-art Ga_2O_3 material and device technologies will be introduced, based on world-wide recent research activities conducted by both our group and external research organizations. In addition, a brief outlook on Ga_2O_3 device applications will be given.

A part of the works presented in this talk was supported by the Development Program, "Next-Generation Energy-Saving Devices" of the Ministry of Internal Affairs and Communications, Japan (JPMI00316).

[1] M. Higashiwaki, K. Sasaki, A. Kuramata, T. Masui, and S. Yamakoshi, *Appl. Phys. Lett.* **100**, 013504 (2012).
[2] M. Higashiwaki and G. H. Jessen, *Appl. Phys. Lett.* **112**, 060401 (2018).
[3] M. Higashiwaki, *Phys. Status Solidi RRL* **15**, 2100357 (2021).

Radiation Effects in Wide Bandgap Materials

Katharina Lorenz [1,2], **Duarte M. Esteves** [1,2], **Daniela R. Pereira** [1,2], **Dirkjan Verheij** [1,2], **Luís C. Alves** [3], **Marco Peres** [1,2]

[1] *Instituto de Engenharia de Sistemas de Computadores-Microsystems and Nanotechnology (INESC MN), Rua Alves Redol 9, 1000-029 Lisboa, Portugal*

[2] *IPFN and DECN, Instituto Superior Técnico, University of Lisbon, Estrada Nacional 10, 2695-066 Bobadela, Portugal.*

[3] *C2TN and DECN, Instituto Superior Técnico, University of Lisbon, Estrada Nacional 10, 2695-066 Bobadela, Portugal.*

Wide bandgap semiconductors (WBS) enable electronic devices to operate at high power, high frequency and high temperature. Moreover, many WBS are considered more radiation-resistant than conventional semiconductors such as Si or GaAs, making them interesting for applications in extreme radiation environments, such as space. However, radiation effects in WBS are usually very complex due to the diversity of the lattices of these compound crystals which often have nonequivalent lattice sites, mixed bonding schemes or different polymorphs. Moreover, the high mobility of point defects can promote the formation of extended defects.

Benefiting from the remarkable radiation resistance of GaN, we developed radiation sensors based on single GaN microwires [1]. Their potential for the detection of ionising radiation as well as their degradation upon high fluence ion irradiation will be discussed. Interestingly, radiation defects are not always a nuisance. Two examples will show how ion beams can be used to tune the electrical and optical properties of WBS. In MoO_3, the electrical conductivity can be controlled over several orders of magnitude by oxygen implantation [2]. In Ga_2O_3, irradiation defects interact with chromium dopants, promoting their optical activation [3, 4]. Such defect engineering strategies will allow novel processing techniques and device designs.

[1] D. Verheij et al., *Appl. Phys. Lett.* **118,** 193501 (2021).
[2] D. R. Pereira et al., *Acta Materialia*, **169**, 15 (2019).
[3] M. Peres et al., *Appl. Phys. Lett.* **120**, 261904 (2022).
[4] D. M. Esteves et al., *Scientific Reports* **13**, 4882 (2023).

"ACS Omega": A High Quality, Global, Open Access Journal from the American Chemical Society

Dinesh Soares

American Chemical Society International, ACS Publications, Binsey House, Wallbrook Court, North Hinksey Lane, Oxford, United Kingdom

"ACS Omega" was launched in 2016 as the first gold open access journal in the ACS Publications portfolio. In this talk, I will introduce you to the American Chemical Society and ACS Publications, share information about "ACS Omega", its scope, mission, and editorial board, and take you through its key performance metrics from its inception to its current status as one of the world's largest, high-quality Open Access journals in the chemical sciences and interfacing areas.

"Nextnano" Workshop at Jaszowiec 2023

Herbert S.Mączko

nextnano GmbH, Konrad-Zuse-Platz 8, 81829 München, Germany

Are you interested in getting started with our next-generation nanotechnology software?Look no further than nextnano Workshop, providing the perfect opportunity for education and skill-building.

Led by our experienced instructors, the workshop offers a comprehensive introduction to the software. You will learn how to create simulations of nanoscale devices and how to analyze simulation results.

Topics Covered:

- Overview of all capabilities of the nextnano software
- Documentation
- How to use the nextnano software efficiently
- Learning nextnano++ on examples
    - structure definition
    - introducing strain
    - Poisson solver (pn junction)
    - Current-Poisson solver (IV curve of pn junction)
    - Schrödinger solver (quantum dot)
    - Schrödinger-Poisson solver (2DEG)
    - Schrödinger-Poisson-Current solver (LED)
    - optical spectra (quantum wire)
- Material database
- nextnano support

To make the most of the workshop, we recommend you bring your own laptop. Don't miss out on this opportunity to learn from the best and take your understanding of semiconductors to the next level. All participants will get evaluation licenses for nextnano++ package for 3 months

Magnetophonon resonances in graphene

M.T. Greenaway[1,2], P. Kumaravadivel [3,4], J. Wengraf [3,5], L.A. Ponomarenko[3,5], A.I. Berdyugin[3], J. Li[6], J.H. Edgar[6], R. Krishna Kumar[3], A.K. Geim[3,4], and L. Eaves[2]

[1]Department of Physics, Loughborough University,
[2]School of Physics and Astronomy, University of Nottingham,
[3]School of Physics and Astronomy, University of Manchester,
[4]National Graphene Institute, University of Manchester,
[5]Department of Physics, University of Lancaster,
[6]Tim Taylor Department of Chemical Engineering, Kansas State University.

Resonant magnetoresistance measurements on monolayer graphene FETs under "ohmic" low current conditions have been used to study a wealth of novel physics. Recently, we observed magnetophonon resonance (MPR) in graphene, where peaks, periodic in inverse magnetic field, emerge in the magnetoresistance due to inelastic acoustic phonon scattering of electrons between Landau levels [1]. MPR provides a measurement of the transverse (TA) and longitudinal (LA) acoustic phonon velocities and gives insight into the nature of electron-phonon coupling.

At high currents (up to 100 Am^{-1}), electrons are driven far from equilibrium so that their kinetic energy can exceed the thermal energy of the phonons. We observe three non-equilibrium phenomena in monolayer graphene at high currents [2]: (i) a "Doppler-like" shift and splitting of the frequencies of the TA phonons, revealed by shifts of the MPR resonant peaks in the differential resistance, r_y (see Fig. 1a); (ii) an intra-LL Mach effect with the emission of TA phonons when the electrons approach supersonic speed ($\sim$1.4 x 10^4 ms^{-1}), revealed by a broad magnetic field-independent peak in r_y at $I \sim 1$ mA ($\sim$ 70 Am^{-1}) and (iii) the onset of elastic inter-LL transitions and an associated resonance maximum in r_y at a critical carrier drift velocity (see Fig 1b). The third phenomenon is analogous to a "superfluid" Landau velocity and the formation of magneto-excitons involving a quantum jump, h/m, in the electron LL circulation. All three phenomena can be unified in a generic resonance equation. They offer avenues for research on out-of-equilibrium phenomena in other two-dimensional systems.

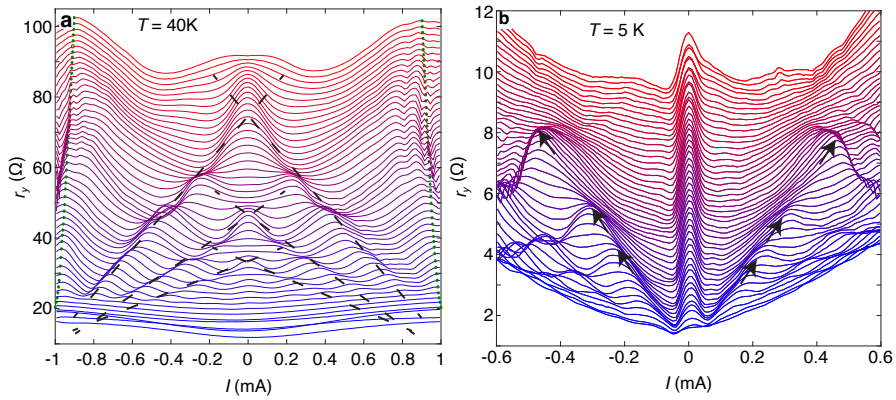

Fig. 1. (a) Plot of the dependence of differential resistance $r_y(I)$ on current for magnetic fields, B, between 0 and 2 T in 0.04 T intervals, measured at a carrier density $n = 3.16 \times 10^{12}$ cm^{-2}. Curves are offset by 1.5 Ω and the dashed lines highlight the shift of the positions of the magnetophonon resonance peaks. The green markers close to $I = \pm 1$ mA show the position of the B-independent peak in $r_y(I)$ when the electrons approach supersonic speed. (b) Plot of $r_y(I)$ for values of B between 0 to 1.2 T. Black arrows highlight the shifts of the resonant peaks in r_y due to elastic inter-LL transitions that arise when the electron velocity approaches the Landau velocity.

[1] P. Kumaravadivel *et al.*, *Nature Communications* **10,** 3334 (2019)
[2] M.T. Greenaway *et al.*, *Nature Communications* **12**, 6392 (2021)

Kardar-Parisi-Zhang universality in a one-dimensional polariton condensate

S. Ravets[1]

[1] *Université Paris-Saclay, CNRS, Centre de Nanosciences et de Nanotechnologies (C2N), 91120, Palaiseau, France*

Cavity polaritons are hybrid exciton-photon quasi-particles emerging from the strong coupling regime between photons confined in an optical cavity and excitons confined in quantum wells. They present physical properties reflecting their mixed nature. From the photon part, they inherit a small effective mass and can be confined in lattices with typical dimensions of the order of a few microns. Their excitonic part endows them with inter-particle interactions resulting in a giant Kerr non linearity. Cavity polaritons exhibit fascinating properties such as Bose Einstein condensation at elevated temperature, superfluidity, multistability... Importantly, the system is driven-dissipative in nature: the driving field maintains an out-of-equilibrium steady-state by compensating the constant leakage of photons.

Recent theoretical works have shown that the phase dynamics of out-of-equilibrium condensates obeys the celebrated Kardar Parisi Zhang (KPZ) equation [1-3]. In this talk, I will present our recent experimental observation of universal KPZ scaling laws in the first order coherence of a 1D polariton condensate [4]. I will first explain how we generated highly elongated polariton condensates in a 1D polariton lattice. I will then describe our measurements of the condensate coherence. Finally, I will show that data points lying within a well-defined spatio-temporal window collapse onto a single scaling function, characteristic of the KPZ universality class.

[1] Altman, E., Sieberer, L. M., Chen, L., Diehl, S., and Toner, J. *Physical Review X* **5**, 011017 (2015).
[2] Ji, K., Gladilin, V. N., and Wouters, M. *Physical Review B* **91**, 045301 (2015).
[3] He, L., Sieberer, L. M., Altman, E., and Diehl, S. *Physical Review B* **92**, 155307 (2015).
[4] Q. Fontaine, D. Squizzato, F. Baboux, I. Amelio, A. Lemaître, M. Morassi, I. Sagnes, L. Le Gratiet, A. Harouri, M. Wouters, I. Carusotto, A. Amo, M. Richard, A. Minguzzi, L. Canet, S. Ravets, and J. Bloch, *Nature* **608**, 687 (2022).

Time-resolved nonlinear optical spectroscopy of basic excitations in 2D materials

Daniel Wigger

School of Physics, Trinity College Dublin, Ireland

Since their discovery in 2010, the study of optically active 2D materials in the form of transition metal dichalcogenides, has grown to a distinguished area of research in solid state optics. In these materials tightly bound excitons dominate the optical response and lead to rich multi-particle physics based on the interplay with light, phonons, single charges, and other excitons. While microscopic descriptions, e.g., based on semiconductor Bloch equations, reveal many effects arising from the different coupling mechanisms, we have employed a handy mean-field extension of the optical Bloch equations. We take a local field coupling and excitation-induced dephasing into account, which account for exciton-exciton interactions [1]. The appeal of this approach lies in the fact that it allows to derive analytic expressions for optical signals even for complex nonlinear wave-mixing experiments in the limit of ultrafast pulses [2]. The local field model has proven to reproduce pump-probe [3], four-wave mixing [4, 5], and even six-wave mixing features [4] surprisingly well, despite its mathematical simplicity. In the first part of my talk I will explain the basic consequences of the local field model and present our recent results on four-wave mixing spectroscopy on gate-controlled $MoSe_2$ monolayers, which reveal the coherence properties and couplings of different exciton complexes when changing the electronic density in the system [5].

In the second part I will move to the van der Waals insulator hexagonal boron nitride (hBN), which is recently gaining significant attention because it can host bright colour centres operating as single photon emitters at room temperature. These quantum emitters also stand out due to their remarkably strong coupling to optical and acoustic phonons. In the second part of my presentation I will discuss our recent coherent control study of phonon-assisted excitation of single hBN colour centres [6]. Through this Ramsey–interferometry-like method we were able to determine the coherence times of bare and optical–phonon-assisted excitations and demonstrate the coherence loss induced by the emission of acoustic phonon wave packets.

[1] M. Wegener, D. S. Chemla, S. Schmitt-Rink, and W. Schäfer, *Phys. Rev. A* **42**, 5675 (1990).

[2] T. Hahn, J. Kasprzak, P. Machnikowski, T. Kuhn, and D. Wigger, *New J. Phys.* **23**, 023036 (2021).

[3] A. Rodek, T. Hahn, J. Kasprzak, T. Kazimierczuk, K. Nogajewski, K. Watanabe, T. Taniguchi, T. Kuhn, P. Machnikowski, M. Potemski, D. Wigger, and P. Kossacki, *Nanophotonics* **10**, 2717 (2021).

[4] T. Hahn, D. Vaclavkova, M. Bartos, K. Nogajewski, M. Potemski, K. Watanabe, T. Taniguchi, P. Machnikowski, T. Kuhn, J. Kasprzak, and D. Wigger, *Adv. Sci.* **9**, 2103813 (2022).

[5] A. Rodek, T. Hahn, J. Howarth, T. Taniguchi, K. Watanabe, M. Potemski, P. Kossacki, D. Wigger, and J. Kasprzak, arXiv:2302.13109 (accepted in 2D Mater.).

[6] J. A. Preuß, D. Groll, R. Schmidt, T. Hahn, P. Machnikowski, R. Bratschitsch, T. Kuhn, S. Michaelis de Vasconcellos, and D. Wigger, *Optica* **9**, 522 (2022).

The study of resonant Raman scattering in semiconducting layered GeS

L. Bryja [1], J. Andrzejewski [1], J. Debus [2], C.-H. Ho [3] and J. Jadczak [1]

[1] *Department of Experimental Physics, Wroclaw University of Science and Technology, Wroclaw, Poland*
[2] *TU Dortmund University, 44227 Dortmund, Germany*
[3] *Graduate Institute of Applied Science and Technology, National Taiwan University of Science and Technology, Taipei, 106, Taiwan*

Semiconducting layered group IV monochalcogenides such as black phosphorous and germanium sulfide with an anisotropic puckered crystalline structure in each layer have recently attracted much attention due to their unique optical and electronic properties and anticipated applications in optoelectronics [1]. Resonant Raman scattering (RRS) is an efficient tool for studding of vibrational properties as well as electron-phonon interactions. Here, we report on investigation of low temperature (T = 7 K), polarization-resolved, resonant Raman scattering experiments on GeS flakes in the range from 90 to 720 cm^{-1}. The RRS measurements are performed in back scattering configuration using a DCM dye laser with a tunable wavelength from 670 to 690 nm (Fig. 1). In order to determine the energy and optical polarization of the neutral exciton (X) complementary photoluminescence (PL) and reflectance (R) experiments are performed. In non-resonant RS spectra four Raman active modes A^2_g, A^3_g, A^4_g and B^2_{1g} are observed, however, when the excitation energy is tuned towards to the energy of the X we can resolve in the Raman spectra 18 peaks, among which 14 have not been reported previously in the back scattering configuration. Intensity of all the new Raman features significantly increases as they are brought into resonance with the neutral exciton. Additionally, they exhibit almost the same polarization dependence as the X. Analysis of the origin and assignment of new phonon modes are based on their energies, polarization-dependent intensities, numerical calculations and comparison with previous experimental and theoretical studies of the Raman scattering in GeS and resonant Raman scattering in other materials. Accordingly, new features in the RRS spectra are attributed to infrared active and second-order phonon modes.

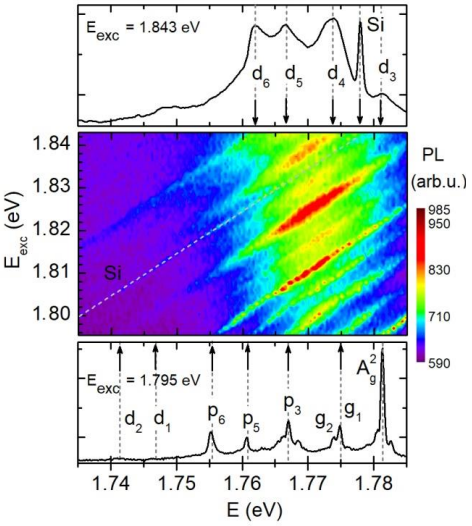

Fig. 1 False-color map of low-temperature PLE/RRS spectra of GeS as a function of the excitation energy E_{exc}.

[1] C.H. Ho et al., *Adv. Optical Mater* **5**, 1600814 (2017).

Quantum anomalous Hall insulator in ionic Rashba lattice of correlated electrons

Marcin M. Wysokiński[1] **and Wojciech Brzezicki**[1,2]

[1] *International Research Centre MagTop, Institute of Physics,Polish Academy of Sciences*
Aleja Lotników 32/46, PL-02668 Warsaw, Poland
[2] *Institute of Theoretical Physics, Jagiellonian University,*
Prof. Stanisława Łojasiewicza 11, PL-30348 Kraków, Poland

We propose an exactly solvable two-dimensional lattice model of strongly correlated electrons that realizes a quantum anomalous Hall insulator with Chern number $\mathcal{C} = 1$. We show that the interplay of ionic potential, Rashba spin-orbit coupling and Zeeman splitting leads to the appearance of quantum anomalous Hall effect. Moreover, we calculate in an exact manner Chern number for the correlated system where electron-electron interactions are introduced in the spirit of Hatsugai-Kohmoto model using two complementary methods, one relying on the properties of many-body groundstate and the other utilizing single-particle Green's function, and subsequently we determine stability regions. By leveraging the presence of inversion symmetry we find boundaries between topological and trivial phases on the analytical ground. Notably, we show that in the presence of correlations onset of topological phase is no longer signalled by a spectral gap closing. We provide a clear understanding of this inherently many-body feature by pinpointing that the lowest energy excited states in the correlated system are no longer of the single-particle nature and thus are not captured by a spectral function.

[1] M. M. Wysokiński, W. Brzezicki *arXiv:2303.04454* (2023)

Exciton Diffusion in an Ensemble of Self-Assembled Semiconductor Quantum Dots

Karol Kawa and Paweł Machnikowski

Institute of Theoretical Physics, Wrocław University of Science and Technology, 50-370 Wrocław, Poland

Electron-hole kinetics is at the heart of semiconductor physics. Coupled electron-hole pairs, which are the fundamental excitations in a semiconductor, are able to move. In particular, exciton transfer occurs in self-assembled semiconductor quantum dot (QD) ensembles [1]. Despite the possible tunneling of carriers between QDs (Dexter-like transfer), the experiment [1] revealed enhanced transport in (two-dimensional) ensembles with a low spatial density of QDs where tunneling is inefficient. This suggests Förster resonance energy transfer (FRET) [2] as the transfer mechanism, that is, the photon-assisted process by which an exciton is annihilated in one dot and simultaneously created in another.

Therefore, we theoretically study exciton diffusion due to Förster transfer in an inhomogeneous ensemble of QDs randomly distributed on a circular mesa. QDs are assumed to be quantum emitters with one ground- and one excited state selected by the light polarization. The analytical formula of the Förster coupling is known for the general ensemble of quantum dipole emitters [3, 4]. It has the form of a sum of three power-law terms decreasing with distance, each multiplied by an oscillating factor. The inhomogeneity is given by a random distribution of the fundamental transition energy in each QD. In addition, a finite exciton lifetime is included. We derive and solve the equation of motion for the density matrix using the stochastic simulation method with a given exciton decay rate or by exact diagonalization for idealistic nondissipative systems.

Diffusion is described by time-dependent mean square displacement (MSD) and exciton density distrubution in space and time. Exciton diffuses in three subsequent time stages. First, there is a ballistic motion followed by a normal diffusion, which ends at saturation. The exciton density reveals a similar time dependence as MSD and a power-law localization in space. Furthermore, stochastic simulation allows us to trace the time dependence of the intensity of photoluminescene.

Finally, we present an approximate analytical solution, developed by us in [5, 6], which covers most of the effects predicted by the simulations, especially the triple-stage diffusion. The relatively small Förster coupling compared to the energy inhomogeneity of the ensemble validates the first-order approximation in which only direct transfer to remote QDs is important and allows one to express the MSD and exciton density analytically.

[1] F. V. de Sales et al., Phys. Rev. B 70, 235318 (2004).
[2] T. Förster, Ann. Phys., 437, 55 (1948).
[3] M. J. Stephen, J. Chem. Phys. 40, 669 (1964).
[4] R. H. Lehmberg, Phys. Rev. A 2, 883 (1970).
[5] K. Kawa and P. Machnikowski, Phys. Rev. B 102, 174203 (2020).
[6] K. Kawa and P. Machnikowski, Phys. Rev. B 105, 184204 (2022).

Introducing the step Monte Carlo method for simulating dynamic properties

Dariusz Sztenkiel

Institute of Physics, Polish Academy of Sciences, al. Lotników 32/46, 02-668 Warszawa, Poland

The Monte Carlo (MC) approach is now an essential ingredient in many quantitative studies and branches of science including physics, finance-economics, biology, engineering, etc. In the field of condensed matter physics and materials science MC can be used to study, among many others, system of classical particles [1], classical spin systems [2], percolation and fractals problems. The MC algorithm is the natural choice for studying the static properties of a system, where dynamical effects are not required. Then, the advantages of Monte Carlo are the relative ease of implementation and the rapid convergence to steady state.

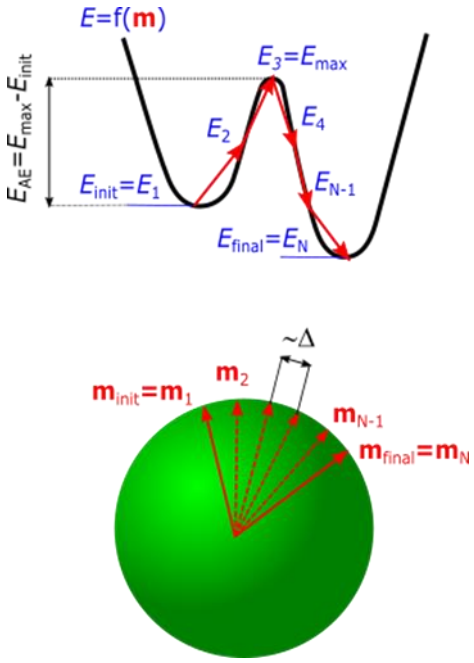

Fig. 1. Schematic illustration of the step Monte Carlo (sMC) method for the case of magnetization process (one Monte Carlo move). The magnetization direction $\mathbf{m}$ (bottom panels) can take any point on the unit sphere with energy $E = f(\mathbf{m})$ (top panels). $\mathbf{m}_{init}$ and $\mathbf{m}_{final}$ are initial and final (trial) direction of magnetic moment with energy E_{init} and E_{final} respectively. In the sMC approach the probability of accepting the final random state $\mathbf{m}_{final}$ depends on the activation energy $E_{AE} = E_{max} - E_{init}$, not on the relative energy $E_{final} - E_{init}$.

In the modified MC approach proposed here (similarly to the kinetic MC approach) the probability of accepting the final state depends on the activation energy, not on the relative energy between the final and initial state [3]. However, the barrier height is calculated on an ongoing basis, by generating intermediate states with a predefined step Δ. Therefore, we name this method step Monte Carlo (sMC) [3]. Importantly, the sMC method correctly takes into account the presence of various local barriers and it obeys the detailed balance condition, even if the system is not in equilibrium. As a result, the appropriate dynamics of the tested system is simulated. The details of sMC algorithm are explained for the case of magnetization process. To test the correctness of sMC, we compare its results with those obtained by stochastic Landau-Lifshitz-Gilbert (sLLG) approach.

[1] D. Frenkel and B. Smit, "Understanding Molecular Simulation: From Algorithms to Applications", Academic Press, San Diego (2002).

[2] M. Sawicki, T. Devillers, S. Galeski, C. Simserides, S. Dobkowska, B. Faina, A. Grois, A. Navarro-Quezada, K. N. Trohidou, J. A. Majewski, T. Dietl, and A. Bonanni, *Phys. Rev. B*, **85**, 205204 (2012)

[3] D. Sztenkiel, "Introducing the step Monte Carlo method for simulating dynamic properties," arXiv:2209.08961 (2022).

Novel Te-bearing half-Heusler phases and their potential thermoelectric performance

Kaja Bilińska [1], **Maciej J. Winiarski** [1]

[1] *Institute of Low Temperature and Structure Research, Polish Academy of Sciences, Okólna 2, 50-422 Wrocław, Poland*

Theoretical predictions from first principles were conducted on nine half-Heusler tellurides ($M^{IV}M^{VIII}Te$, where M^{IV} = Ti, Zr, Hf, and M^{VIII} = Fe, Ru, Os), each possessing 18 valence electrons. Among the compounds investigated, eight were found to be novel and mechanically stable according to the Born criteria for elastic constants. The MBJGGA approach predicted eight of the examined compounds to be semiconductors, with band gaps ranging from 0.395 eV (ZrOsTe) to 1.247 eV (ZrRuTe). Detailed analysis was conducted on the band gaps, spin-orbit splitoffs of heavy- and light-hole bands, elastic constants, and effective masses in the half-Heusler tellurides. Chemical trends were observed for the transition metal ions considered, with Fe-bearing compounds exhibiting the widest band gaps. The compounds ZrOsTe and HfRuTe are expected to have potential applications in thermoelectric devices due to Mahan's '10 k_B T rule'. The thermoelectric performance was discussed based on transport calculations, the deformation potential theory approximation for the relaxation time of carriers, and Slack's approximation for the lattice thermal conductivity. ZT (figure of merit) values as high as 2.76 and 4.14 at 1100 K were predicted for ZrOsTe and HfRuTe, respectively. This comprehensive investigation of half-Heusler tellurides presents interesting systems for further experimental research.

Calculations were performer in Wroclaw Center for Networking and Supercomputing (Project no. 158).

[1] K. Bilińska, D. Goles, M. J. Winiarski, *under review (Journal of Physics and Chemistry of Solids)*.

[2] K. Bilińska, M. J. Winiarski, *under review (Solid State Communications)*.

[3] M. J. Winiarski, K. Bilińska, D. Kaczorowski, K. Ciesielski, J. Alloys Compd. **762**, 901 (2018).

[4] M. J. Winiarski, K. Bilińska, Intermetallics **108**, 55 (2019).

[5] M. J. Winiarski, K. Bilińska, Acta Phys. Pol. **138**, 533 (2020).

Optimizing the cap thickness in fabrication of quantum dot photonic structures by focused ion beam

Maciej Jaworski[1,2], Aleksandra Chudzyńska[2,3], Paweł Mrowiński[1], Grzegorz Sęk[1]

[1] *OSN Laboratory, Department of Experimental Physics, Wrocław University of Science and Technology, Wybrzeże Wyspiańskiego 27, 50-370 Wrocław, Poland*
[2] *Nanores, Bierutowska 57-59, 51-317 Wrocław, Poland*
[3] *Department of Optical Spectroscopy W. Trzebiatowski Institute of Low Temperature and Structural Research of the Polish Academy of Sciences, Okólna 2 Wroclaw 50-422, Poland*

In recent years, much attention has been paid to the fabrication and investigation of various photonic structures, such as micro-mesas, micro-lenses, micropillar cavities or photonic crystal slabs integrated with quantum dot emitters to optimize the performance in terms of non-classical light sources for quantum technology applications. There exists different fabrication methods of such structures. In this work, we use a focused xenon ion plasma beam (Xe-PFIB), which on one hand can suffer from a possible destructive influence on the crystal structure due to ion implantation, thus reducing the internal quantum efficiency of the source, i.e. intensity of photoluminescence from quantum dots.

Therefore, the goal of this study is to find the optimal range of cap layer thickness which assures efficient emission. The processes have been made on an exemplary QD material system of InGaAs/GaAs with the emission in the application-relevant range of the 2nd telecommunication window. By using wet chemical etching process, first we prepared samples with the cap thickness in the range from above 600 nm down to approx. to 50 nm. Next, a series of cylindrical micro-mesas of 4 μm in diameter were fabricated using the Xe-PFIB. The ion beam energy of 30 keV and the beam current of 1nA were selected according to our preliminary tests. The fabricated pillar-like photonic structures in function of the cap thickness were then characterized by low-temperature micro-photoluminescence (μ-PL) measurements. Based on the single dot emission intensity dependence on the decreasing of the cap layer thickness, we found that the minimum cap thickness lies between 200 nm and 150 nm, for the given beam parameters and the chosen material system. Last, we considered further optimization steps, which relied on the carbon layer deposition to protect from the unwanted ion implantation, could potentially allow for the Xe-PFIB processing for even thinner cap layers.

This work has been supported by the “Implementation doctorate” program of the Polish Ministry of Education and Science within grant No. DWD/4/50/2020. We would also like to thank Sven Rodt and Stephan Reitzenstein from Technische Universität Berlin for providing the semiconductor quantum dot materials used in this study.

Facile Synthesis of Semiconductor Nanostructures with Variable Plasmonic Properties Using Pulsed Laser Ablation Technique

Yury V. Ryabchikov

HiLASE Centre, Institute of Physics of the Czech Academy of Sciences,
Scientific Laser Application Department, 828 Za Radnicí, Dolní Břežany, Czech Republic

Different semiconductor nanostructures such as silicon or carbon nanoparticles are promising nanomaterials in many various applications such linear or nonlinear bioimaging, optical nanothermometry, gas sensing, radio-frequency-induced hyperthermia etc. However, their simultaneous applications in different applications can be considerably limited due to the absence of specific features related to noble metal or magnetic metals. Thus, merging of semiconductor nanostructures with various metallic elements in the form of one nanoparticle by designing of multielement nanocomposites can significantly enlarge the application area of semiconductor nanomaterials.

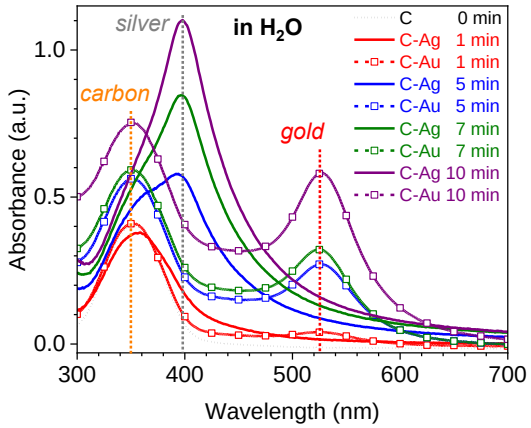

Figure 1. Laser ablation time-dependent plasmonic properties of fluorescent carbon nanocomposites with tuneable plasmonic properties.

In this work, the synthesis of various composite semiconductor-based nanoparticles with variable both efficiency and spectral position of their plasmonic properties was carried out by pulsed laser ablation in liquids (PLALs) techniques providing a facile formation of multi-element nanostructures of high chemical purity. In particular, carbon and silicon nanoparticles with strong linear and nonlinear photoluminescence, respectively, were used for the development of composite nanostructures. The performed laser-induced structural modification of semiconductor nanomaterials provides the strong plasmonic properties whose efficiency can easily be controlled by the laser irradiation time (Figure 1). The structural properties of the synthesized nanocomposites were investigated by different X-ray techniques such as X-ray diffraction (XRD) and X-ray photoelectron spectroscopy (XPS) as well as by electron paramagnetic resonance (EPR). Moreover, an impact of the chemical composition on the emission properties of fluorescence carbon nanodots was studied by the steady-state photoluminescence showing the modification of the fluorescence spectra of carbon nanodots upon the laser ablation time. The performed laser-induced change of the semiconductor nanostructure performance reveals new applications of silicon and carbon nanostructures in the field of nanoplasmonics related to the sensing of different molecules using surface-enhanced effects due to the presence of noble metal elements.

Acknowledgements:

Yu.V.R. acknowledges the European Union's Horizon 2020 research and innovation programme under the Marie Skłodowska-Curie grant agreement No 897231 (LADENTHER) as well as the European Regional Development Fund and the state budget of the Czech Republic (Project BIATRI: CZ.02.1.01/0.0/0.0/15_003/0000445) as well as the Ministry of Education, Youth and Sports (Programs NPU I-Project no. LO1602).

Optical Properties of Silicon Nanowires-Based Composites

Yury V. Ryabchikov

HiLASE Centre, Institute of Physics of the Czech Academy of Sciences,
Scientific Laser Application Department, 828 Za Radnicí, Dolní Břežany, Czech Republic

Nanostructured silicon represent a great class of nanomaterials including various nanostructures such as porous silicon, silicon nanowires, silicon (oxy-)nitride, silicon carbide, silicon nanoparticles formed by pyrolysis, chemical etching or pulsed laser ablation techniques. Formation of low-dimensional materials reveal new unique structural and optical properties as compared to bulk silicon significantly depending on a type of a silicon wafer, used treatment procedure, nanostructuring conditions etc.

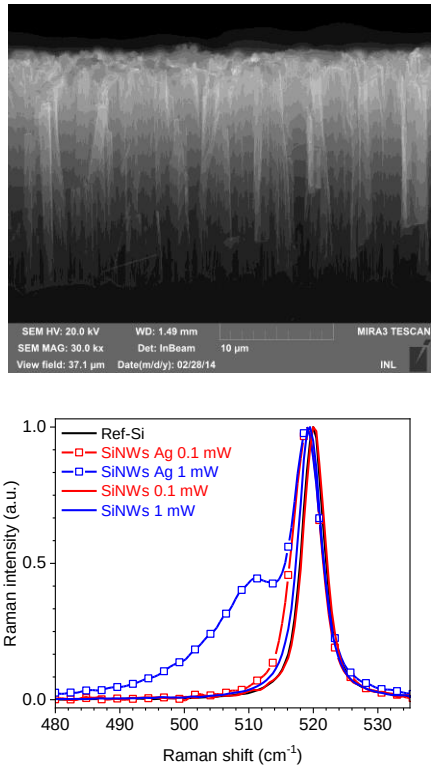

Figure 1. SEM image (on the top) and Raman shift (on the bottom) of Si NWs with and without Ag nanostructures at different laser power (488 nm).

One of the perspective candidates is silicon nanowires (Si NWs) formed by metal-assisted chemical etching of a bulk silicon wafer possessing highly aligned structure of silicon nanocrystals contrary to chaotic one in porous silicon films. It leads to more homogeneous and reproducible structural and optical properties of Si NWs that can be employed for photovoltaic, sensing or biomedical applications. Moreover, highly ordered porous structure of Si NWs makes them a nice matrix for introducing of different kinds of fluorophores, including other types of Si-based nanomaterials, in order to develop multifunctional nanoplatforms.

In this research, Si NWs were formed using different time of chemical etching (from 15 s to 30 min) and their properties were investigated. In particular, Si NWs possess considerable Raman shift at 520 cm^{-1} using various excitation wavelengths at the visible spectral range followed by some signal distortion with the increase of the laser power making Si NWs perspective for optical nanothermometry. Moreover, Si NWs also reveal some PL variable in the range of 600 – 700 nm depending on the used excitation wavelength (343 – 515 nm). Furthermore, introducing of silicon or silicon carbide nanoparticles formed by the chemical etching leads to some spectral shift of the maximum position of Si NWs photoluminescence as well as its intensity.

Thus, optical properties of Si NWs can be varied not only by changing of the synthesis conditions but also by introducing of different silicon-based nanostructures in pores of Si NWs matrix forming silicon composite material.

Acknowledgements:

Yu.V.R. acknowledges the European Union's Horizon 2020 research and innovation programme under the Marie Skłodowska-Curie grant agreement No 897231 (LADENTHER) as well as the European Regional Development Fund and the state budget of the Czech Republic (Project BIATRI: CZ.02.1.01/0.0/0.0/15_003/0000445) as well as the Ministry of Education, Youth and Sports (Programs NPU I-Project no. LO1602).

Non-equilibrium transport theory for dopant arrays in silicon

M. Gawełczyk[1,2], G. W. Bryant[3,4], M. Zieliński[1]

[1] *Institute of Physics, Faculty of Physics, Astronomy and Informatics, Nicolaus Copernicus University, 87-100 Toruń, Poland*

[2] *Institute of Theoretical Physics, Wrocław University of Science and Technology, Wrocław 50-370, Poland*

[3] *Atom Based Device Group, National Institute of Standards and Technology, Gaithersburg, MD, 20899, USA*

[4] *Joint Quantum Institute, University of Maryland, College Park, MD, 20740, USA*

The recent development of precise phosphorus donor placement in silicon [1,2] has attracted attention to the chains and arrays of such sites. Donor arrays have already proven well suited for quantum simulation of the Extended Hubbard [3] and SSH [4] models and are of major interest for future quantum-information devices.

In the experiment, systems of a few sites are gated and studied electrically in terms of so-called stability and Coulomb-blockade diagrams obtained by measuring the current while sweeping gate voltages. The theory aims then to simulate such diagrams and provide a two-way correspondence between the physical system and the simulated model. Thus, the need for a non-equilibrium transport theory of dopant systems arises.

Our approach based on combining exact diagonalization with non-equilibrium Green's functions allows for calculating both terminal and local currents in the arrays and other observables characterizing the system. Typically, by resorting to Green's functions, one loses the information on the underlying eigenstates. Our methodology lets us preserve this knowledge and back-trace states responsible for features of interest. This gives us a way to gain more information about the transport processes than can be obtained directly from transport measurements. Thus, we can, e.g., characterize the many-body configurations that contribute to the current, determine current magnitudes for different channels, and visualize how the electron flow circumvents disturbances in the form of array randomness. We study some of these effects to better understand transport studies of experimentally realized arrays [3].

Supported by the National Science Centre (Poland) under Grant No. 2015/18/E/ST3/00583.

[1] M. Fuechsle, J. A. Miwa, S. Mahapatra, H. Ryu, S. Lee, O. Warschkow, L. C. L. Hollenberg, G. Klimeck, M. Y. Simmons, *Nature Nanotech.* **7**, 242 (2012).

[2] J. Wyrick, X. Wang, R. V. Kashid, P. Namboodiri, S. W. Schmucker, J. A. Hagmann, K. Liu, M. D. Stewart, C. A. Richter, G. W. Bryant, R. M. Silver, *Adv. Funct. Mater.* **29**, 1903475 (2019).

[3] X. Wang, E. Khatami, F. Fei, J. Wyrick, P. Namboodiri, R. Kashid, A. F. Rigosi, G. W. Bryant, R. Silver, *Nature Commun.* **13**, 6824 (2022).

[4] M. Kiczynski, S. K. Gorman, H. Geng, M. B. Donnelly, Y. Chung, Y. He, J. G. Keizer, M. Y. Simmons, *Nature* **606**, 694 (2022).

Elimination of Early Breakdowns in Fully-Depleted Detectors of Ionizing Radiation

Krzysztof Kucharski, Paweł Janus, Andrzej Panas, Grzegorz Głuszko, Daniel Tomaszewski, Konrad Krzyżak

Łukasiewicz-Instytut Mikroelektroniki i Fotoniki, Al. Lotników 32/46, Warsaw, Poland

Reverse-biased P-N junctions are basic elements of many silicon detectors of electromagnetic radiation. They work under high reverse bias conditions (nominally 40 V). Therefore, a so-called early breakdown is a key parameter that determines whether given detector is good or bad. The term early breakdown denotes a rapid increase of the I-V characteristics of the reverse-biased P-N junction below an avalanche breakdown. Only detectors without early breakdowns can be candidates for real applications depending on the value of a so-called "dark" current. This work presents results of our technological experiments aimed at elimination of the early breakdowns in P-N junctions.

Circular diodes (diameter 4 mm) were fabricated on 4-inch high resistivity silicon wafers using different processing sequences. Next, electrical measurements of the junctions were done along the wafer diameter. The following technology variants were taken into consideration:

- devices after so-called "spray" n-type implantation (low dose and energy) of front side of the wafer;
- devices with different methods of doping of contact areas at the back side of the wafer: P implantation or diffusion from the $POCl_3$ source;
- devices with two thicknesses of poly-Si getter at the at the back side of the wafer: 1.1 µm, 1.6 µm;

Results of the experiment were as follows:

- "Spray" n-type implantation of front sides and back side contact implantation eliminated efficiently early breakdowns (Fig. 1). However, such doping methods can lead to degradation of "dark" currents. In such a case "dark currents" can be effectively improved using a poly-Si getter at the wafer back sides.
- Using the standard (thickness 1.1 µm) gettering process without implantation did not eliminate early breakdowns. However an increase of the getter thickness to 1.6 µm allowed to eliminate early breakdowns. Obviously, this method required a longer wafer processing.

a)

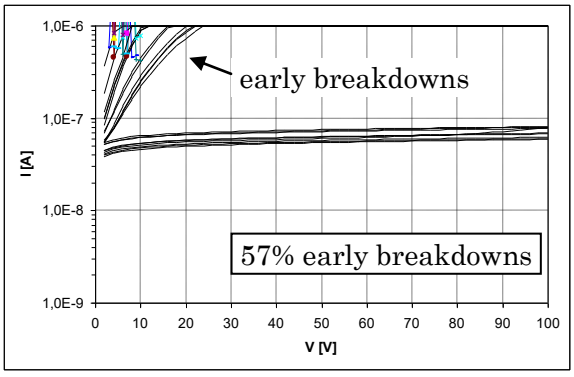

b)

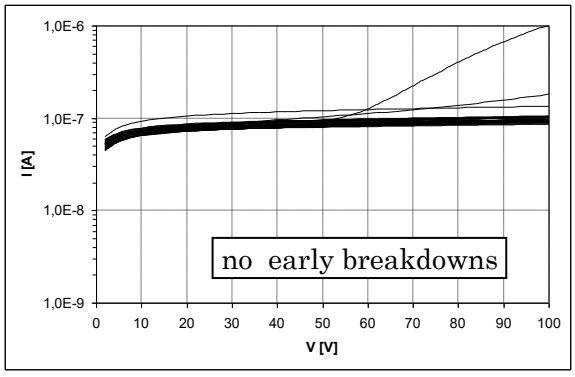

Fig.1 Effect of type of ohmic contact at the back side: a) $POCL_3$, b) P-implant.; in both cases standard, 1.1 µm-thick phosphorus doped poly-Si getter at the back side used.

Intervalley hybridization and optical properties of $Ge_{1-x}Sn_x$ quantum dots

Krzysztof Gawarecki[1], Paweł Scharoch[2], Jakub Ziembicki[2], Norbert Janik[2], Robert Kudrawiec[2]

[1] *Institute of Theoretical Physics, Wrocław University of Science and Technology, Wybrzeże Wyspiańskiego 27, 50-370 Wrocław, Poland*

[2] *Department of Semiconductor Materials Engineering, Wrocław University of Science and Technology, Wybrzeże Wyspiańskiego 27, 50-370 Wrocław, Poland*

The $Ge_{1-x}Sn_x$ alloy attract much attention due to its band gap dependence on the composition. At some critical Sn content (of a few percent), the bulk changes its character from the indirect- to the direct band gap [1, 2]. The other properties of $Ge_{1-x}Sn_x$, like high carrier mobility, makes this material interesting from the point of view of applications for optoelectronic devices [3].

We present a theoretical, atomistic study of electron and optical properties of $Ge_{1-x}Sn_x$ nanostructures. Within the $sp^3d^5s^*$ tight-binding model, we calculate the electron and hole states in $Ge_{1-x}Sn_x$ cubic boxes and colloidal quantum dots. We investigate the interplay of confinement effect and composition-induced indirect-direct band gap transition. We demonstrate an intervalley hybridization of the ground electron state and identify the relevant regimes of sizes and QDs compositions, where they are optically active. We also calculate the absorbance spectra of experimentally-relevant colloidal quantum dots [4].

The simulations are performed within the $sp^3d^5s^*$ tight-binding model [5] combined with the valence force field model to account for strain in the system. We find the parameters via fitting the target Ge, α-Sn and zincblende GeSn band structures calculated using DFT approach with MBJLDA functional [2].

References

[1] W. Wegscheider, K. Eberl, U. Menczigar, G. Abstreiter, Single-crystal Sn/Ge superlattices on Ge substrates: growth and structural properties, Appl. Phys. Lett. 57 (9) (1990) 875–877.

[2] M. Polak, P Scharoch and R Kudrawiec, The electronic band structure of $Ge_{1-x}Sn_x$ in the full composition range: indirect, direct, and inverted gaps regimes, band offsets, and the Burstein–Moss effect, 2017 J. Phys. D: Appl. Phys. 50 195103

[3] Gupta S, Gong X, Zhang R, Yeo Y, Takagi S and Saraswat K 2014 New materials for post-Si computing: Ge and GeSn devices MRS Bull. 39 678–86

[4] V. Tallapally, T. A. Nakagawara, D. O. Demchenko, Ü. Özgür, and I. U. Arachchige, $Ge_{1-x}Sn_x$ alloy quantum dots with composition-tunable energy gaps and near-infrared photoluminescence, Nanoscale **10**, 20296 (2018)

[5] J.-M. Jancu, R. Scholz, F. Beltram, and F. Bassani, Empirical spds* tight-binding calculation for cubic semiconductors: General method and material parameters, Phys. Rev. B **57**, 6493 (1998).

Evaluation of Reaction Parameters in Polymeric Carbon Nitride Hybridized ZnO Nanocomposite for Improving Photocatalytic Activity using Thermal Synthesis

Narayan N. Som[1], Agnieszka Opalinska[1] and Witold Lojkowski[1]

[1] *Institute of High Pressure Physics, Polish Academy of Science, Sokolowska 29/37, 01-142 Warsaw, Poland*

Recently, semiconductor photocatalyst has garnered a lot of interest, as it has significant promise for environmental restoration and the generation of green hydrogen energy. The polymeric carbon nitride (PCN) and ZnO have been investigated in various catalytic reactions such as organic pollutant degradation and water splitting due to their relative inexpensiveness, moderate band gap (2.7 -3.0 eV), high thermal conductivity, and chemical stability [1]. However, the PCN is found to exhibit less applicability as a photocatalyst for water splitting due to the low surface area, high charge recombination probability, and weak visible light absorption, which is also dependent on the synthesis methodology. Since then, many efforts have been dedicated to the enhancement of the photocatalytic activity of PCN. Previously, in our group, we had successfully obtained PCN-AlOOH-ZrO2 nanocomposite, having a higher specific surface area of about 79.5 m^2/g and a band gap of 3.0 eV [2]. We have also shown that the size of ZnO particles can be controlled with the water concentration and achieved the highest specific surface area (59.4 m^2/g) [3].

Primarily, our goal is to present the development of nanomaterial synthesis to obtain the repeatable homogenous nanostructure, having a high specific surface area with narrowing the band gap which will enhance its photocatalytic activity for hydrogen evolution reaction. We have investigated the structural morphology and its stability through SEM, XRD, and ATR-FT-IR. This PCN nanocomposite was obtained by two steps: 1) microwave hydrothermal synthesis of ZnO followed by drying and 2) mixing the ZnO with different proportions of melamine and annealing in air at 550° C using a muffle furnace for 3hrs. The synthesized ZnO nanoparticle has an average grain size of 25 nm with BET_{SA} 45.483 m^2/g and a density of 5.22±0.0.04 g/cm^3. We observed the strong XRD peak of PCN (at 28.33°) and 31.75°, 36.25° and 62.87° XRD peaks for ZnO hexagonal phase, which confirms the PCN-ZnO formation as shown in Figure 1, except 70% of ZnO. In near future, we will investigate other fundamental properties and photocatalytic activities with both experimentally and with density functional theory methodology.

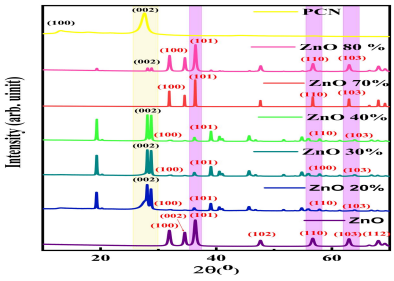

Figure1: XRD diffraction pattern of PCN, ZnO and PCN-ZnO nanocomposite.

Acknowledgement: This work has been supported by the European Union's Horizon 2020 research and innovation programme under Maria Skłodowska-Curie grant agreement No 847639.

[1] Wang, Yajun, Rui Shi, Jie Lin, and Yongfa Zhu, *Energy & Environmental Science* **4**, 2922 (2011).
[2] Koltsov, Iwona, et al., *Molecules* **24**, 874 (2019).
[3] Wojnarowicz, Jacek, et al., *Nanotechnology* **29**, 065601 (2018).

Pressure-driven tuning of bandgap in methylammonium lead iodide

Agnieszka Pieniążek,[1] Filip Dybała,[1] Maciej Polak,[2] Łukasz Przypis,[3] Artur P. Herman,[1] Jan Kopaczek,[1] Robert Kudrawiec[1]

[1] *Department of Semiconductor Materials Engineering, Faculty of Fundamental Problems of Technology, Wroclaw University of Science and Technology, Wybrzeże Wyspiańskiego 27, 50-370 Wrocław, Poland*

[2] *Materials Science and Engineering Department, University of Wisconsin-Madison, Madison, WI 53706, USA*

[3] *Saule Research Institute, Wroclaw Technology Park, 11 Duńska Street, Sigma Building, 54-130 Wrocław, Poland*

Hybrid organic-inorganic perovskites of the composition of AMX_3, where A stands for an organic cation, M is a metal and X is a halide, are promising materials for a wide range of applications, including solar cells, light-emitting devices, photodetectors, and lasers due to low costs and simplicity of preparation, strong light absorption and long diffusion lengths facilitated by long carrier lifetimes and low nonradiative recombination rates.

Hydrostatic pressure can alter bond lengths and valence angles without changing chemical composition, tuning the electronic landscape responsible for basic properties of photovoltaic materials, like the energy bandgap. Moreover, combined with the density functional theory (DFT), it helps recognize structural factors affecting electronic band structure with atomic-level understanding.

In the following, the pressure-generated optical and structural changes of the low-temperature orthorhombic phase (OP) of methylammonium lead iodide were studied experimentally by photoluminescence (PL) and theoretically within DFT. The abnormal bandgap evolution of the OP under pressure with redshift-blueshift-redshift trend observed in both experiment (Figure 1) and theoretical predictions is explained by the competition between Pb-I bond shrinkage and PbI_6 octahedral tilting. Bandgap pressure coefficient within the OP determined from the redshift range of the PL energy is found to be negative and dependent on the temperature (α_{40K}= -36.3±0.1 meV/GPa, α_{80K}=-29.8±0.1 meV/GPa, α_{120K}=-13.3±0.1 meV/GPa). Negative deformation potential results from antibonding character of the bottom of the conduction band and the top of the valence band while dependence on the temperature is related to changes in Pb-I bond length as the atomic configuration approaches temperature-induced phase transition as well as increased transverse acoustic phonon contribution to octahedral tilting at higher temperatures.

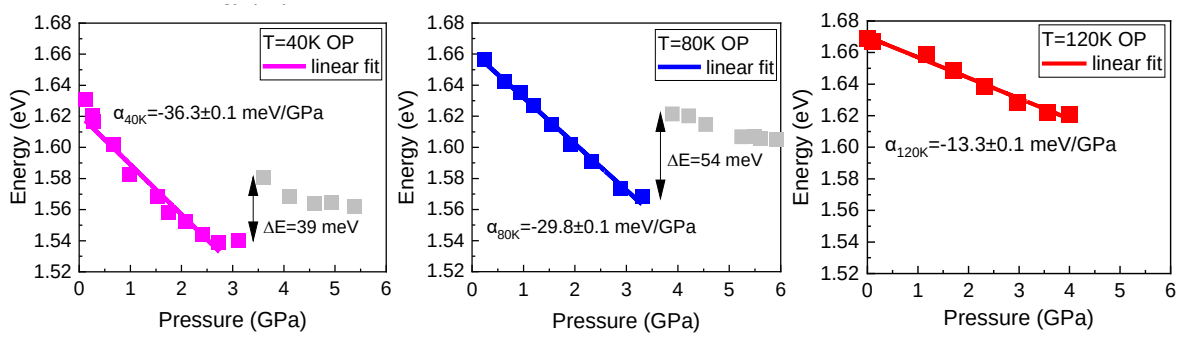

Figure 1. Pressure response of the PL peak positions at (left) 40 K, (middle) 80 K, and (right) 120 K.

Nanoprobe-based electrical characterization of semiconductors nanostructures

Stanislav Tiagulskyi[1], Roman Yatskiv[1], Ondřej Černohorský[1], Nikola Bašinová[1], Šárka Kučerová[1], Jan Vaniš[1], Anna Reszka[2] and Jan Grym[1]

[1]*Institute of Photonics and Electronics of the Czech Academy of Sciences, Chaberská 57, Prague, 18200, Czech Republic*

The miniaturisation of electronic components is running its natural course during the development of the modern electronic industry. Moving to the nanoscale requires specific methods of investigation since macroscale properties of semiconductor materials could not be directly extrapolated to the nanoscale. Here, we present a method of electrical characterisation on the nanoscale that overcomes the drawbacks of conventional characterisation techniques and helps shed light on the fundamental properties of nanoscale semiconductor structures and nanostructured materials.

To study the electrical properties of the nanostructures, we use two nanomanipulators mounted in the chamber of a multifunctional scanning electron microscope (SEM) that is additionally equipped with the focused ion beam (FIB) and the gas injection system (GIS). The FIB and GIS are used for ion beam milling and local deposition of Pt conductive layers with the aim of building more complex nanoscale structures without additional steps (transfer to other substrates, lithographic deposition of contacts, etc.). The manipulators in SEM allow us to measure the current-voltage characteristic of a single nanostructure with desirable morphology controlled by SEM imaging simultaneously with electrical characteriation. Moreover, the vacuum chamber reduces the impact of gas adsorption and light irradiation, which both affect the properties of structures under the test.

We demonstrate examples of the implementation of the nanoprobe-based approach for the electrical characterisation of ZnO/GaN single nanorod heterostructures [1,2], GaN/AlGaN nano-LEDs [3], patterned graphene/ZnO [4] and graphene/Ga_2O_3 interfaces, nanoscale ZnO nanorod/graphene Schottky diodes [5], and single nanowire metal/semiconductor/metal structures [6].

[1] Tiagulskyi, S.; Yatskiv, R.; Faitova, H.; Kucerova, S.; Vanis, J.; Grym, J., *Mater. Sci. Semicond. Process* **107**, 6, (2020).

[2] Tiagulskyi, S.; Yatskiv, R.; Faitova, H.; Kucerova, S.; Roesel, D.; Vanis, J.; Grym, J.; Vesely, J., *Nanomaterials* **10**, 13, (2020).

[3] Reszka, A.; Korona, K.P.; Tiagulskyi, S.; Turski, H.; Jahn, U.; Kret, S.; Bozek, R.; Sobanska, M.; Zytkiewicz, Z.R.; Kowalski, B.J., *Electronics* **10**, 20, (2021).

[4] Tiagulskyi, S.; Yatskiv, R.; Faitova, H.; Cernohorsky, O.; Vanis, J.; Grym, J., *Physica E* **136**, 5, (2022).

[5] Tiagulskyi, S.; Černohorský, O.; Bašinová, N.; Yatskiv, R.; Grym, J., *Mat. Res. Bul. (under review)*, (2023).

[6] Drinek, V.; Tiagulskyi, S.; Yatskiv, R.; Grym, J.; Fajgar, R.; Jandova, V.; Kostejn, M.; Kupcik, J., *Beilstein J. Nanotechnol.* **12**, 1365-1371, (2021).

Young's Modulus and Microhardness of (Pb,Cd)Te Solid Solution Grown by SSVG and MBE Method

Stanisław Adamiak [1], Wojciech Wołkanowicz [2], Anna Juś [1], Elżbieta Łusakowska [2], Roman Minikayev [2], Dariusz Płoch [1], Jędrzej Korczak [2,3], Andrzej Szczerbakow [2,*], and Wojciech Szuszkiewicz [2,$]

[1] *Center for Microelectronics and Nanotechnology, Institute of Materials Engineering, University of Rzeszow, Pigonia 1, 35-959 Rzeszow, Poland*
[2] *Institute of Physics, Polish Academy of Sciences, al. Lotników 32/46, 02-668 Warsaw, Poland*
[3] *International Research Centre MagTop, Institute of Physics, Polish Academy of Sciences, al. Lotników 32/46, 02-668 Warsaw, Poland*

The PbTe, both alone or as a constituent of several systems (solid solutions, low-dimensional structures, composites etc.), attracts an increasing interest. The reasons are related to the new physical findings e.g., such as topological crystal insulators or dynamic local symmetry breaking and important applications, mostly in the harvesting energy area. The solids containing PbTe and CdTe, intensively investigated the last dozen years are one of the systems of today's active research. In particular, a significant hardening of the (Pb,Cd)Te solid solution with an increasing CdTe content could be an attractive property for selected applications of such crystals (see, e.g. [1]).

Recently, it was suggested that selected mechanical property, the microhardness, of PbTe bulk crystals and MBE-grown layers differ substantially [1]. On the other hand, analogous difference seems to be much smaller in case of GaAs [2] and not observed in (Cd,Hg)Te [3]. Therefore the question arises whether this effect exist also in (Pb,Cd)Te solid solution crystals.

All presently investigated samples were obtained at the Institute of Physics PAS. The bulk, single (Pb,Cd)Te solid solution crystals containing a few percent of CdTe were grown by the SSVG method. The samples oriented along three principal crystal directions by the X-ray diffraction were selected for further studies in order to check the microhardness anisotropy. In case of (001) orientation, sample with a natural surface was used, while the (011)- and (111)-oriented samples were etched in a bromine methanol solution. A few micrometers thick, (001)-oriented MBE layers with an analogous chemical composition were grown on GaAs substrates for the comparison. The samples characterized by XRD and AFM were investigated by the nanoindentation method at the University of Rzeszów. The applied load varied from 0.2 mN to 10 mN. The microhardness and Young's modulus, presently determined and compared with our previous results [1,2] and available literature data are given and discussed.

This work was partially supported by the National Science Centre for Development (Poland) through grant TERMOD No. TECHMATSTRATEG2/408569/5/NCBR/2019.

---

* Retired
$ Corresponding author. E-mail address: szusz@ifpan.edu.pl.

[1] R. Kuna, S. Adamiak, S. Petit, *et al.*, *Acta Phys. Pol.* A, **130**, 1245 (2016).
[2] S. Adamiak, E. Łusakowska, E. Dynowska, *et al.*, *Phys. Stat. Sol.* B **256**, 1800549 (2019).
[3] V. Klinger, T. Roesener, G. Lorenz, *et al.*, *Thin Solid Films* **548**, 358 (2013).
[4] R. Minikayev, S. Adamiak, A. Kazakov, *et al.*, *Acta Phys. Pol. A*, **136**, 603 (2019).

Characterization of (Cd,Mn)Te and (Cd,Mn)(Te,Se) material and contact properties

Dominika M. Kochanowska[1], Aneta Wardak[1], Krzysztof Gościński[1], Piotr Sybilski[1], Anna Reszka[1], Adrian Sulich[1] and Andrzej Mycielski [1]

[1] *Institute of Physics, Polish Academy of Sciences, Aleja Lotników 32/46, 02-668 Warsaw, Poland*

The basic parameters of materials used for semiconductor X-ray and gamma-ray detectors are carrier mobility (μ) and their lifetime (τ). Radiation generates hole-electron pairs in semiconductor detector material, an amount proportional to the energy of the incident radiation. Minimalization of carriers concentration results in increasing detector sensitivity. That leads to the creation of a semi-insulating material. The use of special material doping leads to material compensation and results in material resistances of the order of 10^{10}-10^{11} Ωcm. However, obtaining repeatable contacts for such highly resistive materials is very difficult. We have developed a method for obtaining nearly-ohmic contacts using amorphous layers based on CdTe, ZnTe, and (Cd,Mg)Te. The best I-V characteristics were obtained for materials with (Cd,Mg)Te:Sb contact layers and metallization. Properties of these contacts were investigated using scanning electron microscopy (SEM) and X-ray diffraction (XRD). We use current-voltage characteristics to examine the metal/amorphous layer/detector material interface.

For materials with resistivity of about 10^{8}-10^{9} Ωcm we made Schottky contacts. This type of contact is achieved by selecting appropriate contact materials that act as barriers for injecting electrons from one side and holes from the other side of the detector material. Creating a depletion layer in the sample by applying voltage leads to an increase in the signal produced by charge carriers generated by radiation.

In this work, we present such contacts made on (Cd,Mn)Te and (Cd,Mn)(Te,Se) crystals doped with V, In, or V and In, respectively. We measured I-V characteristics, Time of Flight (TOF), and photocurrent as a function of the applied field (PC-V) for selected samples [1]. Data were collected as a function of temperature in the range of 0 to 70°C. The measurements allowed us to obtain mobility values for electrons (≈ 880-980 $cm^2V^{-1}s^{-1}$) and holes (≈ 30-50 $cm^2V^{-1}s^{-1}$). From measurements of parameter μτ ($\mu_e\tau_e \approx 1\cdot10^{-3}$ cm^2V^{-1}), we calculated an electron lifetime of the order of 10^{-6} s.

TOF measurements allow for the estimation of trapping and de-trapping processes. The I-V data enable us to determine barrier heights at the junction [2] and the activation energies of some states in the material's energy gap.

Acknowledgments

This work was partially supported by the Polish National Centre for Research and Development through grant No.TECHMATSTRATEG1/346720/8/NCBR/2017. The authors would like to gratefully acknowledge Janusz Gdański, Stanisław Jabłoński, Michał Kochański, Marcin Dopierała, Adam Marciniak, and Marek Zubrzycki for their technical support during experiments.

[1] A. Mycielski *et al.*, 'Surface Recombination and Space-Charge-Limited Photocurrent-Voltage (PC-V) Measurements in (Cd,Mn)Te Samples–Kinetics of Photocurrent (PC)', *Sensors*, vol. 22, no. 8, 2022, doi: 10.3390/s22082941.

[2] S. J. Bell *et al.*, 'Comparison of the surfaces and interfaces formed for sputter and electroless deposited gold contacts on CdZnTe', *Appl Surf Sci*, vol. 427, pp. 1257–1270, Jan. 2018, doi: 10.1016/j.apsusc.2017.08.077.

Comparison of (Cd,Mn)Te and (Cd,Mn)(Te,Se) Compounds for Room Temperature X- and Gamma-Ray Detection: Optical Properties and Detector Response

Aneta Wardak [1], Dominika M. Kochanowska [1], Michał Szot [1,2], Michał Kochański [1], Marcin Dopierała [1], and Andrzej Mycielski [1,3]

[1] *Institute of Physics, Polish Academy of Sciences, Aleja Lotników 32/46, 02-668 Warsaw, Poland*
[2] *International Research Centre MagTop, Institute of Physics, Polish Academy of Sciences, Aleja Lotników 32/46, 02-668 Warsaw, Poland*
[3] *PUREMAT Technologies, Aleja Lotników 32/46, 02-668 Warsaw, Poland*

Semi-insulating CdTe-based compounds are being tested as materials for room temperature X- and gamma-ray detectors. More recently, selenium has been added to CdTe to increase the hardness of the compound as fewer harmful subgrains have been found in harder materials [1]. We have checked that compounds alloyed with Se are indeed harder. However, this application particularly requires good charge carrier transport, which is ensured by a low concentration of trapping defects.

In this work, two Bridgman-grown (Cd,Mn)Te-based materials were tested in order to compare their optical properties and the ability to detect X and gamma radiation. Our studies covered $Cd_{0.95}Mn_{0.05}Te$ and $Cd_{0.95}Mn_{0.05}Te_{0.98}Se_{0.02}$ crystals – as-grown samples as well as samples annealed in cadmium or selenium vapors. Low-temperature photoluminescence (PL) studies allowed us to discuss the presence of defect states. In both materials, two donor-acceptor pair transitions (DAP) exist. Shallow (s) and deep (d) DAP transitions are about 70 meV and 200 meV below the exciton lines, respectively. Bridgman-grown (Cd,Mn)Te has a high concentration of Cd vacancies, which are acceptors. Annealing in Cd vapors was carried out to reduce their concentration. This process eliminates or reduces the intensity of DAP^d line in (Cd,Mn)Te, whereas in (Cd,Mn)(Te,Se) even double annealing in Cd vapors does not influence the DAP^d line. In PL, the DAP^d line is observed in (Cd,Mn)(Te,Se) up to higher temperatures than in (Cd,Mn)Te. The possible interpretation of the differences between the two compounds might be the existence of a complex containing the Se vacancy in (Cd,Mn)(Te,Se). In principle, it should be a deep donor (analogy to Te vacancy) [2].

Then, the detector response of these two materials was compared. Pixelated detectors were created by the sputtering of metal layers. The room-temperature spectroscopic performance of the detectors was checked using a Co-57 point source. The (Cd,Mn)Te detector distinguishes 122 keV gamma-rays of Co-57 with an energy resolution of ~16%. On the other hand, the (Cd,Mn)(Te,Se) detector recognizes only X-rays of Co-57 at 7 keV with an energy resolution of ~45%, and a trace of gamma-rays at 14.4 keV. We associate the poor response of the (Cd,Mn)(Te,Se) detector with the presence of a deep trap involved in the luminescence of DAP^d. Therefore, (Cd,Mn)Te is a more promising material for use in X-ray and gamma-ray detectors.

Acknowledgements
The authors would like to gratefully acknowledge Janusz Gdański, Stanisław Jabłoński, Adam Marciniak, and Marek Zubrzycki for their technical support during experiments. This work was partially supported by the Polish National Centre for Research and Development through grant No. TECHMATSTRATEG1/346720/8/NCBR/2017.

[1] U. N. Roy et al., *Sci. Rep.* **9**, 1620 (2019).
[2] J.-H. Yang et al., *Semicond. Sci. Technol.* **31**, 083002 (2016).

Mn^{2+}-V_{Zn}^{-} charge transfer complexes in $Zn_{1-x}Mn_xTe$

V.K. Le, A. Avdonin, and A. Mycielski

Institute of Physics, PAS, Al. Lotników 32/46, 02-668 Warsaw, Poland

$Zn_{1-x}Mn_xTe$ dilute magnetic semiconductor (DMS) has recently attracted much attention due to the possibility of creation of the Mn-Mn ferromagnetic coupling [1] and fabrication of highly spin polarized red-green light emitting devices [2]. It is commonly believed that in $II_{1-x}Mn_xVI$ DMSs Mn^{2+} ions are electrically neutral. Recently, we have reported that in $Zn_{1-x}Mn_xTe$ doped with phosphorus (P) the Mn^{2+} ions strongly couple with P-acceptors giving rise to the compensation of the P-acceptors and the creation of Mn^{3+} ions [3].

In this communication, we report the results of the Hall effect, photoluminescence (PL), magneto-PL and electron paramagnetic resonance measurements performed on the undoped ZnTe and $Zn_{1-x}Mn_xTe$ crystals, which show a strong interaction between Mn^{2+} ions and singly negatively charged zinc vacancy defects V_{Zn}^{-} resulting in the formation of the Mn^{2+}-V_{Zn}^{-} charge transfer complexes. The Mn^{2+}-V_{Zn}^{-} coupling causes the transformation of the 0.047 eV $V_{Zn}^{-/0}$ shallow acceptor level, present in ZnTe, into a 0.138 eV $V_{Zn}^{--/-}$ deep acceptor level [see Fig. (a)]. This points to the compensation of the $V_{Zn}^{-/0}$ shallow acceptor level by Mn^{2+} ions. We have suggested a charge transfer mechanism which transforms the Mn^{2+}-V_{Zn}^{-} complexes into Mn^{3+}-V_{Zn}^{--} ones,

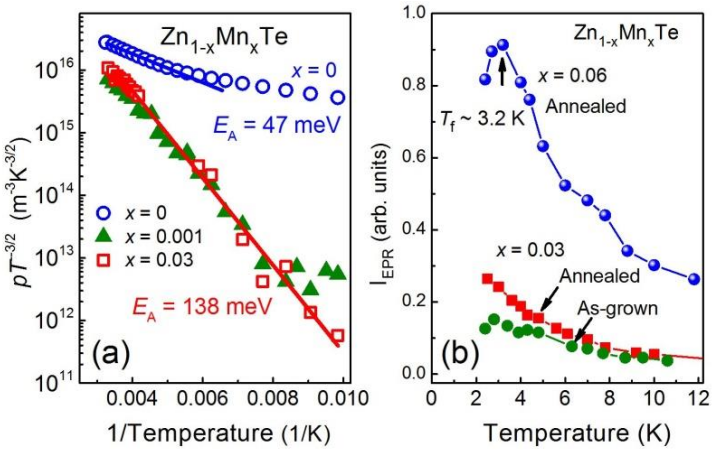

$$Mn^{2+}(3d^5,4s^2) + V_{Zn}^{-} \rightarrow Mn^{2+}(3d^5,4s^1) + V_{Zn}^{--} \rightarrow Mn^{3+}(3d^4,4s^2) + V_{Zn}^{--}.$$

The PL spectra measured under the 2.21 eV excitation for $Zn_{0.96}Mn_{0.04}Te$ sample exhibit two PL bands locating at 1.96 eV and 1.44 eV, which are attributed to the intrashell transitions of Mn^{2+} and Mn^{3+} ions, respectively.

The coexistence of the mixed valence Mn^{2+} and Mn^{3+} states leads to local ferromagnetic (FM) double exchange interaction between Mn^{2+} and Mn^{3+} ions by the Zener double exchange mechanism. The competition between the Mn^{2+}-Mn^{3+} FM double exchange interaction and the intrinsic Mn^{2+}-Mn^{2+} antiferromagnetic superexchange coupling gives rise to the paramagnetic–spin glass phase transition at T_f = 3.2 K in $Zn_{0.94}Mn_{0.06}Te$ sample [see Fig. (b)].

We have observed that the compensation of the acceptor impurities or cation vacancy defects by Mn^{2+} ions is the inherent property not only for $II_{1-x}Mn_xVI$ DMSs but also for $III_{1-x}Mn_xV$ alloys. This finding calls for a new strategy for the efficient *p*-type doping of the Mn-based DMSs.

[1] Le Van Khoi, A. Avdonin, and A. Mycielski, *Phys. Rev. B* **107**, 085206 (2023).
[2] Le Van Khoi and R. R. Gałązka, *Appl. Phys. Lett.* **98**, 112103 (2011).
[3] Le Van Khoi, W. Dobrowolski, T. Kazimierczuk, A. Rodek, P. Kossacki, R.R. Galazka, and W. Zawadzki, *Phys. Rev. B* **101**, 054440 (2020).

Anomalous behavior of the indirect excitons in (Cd,Mn)Te/(Cd,Mg)Te/CdTe double QW structures

V.Yu.Ivanov [1], O.V.Terletski[2], S.M.Ryabchenko[2], V.I.Sugakov[3], G.V. Vertsimakha[3], V.V.Vainberg[2], G.Karczewski[1].

[1] *Institute of Physics Polish Academy of Science al.Lotników 32/46 Warsaw 02-668, Poland*
[2] *Institute of Physics National Academy of Sciences of Ukraine, Kiev, Ukraine*
[3] *Institute of Nuclear Research National Academy of Sciences of Ukraine, Kiev, Ukraine*

Interest in the study of double quantum well (DQW) semiconductor nanostructures is often related to the attempt to create a condensed state of so-called indirect excitons, which have a long exciton lifetime due to the localization of the exciton electron and hole in different QWs. This communication reports a new phenomenon in the photoluminescence (PL) of DQWs constructed from CdTe and CdMnTe QWs separated by a CdMgTe barrier. It has been found that the energy of indirect excitons (IX) in DQWs in the samples studied depends significantly on the energy of the excitation photon. To the best of our knowledge, such an effect has not been discussed previously.

Here we present the results of a study of exciton systems of CdMnTe/CdTe DQW structures consisting of a bound 15 nm width DMS QW, a non-magnetic CdTe QW with width varied in the range 6-10 nm, separated by a 2 nm width CdMgTe barrier. The stationary and time-resolved spectra of PL and PL excitation (PLE) were studied over a wide range of magnetic fields and optical excitation energies and intensities. Fig.1 shows magnetic field dependencies excitons energies at different powers of excitation (a), PL spectra of excitons from DQWs at different excitation energies in the magnetic field (b) and the emission energy dependence of indirect exciton (IX) and trion (T) from CdTe QWs on the excitation photon.

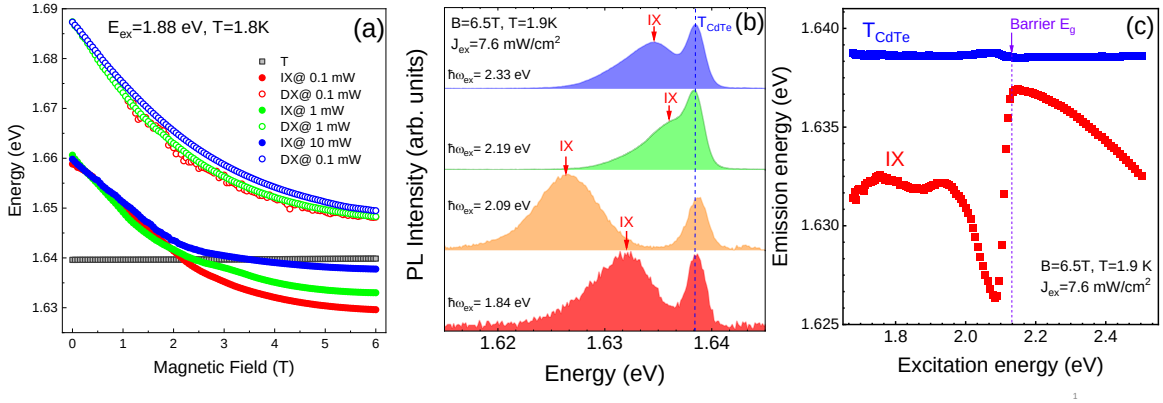

Fig.1 (a) Dependence of the energies of IX, DX from DMS QW and T energies on the magnetic field at different excitation powers; (b) PL spectra at different excitation powers at B=6.5 T; (c) Dependence of the energies of IX and T on the excitation power. The values of temperature, magnetic field and excitation power density are shown in the inset.

Anomalous non-monotonic behavior of the IX emission spectrum is observed near the energy of a (Cd,Mg)Te barrier band edge, while direct exciton from DMS WQ (DX) and trions (T) do not depend on the optical excitation energy. The energy difference between IX and T, i.e. the magnitude of the effect, is generally dependent on the optical excitation power density, but at low excitation power densities, this dependence disappears. We propose that the main mechanism responsible for this effect is due to the accumulation of photo-induced carriers in different QWs, which induces the appearance of an intrinsic electrostatic field that strongly modifies the energy spectrum of IX.

Properties of Infrared Detectors Made of $Pb_{1-x}Mn_xTe$/CdTe Multilayer Composite

S. Chusnutdinow[1,2], A. Kazakov[2], M. Szot[1,2], S. Schreyeck[3], R. Jakieła[1], K. Brunner[3] and G. Karczewski[1,3]

[1]Institute of Physics, Polish Academy of Sciences, Aleja. Lotników 32/46, PL-02-668 Warszawa, Poland
[2]International Research Center MagTop, Aleja Lotników 32/46, PL-02-668 Warszawa, Poland
[3]Physikalisches Institute, Universität Würzburg, Am Hubland, D-97074 Würzburg, Germany

Infrared detectors are widely used for various purposes, such as chemical gas analysis, gas leak detection, IR imaging, remote temperature measurements, etc. In particular, there is continued interest in applications and consequently in the development of IR detectors operating at room temperature. We have shown experimentally that photoresistors made of the PbTe/CdTe multilayer composite are highly sensitive to infrared light, and their detectability at room temperatures is comparable to that of commercially available infrared detectors [1]. The high performance of PbTe/CdTe detectors is due to three factors. The first factor is a significant reduction in the concentration of free carriers in conductive PbTe layers due to their capture by broken bonds located at PbTe/CdTe interfaces. The atomic bonds at the interfaces are broken because of the different crystal structures of PbTe and CdTe, the rock salt and zinc blende, respectively. The second factor is a high mobility of carriers present in the PbTe layers. Despite the huge number of defects at the interfaces, the high mobility is preserved due to the high dielectric constant of PbTe, which effectively screens the scattering centers at the interfaces.

The main objective of the present work is to check how manganese atoms introduced into PbTe layers affect the performance of IR photoresistors made of $Pb_{1-x}Mn_xTe$/CdTe multilayer composite. It is known, that Mn effectively increases the energy gap of $Pb_{1-x}Mn_xTe$ [2], which leads to the increase of carrier effective masses and thus of the density of states. As a result, the concentration of carriers is expected to decrease with the increasing manganese content, x, which in turn should made the of $Pb_{1-x}Mn_xTe$/CdTe photoresistors more sensitive to optical excitation. Properties of $Pb_{1-x}Mn_xTe$/CdTe multilayer composite grown by molecular beam epitaxy on GaAs substrates have been studied. The study included morphological characterization by X-ray diffraction, scanning electron microscopy, secondary ion mass spectroscopy as well as transport and optical measurements. The main focus was on sensing properties of photoresistors made of $Pb_{1-x}Mn_xTe$/CdTe in the infrared spectral region. It was shown that the presence of Mn in $Pb_{1-x}Mn_xTe$ conductive layers shifts the cut-off wavelength toward blue and weakens the spectral sensitivity of the photoresistors. The first effect is due to an increase in the energy gap $Pb_{1-x}Mn_xTe$ with an increase in Mn concentration, and the second is due to a pronounced deterioration in the crystal quality of the multilayer by the presence of Mn atoms as shown by the morphological analysis.

The research in Poland was supported by the National Science Centre through the Grant No.2021/41/B/ST3/03651 and partially supported by the Foundation for Polish Science through the IRA Programme co-financed by EU within SG OP (Grant No. MAB/2017/1) and in Germany by the DFG through the SFB 1170 “ToCoTronics” (project No. A05).

[1] S. Chusnutdinow, S. Schreyeck, S. Kret, A. Kazakov, G. Karczewski, *Applied Physics Letters*, **117**, 072102 (2020).
[2] V. Osinniy, A. Jedrzejczak, W. Domuchowski, K. Dybko, B. Witkowska, T. Story, *Acta Physica Polonica A,* **108**, 803 (2005).

Terahertz Spectroscopy of Hyperbolic Metamaterial Based on $CdTe/Cd_{1-x}Mg_xTe$ Multiple Quantum Wells

J. Łusakowski[1,2], A. Frączak[1], E. Imos[1], A. Siemaszko[1], M. Zaremba[1], K. Karpierz[1], Z. Adamus[3,4], T. Słupiński[3,4], and T. Wojtowicz[4]

[1]*Faculty of Physics, University of Warsaw, ul. Pasteura 5, 02-093 Warsaw, Poland*
[2]*Centera Laboratories, Institute of High Pressure Physics, Polish Academy of Sciences, ul. Sokołowska 29, 01-142 Warsaw, Poland*
[3]*International Research Centre Mag Top, Institute of Physics, Polish Academy of Sciences, al. Lotników 32/46, 02-668 Warsaw, Poland*
[4]*Institute of Physics, Polish Academy of Sciences, al. Lotników 32/46, 02-668 Warsaw, Poland*

The tensor of the dielectric function of hyperbolic materials (HM) is defined by components which real parts are of opposite signs. Then, the surface of the constant frequency in the $\omega - k$ space is a hyperboloid which supports (theoretically) infinite number of wave vectors k for given value of ω. This drastically changes propagation of the electromagnetic wave, leading, e.g., to sub-diffraction imaging or negative refraction. Although some of naurally existing materials show such properties in a certain range of frequency (e.g., hexagonal Boron Nitride in the range 6.3 - 7.3 μm) HM are usually artificially constructed with the help of advanced growth or processing technology. One of such structures, falling into the category of artificial hyperbolic metamaterial (HMM), is an alternating sequence of conducting and isolating layers showing hyperbolic properties for a limited range of wavelenghts λ of electromagnetic radiation (under the condition $\lambda \gg d$, where d is the period of the structure). Then, HMM can be treated as a medium characterized by effective constants $\epsilon_{||}\epsilon_{\perp} < 0$, where $||$ and $\perp$ are defined with respect to the plane of the HMM and in such a HMM the hyperbolic properties are exhibited for the Tranverse Magnetic modes of radiation.

Samples of molecular-beam-epitaxy-grown modulation-doped multiple quantum wells can be considered as appropriate for such studies because alternating doped barriers and quantum wells supplied with free electrons consitite the required sequence of isolating and conducting layers. In the present work, we studied response of such structures, grown in the form of a series of ten CdTe quantum wells, modulation doped in each barrier separating the wells. The total electron concentration estimated by transport measurements was equal to about 10^{12} cm^{-2}. Measurements of transmission of linearly polarized THz radiation through the samples were carried out at 4.2 K (the sample was cooled with an exchange helium gas) as a function of magnetic field up to 9 T and as a function of the angle between the plane of the sample and the magnetic field. Tilting the sample allowed to generate TM modes of the radiation while the magnetic field allowed to tune the efective dielectric tensor of the structure.

We observed a rich response of investigated samples showing an interplay of the tilt, magnetic field and frequncy of radiation. These factors conributed both to the shape as well as to position of spectral features, typically built aroung the magnetic field of the cyclotron resonance. By studying the THz photoresistance we showed that investigated samples could be used as sensitive detectors of THz radiation in magnetic fields below 1 T when Shubnikov - de Haas oscillations become a dominant feature of spectra.

This research was partially supported by the Polish National Science Centre grant UMO-2019/33/B/ST7/02858 and by the Foundation for Polish Science through the IRA Programme co-financed by EU within SG OP (Grant No. MAB/2017/1).

Near-band-gap Optical Properties of Modulation-doped $CdTe/Cd_{1-x}Mg_xTe$ Multiple Quantum Well Structures

J. Łusakowski[1,2], M. Grymuza[1], W. Solarska[1], K. Karpierz[1], Z. Adamus[3], T. Słupiński[3,4], and T. Wojtowicz[3]

[1]*Faculty of Physics, University of Warsaw, ul. Pasteura 5, 02-093 Warsaw, Poland*
[2]*Centera Laboratories, Institute of High Pressure Physics, Polish Academy of Sciences, ul. Sokołowska 29, 01-142 Warsaw, Poland*
[3]*International Research Centre Mag Top, Institute of Physics, Polish Academy of Sciences, al. Lotników 32/46, 02-668 Warsaw, Poland*
[4]*Institute of Physics, Polish Academy of Sciences, al. Lotników 32/46, 02-668 Warsaw, Poland*

Modulation-doped quantum wells (QWs) constitute a system exhibiting properties which may essentially differ from properties of their undoped counterparts. The source of differences is the presence of free carriers in the quantum wells which strongly influence optical response of the system to electromagnetic radiation and, of course, also change the low-frequency conductivity. In general, doping with donors or acceptors leads to, respectively, n-type or p-type gas of charged carriers confined by a two-dimensional potential. In the present case we consider only n-type modulation-doped CdTe-based quantum well structures. At low temperatures, the near-band-gap optical properties of low-doped structures are dominated by excitation or recombination of neutral excitons and negatively charged excitons (trions). In the case of a single quantum well, by increasing doping level, which results in increasing the concentration of a two-dimensional electron gas (2DEG) in a QW, one observes a gradual change of the shape of the luminescence spectrum from that showing sharp lines resulting from recombination of excitions and trions to a broad structure defined rather by a Fermi-edge singularity. Application of magnetic field, perpendicular to the plane of the 2DEG further modifies spectra. In the case of undoped QWs or a low density 2DEG, one observes splitting of excitons or trions levels and optical transitions between split levels according to the relevant polarization selection rules. When the concentration of free electrons is high enough, transitions between Landau levels in the conduction and the valence band dominate the spectra.

In the present work, we studied of photoluminescence and reflectivity of modulation-doped $CdTe/Cd_{1-x}Mg_xTe$ quantum well structures grown by a molecular beam epitaxy. Each of four samples studied comprised ten QWs. Within each sample, parametrs of QWs and the doping of each of them were nominally identical. The samples differed by the doping concentration and the width of the spacer which resulted in differences in the concentration of a two-dimesional electron gas (2DEG). The samples were studied at liquid-helium temperatures and in magnetic fields up to 9 T. A near-band-gap (at about 1.6 eV) photoluminescence was excited with a green laser light while the reflectivity (a halogen lamp was used) was observed in a broader spectral range between 1.6 and 2.5 eV, clearly showing also the spectrum of higher-energy transitions, absent in the luminescence spectra. The measurements allow us to discuss the evolution of the optical response (in the near-band-gap energies) of modulation-doped CdTe-based mutliple quantum well structures as a function of 2DEG concentration which seem to be the first result for this kind of II-VI quantum structures.

This research was partially supported by the Foundation for Polish Science through the IRA Programme co-financed by EU within SG OP (Grant No. MAB/2017/1) and the Polish National Science Centre grant UMO-2019/33/B/ST7/02858.

Terahertz Emission from CdTe-based Multiple Quantum Wells

D. Yavorskiy[1,2], R. Zdunek[3], K. Karpierz[3], Z. Adamus[2,4], T. Słupiński[2,4], T. Wojtowicz[4], and J. Łusakowski[1,3]

[1]*Centera Laboratories, Institute of High Pressure Physics, Polish Academy of Sciences, ul. Sokołowska 29, 01-142 Warsaw, Poland*
[2]*Institute of Physics, Polish Academy of Sciences, al. Lotników 32/46, 02-668 Warsaw, Poland*
[3]*Faculty of Physics, University of Warsaw, ul. Pasteura 5, 02-093 Warsaw, Poland*
[4]*International Research Centre Mag Top, Institute of Physics, Polish Academy of Sciences, al. Lotników 32/46, 02-668 Warsaw, Poland*

Terahertz radiation is a natural candidate to be a game changer in the future electronics and communication systems. The roads towards creation of 6G and 7G systems begun to be explored and it is only the matter of time before full-scale THz systems become a reality. One of the directions leading to these advanced ways of exploring the THz part of the electromagnetic spectrum is defined by the need to construct compact detector - emitter systems that should fulfill challenging requirements of a low-energy consumption, tunability, high spectral resolution and sensitivity. Despite a tremendous progress in THz science and technology over the last two dacades, there are still many open problems to be solved. In particular, new solutions of low-energy consumption emission – detection semiconductor systems are required to fullfil market demands. While the detection part of future systems is well developed, the efficiency of semiconductor emitters is low. That is why, research that can lead to proposing new types of emitter designs is so imprtant.

We have recently shown that low-photon-energy emission, with a maximum at about 1.2 meV was obtained from electrically pumped modulation-doped single GaAs/AlGaAs heterostructure at zero magnetic field. In the present paper, we address the problem of THz emission using electrically pumped semiconductor quantum system at low temperatures and in magnetic fields. The systems under study are multiple CdTe quantum wells modulation-doped with Ioidne. The structures were grown by molecular beam epitaxy on semi-insulating GaAs substrates. Each sample contained ten quantum wells that were 20 nm wide. A series of samples was grown with different doping levels and different width of barriers separating the wells. The presence of free electrons with a total concentration of about 10^{12} cm^{-2} was verified by the cyclotron resonance and magnetotransport (classical and quantum) studies. For emission experiments, the samples were placed at the magnetic field and biased with pulses of the electric power. The emitted radiation was coupled to a Michelson interferometer with a Golay cell as a detector. We show that the emission of THz radiation appears only at a certain magnetic field strongly suggesting that the mechanism responsible for the emission is so called Landau emission, a process of a radiative recombination of electrons from upper to lower Landau levels which can be thought of as an inverse of cyclotron resonance. The magnetic field at which the emission appears is around 1 T, and the spectrum is peaked at energy close to the cyclotron resonance of electrons with the effective mass of CdTe ($0.102m_0$). The present study allows us to determine the design of the multiple CdTe-based quantum structure (doping, spacer and barrier width) to maximize the power of emitted radiation.

This research was partially supported by the Foundation for Polish Science through the IRA Programme co-financed by EU within SG OP (Grant No. MAB/2017/1) and the Polish National Science Centre grant UMO-2019/33/B/ST7/02858.

Simulation of Optical Properties of Terahertz Hyperbolic Metamaterials Based on Multiple Quantum Wells

J. Łusakowski[1,2], and T. Kazimierczuk[1]

[1]Faculty of Physics, University of Warsaw, ul. Pasteura 5, 02-093 Warsaw, Poland
[2]Centera Laboratories, Institute of High Pressure Physics, Polish Academy of Sciences, ul. Sokołowska 29, 01-142 Warsaw, Poland

One of types of hyperbolic metamaterials is a stack of alternating dielectric and metallic layers (thickness d_d, dielectric function $\epsilon_d(\omega)$ and d_m, $\epsilon_m(\omega)$, respectively), where $\omega \sim 1/\lambda$ is the frequency of the electromagnetic wave. Within an effective medium approach, i.e., when the wavelenght $\lambda \gg (d_d + d_m)$ the material behaves as an optically uniaxial medium with the effective dielectric constants $\epsilon_{\|} = p\epsilon_m + (1-p)\epsilon_d$ and $\epsilon_{\perp} = \epsilon_m\epsilon_d/[p\epsilon_d + (1-p)\epsilon_m]$, where $\epsilon_{\|}$ and $\epsilon_{\perp}$ describe the dielectric polarization of the effective medium material for the electric field with zero and non-zero component along the optical axis (which is perpendicular to the surface of the layers) and $p = d_m/(d_m+d_d)$.

Considering the electric field of the wave propagating in this medium, one gets from the Maxwell's equations

$$\left(k_{\perp}^2 + k_{\|}^2 - \epsilon_{\|}\frac{\omega^2}{c^2}\right)\left(k_{\perp}^2\epsilon_{\perp} + k_{\|}^2\epsilon_{\|} - \epsilon_{\perp}\epsilon_{\|}\frac{\omega^2}{c^2}\right) = 0 \tag{1}$$

where c is the speed of light, and $k_{\perp}$ and $k_{\|}$ are components of the wave vector perpendicular and parallel to the layers, respectively.

By equating to zero the first and second term in Eq. 1 one gets equations describing a spherical and ellipsoidal isofrequency surfaces, if $\epsilon_{\perp}\epsilon_{||} > 0$. These solutions correspond to the Transverse Electric (TE) and Transverse Magnetic (TM) modes, respectively. However, if $\epsilon_{\perp}\epsilon_{||} < 0$, TM waves (these with a non-zero component of the electric field of the wave in the direction of the optical axis) are supported by a hyperboloidal isofrequency surface with allowing k-vectors to stretch to infinity (in fact, to $2\pi/a$, where a is the period of the lattice).

The aim of the present paper is to numerically simulate THz optical properties of structures in which conductive and dielectric layers are CdTe quantum wells containing electrons and $Cd_{1-x}Mg_xTe$ barriers, respectively, situated on a SI-GaAs substrate (thickness d_s). The essential difference between our study and the work of other groups is introduction of magnetic field which leads to an anisotropy of the conductive layers and introduces a cyclotron resonance. Numerical simulations are carried out according to a transfer matrix method for anisotropic system. The results are coeffcients of energy transfer for both TE and TM modes and allow to determine the state of polarization of transmitted and reflected waves. Simulations are carried out as a function of geometrical parameters of structures (the number of quantum wells N, d_d, d_m, d_s), the electron concentration in the wells, the magnetic field, the frequency of the wave and the angle of incidence.

We applied the numerical procedure treating the system as composed of N periods of layers characterized by ϵ_m, ϵ_d on a substrate or as a system of the thickness $N(d_d + d_m)$ characterized by effective parameters $\epsilon_{\perp}$, $\epsilon_{||}$. This allows us to establish the validity of the effective medium approach in the presence of magnetic field, which is a new result.

This research was partially supported by the Polish National Science Centre grant UMO-2019/33/B/ST7/02858.

Diffusional dependent structures on the crystal surface

M. Chabowska, M. Załuska-Kotur

Institute of Physics, Polish Academy of Sciences,
Aleja Lotnikow 32/46, PL-02668 Warsaw, Poland

Different patterns can be created on the surface of growing crystals, among which the step bunches and/or step meanders are two of the most studied. The Ehrlich–Schwoebel effect at the surface steps is considered one of the "usual suspects" of such patterning. The combination of a direct and inverse step barrier and the proper selection of the potential of the well between them or changing the height of the direct step barrier leads to the growth of nanocolumns, nanowires, and nanopyramids or meanders, in the same system [1]. Based on our (2 + 1)D vicinal Cellular Automaton model [2,3] we show that not only the combination of step barriers is crucial in the formation of surface structures. In particular, we show that changes only in the diffusion process can lead to different patterns (Fig).

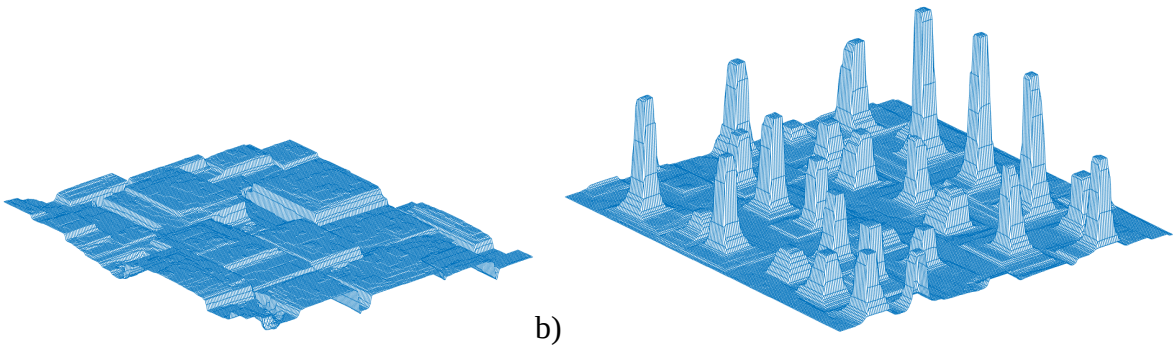

a) b)

Fig. Structures obtained for initial concentration of particles c_0=0.02, Inverse Ehrlich-Schwoebel barrier with jump probability given by P_{ies}=0.2, direct Ehrlich-Schwoebel barrier with jump probability given by P_{des}=0.4, the energy of particle that stays at the bottom of the step p_w=2.5, length of terrace l_0=2 and a) number of diffusional steps n_{DS}=10 which leads to nanopillars b) n_{DS}=40 which leads to nanowires. System size 200 x 200.

[1] M. Załuska-Kotur, H. Popova and V. Tonchev, *Crystals* **11**, 1135 (2021).
[2] A. Krasteva, H. Popova, F. Krzyżewski, M. Załuska-Kotur, M. and V Tonchev, *AIP Conf. Proc.* **1722**, 220014 (2016).
[3] F. Krzyżewski, M.A. Załuska-Kotur, A. Krasteva, H. Popova, and V Tonchev, *J. Cryst. Growth* **474**, 135 (2017).

Fitting parameters of atomic orbitals to reproduce optical properties of III-V systems

Krzysztof Kwas, Krzysztof Gawarecki

[1] *Institute of Theoretical Physics, Wrocław University of Science and Technology, Wybrzeże Wyspiańskiego 27, 50-370 Wrocław, Poland*

The multiband $\boldsymbol{k} \cdot \boldsymbol{p}$ models in the envelope function approximation are commonly used to describe electronic and optical properties of semiconductor nanostructures [1]. However, in some applications, like the modeling of fine structure splitting [2], the precise knowledge of the wavefunction at atomic scale is needed. In consequence, it is crucial to gather some atomic-scale information on Bloch functions calculated within the $\boldsymbol{k} \cdot \boldsymbol{p}$ approach. In particular, it would be beneficial to bridge between the empirical parameters and microscopic properties of the wave functions.

In our work, we model the Bloch states around the single atoms of the crystal. We study the commonly used III-V materials of the zinc-blende structure. The zone-center Bloch states are expressed as combinations of Slater-type atomic orbitals [3], where we take into account the contributions allowed by the irreducible representation related to a given band [4]. Then, we fit the orbital-dependent coefficients and exponential decays to reproduce the optical properties of the considered materials.

The utilized theoretical framework is similar to Ref. [3]. However, we aim to fit a larger set of interband momentum matrix element parameters, which are given in the 30-band $\boldsymbol{k} \cdot \boldsymbol{p}$ Hamiltonian [5].

References

[1] *Multi-Band Effective Mass Approximations*, Vol. 94 of *Lecture Notes in Computational Science and Engineering*, edited by M. Ehrhardt and T. Koprucki (Springer International Publishing, 2014).

[2] P. T. Różański and M. Zieliński *Linear scaling approach for atomistic calculation of excitonic properties of 10-million-atom nanostructures* Phys. Rev. B 94, 045440 (2016)

[3] R. Benchamekh, F. Raouafi, J. Even, F. Ben Cheikh Larbi, P. Voisin, and J.-M. Jancu, *Microscopic electronic wave function and interactions between quasiparticles in empirical tight-binding theory*, Phys. Rev. B 91, 045118 (2015)

[4] J.-M. Jancu, R. Scholz, F. Beltram, and F. Bassani, *Empirical spds* tight-binding calculation for cubic semiconductors: General method and material parameters*, Phys. Rev. B **57**, 6493 (1998).

[5] K. Gawarecki, P. Scharoch, M. Wisniewski, J. Ziembicki, H. S. Mączko, M. Gładysiewicz, R. Kudrawiec, *Invariant expansion of the 30-band k·p model and its parameters for III-V compounds*, Phys. Rev. B 105, 045202 (2022)

Excited Electronic States of Sr_2: *Ab Initio* Predictions and Experimental Observation of the $2^1\Sigma_u^+$ State

J. Szczepkowski[1], M. Gronowski[2], A. Grochola[1], W. Jastrzebski[1], M. Tomza[2] and P. Kowalczyk[3]

[1]*Institute of Physics, Polish Academy of Sciences, al. Lotników 32/46, 02-668 Warszawa, Poland*
[2]*Institute of Theoretical Physics, Faculty of Physics, University of Warsaw, ul. Pasteura 5, 02-093 Warszawa, Poland*
[3]*Institute of Experimental Physics, Faculty of Physics, University of Warsaw, ul. Pasteura 5, 02-093 Warszawa, Poland*

Despite its apparently simple nature with four valence electrons, the strontium dimer constitutes a challenge for modern electronic structure theory. Here we focus on excited electronic states of Sr_2, which we investigate theoretically up to 25000 cm^{-1} above the ground state, to guide and explain new spectroscopic measurements. In particular, we focus on potential energy curves for the $1^1\Sigma_u^+$, $2^1\Sigma_u^+$, $1^1\Pi_u$, $2^1\Pi_u$, and $1^1\Delta_u$ states computed using several variants of *ab initio* coupled-cluster and configuration-interaction methods to benchmark them. In addition, a new experimental study of the excited $2^1\Sigma_u^+$ state using polarisation labelling spectroscopy is presented, which extends knowledge of this state to high vibrational levels, where perturbation by higher electronic states is observed. The available experimental observations are compared with the theoretical predictions and help to assess the accuracy and limitations of employed theoretical models.

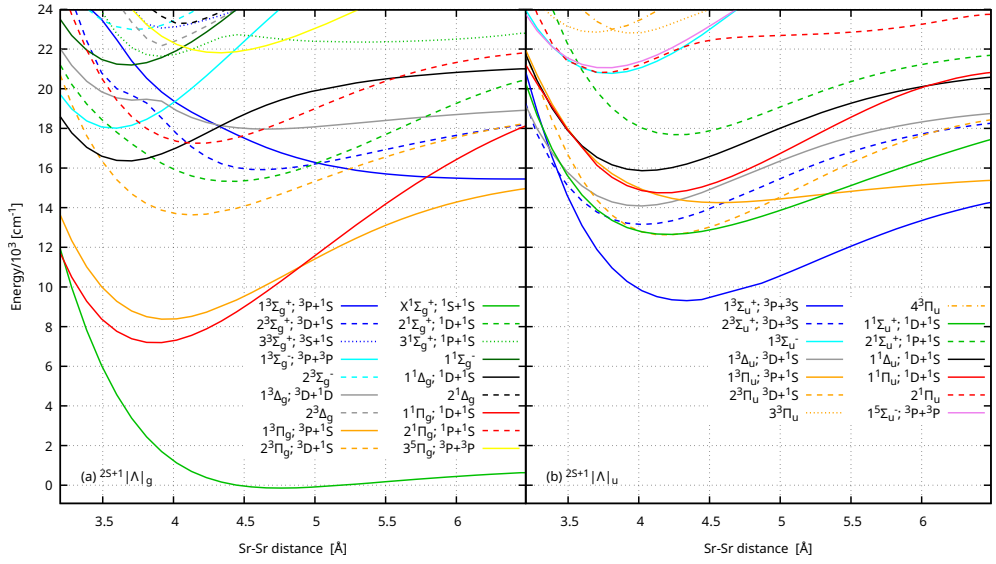

Figure 1: Potential energy curves for the ground and excited electronic states of Sr_2 obtained using the non-relativistic spin-free sMRCI+Q/5Z method with the scalar-relativistic small-core pseudopotential.

Financial support from the National Science Centre Poland is gratefully acknowledged: grant no. 2021/43/B/ST4/03326.

[1] J. Szczepkowski, M. Gronowski, A. Grochola, W. Jastrzebski, M. Tomza and P. Kowalczyk, *J. Phys. Chem. A* (2023) available online at doi:10.1021/acs.jpca.3c02056.

Excellent excitonic properties of novel hexagonal MA_2Z_4 monolayers

Tomasz Woźniak[1,2,3], Paulo E. Faria Junior[4], Umm-e-hani[2,3], Muhammad S. Ramzan[2,3,5], Agnieszka B. Kuc[2,3]

[1] *Wrocław University of Science and Technology, wyb. Wyspiańskiego 27, 50-370 Wrocław, Poland*
[2] *Helmholtz-Zentrum Dresden-Rossendorf, Bautzner Landstraße 400, 01328 Dresden, Germany*
[3] *Jacobs University Bremen, Campus Ring 1, 28759 Bremen, Germany*
[4] *University of Regensburg, Universitätsstraße 31, 93053 Regensburg, Germany*
[5] *Carl von Ossietzky Universität Oldenburg, Ammerländer Heerstraße, 114-118 26129 Oldenburg, Germany*

MA_2Z_4 monolayers form a new class of hexagonal non-centrosymmetric materials hosting extraordinary spin-valley physics. While only two compounds ($MoSi_2N_4$ and WSi_2N_4) have been synthesized so far [1], theory predicts interesting (opto)electronic properties of a whole new family of such two-dimensional materials, as analogs of transition metal dichalcogenides [2]. We study within Density Functional Theory the electronic structure of selected MSi_2Z_4 (M = Mo, W; Z = N, P, As, Sb) monolayers. They exhibit direct band gaps and significant spin-orbit splittings of bands at K valleys. Effective Bethe–Salpeter-equation-based calculations reveal exciton binding energies up to 450 meV. The wave functions of electrons and holes are confined to the inner Z-M-Z layer. Evolution of excitonic energies under external magnetic field is predicted by providing their effective g-factors and diamagnetic coefficients, which can be directly compared to experimental values. In particular, large positive g-factors are predicted for excitons involving higher conduction bands. Additionally, a spin-orbit induced bands inversion is observed in the heaviest studied compound, WSi_2Sb_4, a hallmark of its topological nature.

In view of these predictions, MA_2Z_4 monolayers yield a new platform to study excitons and are attractive for optoelectronic devices, also as new building blocks of van der Waals heterostructures.

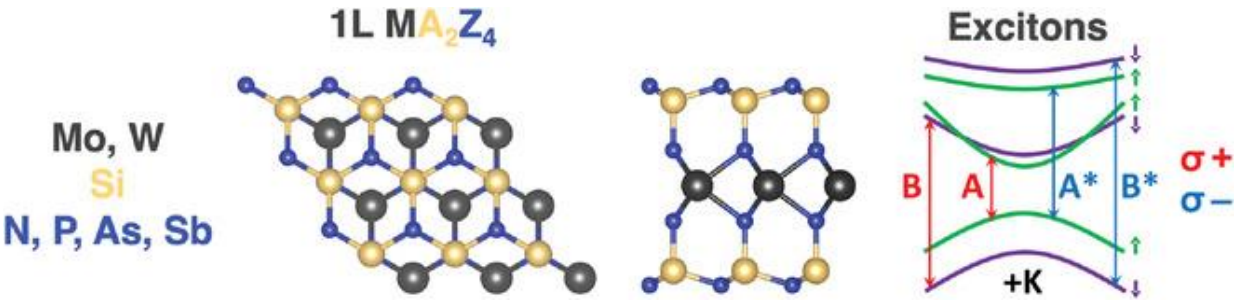

Figure 1. Top and side view of atomic structure of the studied MA_2Z_4 monolayers. Circularly polarized excitonic transitions at +K valley.

[1] Y.-L. Hong, Z. Liu, L. Wang, W. Ren et al., *Science* **369**, 670 (2021).
[2] L. Wang, Y. Shi, M. Liu, X.-Q. Chen et al., *Nature Commun.* **12**, 2361 (2021).
[3] T. Woźniak, Umm-e-hani, P.E. Faria Junior, M. S. Ramzan, A. B. Kuc, *Small*, 202206444 (2023).

Macroscopic Quantum Tunneling of a Topological Ferromagnet

Kajetan M. Fijalkowski, Nan Liu, Pankaj Mandal, Steffen Schreyeck, Karl Brunner, Charles Gould, and Laurens W. Molenkamp

Faculty for Physics and Astronomy (EP3), Universität Würzburg, Am Hubland, D-97074, Würzburg, Germany
Institute for Topological Insulators (ITI), Am Hubland, D-97074, Würzburg, Germany

Since the early days of quantum mechanics, physicists have been trying to understand how the laws governing the microscopic world merge into those describing the classical mechanics at macroscopic size scales. A trademark quantum mechanical phenomenon that has no direct analog in classical physics is quantum tunnelling between different eigenstates of the system. This posed an intriguing question regarding the possibility of existence of quantum tunnelling in systems that can be regarded as macroscopic.

Only in the recent couple of decades the experimental techniques have reached a level of advancement that allowed to directly address that question experimentally. This was done in the context of macroscopic quantum tunnelling between different states in the Josephson junctions [1], as well as quantum tunnelling of magnetic domain walls [2], and magnetization [3] in magnetic systems.

Here, we investigate the electronic transport in a $(V,Bi,Sb)_2Te_3$ ferromagnetic topological insulator nanostructure in the quantum anomalous Hall regime. This provides access to the dynamics of an individual ferromagnetic domain. Telegraph noise resulting from the magnetization fluctuations of this domain is observed in the Hall signal. Careful analysis of the domain switching statistics provides evidence for macroscopic quantum tunneling of magnetization [4]. This ferromagnetic macrospin is not only the largest magnetic object in which quantum tunneling has been observed, but also the first observation of the effect in a topological state of matter.

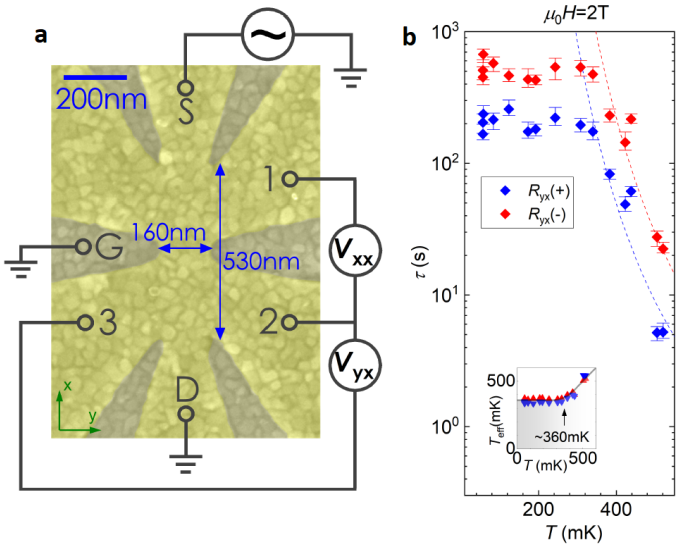

Figure 1: (a) High magnification false color SEM image of the device together with a circuit diagram schematic. (b) Evolution of lifetime τ for each state with temperature, demonstrating a low temperature saturation caused by macroscopic quantum tunneling of magnetization [4].

[1] R. F. Voss et al., *Phys. Rev. Lett.* **47**, 265 (1981)
[2] J. Brooke et al., *Nature* **413**, 610 (2001)
[3] L. Thomas et al., *Nature* **383**, 145 (1996)
[4] K. M. Fijalkowski et al., *ArXiv*:2206.03972 (2022)

Anomalous transverse response in topological magnet CeAlSi

Md Shahin Alam [1], Fazel Tafti [2], Carmine Autieri [1], Marcin Matusiak [1,3]

[1] *International Research Centre MagTop, Institute of Physics, Polish Academy of Sciences, Aleja Lotników 32/46, PL-02668 , Warsaw, Poland*
[2] *Department of Physics, Boston College, Chestnut Hill, Massachusetts 02467, USA*
[3] *Institute of Low Temperature and Structure Research, Polish Academy of Sciences, ul. Okólna 2, 50-422 Wrocław, Poland*

A non-zero Berry curvature, which is a characteristic feature of topological materials, especially in the electronic structure, can be accessed through measurements of the anomalous Hall and Nernst effect [1]. A good candidate for such studies is CeAlSi, a ferromagnetic Weyl semimetal in which Weyl nodes can be tunable in the time reversal breaking regime [2]. We investigated the anomalous Hall conductivity for two different orientations of the magnetic field (B), namely σ^A_{yz} for $B \parallel a$, and σ^A_{xy} for $B \parallel c$ (a and c are crystallographic axes). In the low temperature limit σ^A_{xy} and σ^A_{yz} turn out to be of opposite sign, which was attributed to shifting of the Weyl point due to reconstruction of the band structure driven by spin reorientation. The anomalous contribution has been also detected in the Nernst conductivity (α^A_{xy}/T) measured with B oriented along c - axis. α^A_{xy}/T turns out to be large in the low temperature phase and slowly decreases at high temperatures. The ratio of σ^A_{xy} and α^A_{xy} is a sizable fraction of k_B/e at $\sim 52\,K$ indicating that the anomalous transverse response is fundamentally associated with the nontrivial band structure [3]. Using a single band toy-model assuming a non-zero Berry curvature in the vicinity of the Weyl node, we were able to recreate the temperature dependences of σ^A_{xy} and α^A_{xy}/T at high temperatures. In this region, large σ^A_{xy} and non-vanishing α^A_{xy} appear to be consequences of the fact that the Fermi level lies close to the band crossing point.

[1] Jonathan Noky, Johannes Gooth, Claudia Felser, and Yan Sun, *Phys. Rev. B.* **98**, 241106(R) (2018).

[2] Hung-Yu Yang, Bahadur Singh, Jonathan Gaudet, Baozhu Lu, Cheng-Yi Huang, Wei-Chi Chiu, Shin-Ming Huang, Baokai Wang, Faranak Bahrami, Bochao Xu, Jacob Franklin, Ilya Sochnikov, David E. Graf, Guangyong Xu, Yang Zhao, Christina M. Hoffman, Hsin Lin, Darius H. Torchinsky, Collin L. Broholm, Arun Bansil, and Fazel Tafti, *Phys. Rev. B.* **103**, 115143 (2021).

[3] Liangcai Xu, Xiaokang Li, Linchao Ding, Taishi Chen, Akito Sakai, Benoît Fauqué, Satoru Nakatsuji, Zengwei Zhu, and Kamran Behnia, *Phys. Rev. B.* **101**, 180404(R) (2020).

Superconductivity in PbTe/SnTe semiconductor heterostructure: a candidate for spin-triplet superconductor

P. Sidorczak[1,2], W. Wołkanowicz[3], K. Gas[3], A. Kaleta[3], S. Gierałtowska[3], R. Minikayev[3], S. Kret[3], M. Sawicki[3], T. Wojtowicz[2], D. Wasik[1], M. Gryglas-Borysiewicz[1], K. Dybko[2,3]

[1] *Faculty of Physics, University of Warsaw, ul. Pasteura 5, 02-093, Warsaw, Poland*
[2] *International Research Centre MagTop, Institute of Physics, Polish Academy of Sciences, al. Lotników 32/46, 02668, Warsaw, Poland*
[3] *Institute of Physics, Polish Academy of Sciences, al. Lotników 32/46, 02668, Warsaw, Poland*

The superconductivity of IV-VI semiconductor heterostructures has been a puzzling phenomenon for many years [1,2]. The underlying mechanism seems to be based on the inversion of the band structure induced by compression due to periodic dislocation grids on the interfaces, which gives rise to topological crystalline insulator surface states [3]. At the same time, the resulting periodically varying strain acting on these states creates topological flat band, which promotes superconducting phase transition [4]. However, the pairing mechanism behind this superconductivity has not yet been fully demonstrated, to the best of our knowledge.

Here we present the results of soft point contact spectroscopy (PCS) of superconducting PbTe/SnTe heterostructures, in which the presence of dislocations was revealed using transmission electron microscopy. The PCS experiments exhibit a distinct zero-bias conductance peak (ZBCP). It can be fitted within a theoretical model involving an Anderson-Brinkman-Morel electron pairing potential [5]. This superconducting mechanism realizes p-wave pairing symmetry and was initially introduced to explain the spin-triplet phase of the superfluid ^{3}He. Recent works have expanded this formalism to explain flatband-induced superconductivity [6].

In the PCS experiments, we used both silver and nickel contacts (normal metal and highly spin-polarized metal). The observed spectra do not depend on the spin polarization, which is a signature of p-wave pairing potential [5]. We will present a discussion that sheds light on the mechanism of the unconventional superconductivity observed in this class of narrow-gap semiconductor heterostructures.

The research was partially supported by the Foundation for Polish Science through the IRA Programme co-financed by EU within SGOP and the National Science Centre (Poland) through OPUS (UMO-2017/27/B/ST3/02470) project.

[1] K. Murase et al., *Surf. Sci.* **170**, 486 (1986).
[2] N. Ya. Fogel, et al. *Phys. Rev. B* **66**, 174513 (2002).
[3] Timothy H. Hsieh, et al. *Nature Communications* **3**, 982 (2012).
[4] E. Tang, L. Fu, *Nat. Phys.* **10**, 964 (2014).
[5] J. C. He, Y. Chen *Phys. Rev. B* **106** , 224508 (2022).
[6] M.A. Silaev, G.E. Volovik *J. Exp. Theor. Phys.* **119**, 1042-1057 (2014).

Peculiar magnetic phase in antiferromagnet MnTe

K. P. Kluczyk[1], K. Gas[2], M. J. Grzybowski[1], M. A. Borysiewicz[3], T. Fąs[1], J. Suffczyński[1], E. Łusakowska[2], W. Wołkanowicz[2], J. Z. Domagała[2], P. Skupiński[2], K. Grasza[2], A. Mycielski[2], K. Výborný[4], M. Baj[1] M. Sawicki[2], and M. Gryglas-Borysiewicz[1]

[1]*Faculty of Physisc, University of Warsaw, Pasteura 5, Warsaw, Poland,*
[2]*Institute of Physics, Polish Academy of Sciences, Al. Lotników 32/46, Warsaw, Poland,*
[3]*Łukasiewicz Research Network - Institute of Microelectronics and Photonics, Al. Lotników 32/46, Warsaw, Poland,*
[4]*Institute of Physics, Academy of Sciences of the Czech Republic, Cukrovarnická 10, Praha, Czech Republic,*

Antiferromagnets get increasing attention nowadays as their magnetic state is coupled to its resistivity state and importantly, it may be influenced by electric current [1, 2]. A new puzzling chapter has opened with the developments of topology - in particular, some antiferromagnets have been predicted to exhibit exceptional properties, induced just by the crystal symmetry and not by relativistic effects [3], e.g. existence of anomalous Hall effect (even in a magnetically-compensated system). Recently, experimental evidence was made for RuO_2 [4] and thin MnTe films [5].

Hexagonal MnTe is a semiconductor with a moderate band gap (about 1.3 eV), room temperature resistivity of about a few Ω·cm and the Néel temperature T_N of 308 K. We performed structural, optical, transport and magnetic studies of state-of-the-art bulk samples in wide temperature and magnetic field range. We have traced the Hall voltage behaviour revealing nonlinearities in $\rho_{xy}(B)$ dependence. The observed data were fitted in multi-carrier model, providing two hole and one electron channel. The results will be referred to the recent band structure calculations [6]. Moreover, similiarly to [5] we have observed a clear hysteresis loop in $\rho_{xy}(B)$ seen exclusively below T_N. However, the loop is flipped with respect to the one observed in epitaxial MnTe [5]. The presence of hysteresis in the Hall resistivity coincides with a weak ferromagnetic signal, resolved in SQUID magnetometry. A discussion about the origin of the observed phenomena will be provided.

[1] P. Wadley et al., *Science* **351**, 587–590 (2016).
[2] L. Baldrati et al., *Phys. Rev. Lett.* **123**, 177201 (2019)
[3] L. Šmejkal et al., *Phys. Rev. X* **12**, 040501 (2022)
[4] Z. H. Zhu et al., *Phys. Rev. Lett.* **122**, 017202 (2019)
[5] R. D. G. Betancourt et al., *Phys. Rev. Lett.* **130**, 036702 (2023)
[6] P. E. de Faria et al., *"Sensitivity of the MnTe valence band to the orientation of magnetic moments"*, *Phys. Rev. B*, accepted: 8 February 2023.

This work was partially supported by the Polish National Centre for Research and Development through grant TECHMATSTRATEG1/346720/8/NCBR/2017.

Photoluminescence studies of the futuristic SnSe semiconductor

M. Szot[1,2], P. Wojnar[1], J. Korczak[1,2], W. Zaleszczyk[1,2], L. Kowalczyk[1], S. Chusnutdinow[1], R. Minikayev[1], W. Wołkanowicz[1], T. Story[1,2], G. Karczewski[1]

[1] Institute of Physics, Al. Lotników 32/46, PL-02668 Warsaw, Poland
[2] International Research Centre MagTop, Institute of Physics Polish Academy of Sciences, Al. Lotników 32/46, PL-02668 Warsaw, Poland

SnSe semiconductor belongs to the family of binary IV-VI chalcogenide compounds (Sn-X; X=Se,S), which owe the interest of researchers to the similarity of their layered crystal structure to molybdenum dichalcogenides - a prototype 2D systems. In particular, SnX_2 chalcogenides have been extensively studied as they exhibit high optical absorption coefficient and strong photo-responsivity in the near infrared spectral range allowing their wide application in a new generation of optoelectronic and photonic systems. Unlike rock salt lead monochalcogenides tin-based chalcogenides crystallize in hexagonal and monoclinic phases for SnX_2 or orthorhombic phase for SnX compounds. The layered orthorhombic structure (distorted rock salt structure) of SnSe leads to anisotropy and anharmonicity of chemical bonds responsible for extremely low thermal conductivity along the plane with zig-zag ordering of ions and finally for the very high value of the thermoelectric figure of merit parameter *ZT* reaching 2.6 [1]. The excellent thermoelectric properties of monocrystalline SnSe have become a new inspiration for research on SnX materials. Therefore, tin chalcogenides appear as a family of semiconductors with the possibility of dual use in the field of photovoltaic and thermoelectric energy conversion, important from the point of view of environmental protection. In addition, the exciton binding energy and the energy gap of SnSe significantly depend on dimensionality of the structures (due to strong quantum confinement) and on the method of material preparation. For SnSe bulk samples an indirect bandgap of about 0.9 eV is expected, while for single-layer material the indirect and minimum direct gap differs slightly and amount to 1.63 eV and 1.66 eV, respectively [2]. Since SnX chalcogenides are generally less investigated than SnX_2 compounds, systematic study of their optical properties is needed. In particular, the results of luminescence (PL) studies of these compounds are rarely reported.

In this paper we discuss the results of PL measurements of monocrystalline SnSe synthesized in a direct reaction between the elements in a vacuum-sealed quartz ampoule at 950 °C. Orthorhombic structure of the resulting crystal was confirmed by XRD analysis. For these crystals excited with a 405 nm laser at cryogenic temperatures we observed several PL lines with energies of 0.9 eV, 0.94 eV and 1 eV, the position of which is weakly dependent on temperature. We assign the weakest line with the lowest energy to the indirect bandgap transition expected for bulk SnSe material. Higher energy lines, which are 5 to 10 times stronger, we associate with direct transitions in layered terraces-like structures (revealed on the surface of our SnSe crystals in SEM microscopic measurements), because the energy positions and amplitudes of these lines depend on the spatial position at the sample in which measurement has been taken. Our interpretation of the obtained PL spectra will be discussed in detail, taking into account the results of micro- and cathodo-luminescence measurements.

Acknowledgments

The research was partially supported by by the Foundation for Polish Science through the IRA Programme co-financed by EU within SG OP (Grant No. MAB/2017/1) and by the National Science Centre through Grant No. 2021/41/B/ST3/03651.

References

[1] L. Zhao et al., *Nature* **508**, 373 (2014)
[2] W. Shi et al., *Adv. Sci.* **5**,1700602 (2018)

Investigating of the topological phase transition in $Pb_{1-x}Sn_xTe$ topological crystalline insulators by using nonlinear Hall effect measurements

M. Ahmad[1], W. Wołkanowicz[2], S. Dad[2], P. Dziawa[2], T. Wojtowicz[1] and K. Dybko[1,2]

[1] *International Research Centre MagTop, Institute of Physics, Polish Academy of Sciences, Aleja Lotnikow 32/46, PL-02668 Warsaw, Poland*
[2] *Institute of Physics Polish Academy of Sciences, Aleja Lotnikow 32/46, PL-02668 Warsaw, Poland*

The linear Hall conductivity occurs in the systems, which have broken time-reversal symmetry either by the intrinsic or external magnetic field. However, recently predicted nonlinear Hall effect (NLHE) preserves time-reversal symmetry but it breaks inversion symmetry [1]. NLHE appears from the anomalous velocity of the Bloch electrons due to Berry curvature. Therefore, topological crystalline insulators and the Weyl semimetals are the potential candidates for NLHE due to a Berry curvature dipole [1-3]. The surface of topological crystalline insulators hosts massless Dirac fermions protected by mirror symmetries [2]. At low temperatures, ferroelectric transition caused one of the mirror symmetries to be broken. In the case of thin film, the small mismatch of the lattice parameter can also break the mirror symmetry. The present study reports a NLHE in the $Pb_{1-x}Sn_xTe$ topological crystalline insulator thin films with varying Sn composition. The thin film samples of $Pb_{1-x}Sn_xTe$ with compositions x=0.35 and x=0.42 were grown by molecular beam epitaxy (MBE) on (100) oriented CdTe (4 µm) // GaAs substrates. The nonlinear Hall signal appeared only when the AC excitation was applied along the mirror axis i.e. [110] in our case. The measurements of a nonlinear Hall voltage follows the same geometry as used in ordinary Hall effect, but the transverse voltage is measured at double-frequency, $V_2\omega$ and zero-frequency (DC) V_0 by using lock-in amplifiers. Both voltages quadratically depend on the perpendicular driving current and decrease when reaching transition from topological to trivial band ordering with rising temperature. The observed phenomenon opens the possibility of exploring topological phase transition as a function of temperature, composition and hydrostatic pressure in topological crystalline insulators.

This work is supported by the Foundation for Polish Science through the IRA Programme co-financed by EU within SG OP.

[1] Sodemann, Inti and Fu, Liang, *Phys. Rev. Lett.* **115**, 216806 (2015).
[2] P. Dziawa, B. J. Kowalski, K. Dybko, R. Buczko, A. Szczerbakow, M. Szot, E. Łusakowska, T. Balasubramanian, B. M. Wojek, M. H. Berntsen, O. Tjernberg and T. Story, *Nat. Mater.* **11**, 1023–1027 (2012).
[3] Kang, K., Li, T., Sohn, E. *Nat. Mater.* **18**, 324–328 (2019).

Electrical Properties of Anisotype ZnO:Al/ZnSe/*p*-CdTe Heterostructures

Eduard V. Maistruk, Ivan G. Orletskyi, Maria I. Ilashchuk, Ivan P. Koziarskyi and Dmytro P. Koziarskyi

Yuriy Fedkovych Chernivtsi National University,
Kotsubinsky Str., 2, 58002, Chernivtsi, Ukraine

Solar cells based on CdTe, fabricated in the form of ITO/CdS/CdTe heterostructures, achieved an efficiency of more than 22% when the buffer layer from the CdS compound was replaced by a wide-gap MgZnO solid solution. The wider band gap of zinc selenide (2.7 eV), higher transparency, and a small difference in electron affinities (0.19 eV) contribute to the use of ZnSe as an alternative to CdS buffer layer in these solar cells to increase their efficiency [1].

The investigated ZnO:Al/ZnSe/*p*-CdTe heterostructures were produced by sequentially deposition of ZnSe and ZnO:Al thin films by high-frequency magnetron sputtering on the surface of freshly cleaved plates from the crystalline parts of a CdTe ingot. Cadmium telluride crystals were grown by the vertical Bridgman method with a low pressure of cadmium vapor in an ampoule to form acceptor defects of cadmium vacancies (V_{Cd}^{-}, V_{Cd}^{-2}), which determine the hole conductivity of the semiconductor. The kinetic parameters of *p*-CdTe at T= 295 K were: specific electrical conductivity $\sigma = 3\cdot10^{-3}$ $\Omega^{-1}\cdot cm^{-1}$, hole concentration and mobility $p= 3.5\cdot10^{14}$ cm^{-3} and $\mu_H = 56.0$ $cm^2\cdot V^{-1}\cdot s^{-1}$, respectively. The problem of making ohmic contacts to *p*-CdTe was solved by creating a p^+-region in the near-surface layer of the semiconductor when irradiated with ruby laser pulses (wavelength l = 0.694 μm, absorption coefficient $a = 6\cdot10^4$ cm^{-1}).

The rectifying properties of ZnO:Al/ZnSe/*p*-CdTe heterojunctions are determined by a potential barrier of ~1.0 eV formed in the near-contact region of *p*-CdTe. Current rectification coefficient: ~10^2. The *I-V*–characteristics of the structures are well explained within the framework of the theory of currents limited by the space charge (which is caused by the formation of an inverse layer in the near-surface region of *p*-CdTe), both in the region of small forward biases ($3kT/q < V <$ 0.45 V) and in the region reverse biases (-0.6 V < V < $-3kT/q$). As the forward voltage increases, the main mechanism of current transfer is electron tunneling through a thin potential barrier from the conduction band of the film to the conduction band of *p*-CdTe. In the region of higher reverse biases (V < -0.6 V), the current is formed by the tunneling of electrons from deep energy levels ΔE = 0.5 eV located in the band gap of cadmium telluride in the region of the inversion layer.

The C-V–characteristics of ZnO:Al/ZnSe/*p*-CdTe heterojunctions in the region of reverse biases at high frequencies (f = 600 – 1000 kHz) correspond to sharp surface-barrier structures. The dependence of the capacitance on the frequency of the alternating signal observed at low frequencies (f = 10 – 100 kHz) is explained by the influence of the charge of deep surface levels at the ZnSe/*p*-CdTe interface.

The constructed energy diagram of the ZnO:Al/ZnSe/*p*-CdTe heterostructure (taking into account the energy parameters of the materials) well explains the obtained experimental results.

[1] A. A. Khurram, M. Imran, Nawazish A. Khan, M. Nasir Mehmood, *J. Semiconductors* **38**, 093001 (2017)

Current Transfer Mechanisms in $CuMoO_4$/*n*-Si Heterostructure

Ivan P. Koziarskyi, Eduard V. Maistruk and Dmytro P. Koziarskyi

Yuriy Fedkovych Chernivtsi National University,
Kotsubinsky Str., 2, 58002, Chernivtsi, Ukraine

Delafossite ($CuMoO_4$), together with other minerals of its group, is known for a wide range of electrical properties. Its conductivity can vary from insulating to metallic materials. $CuMoO_4$ nanocomposites can be used for the manufacture of electroluminescent devices as a photocatalyst. This compound also refers to transparent conducting oxides (TCO) – these are semiconductors that combine transparency to visible light and high electrical conductivity in one material. The development of *p*-type TCO will give us opportunities that cannot be used only with *n*-type materials, such as transparent *p*-*n* heterojunction, diodes, transistors.

Thin films of $CuMoO_4$ (thickness ~ 100 nm) were obtained by RF magnetron sputtering on glass substrates (for optical studies) and on plane-parallel *n*-Si plates (for obtaining heterostructures). A stoichiometric mixture of CuO and MoO_2 was used to manufacture the target. The temperature of the substrate T_S = 613 K, sputtering was carried out for 30 min, with a magnetron power of 180 W.

To determine optical coefficients, a method based on independent measurement of transmission and reflection coefficients was used. For the obtained films, transmission coefficient ~ 30 – 40% in the visible region. The presence of a straight section near the region of the own absorption edge on the dependences $(\alpha h\nu)^2 = f(h\nu)$ confirms the fact that the process of absorption of light photons takes place with the help of direct optical transitions. For the studied films, by extrapolation, the optical band gap E_g^{op} = 4.1 eV was determined.

On the basis of the *I*-*V*-characteristics obtained at different temperatures (Fig. 1) by extrapolation of linear sections of forward branches, the value of the height of the potential barrier was estimated and its temperature dependence was constructed (Fig. 1, inset), from which the temperature coefficient of change in the height of the potential barrier was determined and its values at 0 K, which are equal to $d(q\varphi_k)/dT$ = -1.9·10^{-3} eV/K and $q\varphi_k$(0 K) = 0.75 eV, respectively.

Fig. 1 shows that the *p*-$CuMoO_4$/*n*-Si heterostructure has rectification properties, the rectification ratio $RR \approx 120$ for $|V| = 0.4$ V and $T = 294$ K. According to the slope of the temperature dependence $ln(R_s) = f(10^3/T)$, the activation energy of charge carriers is determined, which is E_a = 0.25 eV.

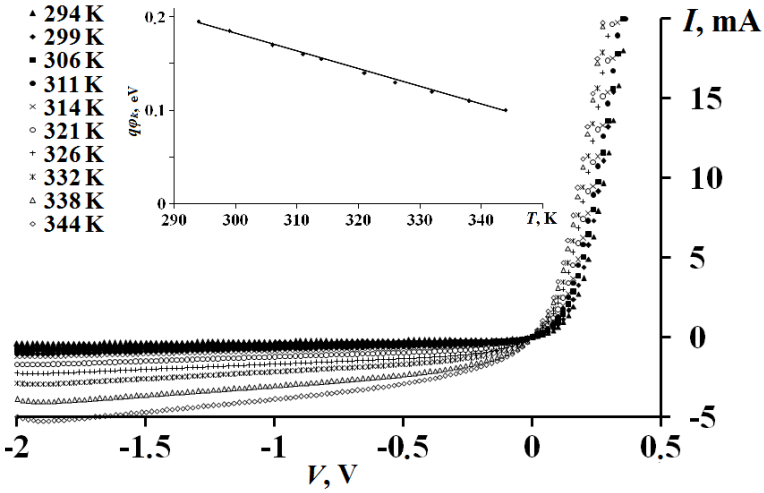

Fig. 1. *I*-*V*-characteristics of the *p*-$CuMoO_4$/*n*-Si heterostructure at different temperatures (inset: $q\varphi_k = f(T)$)

At forward biases of $3kT/q$ V < *V* < 0.2 V, the generation-recombination mechanism of current transfer prevails in the *p*-$CuMoO_4$/*n*-Si structure. The reverse current at biases -2 V < *V* < -$3kT/q$ V is determined by tunneling processes involving surface states.

The *p*-$CuMoO_4$/*n*-Si heterostructure is photosensitive under reverse bias under AM1.5 radiation conditions.

Kinetics of Fe Island Films degradation in Air

K.A. Korotkov[1], A.M. Kasumov[1], A.I. Dmiriev[1], V.M. Karavaeva[1], A.I. Ievtushenko[1]

[1] *I.M. Frantsevich Institute for Problems of Material Science, National Academy of Sciences of Ukraine, 3 Krzhizhanovskogo Str.,Kyiv, 03142, Ukraine*
kasumov@ipms.kiev.ua

Iron island films are a promising material for nanotechnologies and spintronic. However, due to their high reactivity, they quickly oxidize in air and can only be used under conditions of ultrahigh ($< 10^{-9}$ Torr) vacuum. The aim of this work is to study the degradation kinetics of Fe island films in air and the effect of this process on such properties as resistivity ρ, optical transmission T, and thickness.

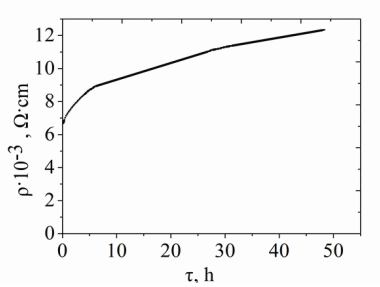

Figure 1.

Figure 1 shows the growth kinetics ρ of the Fe film depending on the time τ of its exposure to air. The initial film thickness is 20 nm, which, according to [1], corresponds to island morphology and the tunneling mechanism of charge transfer between islands. It can be seen from this figure that due to air oxidation, the resistance ρ of the Fe island film rapidly increases in a power-law dependence on the exposure time: $\rho = a\tau^{\kappa}$, where $a = 7.5\ 10^{-3}$ Ω/h, $\kappa = 0.08$. The growth constant κ of the oxide layer is much less than the value of 0.5 observed during reaction diffusion in continuous films [2]. This may be due to the specific morphology of the island film, in which the empty spaces between the islands do not take part in the oxidation process. In addition, at room temperature of the experiment, the low-temperature Mott oxidation mechanism should also take place under the influence of electric field that arises in interface by sorbet oxygen atoms and Fe atoms. This mechanism has a lower rate of oxidation.

After 14 hours of exposure, ρ of the Fe film begins to correspond to Fe_3O_4. And then it increases at a slower rate, approaching Fe_2O_3.

Figure 2 shows the spectral dependence of the optical transmission T(λ) of the Fe island film before (1) and after (2) exposure to air for 48 hours.

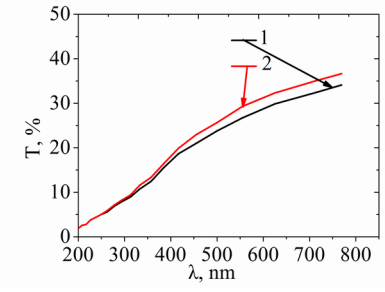

Figure 2

As can be seen from this figure, the process of Fe oxidation is accompanied by film bleaching, which manifests itself to the greatest extent in the long-wavelength region of the spectrum. It is obvious that the transparency of the film is associated with a decrease in its reflection coefficient as the composition changes from metal (Fe) to semimetal (Fe_3O_4) and then to semiconductor (Fe_2O_3).

The thickness of the Fe film in the process of oxidation increases from 20 nm to 40 nm in 48 hours of exposure to air. The increase in thickness caused by the incorporation of oxygen atoms should change the configuration of the islands and additionally affect the change in ρ and T shown in Figures 1 and 2.

[1] K.A. Korotkov, A.M. Kasumov, et all, *Int. Conf. CICS-2022,* 96 (Ukraine, Kyiv, 2022).
[2] B.I. Boltaks, *Diffusion in semiconductors* (Academic Press, 1 January 1963)

Isolation of responsive elements of coordinate *p-i-n* photodiodes by p^+-layer

Kukurudziak M. S.[1, 2]

[1]*Rhythm Optoelectronics Shareholding Company, 244 Holovna St., 58032 Chernivtsi, Ukraine*
[2]*Yu. Fedkovych Chernivtsi National University, 2 Kotsyubynsky St., 58002 Chernivtsi,Ukraine*

An urgent task of modern optoelectronics and photoelectronics is the development of systems for detecting the coordinates of various objects. Coordinate multi-element or matrix *p-i-n* photodiodes (PD) are most often used in such systems. The coordinate PD is usually a two- or four-element (sometimes more) photodiode on one semiconductor plate, and the responsive elements (RE) of photodiodes are separated by gaps smaller than the size of the light probe [1]. An important task in the manufacture of multi-element PDs is to ensure proper insulation of the REs among themselves, since the formation of inversion layers at the Si-SiO_2 interface can significantly deteriorate the insulation resistance of the active elements. There are various methods of isolation of REs. A classic option in planar technology is insulation with a base material and a dielectric gap on the surface, most often SiO_2 (Fig. 1a). This method provides insulation resistance between elements R_{con}=1-15 MΩ. But with an increase in the level of positive charge in the oxide, a sharp deterioration of this parameter is possible. A common method of isolation is the formation of a mesastructure, where the dielectric is air (R_{con}=6.7-20 MΩ) (Fig. 1b). But this method does not exclude the formation of inversion channels at the Si-SiO_2 interface. An effective method of isolation of the REs is the formation in the gaps between the active elements of areas of restriction of channels of leakage of charge carriers isotypic with the material of the substrate (in this case, p^+-type, R_{con}=18-50 MΩ) (Fig. 1c). In the case of *p-i-n* PD, this is embodied by the introduction of additional thermal operations - diffusion of boron into the gaps between the REs and oxidation, as well as one photolithography, which significantly increases the cost of the products.

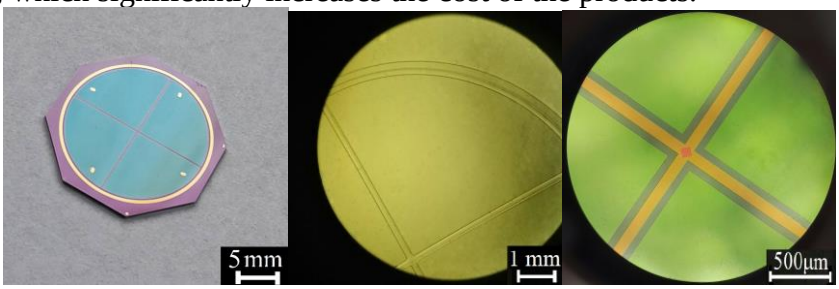

a) b) c)

Fig. 1. Image of crystals of PDs: a) classic PD; b) PD with mesastructure; c) PD with p^+- area between REs.

We proposed to first carry out boron diffusion in the entire front surface of the substrate with a low concentration, and then the sequence of operations will correspond to the classical route [1]. Boron diffusion in this case was carried out at a temperature of 1073-1123 K for 1-2 min, the surface resistance after diffusion reached R_S=150-200 Ω/□. Accordingly, the formation of p^+-type areas was ensured by the introduction of one "low-temperature" thermal operation and without the introduction of additional photolithography. The insulation resistance between REs with such a crystal design reached R_{con}=15-30 MΩ. It was noted that the introduction of a small concentration of boron significantly reduces the density of dislocations that are formed during the diffusion of phosphorus. This is caused by the compensation of mechanical stresses introduced by phosphorus atoms, which have a larger diameter than silicon, since the diameter of boron atoms is lower than in silicon.

[1] M. S. Kukurudziak, *Phys. Chem. Solid St.* **23(4)**, 756-763 (2022).

Damping of open circuit photovoltage in a Si homojunction

Bronislaw A. Orlowski[1], Katarzyna Gwozdz[2], Krzysztof Goscinski[1], Marta Chabowska[1], Elżbieta Guziewicz[1], Bogdan J. Kowalski[1]

[1]*Institute of Physics, Polish Academy of Sciences, Al. Lotników 32/46 ,Warsaw, Poland*
[2]*Wroclaw University of Science and Technology, Wybrzeże Wyspiańskiego 27, 50-370 Wrocław, Poland*

The paper continues the study of interaction of free electrons and holes with defect states in the illuminated photo junction [1]. The laser beam of selected energy photons was used to measure open circuit voltage V_{oc} versus illumination intensity dependence. Obtained results are compared with the proposed theoretical model [2,3].

In general, photo junctions are build of two different semiconducting materials with different crystal structure, electronic band structure as well as different minority and majority carriers. Free and trapped electrons and holes interact in the junction. In such a case the junction has different electrons and holes concentrations, n_{10} and p_{10} on side 1, and n_{20} and p_{20} on side 2. Under illumination in steady state conditions they change to new concentrations of n_{11}, p_{11} and n_{21}, p_{21}. The achieved steady state conditions will be approximately (Maxwell-Boltzmann approximation) described by the energy shifts corresponding to four values of quasi Fermi levels energies: $F_{1n1}=kT\ln(n_{11}/n_{10})$, $F_{1p1}=kT\ln(p_{11}/p_{10})$, $F_{2n1}=kT\ln(n_{21}/n_{20})$ and $F_{2p1}=kT\ln(p_{21}/p_{20})$ different from the common energy of the thermal equilibrium Fermi level F=0. The created difference of chemical potential between the sides of the junction are equal to $(F_{1n1}-F_{2n1})/e$ for electrons and $(F_{1p1}-F_{2p1})/e$ for holes. This difference of energies contribute to an open circuit voltage value $V_{oc1}=(F_{1n1}-F_{2n1})/e + (F_{1p1}-F_{2p1})/e$.

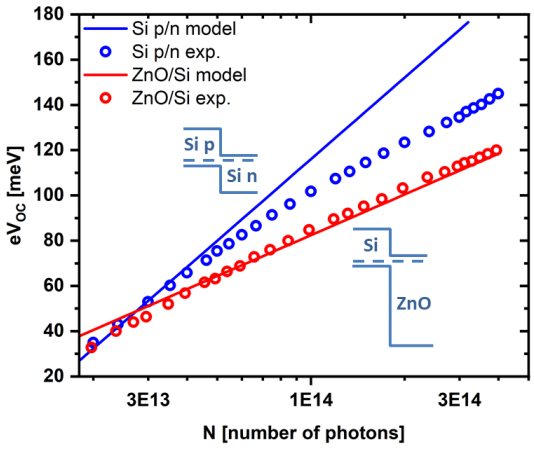

Fig. 1. A comparison of the measured open-circuit voltage with predictions of the presented model for a homo- and heterojunction.

We test the described model by comparing predictions derived from it with the results of the open circuit voltage measurements performed for two systems: a heterojunction n-type ZnO/p-type Si and a homojunction made of n-type and p-type Si. In the former, the ZnO top layer (Eg = 3.37 eV) is transparent to the photons of the energy hν = 1.91eV, so electrons and holes are generated only in the Si layer (the absorption edge at about 1.1eV). In the latter, the laser beam radiation is absorbed in both parts of the junction. The model satisfactorily describes the measured open circuit voltage in the heterojunction (Fig. 1), while for homojunction it fails to describe the experimental results for the high intensity illumination. Likely, stronger influence of the interface imperfections reducing the efficiency of the junction has to be taken into account if both sides of it are populated with electron-hole pairs.

References

1. W. Schröter, J. Kronewitz, U. Gnauert, F. Riedel, M. Seibt, *Phys. Rev. B* **52**, 13726 (1995)
2. B.A. Orlowski, K. Gwozdz, M. Galicka, S. Chusnutdinow, E. Placzek-Popko, M.A. Pietrzyk, E. Guziewicz, B.J. Kowalski, *Acta Phys. Pol. A* 134, 590 (2018)
3. B.A. Orlowski, K. Gwozdz, K. Goscinski, S. Chusnutdinow, M. Galicka, E. Guziewicz, B.J. Kowalski, *Acta Phys. Pol.* A.141.548 (2022).

Epitaxial Hexagonal Boron Nitride – Growth, Properties and Applications

Johannes Binder

Faculty of Physics, University of Warsaw, Pasteura 5, 02-093 Warsaw, Poland

Hexagonal boron nitride (h-BN) is a two-dimensional (2D) material and a member of the III-nitride family that has recently attracted great interest due to its versatile range of applications. One of the most prominent examples is the use of h-BN as a substrate for other 2D materials. The lack of dangling bonds, the atomically flat surface and the homogenous dielectric environment lead to a significant improvement of the electrical and optical properties of adjacent 2D materials and render h-BN the prototype 2D-insulator for van der Waals (vdW) heterostructures that consist of stacks of many different 2D materials.

However, most of the work on vdW heterostructures is so far based on exfoliated flakes of h-BN. It is clear that the bottleneck for industrial applications of 2D materials will be the possibility to fabricate high-quality large-area layers.

In the first part of my presentation I will address this issue and show results on the growth of epitaxial h-BN on sapphire by metalorganic vapour-phase epitaxy (MOVPE) [1-3], which is currently regarded as one of the most promising growth techniques. I will show that the growth of a 2D material on a conventional substrate at high temperatures followed by a cool down to room temperature will lead to wrinkle formation [1,4], which can be used to assess the quality of the grown layer.

In the second part, I will focus on the properties of h-BN in general and of our epitaxial h-BN in particular, with a detailed characterization and discussion of the properties.

The last part will be dedicated to applications of our MOVPE-grown h-BN ranging from large-area growth of vdW heterostructures [5], single photon emitting defects [6], photonic applications like the growth of Bragg mirrors [7] to hydrogen generation and storage applications [1].

[1] J. Binder, A. K. Dabrowska, M. Tokarczyk, K. Ludwiczak, R. Bozek, G. Kowalski, R. Stepniewski, A. Wysmolek *Nano Letters* **23**, 1267−1272 (2023)
[2] M. Tokarczyk, A. K. Dabrowska, G. Kowalski, R. Bozek, J. Iwanski, J. Binder, R. Stepniewski, A. Wysmołek *2D Materials* **10**, 025010 (2023)
[3] A. K. Dabrowska, M. Tokarczyk, G. Kowalski, J. Binder, R. Bozek, J. Borysiuk, R. Stepniewski, A. Wysmołek *2D Materials* **8**, 015017 (2021)
[4] J. Iwanski, P. Tatarczak, M Tokarczyk, A. K. Dabrowska, J. Pawlowski, J. Binder, G. Kowalski, R. Stepniewski, A. Wysmolek *Nanotechnology* **34**, 015202 (2023)
[5] K. Ludwiczak, A. K. Dabrowska, J. Binder, M. Tokarczyk, J. Iwański, B. Kurowska, J. Turczyński, G. Kowalski, R. Bożek, R. Stępniewski, W. Pacuski, A. Wysmołek *ACS Appl. Mater. Interfaces* **13**, 47904 (2021)
[6] M. Koperski, K. Pakuła, K. Nogajewski, A. K. Dąbrowska, M. Tokarczyk, T. Pelini, J. Binder, T. Fas, J. Suffczynski, R. Stepniewski, A. Wysmolek, M. Potemski *Scientific Reports* 11:15506 (2021)
[7] A. Ciesielski, J. Iwański, P. Wróbel, Rafał Bożek, S. Kret, J. Turczyński, J. Binder, K. P. Korona, R. Stępniewski, A. Wysmołek *arXiv:*2206.02168 (2022)

h-BN bubbles – a step towards deterministic activation of single photon emission

P. Tatarczak*, J. Iwański, J. Binder, A. K. Dąbrowska, M. Tokarczyk, R. Stępniewski and A. Wysmołek

Faculty of Physics, University of Warsaw, Pasteura 5, 02-093 Warsaw, Poland

Hexagonal boron nitride (h-BN) is a wide bandgap (~6 eV) two-dimensional semiconductor which can be easily integrated with other materials. Point defects hosted by h-BN were found to act as single photon emitters even at the room temperature [1]. Therefore, h-BN is regarded as a promising material in terms of quantum optoelectronics. However, it was shown that single photon emission needs to be activated e.g. by annealing or by bending the material [2]. We address this issue by the deterministic creation of h-BN bubbles. Via electron irradiation [3] of our MOVPE material grown on sapphire substrates [4], we initialize the radiolysis of interfacial water. This leads to the creation of stable hydrogen-filled h-BN bubbles (Fig. 1a).

Here, we discuss the optical properties of the obtained h-BN bubbles. To study the impact of created deformation on defect-related emission in different spectral ranges, we performed photoluminescence (PL) measurements using different excitation wavelengths. PL mapping measurements show that bubbles enhance the total light emission (Fig. 1b) and prove that they can activate additional spectral lines impossible to observe on flat h-BN (Fig. 1c), which are candidates for single-photon emitters. Since bubbles are non uniform, they create a inhomogeneous strain distribution that can shift the energy. Therefore they can also tune the energy of emitted light. The key point is that bubbles are created only in irradiated precisely selected locations. Therefore, h-BN bubbles seem to be a useful tool to deterministically locate and activate quantum emitters on demand.

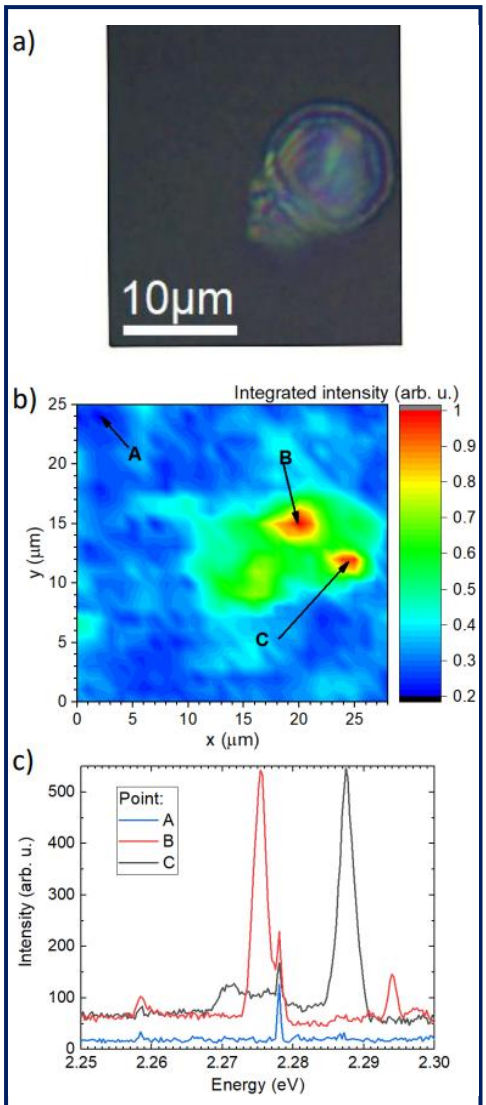

Fig. 1. PL measurements of one single h-BN bubble with 532 nm laser excitation at 4.2 K: a) Optical image of the h-BN bubble, b) total integrated intensity (2.06-2.30 eV), c) results for specific points marked at b).

Acknowledgement: This work has been partially supported by the National Science Centre Poland under decisions no. and 2020/39/D/ST7/02811 and 2022/45/N/ST7/03355

References:

[1] T. T. Tran et al., *Nature Nanotech* **11**, 37 (2016)
[2] N. V. Proscia et al., *Optica* **5**, 1128 (2018).
[3] J. Binder et al., *Nano Lett.* **23**, 1267 (2023)
[4] A. K. Dąbrowska et al., *2D Mater.* **8**, 015017 (2021)

Nature of UV (3 – 5 eV) Emission from Hexagonal Boron Nitride

K. P. Korona[1*], A. K. Dąbrowska[1], J. Iwański[1], T. Korona[2], A. Reszka[3], J. Binder[1], R. Stępniewski[1], A. Wysmołek[1]

[1] *Faculty of Physics, University of Warsaw, Pasteura 5, 02-093 Warsaw, Poland*
[2] *Faculty of Chemistry, University of Warsaw, Pasteura 1, 02-093 Warsaw, Poland*
[3] *Institute of Physics, Polish Academy of Sciences, Al. Lotników 32/46, 02-668 Warsaw, Poland*
*e-mail: kkorona@fuw.edu.pl

Boron nitride (BN) is a semiconductor with energy gap of about 6 eV. In spite of wide interest in BN properties, there are still many discrepancies in reports on its photoluminescence (PL) spectra. In the present work we aim to analyze nature of bright UV PL emission from defects in hexagonal BN (h-BN) by means of a joint experimental and theoretical study.

The experimental part was performed on the boron nitride layers grown on sapphire substrates using the Metal Organic Vapor Phase Epitaxy (MOVPE) [1]. The growth temperature, t_{gr}, for a series of samples was between 1050°C and 1300°C.

The photoluminescence was excited with the 215 nm (5.8 eV) light generated as fourth harmonic of the Ti:Sapphire laser line. Micro-PL spectroscopy was performed with the mirror objective. Time-resolved PL (TRPL) was measured with a UV-designed streak camera equipped with quartz optics.

In the PL a high-energy emission was observed at 230 nm (5.4 eV) and several bright lines were at range of 300 nm (4.1 eV) and 380 nm (3.2 eV). The C300 emission spectra consisted of a few sharp lines with nearly identical lifetimes (about 0.9 ns). The identical lifetimes suggest that these are phonon replicas what was confirmed by comparison with phonon energies. The lifetimes of the C380 set of lines were about 1.8 ns with a similar phonon replica structure. The lines were narrow (0.6 nm width) showing that the C300 and C380 emissions have a character of color centers. The lifetimes were nearly constant in temperature range from 6 to 300 K, what means that their PL efficiency was high. A strong dependence between the C300 and C380 intensity and t_{gr} has been observed. The color center lines vanished for $t_{gr} > 1200$°C, and were replaced by broad bands (D330 and D400) centered at similar wavelengths.

Based on the theoretical results [2], we postulate that the 300-nm and 380-nm lines can be assigned to pairs of carbon atoms, which is expected in our samples due to the use of organic precursor $(C_2H_5)_3B$ during the growth. In the theoretical calculations the defects of h-BN were simulated by the BN clusters modified with various carbon-related defects. Their electronic spectra were calculated by time-dependent density-functional theory. The introduced defects gave electronic excitations of lower energies, 4.8 eV and 3.7 eV for two simple configurations of C_2 (1,2-C_BC_N and 1,4-C_BC_N), what is in a good agreement with energies of the observed C300 and C380 defects.

The observed temperature dependence enables us to control number of the color centers. Such intentionally introduced centers are important for applications like deep UV emission or quantum information.

This work was supported by NCN (Poland) grants 2019/33/B/ST5/02766 and 2020/39/D/ST7/02811.

[1] A. K. Dąbrowska, *et al.* 2D Materials **8**, 015017 (2021)
[2] T. Korona, M. Chojecki, Int. J. Quantum Chem. 119:e25925 (2019)

Optically Detected Magnetic Resonance of p- and n-type Doped (Cd,Mn)Te QWs

Aleksandra Łopion, Aleksander Bogucki, Zuzanna Śnioch, Karolina E. Połczyńska, Wojciech Pacuski, Tomasz Kazimierczuk, Andrzej Golnik and Piotr Kossacki

Faculty of Physics, Institute of Experimental Physics, University of Warsaw, ul. Pasteura 5, 02-093 Warszawa, Poland

In this work, we combine magnetooptical measurements and optically detected magnetic resonance (ODMR) technique to study magnetic system composed of Mn^{2+} ions in (Cd,Mg)Te/(Cd, Mn)Te QWs with carrier gas.

The advantage of the ODMR technique is the possibility to study local properties of magnetic ions incorporated in well-defined position of nanostructure. The basic information extracted from the ODMR spectra is the energy level structure of the Mn^{2+} ion, which depends, e.g., on the local strain [1]. Although the ODMR technique in diluted magnetic semiconductors is sensitive selectively to the magnetic ions, the detailed analysis of the measured signal reveals interactions within the magnetic ion system or between ions and charge carriers [2].

The nominally undoped (Cd,Mn)Te/(Cd,Mg)Te quantum wells are typically p-type [3]. The hole gas originates from the background doping of the (Cd,Mg)Te barrier material or from the surface states. By covering the (Cd,Mn)Te/(Cd,Mg)Te QW structure with a nickel metallic layer, we produced a sample with different carrier gas properties. As we observe by magnetooptical measurements, the hole gas is replaced by electron gas in the QW. Additionally, the application of the voltage to the nickel gate gives us an opportunity to tune the electron density.

Depending on the conditions, we have observed that the ODMR signal is affected by the carriers present in the sample in two ways. The first effect is the shift between the ODMR signals obtained on neutral and charged exciton (Knight shift). The second one is a change of the spin-lattice relaxation (SLR) rate in the presence of the carriers.

Our results clearly highlight the asymmetry between electron and hole systems. The observed change of effective g-factor in the Knight shift is positive (shift towards lower magnetic fields) and much more pronounced for p-type than for n-type case. Interestingly, for both types of carrier gas we observe significant acceleration of the SLR.

[1] Bogucki A., et al., *Phys. Rev. B* **105**, 075412 (2022).
[2] Łopion A., et al., *Phys. Rev. B* **106**, 165309 (2022).
[3] Maślana W., et al., *Appl. Phys. Lett*. **82**, 1875 (2003).

Magnetic signatures in structural, electronic and optical properties of 2D MPX_3 crystals

[1]Magdalena Birowska

[1]*Institute of Theoretical Physics, Faculty of Physics, University of Warsaw, Pasteura 5, 02-093 Warsaw, Poland*

Since recent years the magnetism in two-dimensional (2D) materials has emerged as one of rapidly growing research areas, with many exciting properties and potential applications in low-power spintronics, and optical communication [1]. The current study focuses on the transition metal phosphorous trichalcogenides semiconductors (MPX_3, M=Mn, Ni, Fe, X=S, Se), which are layered antiferromagnetic semiconductors. These materials are stable in air and exhibit facinating properties, such as recenlty predicted giant excitionic binding energies sensitive to the polarization of light [2].

In this report, we adress a following scientific questions: what mechanism sustains the long-range AFM ordering, and whether the type of magnetic arrangement can be manipulated? Here, we report a comprehensive theoretical *ab initio* results of the structural, electronic and optical properties of the series of MPX_3 monolayers (M=Mn, Ni, Fe, and X=S,Se). We also present the results for alloy systems with magnetic [3] and nonmagnetic substitution [4]. In particular, for the AFM-Neel magnetic ordering, the inclusion of the spin-orbit interaction (SOI) causes an in-equivalency of the pair of valleys (K+,K-), resulting in sizeable valley splitting, which can be tuned by the rotation angle of the spins. In the case of $MnPS_3$, $MnPSe_3$ and $FePS_3$ monolayers, we have demonstrated that the band edge direct transitions are optically active and sensitive to the polarization of light. In addition, our results reveal an effective tuning of magnetic interactions and anisotropies in both $MnPS_3$ and $NiPS_3$ upon nonmagnetic substitution [4]. Finally, we highlight the importance of the structural anisotropy in monolayer of $FesPS_3$, resulting in local inversion symmetry breaking, leading to lifted spin degeneracy of K+/K- valleys, and two optically active transitions visible in experiments [5]. Such efficient engineering of the magnetism in MPX_3 materials provides a suitable platform to understand the magnetism in thin samples

[1] M. Gibertini, M. Koperski, A. F. Morpurgo, K. S. Novosolev, *Nat. Nanotech.* **14**, 408 (2019).
[2] M. Birowska, P.E.F. Junior, J. Fabian, J, Kuntsmann, *Phys. Rev. B* **103**, L121108 (2021).
[3] C. Autieri, G. Cuono, C. Noce, M. Rybak, K. M. Kotur, C. E. Agrapidis, K. Wohlfeld, M. Birowska, *J. Phys. Chem. C* **126**, 6791 (2022).
[4] R. Basnet, K. Kotur, M. Rybak, C. Stephenson, S. Bishop, C. Autieri, M. Birowska, J. Hu, *Phys. Rev. Research* **4**, 023256 (2022).
[5] E. Geraffy, S. Zuri, M. M. Rybak, F. Horani, A. K. Budniak, Y. Amouyal, M. Birowska, E. Lifshitz, *arxiv.org/pdf/2208.10890*.

Magneto-spectroscopy of excitons in two-dimensional layered perovskites

M. Dyksik[1], A. Surrente[1], M. Baranowski[1], D. K. Maude[2], and P. Plochocka[1,2]

[1] *Wroclaw University of Science and Technology, Wroclaw, Poland*
[2] *Laboratoire National des Champs Magnétiques Intenses, Toulouse, France*

Over the past few years we have witnessed a booming interest in the field of two-dimensional (2D) layered metal halide perovskite. The revival of this class of materials is driven in part by their increased environmental stability with respect to the 3D perovskites as well as their outstanding performances in photovoltaic and light-emitting devices [1]. The reduction of dimensionality allows material engineering to go beyond the mere control of the thickness of the inorganic quantum wells. In such a hybrid organic-inorganic materials, the plethora of available organic molecules not only allows to tailor various material functionalities, but also gives rise to a considerable structural diversity. Due to the high contrast of dielectric constant of organic/inorganic sublattices, the 2D perovskites are characterized by very large exciton binding energies with low effective Bohr radius. As a result of large binding energies, the exchange interaction between the electron and hole spins is greatly enhanced, which in turn increases considerably the exciton fine structure. On top of that, the ionic nature and the softness of the perovskite lattice results in a significant coupling of electronic excitations to the lattice vibration (*i.e.*, electron-phonon interactions). Such coupling has a pronounced impact on the optoelectronic properties of 2D perovskites and is manifested in a complex absorption and emission spectra [2], which usually consist of multiple, equally spaced (in energy scale) resonances [3]. As the result, the mutual understanding of electronic and lattice excitations and their correlation – polarons – is crucial to adequately describe this material system.

In this work, we highlight our recent results on the determination of excitonic and polaronic properties of various 2D layered perovskites. In order to access such parameters, spectroscopy in high magnetic field, up to 160 T was employed. By these experiments, we not only determine important material parameters such as effective mass, exciton binding energy and exciton Bohr radius [4], but we also address the longstanding open question about the exciton fine structure in 2D perovskites. We elucidate the order of excitonic states and determine the bright–dark splitting energy [5]. Finally, by correlating the magneto-spectroscopy data with resonant Raman scattering we explain the complex multi-peak absorption response of 2D layered perovskites as being dominated by exciton-polarons.

[1] Gong *et al.*, *Nat. Mater.* **17**, 550 (2018).
[2] Urban *et al.*, *J. Phys. Chem. Lett.* **11**, 5830 (2020).
[3] Dyksik *et al.*, *ACS Energy Lett.* **5**, 3609 (2020).
[4] Dyksik *et al.*, *J. Phys. Chem. Lett.* **12**, 1638 (2021).
[5] Dyksik *et al.*, *Sci. Adv.* **7**, 1 (2021).

Temperature Dependence of Effective Masses in Three-dimensional Methylammonium Lead Trihalides

Andrzej Nowok[1,2], Michał Baranowski[2], Mateusz Dyksik[2], Alessandro Surrente[2] Mirosław Mączka[3] and Paulina Płochocka[1,2]

[1] *Laboratoire National des Champs Magnetiques Intenses, CNRS, 143 avenue de Rangueil, Toulouse, France*
[2] *Department of Experimental Physics, Wrocław University of Science and Technology, Wybrzeże Stanisława Wyspiańskiego 25, Wrocław, Poland*
[3] *Institute of Low Temperature and Structure Research, Polish Academy of Sciences, P.O. Box 1410, Wrocław, Poland*

Perovskite methylammonium lead trihalides ($CH_3NH_3PbX_3$ with X=Cl, Br, I) have gained particular research interest as promising hybrid compounds with excellent sunlight-to-energy conversion abilities [1]. They constitute a particular semiconducting materials system, in some aspects very different from the well-known family of epitaxial semiconductors. The soft, ionic lattice which mixes crystalline, liquid and glassy behaviour is often invoked to explain the superior characteristic of perovskite materials in applications. At the same time particular mechanical properties of perovskites create a complex background for electronic excitation where polaronic effects cannot be neglected and often challenge our understanding of fundamental parameters describing any semiconductors, for example, carrier mobility or effective mass μ [2,3].

For instance, theoretical prediction points that the soft, ionic lattice together with the unusual temperature dependence of the bandgap characteristic for these materials can lead to a significant rise of the carriers' effective mass with temperature [4,5]. Unfortunately, the temperature-induced rise of the carrier's effective mass in $CH_3NH_3PbX_3$ has never been confirmed experimentally so far. Understanding temperature dependence of reduced effective mass μ is particularly relevant in the context of solar cell applications as it affects carrier mobility.

Here we address the problem of temperature evolution of carrier effective mass by means of magneto-optical studies as μ can be directly extracted from the quantization of the free carrier states into Landau levels. We investigate three crystals methylammonium lead iodide ($MAPbI_3$), bromide ($MAPbBr_3$) and their mixed bromide-chloride analogue ($MAPbBr_{1.5}Cl_{1.5}$) under various temperatures. Using an extreme pulsed magnetic field up to 90 T we observe well-resolved Landau levels in each of the crystals even at temperatures exceeding 100 K. The temperature evolution of the Landau levels clearly points to the rise of the carrier effective mass as a function of temperature corroborating theoretical predictions. Importantly the observed rise of carriers' effective mass cannot be simply attributed only to the bandgap opening with temperature highlighting the importance of polaronic effects for metal-halide perovskites semiconductors.

[1] Y. Zhao and K. Zhu, *Chem. Soc. Rev.* **45**, 655 (2016).
[2] D. A. Egger, A. Bera, D. Cahen, et al., *Adv. Mater.* **30**, 1800691 (2018).
[3] M. J. Schilcher, P. J. Robinson, D. J. Abramovitch, *et al.*, *ACS Energy Lett.* **6**, 2162 (2021).
[4] M. Schlipf, S. Poncé and F. Giustino, *Phys. Rev. Lett.* **121**, 086402 (2018).
[5] Y.-B. Lu, H. Yang, W.-Y. Cong, *et al.*, *Appl. Phys.Lett.* **111**, 253902 (2017).

Spin dimensionality in chromium trihalides

N. Zawadzka[1], M. Grzeszczyk[2], Z. Chen[2], M. I. Katsnelson[3], M. R. Molas[1], and M. Koperski[2]

[1] *Institute of Experimental Physics, Faculty of Physics, University of Warsaw, Warsaw, Poland*
[2] *Institute for Functional Intelligent Materials, National University of Singapore, Singapore*
[3] *Institute for Molecules and Materials, Radboud University, Nijmegen, The Netherlands*

Ferromagnetism in layered van der Waals materials that preserve up to the monolayer regime attracts the exceptional attention of scientists [1]. Intensively examined chromium trihalide compounds (CrX_3, where X=I, Br, or Cl) are layered magnetic materials of ferromagnetic order within a layer. $CrBr_3$ layers are ferromagnetically coupled, while CrI_3 and $CrCl_3$ possess antiferromagnetic coupling. Furthermore, the spins in $CrBr_3$ and CrI_3 are preferentially aligned in the out-of-layer direction, whereas in $CrCl_3$ they are characterized by the in-plane orientation [2].

In this work, we study the spin dimensionality of CrX_3 compounds by applying the magnetic field in the out-of-plane (Faraday) and in-plane (Voigt) configurations in reference to the sample, see Figure (a). Magnetization was studied by the polarization-sensitive photoluminescence technique. Circularly polarized excitation and detection were used to evaluate circular dichroism in CrX_3 arising from unequal absorption coefficients for photons characterized by opposite circular polarization.

The inspection of the PL intensity as a function of applied out-of-plane magnetic field sweeping in both directions for CrI_3 and $CrBr_3$ revealed the hysteresis as seen in Fig. (b,c). Hysteresis indicates intrinsic ferromagnetic ordering. $CrCl_3$ not present hysteresis due to strong in-plane orientation of spins, see Fig. (d). Magneto-PL intensity in Voigt configuration reveals complex hysteresis with unusual shape, see Fig. (e)-(g). The comparison of coercive fields in both configurations of the magnetic field provides information about spin dimensionality, which is consistent with theory [2]. $CrBr_3$ can be described by an isotropic Heisenberg model with 3D spin dimensionality. CrI_3 has a greater out-of-plane anizotropy than $CrBr_3$, which suggests an 1D spin dimensionality described by an Ising model. $CrCl_3$ presents the 2D spin dimensionality described by an XY model.

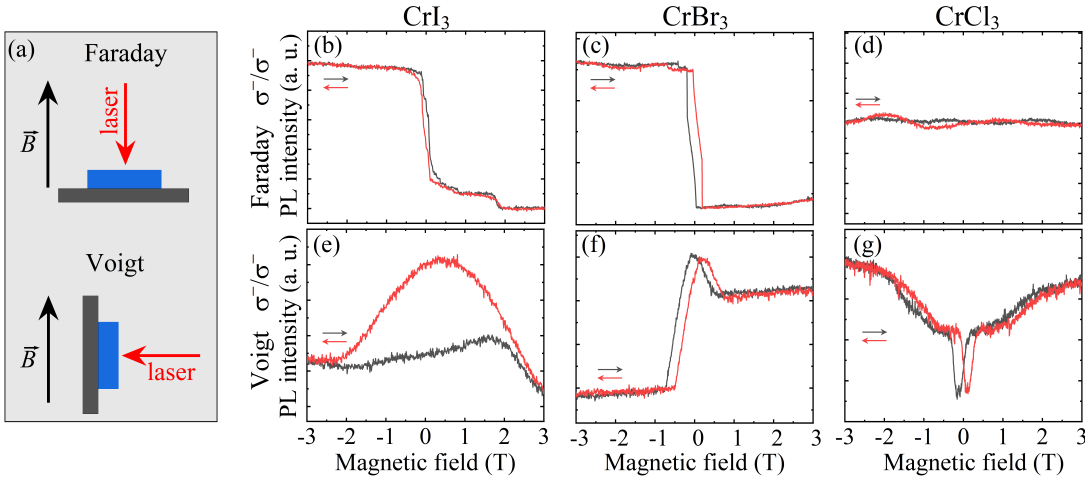

Figure: (a) The schemes of Faraday and Voigt configurations of placement sample in magnetic field. The magneto-PL intensity in Faraday (b,c,d) and Voigt (e,f,g) configurations.

[1] M. Gilbertini, et. al., *Nature Nano.* **14**, 408 (2019).
[2] R. Yadav, et. al., *arXiv:2208.02195* (2022).

INDEX OF AUTHORS